

# **Pavement moisture measurement to indicate risk to pavement life March 2017**

G Arnold (Road Science)

P Fon Sing (Downer)

T Saarenketo and T Saarenpaa (Roadscanners Oy)

ISBN 978-1-98-851213-6 (electronic)  
ISSN 1173-3764 (electronic)

NZ Transport Agency  
Private Bag 6995, Wellington 6141, New Zealand  
Telephone 64 4 894 5400; facsimile 64 4 894 6100  
research@nzta.govt.nz  
www.nzta.govt.nz

Arnold, G, P Fon Sing, T Saarenketo and T Saarenpaa (2017) Pavement moisture measurement to indicate risk to pavement life. *NZ Transport Agency research report 611*. 160pp.

Road Science was contracted by the NZ Transport Agency in 2014 to carry out this research.



This publication is copyright © NZ Transport Agency. This copyright work is licensed under the Creative Commons Attribution 4.0 International licence. You are free to copy, distribute and adapt this work, as long as you attribute the work to the NZ Transport Agency and abide by the other licence terms. To view a copy of this licence, visit <http://creativecommons.org/licenses/by/4.0/>. While you are free to copy, distribute and adapt this work, we would appreciate you notifying us that you have done so. Notifications and enquiries about this work should be made to the Manager National Programmes, Investment Team, NZ Transport Agency, at [research@nzta.govt.nz](mailto:research@nzta.govt.nz).

**Keywords:** drainage, ground penetrating radar, laser scanner, moisture, monitoring, water content

## **An important note for the reader**

The NZ Transport Agency is a Crown entity established under the Land Transport Management Act 2003. The objective of the Agency is to undertake its functions in a way that contributes to an efficient, effective and safe land transport system in the public interest. Each year, the NZ Transport Agency funds innovative and relevant research that contributes to this objective.

The views expressed in research reports are the outcomes of the independent research, and should not be regarded as being the opinion or responsibility of the NZ Transport Agency. The material contained in the reports should not be construed in any way as policy adopted by the NZ Transport Agency or indeed any agency of the NZ Government. The reports may, however, be used by NZ Government agencies as a reference in the development of policy.

While research reports are believed to be correct at the time of their preparation, the NZ Transport Agency and agents involved in their preparation and publication do not accept any liability for use of the research. People using the research, whether directly or indirectly, should apply and rely on their own skill and judgement. They should not rely on the contents of the research reports in isolation from other sources of advice and information. If necessary, they should seek appropriate legal or other expert advice.

# Acknowledgements

The researchers acknowledge the financial assistance by the NZ Transport Agency and the kind assistance from Downer staff for the road trial and asset data. From Roadscanners, Olli Ervelä was in charge of the field data collection, and Timo Rytilahti and Kent Middleton were mainly in charge of the data analysis. Pekka Maijala and Rani Hamrouche developed the MDI algorithms.

# Abbreviations and acronyms

$\epsilon_r$	dielectric value
2D	two-dimensional space
3D	three-dimensional space
AC	alternating current
ASTM	American Society for Testing and Materials
DC	direct current
FWP	forward works programme
GPR	ground penetrating radar
GPS	global positioning system
ISO	International Organization for Standardization
LIDAR	light detection and ranging
MDI	moisture damage index
NMM	neutron moisture meters
NMR	nuclear magnetic resonance
ns	nano second(s)
PA-CEP	pulled-array continuous electrical profiling technique
RF	radio frequency
RSAD	radar surface arrival detection
TDR	time-domain reflectometry (a measuring method); time-domain reflectometer (an instrument used for time-domain reflectometry)
T-R	direct wave – transmitter-receiver direct wave
UAV	unmanned aerial vehicle
WARR	wide-angle reflection and refraction



# Contents

- Executive summary .....7**
- Abstract ..... 10**
- 1 Introduction ..... 11**
  - 1.1 Background ..... 11
  - 1.2 Why measure moisture in roads? ..... 11
  - 1.3 Objectives of the field trial ..... 14
- 2 Research methodology..... 15**
  - 2.1 General..... 15
  - 2.2 Survey methods ..... 16
    - 2.2.1 Ground penetrating radar tests ..... 17
    - 2.2.2 Laboratory tests in Finland and New Zealand..... 17
    - 2.2.3 Moisture damage index calculation ..... 22
    - 2.2.4 Field data collection and basic processing..... 22
    - 2.2.5 Air coupled horn antenna data analysis ..... 23
    - 2.2.6 Repeatability tests ..... 25
  - 2.3 Laser scanner data analysis ..... 26
  - 2.4 Tests with thermal cameras..... 28
  - 2.5 Presentation of results ..... 29
- 3 Research results ..... 31**
  - 3.1 Moisture damage index analysis results ..... 31
  - 3.2 Integrated moisture diagnosis..... 33
  - 3.3 GPR horn antenna data analysis ..... 36
- 4 Validation of results..... 38**
  - 4.1 Introduction..... 38
  - 4.2 No. 2 line test pits ..... 38
    - 4.2.1 RP 3680 decreasing side..... 38
    - 4.2.2 RP 3690 increasing side..... 39
    - 4.2.3 RP 5804 decreasing side..... 40
    - 4.2.4 RP 5844 increasing side..... 41
  - 4.3 No. 3 line test pits ..... 42
    - 4.3.1 RP 670m decreasing side (wet location) ..... 42
    - 4.3.2 RP 670m increasing side (dry location)..... 43
    - 4.3.3 RP 1975m centreline (wet location) ..... 44
    - 4.3.4 RP 1970m increasing (wet location) ..... 45
  - 4.4 London St Pt2 test pits ..... 46
    - 4.4.1 RP 200m increasing side..... 46
    - 4.4.2 RP 200m decreasing side..... 47
  - 4.5 Test pit summary..... 48
  - 4.6 Summary of results ..... 49
- 5 Use of moisture survey in asset management..... 53**
- 6 Conclusions ..... 58**
- 7 Recommendations..... 60**

**8**    **References**.....61  
**Appendix A: Literature review** .....62  
**Appendix B: Field test results in New Zealand October 2015** ..... 121

# Executive summary

This research project was commissioned to address the current lack of knowledge of moisture content in New Zealand pavements, and improve the understanding of the effectiveness of road drainage. The main purpose of the research was to determine how can we measure, simply, the moisture content in a pavement; and determine what its optimum level is before drainage intervention is needed. Further, the moisture measurement was investigated to determine the effectiveness of pavement moisture control techniques.

Currently, we observe external indicators of ineffective drainage through flushing, cracks with pumping, pavement deterioration, etc. These are not definitive measures; thus we need an objective measure. The development of such a moisture measurement technology would quantify the effectiveness of drainage and whether it needs to be improved.

Stage 1 of the research was a literature review which listed a range of moisture measuring techniques, most of which were manual measurements at a project level. The system which showed the greatest potential for use in New Zealand, with ability to survey the whole road network at speeds of 60 to 80km/h, was moisture detection equipment from Roadscanners in Finland. This used air and ground coupled ground penetration radar (GPR) at low and high frequencies 500MHz and 2.2GHz, with high definition video and 2D LIDAR coupled with Road Doctor software to view the results and output data to other databases like RAMM, Juno Viewer and/or a geographic information system (GIS). Results of the literature review are detailed in appendix A of this report.

As a result of the literature review it was agreed to fund stage 2 of this research for a field trial using Road Scanners' moisture detection equipment to survey a selection of roads in New Zealand. Results of the field trial are documented in this report which compares the moisture detected within the pavement layers and subgrade together with the surface defects due to moisture and some results of findings from the test pits.

Studies by Henning et al (2014) on the long-term pavement performance (LTPP) sites found poor drainage was the number one factor affecting the rate of rutting and roughness deterioration. Two trends were observed: one for sites having adequate drainage and the other for sites having inadequate drainage. There was a slight difference between the deterioration rates of the two drainage states; sites with inadequate drainage had approximately 2.5 times the deterioration rate of sites with adequate drainage. Thus there would be significant benefits in improving drainage on sites identified by the drainage survey.

The moisture survey was conducted on a range of roads in the lower North Island using LIDAR laser scanning, GPR and video camera. The survey resulted in data that can be viewed in the free Road Doctor viewer software.

The moisture survey data can be used in several ways for managing the asset. At the network level the moisture damage index (MDI) data can be outputted to GIS or Google maps and colour coded where black indicates the highest values and areas that can be looked at more closely to determine and prioritise appropriate improvements in drainage and waterproofing the surface. Actual raw data from the moisture survey is MDI values at three depths, LIDAR rut depths, roughness and pavement depths (if calculated from GPR) every 2m increment. The data is compatible with various GIS and asset management systems.

The Road Doctor viewer software is used at a project level where a particular location is studied more closely to determine whether or not drainage improvement is needed and also to determine the type of drainage improvement required at locations scheduled for maintenance patch repairs, reseal, pavement renewal or simply a section prioritised for drainage improvement (from the moisture maps or surface and pavement distress indicating moisture problems). The type of drainage improvement for each case will

differ depending on where the water is – the viewer software is an excellent means of determining this. Further, a cross-section view can be obtained from the viewer software to determine whether the ditch depth is adequate and if there is high shoulder lip trapping the water.

Relevant asset managers within Downer have a copy of the Road Doctor viewer software installed on their computers along with the survey data and use it regularly in planning forward works programmes on the network. Its operation is similar to Road Runner with a video view of the road but the Road Doctor view also gives information on rutting and moisture at different depths in the pavement. Another advantage of the Road Doctor software displaying the LIDAR rut depth information is small localised areas can be seen showing depressions and problem areas with moisture where the size of these areas is more akin to the common patch size being around 20m in length. The Road Doctor viewer software can also be used when scheduling patch repairs in the network to determine if any drainage improvements are required alongside the patched areas. Improving drainage alongside patch repairs should extend the life of the patch. The width of the rutting is also an indicator of where the rutting occurs; if the rutting is wide then the rutting is deeper in the subgrade level.

### **Further conclusions from the survey**

This report presents the results of moisture detection surveys at high speed (60 to 80km/h or 30 to 50km/h in 50km/h speed zones). The equipment used was a transverse LIDAR, ground penetration radar (air and ground coupled) and video camera with analysis and presentation of the results using Road Doctor software. A range of roads were surveyed in the North Island where Downer was the maintenance contractor for ease of in kind traffic management and asset data. This survey yielded the following conclusions.

- There are significant benefits both short and long term by proactively improving drainage and surface waterproofness at locations where the moisture detection survey indicated high levels of moisture combined with moisture sensitive materials.
- Despite the high capital cost the moisture survey technique and data analysis was routine and involved only a few days set up and calibration before the survey could be conducted;
- The calibration with boxes of aggregate proved the GPR (air and ground) correlates with increasing saturation/moisture levels.
- The dielectric constant used as an indicator of moisture from the air-coupled GPR was found to be a poor indicator of moisture below the surface.
- A New Zealand specific MDI was developed from the calibration boxes and the complete set of moisture survey results using data mostly from ground coupled radar which allowed the moisture to be detected at three depths below the surface (0 to 200mm; 200 to 400mm and 400 to 600mm).
- The viewing software included both MDI values at different depths along with video and laser LIDAR rut depths where areas of high MDI values often corresponded to moderate to high rutting.
- Test pits conducted seven months after the moisture survey confirmed the results of the moisture survey 80% of the time.
- Results of the moisture survey can be easily outputted to other databases. Downer imported the results into their GIS maps and also into the Juno viewer to enable other pavement distress and maintenance history data to be displayed alongside the moisture data.

- There are significant benefits to proactively improving drainage and surface waterproofness as determined by the moisture survey where studies from the LTPP sites show the life of a pavement can be extended by 2.5 times.
- The theory and technology from literature review (appendix A) was confirmed through the surveys.
- The technology is applicable to New Zealand roads.
- The technology is a suitable tool allowing the asset owner to understand the effectiveness of road drainage using objective measures.
- The MDI is a suitable measure.
- Multiple data types were captured as part of the survey.
- The data is transferable to other systems allowing macro and micro analysis

### **Recommendations**

There are significant benefits in utilising the results of the moisture survey. The first is to be able to quantify and prioritise the drainage improvements needed on the road network along with determining the most appropriate moisture mitigation treatment (either deep to remove water from the subgrade or shallow to remove from the basecourse). To maximise this benefit it is recommended that the complete road network is surveyed around the same time to minimise seasonal effects and determine which networks and areas within networks need drainage improvements. These improvements could include deep subsoil drains at locations where the subgrade was identified to have high moisture levels. However, as part of the network survey further test pits should be undertaken soon after the survey to measure moisture and susceptibility to moisture of the pavement materials to further validate and give confidence in the roads. Further full-scale road trials could be constructed with controlled amounts of water added and measurements undertaken to obtain an improved calculation of the MDI. This further research should use and build on the similar research being conducted by the Finnish road agency.

For networks that are surveyed for moisture it is recommended that the effectiveness of drainage improvements is assessed in terms of moisture detected and the rate of deterioration in relation to different soil types, rainfall, road classification and traffic loading. During the survey period research is required to study how the results of the survey change the way the road network is managed. Also, through monitoring rutting with the LIDAR laser together with maintenance costs determine the financial benefits from proactive drainage improvements based on the moisture survey. For comparison, moisture surveys should also be conducted on local roads as the moisture technology is transferable between state highways and local authorities.

## Abstract

High moisture within pavements accelerates pavement deterioration. Ensuring water is kept out of these pavement layers increases life and saves maintenance costs. A high-speed moisture survey technique employed overseas, utilising ground penetrating radar combined with video and laser LIDAR, was used on a range of roads in the lower North Island. A unique moisture damage index was developed for use in New Zealand to enable the identification of high moisture levels at three different depths (top; middle; bottom) in 2m increments along the road using results from the ground and air coupled radar. In the free viewer software the road cross section can also be displayed to determine the rut depth, ditch depths, cross fall and high lip, which aid in determining the most appropriate improvement in drainage. The New Zealand trial of the moisture detection equipment showed higher rutting in road sections with high moisture, while low moisture was detected in areas of nil or low rutting. Ten test pits measuring moisture at top, middle and bottom depths showed the moisture detection survey conducted seven months earlier was correct in the assessment of high and low moisture for 80% of the time.

# 1 Introduction

## 1.1 Background

This research project was commissioned to address the current lack of knowledge of moisture content in New Zealand pavements, and improve the understanding of the effectiveness of road drainage. The main purpose of the research was to determine how can we measure, simply, the moisture content in a pavement; and determine what its optimum level is before drainage intervention is needed. Further, the moisture measurement was investigated to determine the effectiveness of pavement moisture control techniques.

Stage 1 of the research was a literature review which listed a range of moisture measuring techniques, most of which were manual measurements at a project level. The system which showed the greatest potential for use in New Zealand and able to survey the whole road network at speeds of 60 to 80km/h was moisture detection equipment from Roadscanners in Finland. This used air and ground coupled ground penetration radar (GPR) at low and high frequencies 500MHz and 2.2GHz with high definition video and 2D LIDAR coupled with Road Doctor software to view the results and output data to other databases like RAMM, Juno Viewer and/or a geographic information system (GIS). Results of the literature review are detailed in appendix A of this report.

As a result of the literature review it was agreed to fund stage 2 of this research for a field trial using Road Scanners' moisture detection equipment to survey a selection of roads in New Zealand. Results of the field trial are documented in this report which compares the moisture detected within the pavement layers and subgrade together with the surface defects due to moisture and some results of findings from the test pits.

## 1.2 Why measure moisture in roads?

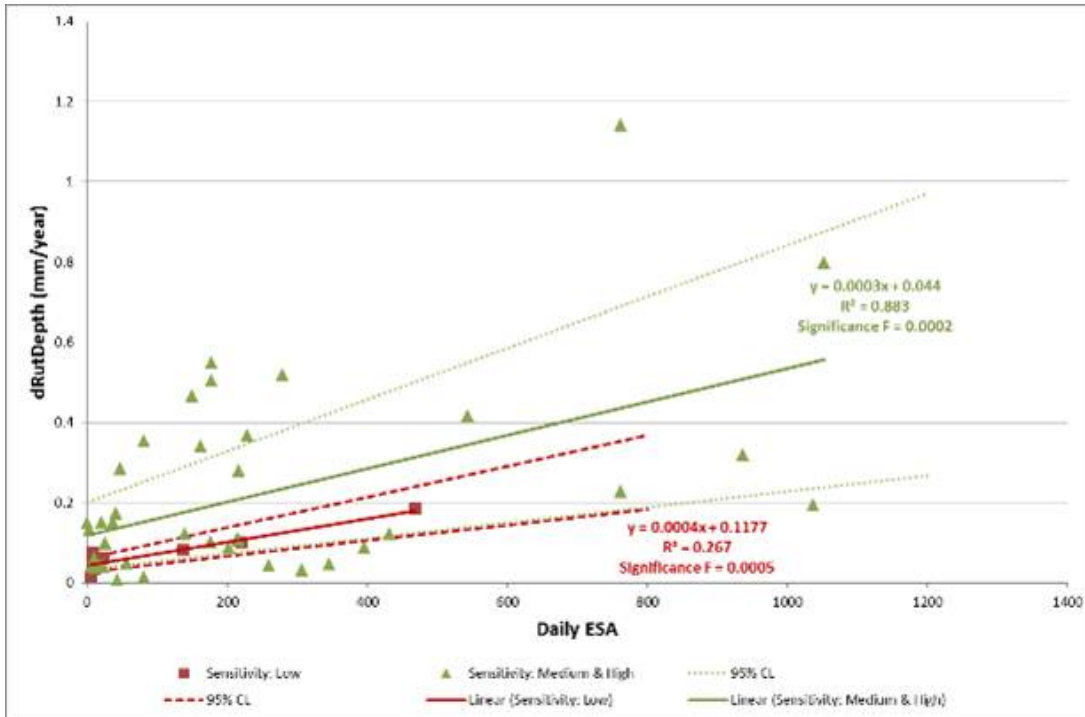
Water plays a key role in the mechanical performance and lifetime of any traffic infrastructure. The fact, known for centuries, is that as long as there is no excess water in road structures and subgrade soil the road will perform well. Increased water content reduces the bearing capacity of a soil or aggregate, which under traffic loading will increase the rate of deterioration and shorten the lifetime of the road. In such cases, the road will need maintenance measures and rehabilitation more often than a well-drained road structure. For this reason, road drainage systems need to work effectively over the whole lifetime of the pavement, not just for a few years. Current predictions of the likely effects of climate change only magnify this issue and modern asset management principles are rightly forcing road owners to consider ways to maximise the use of their available budgets and improve road lifetimes (Matintupa and Saarenketo 2011; ROADEX 2012).

Recent road condition research projects have clearly shown that good drainage maintenance practices are the most effective way to improve road condition, increase road durability, and decrease permanent deformation and spring thaw weakening. A further important matter that directly relates to road drainage is the increasing number of floods as a result of climate change. The frequency and severity of flooding caused by continuous heavy rains have been globally increasing over recent years.

However, one big challenge for road owners is how to monitor the water content in pavement structures and subgrade soils and how to monitor whether the drainage system is effective enough to drain the structures sufficiently to ensure adequate bearing capacity in the road network. Another challenge is how to ensure after flooding that the flooded road sections are safe enough to be opened to heavy traffic.

Studies by Henning et al (2014) on the long-term pavement performance (LTPP) sites found poor drainage was the number one factor affecting the rate of rutting and roughness deterioration. Two trends were observed: one for sites having adequate drainage and the other for sites having inadequate drainage. There was a slight absolute difference between the deterioration rates of the two drainage states with sites with inadequate drainage having approximately 2.5 times the deterioration rate compared with those sites with adequate drainage (figure 1.1). For example, at 400 ESA per day the rut rates are 0.65 and 0.25 for inadequate and adequate drainage respectively.

**Figure 1.1 Rut progression as a function of traffic loading and environment (Henning et al 2014)**



Knowing where on the network the pavement and/or subgrade layers are saturated will result in significant savings in maintenance costs by proactive improvements in drainage and surface waterproofness based on the results of a moisture survey as detailed in table 1.1. Further annual moisture surveys will help prioritise where to spend the drainage improvement budget and measure the effectiveness of any drainage improvements to the road network.

**Table 1.1 Benefits of conducting a network wide moisture survey.**

Item	Short- term benefits	Long- term benefits
1 Prioritise the drainage spend Identify sites high in moisture needing drainage improvement and type of drainage improvement (ie surface, pavement layers and/or deeper in the subgrade).	Using drainage improvement funds wisely: <ul style="list-style-type: none"> <li>only fixes drainage where needed</li> <li>is doing the right type of drainage improvement to get rid of water in either the subgrade or basecourse aggregate</li> </ul> The survey gives evidence and justification for the amount of drainage improvement needed which may be more or less than originally budgeted for.	Gives confidence that the amount of funds allocated for drainage improvement is appropriate and applied in the right locations. Because of this, pavements will last longer. If the moisture survey is done once a year it provides a tool to check the effectiveness of the drainage improvement.



Item	Short- term benefits	Long- term benefits
<p>2 Drainage improvement with maintenance patches</p> <p>The moisture survey results could be used together with the all faults inspection data when programming patch repair treatments. At locations where an in situ stabilisation patch repair is scheduled the moisture survey could be used to determine if drainage improvement is also required.</p>	<p>Fixing drainage properly (based on where the water is from the moisture survey) alongside patch repairs will result in the following benefits:</p> <ul style="list-style-type: none"> <li>• The patch repairs should not fail early and will reduce the amount of rework.</li> </ul>	<p>There is a possibility the patch repairs with the drainage improvement could revert a weak area into a typical strength pavement lasting 40 years and thus ensure savings in maintenance.</p> <p>If the client pays every time the road is repaired then increasing the life of a maintenance patch will result in savings.</p>
<p>3 Extending pavement life</p> <p>The moisture survey could be used to identify sites that are only slightly rutted and high in moisture needing drainage improvement. The survey would identify whether the moisture is in the pavement or subgrade and an effective type of drainage improvement could be put in place. The GPR also helps show up broken culverts and pavements with buried seal layers where water is trapped.</p>	<ul style="list-style-type: none"> <li>• Fewer areas need patch repairs as the network will deteriorate at a slower rate (extends the pavement life by 2.5 times).</li> <li>• Ability to more easily meet network roughness and rutting indicators.</li> <li>• Fewer chipseal flushed areas caused by trapped water in the basecourse aggregate under the seal.</li> </ul>	<ul style="list-style-type: none"> <li>• Less maintenance needed.</li> <li>• Less pavement renewals needed – both because there is less flushing and rutting and lower roughness.</li> <li>• Pavement network is smoother and less rutted.</li> <li>• Fewer ruts result in less risk of aquaplaning vehicles and thus improved safety.</li> <li>• Less water cutting for chipseal flushing.</li> </ul>
<p>4 Assisting in pavement renewal design and investigation</p> <p>For the pavement renewal sites the moisture survey gives valuable information to determine whether or not water is to blame for the failure. Also continuous pavement depths can be determined followed by a suitable drainage improvement method as part of the pavement renewal design.</p>	<ul style="list-style-type: none"> <li>• The risk of early failure is lessened if drainage is improved using a suitable treatment.</li> <li>• Performance criteria of the pavement renewals is met.</li> <li>• Survey aids in providing existing pavement depth in the pavement renewal design to determine the most appropriate treatment (fewer test pits needed or complements test pit information as can get 100% coverage over the length).</li> <li>• LIDAR laser survey of treatment length can be exported into computer aided design for geometric design and aggregate overlay quantity calculations – thus saves survey costs.</li> <li>• If identifying drainage and high moisture is main reason for pavement deterioration, the survey could justify a cheaper treatment of fixing the drainage with smooth ruts and reseal – ‘a do something option’.</li> </ul>	<ul style="list-style-type: none"> <li>• Pavement renewals are designed and constructed correctly, and surfacing and drainage maintained will last at least 40 years exceeding the 25-year design life.</li> <li>• More evidence and confidence in the chosen treatment and drainage improvement method proposed by the contractor.</li> <li>• Opportunity to change pavement renewal to a cheaper ‘do something’ by improving drainage and waterproofing the surface, if the moisture survey detected this was the main reason for pavement deterioration.</li> </ul>

Item	Short- term benefits	Long- term benefits
<p>5 Unsealed roads asset management</p> <p>The moisture survey with GPR and laser LIDAR can determine wet areas, gravel depths, rutting, corrugations, roughness, geometry and ditch depths. This information helps determine where and how much re-gravelling is required, along with where drainage and shape (eg crossfall) improvements are required.</p>	<ul style="list-style-type: none"> <li>• Expenditure on the unsealed road network is prioritised.</li> <li>• Savings in unsealed road maintenance.</li> <li>• Existing gravel depths for determining re-gravelling programmes are provided (sustainable metal usage).</li> <li>• Monitoring rutting and corrugations along with gravel loss can help justify more robust treatments like Notta Seal in locations that deteriorate quickly.</li> <li>• The survey will assist with implementation of the One Network Road Classification and possible conversion from sealed to unsealed roads.</li> </ul>	<ul style="list-style-type: none"> <li>• Pavement renewals are designed and constructed correctly, and surfacing and drainage maintained will last at least 40 years exceeding the 25-year design life.</li> <li>• More evidence and confidence in where the funds are spent to maintain gravel roads.</li> <li>• Overall expenditure on gravel roads could be reduced.</li> </ul>
<p>6 Identifying vulnerable areas of the network</p> <p>The moisture survey combined with laser rutting will enable the road sections vulnerable to moisture damage to be identified to proactively treat these areas to prevent expensive repairs.</p>	<ul style="list-style-type: none"> <li>• Proactive treatments will save in maintenance costs.</li> </ul>	<ul style="list-style-type: none"> <li>• Potentially prevents long-term need for pavement renewal and in the long term will reduce the overall maintenance expenditure by an estimated 20%.</li> </ul>

### 1.3 Objectives of the field trial

The principal objectives of the research were to:

- demonstrate moisture detection equipment can identify saturated pavement areas along the road together with a probable cause (eg the moisture ingress is due to either a cracked seal as found from the thermal imaging camera or inadequate drainage)
- investigate and inspect pavement areas of the road network surveyed that were identified as being saturated and in need of drainage improvement to confirm or otherwise the accuracy of the surveys and the accuracy of the probable cause
- report on the practicality, cost and success or otherwise of the moisture detection equipment trial in New Zealand.

## 2 Research methodology

### 2.1 General

A range of roads was selected based on Transport Agency and local authority contracts where asset information on pavement and surfacing defects were known. Test pits were used to assist in validating the results. The location of these roads is shown in figure 2.1 and detailed in table 2.1. The roads chosen were based on those where some small areas were thought to have problems due to water ingress in the pavement or subgrade soil layers. Thus the survey covered both wet and dry areas along the full length of the road surveyed, although the reason for the pavement and surfacing distress on these roads had never been determined and water was an 'educated guess'. This moisture detection survey would determine whether or not the surface and pavement distress was due to water. The sites surveyed in the Waikato were in addition to this research and were surveyed to assist the Transport Agency identify some broken culverts and wet areas in newly built state highways.

**Figure 2.1** Locations of each test areas in the North Island of New Zealand.



**Table 2.1** Locations of moisture detection survey.

Region	Road name	Road length	No. of lanes	Passes per lane	Length
		km	no	no	km
Porirua	Lyttleton Avenue	1	2	2	4
	Titahi Bay Road	3.4	3	1	10.2
	Prosser St	0.6	2	1	1.2

Region	Road name	Road length	No. of lanes	Passes per lane	Length
	Raiha St	1.9	2	1	3.8
					0
Kapiti	Ruapehu St	1.2	2	1	2.4
	Te Moana	4.6	2	1	9.2
	Kapiti Road	3.5	2	1	7
					0
Taranua	Carlson St	0.7	2	1	1.4
	Otanga Rd	3.9	2	1	7.8
	Rte 52	1.02	2	1	2.04
					0
Hawke's Bay	SH50	2.77	2	1	5.54
	SH2	3.25	2	1	6.5
					0
Taranaki	SH3 Egmont to Stratford	27	2	1	54
	SH3 Mount Messenger	5.4	2	1	10.8
					0
Whanganui	No. 3 line	2.6	2	1	5.2
	No. 2 line	6.1	2	1	12.2
	Kaimatira Rd	2.4	2	1	4.8
	London St	1.1	2	2	4.4
	Wicksteed St	0.2	2	1	0.4
	Glasgow St	1.5	2	2	6
	Springvale Rd	2	2	1	4
	Brunswick	5	2	1	10
	Heads Road	1.5	2	2	6

## 2.2 Survey methods

The survey methods used in the New Zealand field tests were selected to be fitted in an optimal way to the proactive pavement maintenance processes. Ideally, the techniques needed to:

- indicate the road sections where moisture content was increasing to the extent the pavement structure had become susceptible to failure and permanent deformation
- diagnose the reasons for the moisture
- develop a system to help maintenance crews locate the exact problem section and perform maintenance actions as needed.

The basic drainage condition analysis and moisture content survey methods used in the field tests in New Zealand were selected based on the literature review in appendix A and on the positive experiences in the EU ROADDEX project and later in the PEHKO project in Finland. The tested methods were (1) ground penetrating radar 400 MHz ground coupled antenna frequency analysis, (2) ground penetrating radar air

coupled horn antenna technique, (3) laser scanner (LIDAR) data analysis, (4) digital video analysis and (5) thermal camera analysis. The data collection and analysis software belong to the Road Doctor software family made by Roadscanners in Finland. Some of these methods were developed further within this project. The theory and basic principles of all techniques are set out in the literature review.

The following survey technique and laboratory tests were carried out in New Zealand.

### 2.2.1 Ground penetrating radar tests

GPR systems use discrete pulses of radar energy with a central frequency varying from 10MHz up to 2.5GHz to resolve the locations and dimensions of electrically distinctive layers and objects in materials. Pulse radar systems transmit short electromagnetic pulses into a medium and when the pulse reaches an electric interface in the medium, some of the energy will be reflected back while the rest will proceed forwards. The reflected energy is collected and displayed as a waveform showing amplitudes and time elapsed between wave transmission and reflection. When the measurements are repeated at hertz frequencies (currently up to 1000 scans/second) and the antenna is moving, a continuous profile is obtained across the target (Saarenketo 2006). In addition to pulse radar GPR systems stepped frequency radar systems are also entering the road survey markets.

The propagation and reflection of the radar pulses is controlled by the electrical properties of the materials, which comprise 1) magnetic susceptibility, ie magnetism of the material, 2) relative dielectric permittivity and 3) electrical conductivity. The magnetic susceptibility of a soil or road material is regarded as equal to the value of the vacuum, and thus does not normally affect the GPR pulse propagation. The most important electrical property affecting GPR survey results is dielectric permittivity and its effect on the GPR signal velocity in the material and, as such, it is very important to know precisely how to calculate the correct depth of the target (Saarenketo 2006).

GPR technique has been used since 1980s for measuring mainly thickness for different pavement structure layers but recently the technique has been increasingly used to survey material properties such as water content and moisture susceptibility. The literature review provides detailed information about the basic principles of the technique and how it can be used in monitoring the moisture content of road materials (appendix A, section A4.3.1).

### 2.2.2 Laboratory tests in Finland and New Zealand

GPR technique in measuring moisture content has been so far mainly related to air coupled antenna surface reflection technique, which provides information only from the basecourse surface (appendix B). However, in this project one of the goals was to test how the frequency analysis technique, which has given promising results in recent Roadscanners moisture monitoring projects, could be used to measure moisture content at different depths in the pavement structure in New Zealand roads.

The basic idea of the frequency analysis is the same as with acoustic waves. When 'knocking' wet material the sound reflected from the material is lower compared with knocking dry material. In this case the system uses electromagnetic waves and non-contact techniques which lead to much more complex problems with data collection and processing. That is why a GPR calibration study with different road materials was planned for this project.

The preliminary calibration study for road moisture analysis was performed both in Finland at the Roadscanners main office in Rovaniemi and later in New-Zealand in the Downer laboratory in Tauranga. The goal was to study in a controlled environment the GPR frequency response of the sub-unbound basecourse materials at different moisture content and before developing a correlation model that would allow a reliable estimation of high saturation degree in pavement structure in the field.

For the laboratory tests two test boxes with different sizes were built in Finland and three additional boxes in New-Zealand. The materials used in these tests were the following:

Finland boxes 1 and 2: gravel sand aggregate from Hietavaara, Finland.

New-Zealand box 1: Winstone aggregates GAP40.

New-Zealand box 2: Poplar Lane Quarry basecourse aggregate.

The tests were conducted using a GSSI SIR-30 GPR unit with an air coupled 2GHz horn antenna and a ground coupled 400MHz antenna. At the same time, for each GPR measurement, a percometer (a handled device to measure dielectric constant of soils and aggregates) was used to measure the relative dielectric permittivity ( $\epsilon_r$ ). The same testing methodology was applied to all boxes as follows:

- 1 Before starting GPR testing a sample for grading analysis and initial water content was taken to be analysed in the laboratory.
- 2 First GPR measurements were made with two different antennas and with the percometer surface probe and box weighed. Then two litres of water were added to the material surface.
- 3 After 1.5 hours the GPR and percometer measurements were repeated and box was weighed.
- 4 This process was repeated until water saturation was apparent.

**Figure 2.2 Performing 'box tests' in Downer laboratory in Auckland. In this case measurements are carried out using 400 MHz ground coupled antenna**



After measurements, the collected data was processed and a spectrum analysis was conducted to study the frequency response of the aggregate at different levels of saturation and in different depths from the surface to the bottom of the box. Analysing the signal spectrum, dominant frequency, power, bandwidth

and other spectral components of the collected signal allowed changes, which are not easily detectable in time domain waveforms, to be observed. For this, Road Doctor® 3 and MATLAB®, the two advanced software tools for signal analysis, were used.

Further analysis of the 'box tests' showed one basic problem with the box test design. The box where the material was compacted and tested was too small and reflections from the box walls were disturbing signal analysis. That is why the final model between the GPR frequency response and the saturation degree could not be made, and in future will require a small-scale road structure test to be undertaken.

However, a lot of valuable analysis could be made from the box test data and results were obtained leading to a confirmation of the correlation between volumetric water content or saturation degree, and the changes in frequency response. The results also indicated the possibilities and limits helping to define the best MDI procedure for moisture calculation of GPR data collected on roads, using Road Doctor® 3.

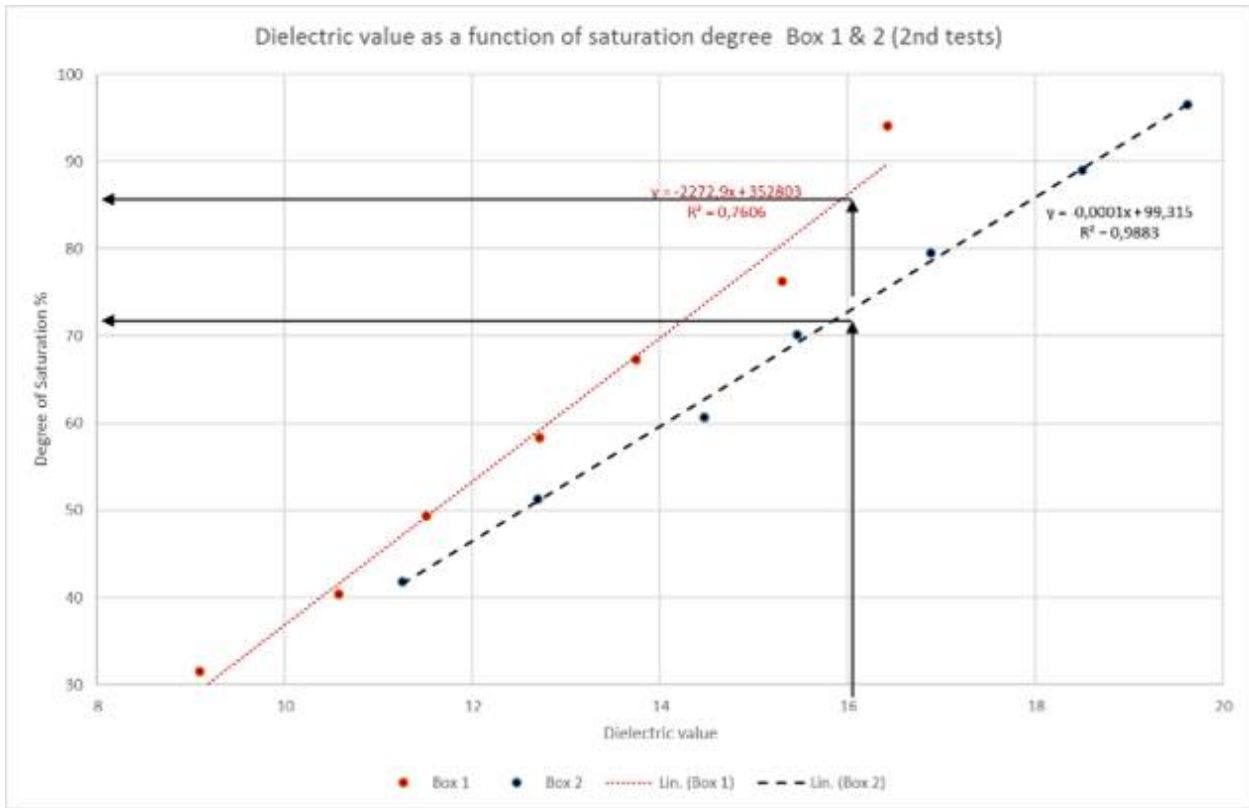
Figure 2.3 presents a good correlation between dielectric value  $\epsilon_r$  and the saturation degree of box 1 Winstone aggregate and box 2 Poplar Lane Quarry material from New Zealand calculated from the 2 GHz horn antenna propagation time between the surface and bottom of the box. Figure 2.3 confirms the critical dielectric value of 16, which several studies have reported to be limited to material susceptible to permanent deformations, matches well with the saturation degree of 70–80%. After that, air bubbles in the material start to be occluded increasing pore water pressure and weakening the material causing wheel track rutting and shear failure from heavy vehicles. At the same time the material becomes extremely susceptible to frost.

Figure 2.4 confirms that surface coupling of the ground coupled antenna is a function of saturation degree and dielectric value, and this knowledge can be used to measure moisture anomalies close to the pavement surface.

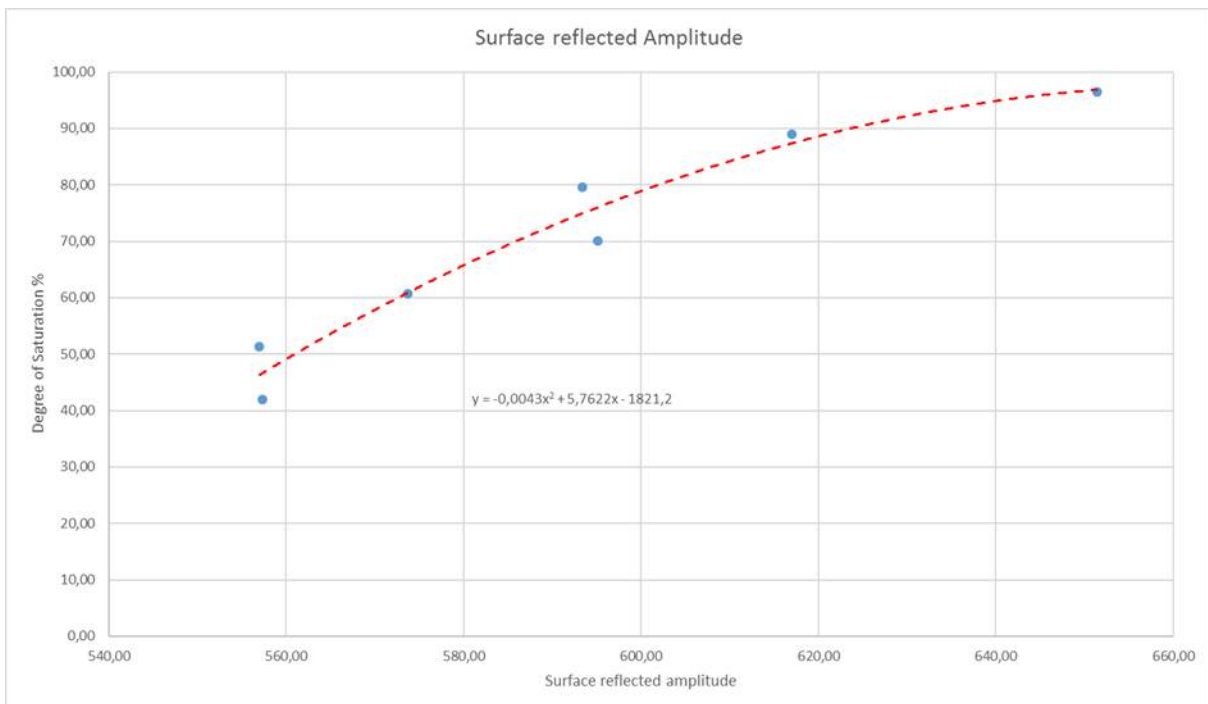
Figure 2.5 demonstrates the effect of an important feature that needs to be taken into account when making a model to calculate the MDI at a different depth in the pavement structure. This is signal attenuation as a function of saturation degree, which is calculated in this case from the test box bottom reflection.

Finally the correlation between frequency response and saturation degree of the basecourse materials is presented in figure 2.6. This verifies that frequency attenuation is partly material dependent and must be considered when calculating MDI in deeper pavement layers.

**Figure 2.3** Correlation between dielectric value  $\epsilon_r$  and the saturation degree of box 1 Winstone aggregate and box 2 Poplar Lane Quarry material from the 2 GHz horn antenna.

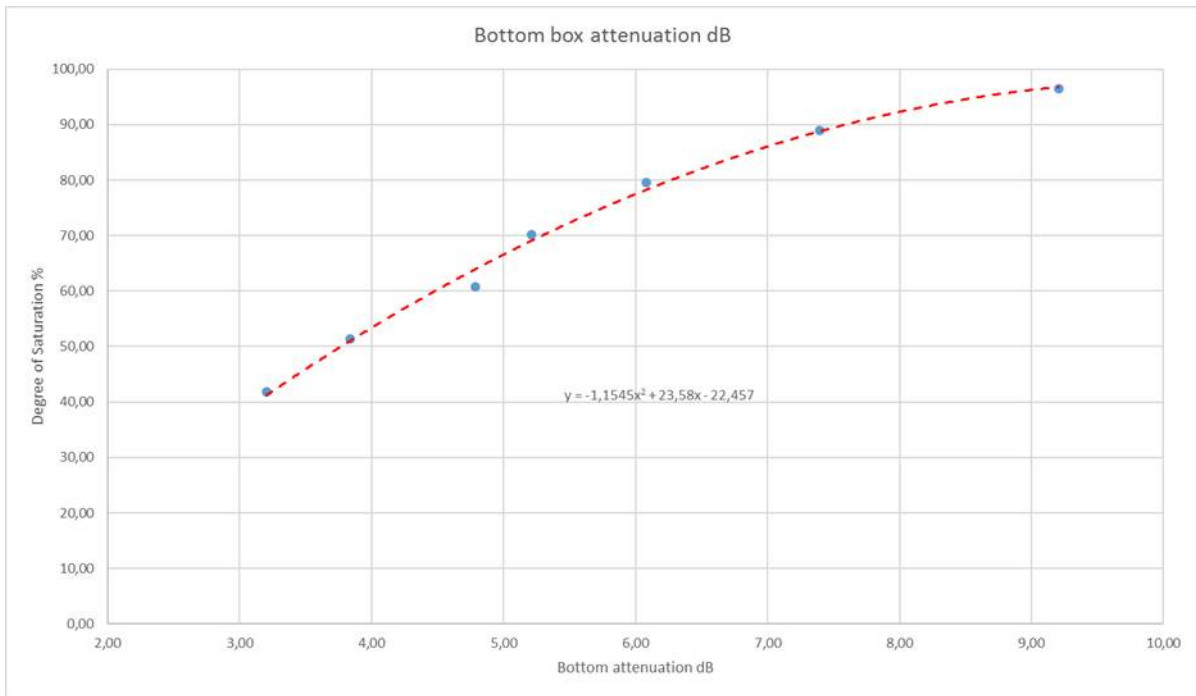


**Figure 2.4** Correlation between surface amplitude from 400 MHz antenna and saturation degree of Poplar Lane Quarry basecourse aggregate

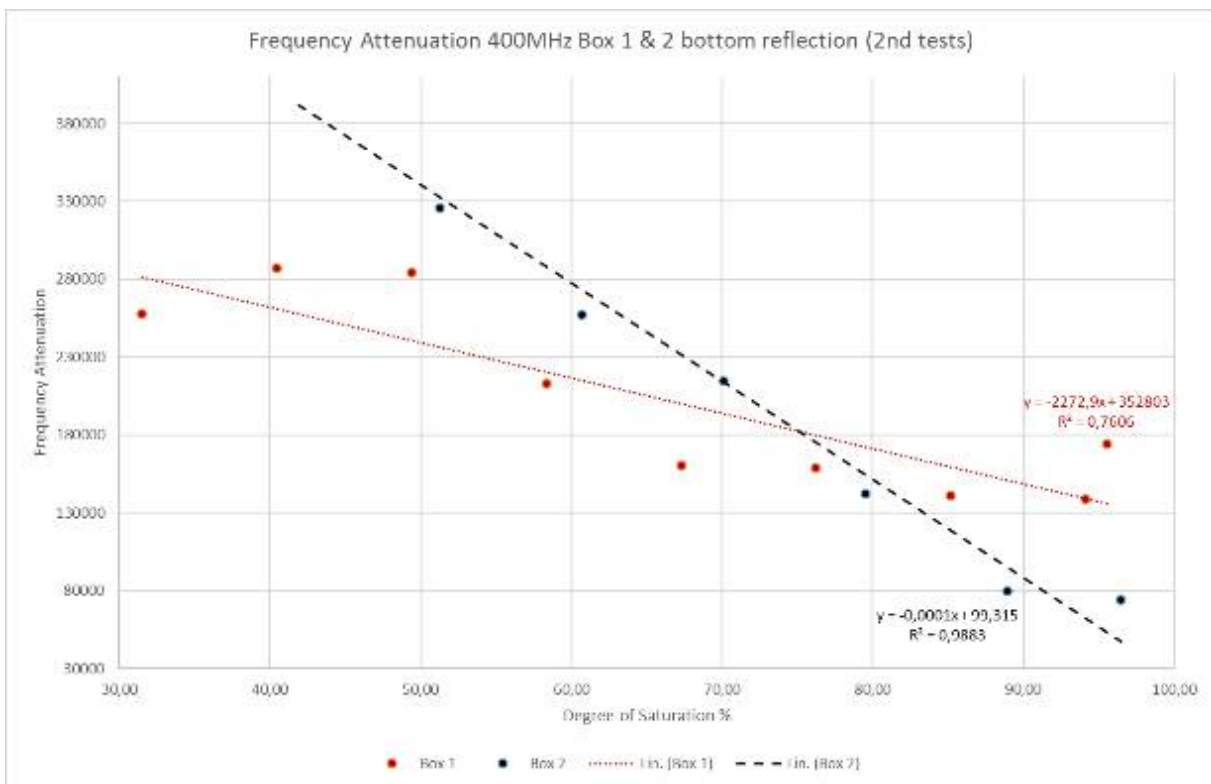




**Figure 2.5** Correlation between signal attenuation of 400 MHz antenna and saturation degree of Poplar Lane Quarry basecourse aggregate. Attenuation is calculated from the test box bottom reflection



**Figure 2.6** Correlation between frequency attenuation and saturation degree of Winstone aggregate (box 1) and Poplar Lane Quarry basecourse aggregate (box 2)



### 2.2.3 Moisture damage index calculation

For the final analysis the MDI was calculated from 400MHz antenna data (ground coupled antenna). This is because, based on the calibration measurements, the 400MHz antenna data was found to be the best suitable for use with frequency analysis. This data includes information from the lower frequencies, which will dominate if moisture and/or highly dispersive materials are present. The MDI was also developed because there was a need to develop an index that describes moisture content and moisture sensitivity of the material between certain depths and not at a single depth level, which is normally done in GPR analysis. The given MDI is a relative value, because actual in-situ calibration measurements could not be used.

The frequency response was calculated at 0–350 MHz interval. The response was an average of 2m long sections which included about 20 scans each. Before the calculation, only the constant background was removed from data. This was used to correct the direct current (DC) level and subtract the direct antenna coupling interferences from the data. The upper part of the data was divided into three 4-nano-second (ns) time intervals: 0–4ns, 4–8ns and 8–12ns. These corresponded to depths of 0–23cm, 23–45cm and 45–70cm, assuming average dielectric value of 7. In places where there were drainage problems and the dielectric value was much higher, these depth intervals were smaller.

The averaged amplitude at the given frequency window was calculated in all three time windows. All the amplitudes were normalised to the amplitude in the first time window. Average normalising factors were calculated from 18 GPR profiles representing all New Zealand test roads. This normalising factor was used to compensate the signal attenuation. The method was based on the assumption that in a very large dataset the frequency content at low frequency window, should be approximately the same in all three time windows. After the multiplications, most of the values were varying between 10 (very dry) and 120 (saturated).

The MDI for the whole pavement structure including subgrade to a depth of 700mm was calculated using a weighted average of all three values of MDI at top, middle and bottom depths. This formula shown below places more weighting on the MDI in the top layer as it is considered the high water content in this layer is the most critical parameter leading to permanent deformations:

$$MDI_{TOTAL} = 0.5MDI_{TOP} + 0.3MDI_{MIDDLE} + 0.2MDI_{BOTTOM} \quad (\text{Equation 2.1})$$

It was found this MDITOTAL calculation above was useful at a network level to generate maps showing sections of road with the highest moisture. However, at a project level it was beneficial to look at the MDI values at all three different depths individually to identify the location of the moisture for determining the best drainage treatment.

### 2.2.4 Field data collection and basic processing

The data collection in New Zealand started in early October 2015 with setting up Roadscanners ground penetrating equipment, GPS, video and laser scanner to a Downer vehicle (figure 2.7). The GPR unit was GSSI SIR-30 equipped with 2 GHz air coupled and 400 MHz ground coupled antenna mounted in the rear. The GPR data was collected with 10 scans per metre and 1,024 samples per scan. The air coupled antenna had 25ns time window, while the ground coupled was set to use 100ns time window. The video was in the front of the van collecting the data from the road surface and surroundings. The laser scanner was in the rear of the vehicle, elevated to 3m in height to be able to scan the road surface as well as the surroundings (ditches and side slopes).

Weather conditions varied from cloudy to sunny and from half cloudy to light rain. One day the surveys were paused in the middle of the day because of heavy rain. The weather was mostly half cloudy interspersed with bright sunshine. This created some challenges for video image quality especially in small curvy roads where

the surveyed route would wind from plain fields to dark forest with heavy canopy and back to bright sunlight. The surveys took several days but proceeded smoothly within the planned schedule.

The data was processed according to normal routines including editing length if necessary and reversing files to present both lanes in same direction. The air coupled data was pre-processed to calculate the height correction and surface reflection with a metal pulse. For interpretation purposes the data was processed with basic vertical and horizontal filtering.

The laser scanner data was processed through normal routines to create point clouds and rut maps. GPS coordinates were filtered to erase irrational points.

**Figure 2.7** The survey van equipped with video camera (top front), laser scanner (high up), GPR ground coupled antenna (red box with wheels, elevated) and air coupled antenna (orange box far rear)



### 2.2.5 Air coupled horn antenna data analysis

One of the project's tasks was to measure pavement thickness in the selected test roads and determine what kind of moisture information could be collected from the air coupled horn antenna data. Pavement thickness was interpreted from 2 GHz air coupled horn antenna data using the Road Doctor software GPR module. This work was challenging in some test sections as the pavement thickness was very thin. However, with 2 GHz horn antenna and Road Doctor software it should normally be possible to detect pavements as thin as 25–30 mm (figure 2.8).

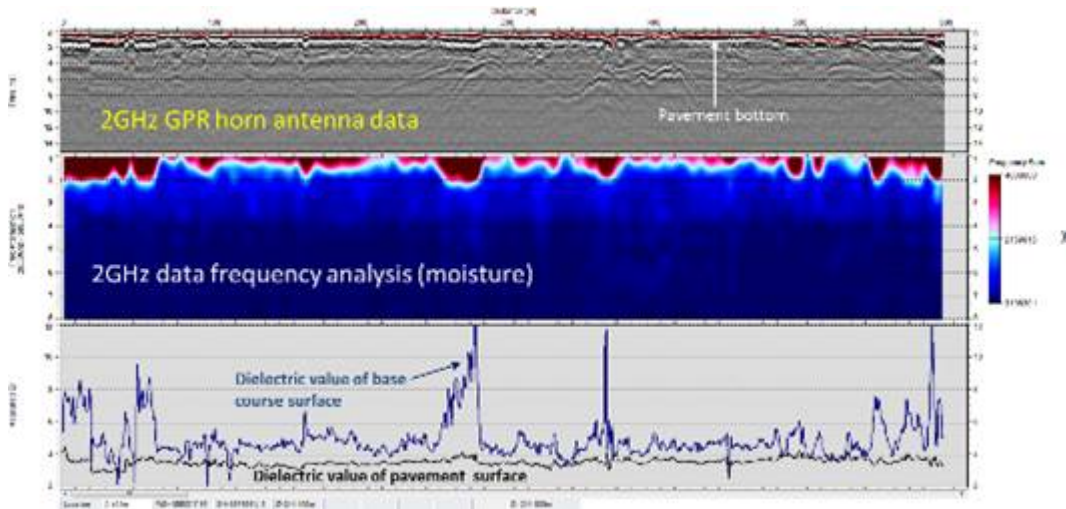
The 2 GHz horn antenna test methods were frequency component analysis and surface reflection technique and results of these analyses can be seen in figure 2.8. This shows that both techniques present moisture anomalies in exactly same places even though they were calculated using two independent methods. This, however, was not the case everywhere as the frequency component moisture analysis was found to be more reliable than the surface reflection technique. The problem with the latter is high signal attenuation with 2 GHz GPR data and thus moisture information can be collected only from the top part of the pavement structure.

In addition, horn antenna elevation information could be used to describe the roughness of the road. This was done by measuring the distance from the horn antenna to the pavement surface, which varied greatly on rough pavement surfaces (figure 2.9).

The surface reflection analysis of the 2 GHz air coupled antenna data revealed an interesting finding for the pavement materials used in New Zealand. On special road sections the dielectric value calculated from

the pavement surface was unrealistically high, approximately at the level of 40 (figure 2.10). The explanation was that in these sections the surface treatment material was steel slag made from a steel mill that uses magnetite beach sands in its process. Magnetite in steel slag increases magnetic permeability of the material and this has a great effect on GPR signal behaviour. After 2,250m, when the steel slag section ends the dielectric values drop back to a normal level. This finding is quite unique and in the literature magnetite susceptibility has been reported to affect the GPR road survey results only in Mexico (Saarenketo 2006).

**Figure 2.8 Example of 2 GHz horn antenna data analysis**



The top field in figure 2.8 presents processed 2 GHz data with thickness interpretation (red line). The middle field presents frequency analysis data where the red colour presents high moisture content and the bottom field presents dielectric values from the pavement surface (black) and basecourse surface (blue) calculated using the surface reflection technique.

Extra information that can be collected from air coupled horn antenna data is antenna elevation measurement for roughness detection, a parameter that has been also called the 'poor man's international roughness index'. Figure 2.9 describes the basic principle of the measurement technique and results of this data can be seen in different figures in this report.

**Figure 2.9** Antenna elevation analysis for roughness surveys (exact distance from antenna to pavement surface is measured continuously)



**Figure 2.10** Example of steel slag made from magnetite sand on dielectric value of pavement surface on SH3 Mount Messenger

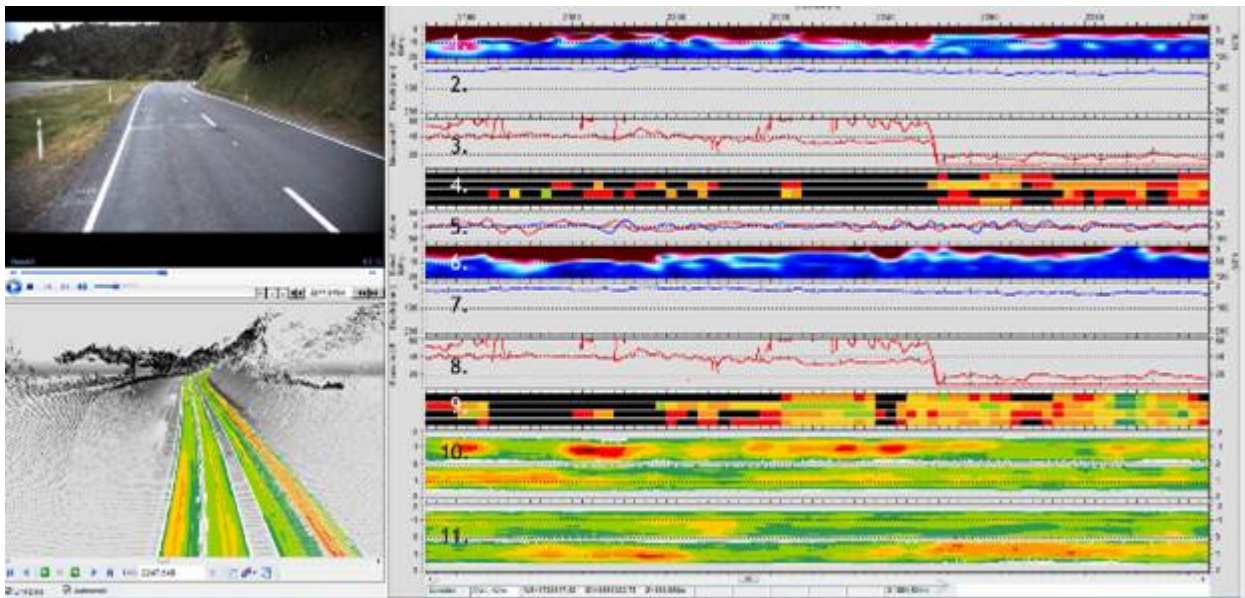


Figure 2.10 shows fields 1 and 6 present 400MHz GPR moisture profiles (left and right lanes), fields 2 and 7 present bituminous pavement thickness and fields 3 and 4 present dielectric values from pavement surface (lower line) and basecourse surface (higher line). Fields 4 and 9 present MDI data. Field 5 presents antenna elevation data and fields 10 and 11 present rut depth maps from left and right lanes.

### 2.2.6 Repeatability tests

Moisture monitoring survey repeatability was tested in Route 52 test site where the same section was surveyed two times roughly at two-hour intervals. Both data sets were analysed the same way and the results in figure 2.11 and 2.12 show a very good repeatability with these two surveys.



Figure 2.11 Repeatability test results from Route 52. (The top 5 windows present moisture monitoring results from survey 1 and bottom 5 windows from survey 2. The bottom window present roughness (antenna elevations) results from two runs (blue= survey 1 and red=survey2))

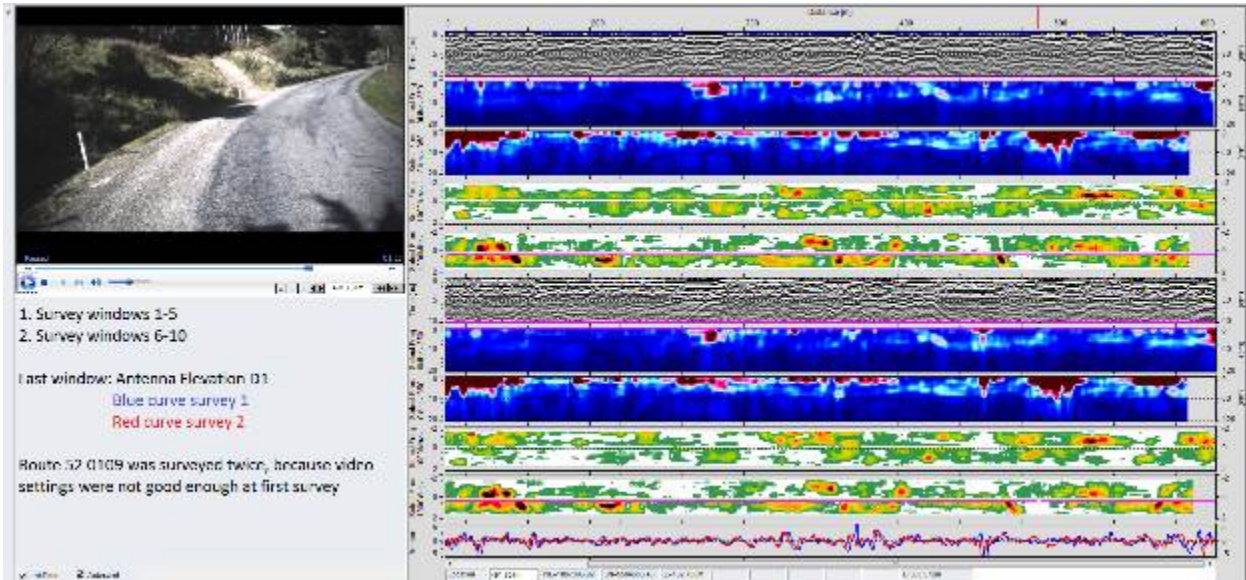
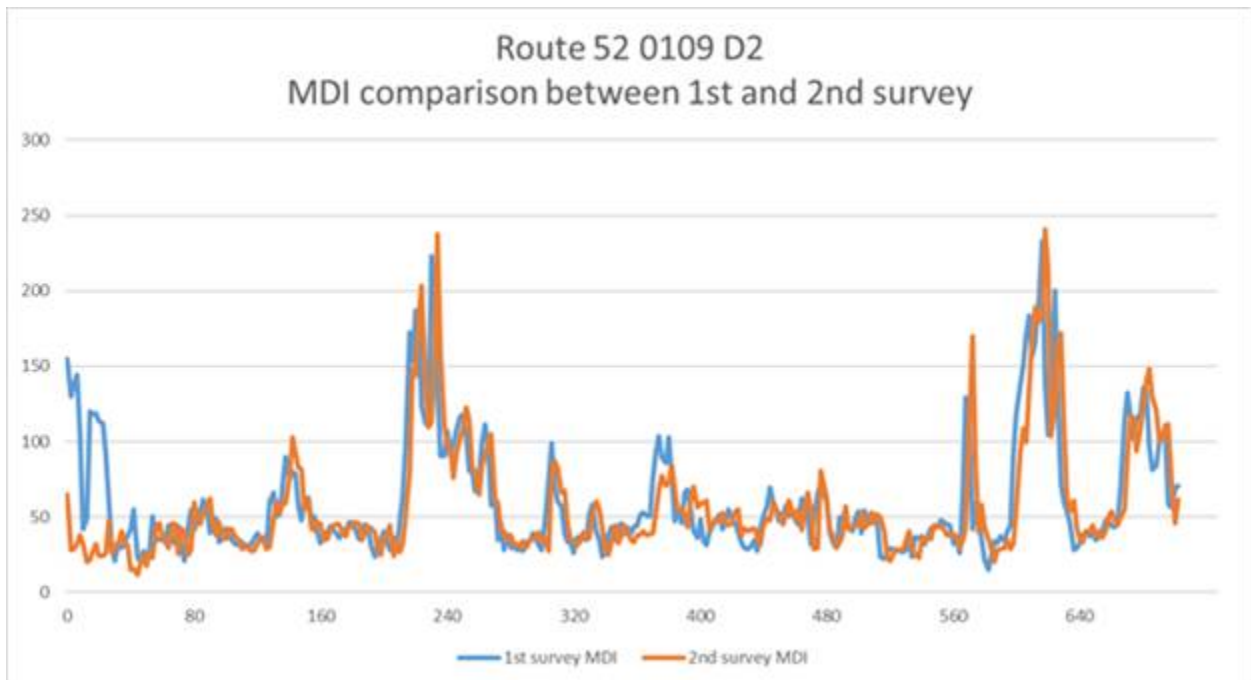


Figure 2.12 MDI repeatability test results from Route 52, direction 2

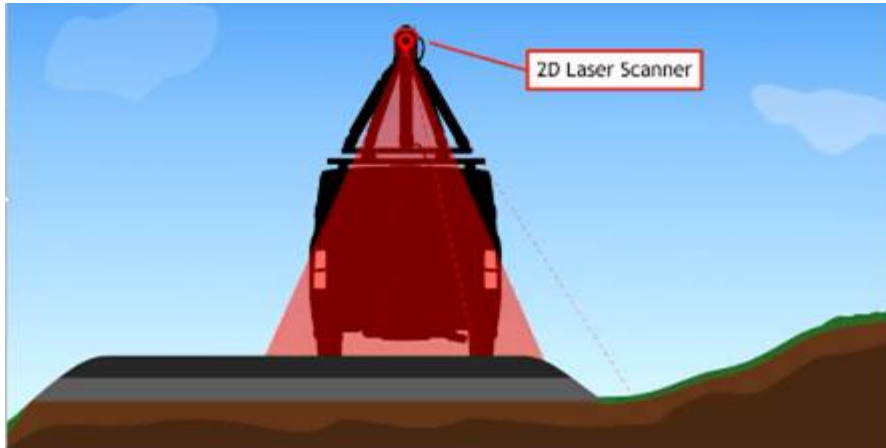


## 2.3 Laser scanner data analysis

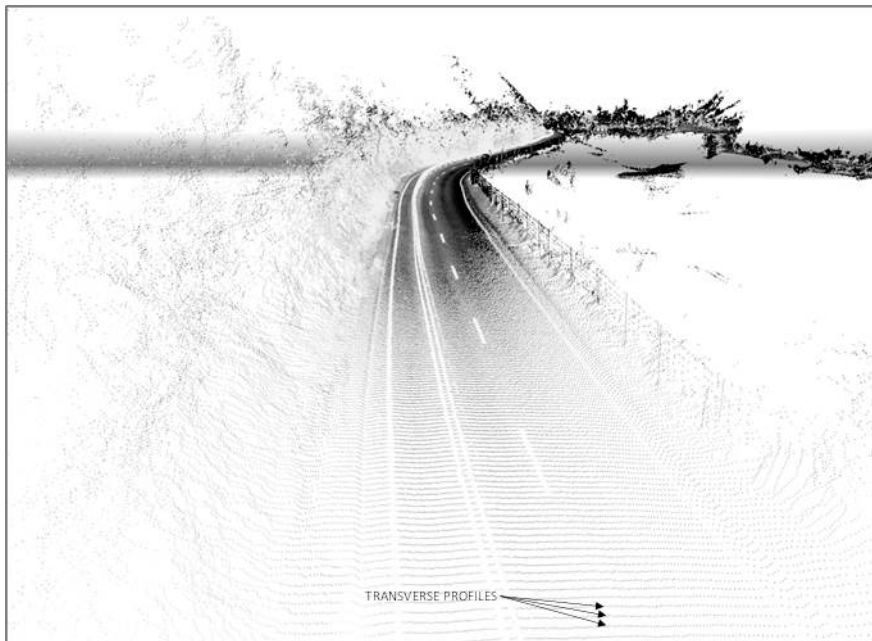
A laser scanner was used to measure information about road surroundings and the shape of the road surface (figure 2.13). The laser scanner used in this survey measured 50m wide transverse profiles approximately every 10cm. Since laser scanners measure 100 scans/second and the interval of transverse profiles depends on survey speed, normally a cross section is collected at 0.05–0.1m intervals. These

cross-section profiles can then be used to create point clouds presented in figure 2.14. Different kinds of road properties and damage indicators can be calculated from the point cloud data. In this project, focus was on analysing deformations (rutting) in the road surface, as shown in figure 2.15.

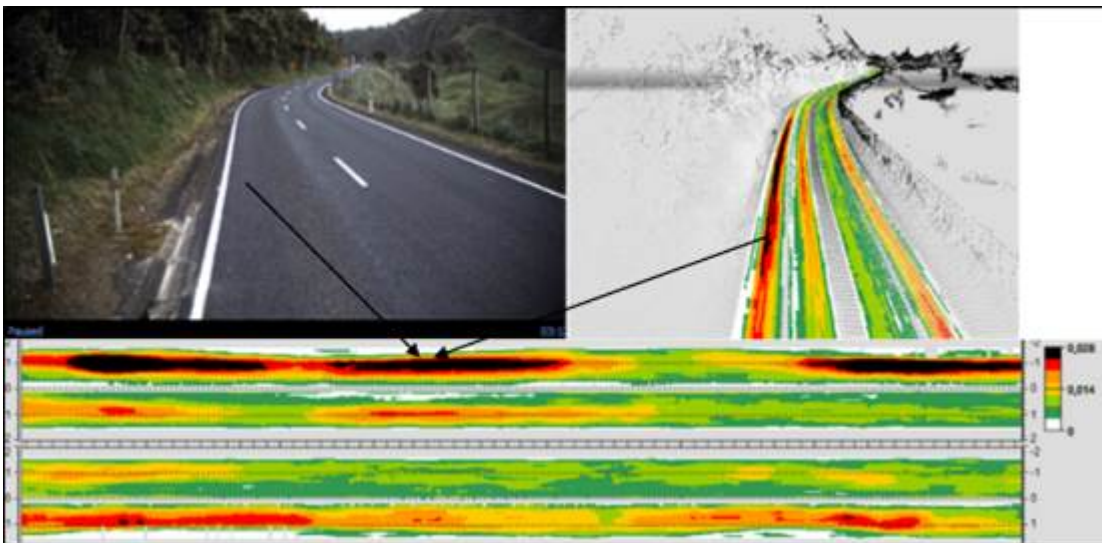
**Figure 2.13 Basic principle of laser scanner data collection from the road surface and its surroundings**



**Figure 2.14 Pointcloud created from scanned transverse profiles. White stripes in the lane centre are caused by the air coupled horn antenna support rods (see figure 3.12)**



**Figure 2.15 Rutting information calculated from the laser scanner data and presented in the form of point cloud video and rut depth map**



## 2.4 Tests with thermal cameras

As a part of this moisture research project, a thermal camera was tested to see if it could be used for detecting cracks on pavements. These tests were made on four streets in the Porirua area. Surveys were planned to take place at night to avoid direct sun and shadows. The theory behind the method is that the sun will heat the road surface during the day and after sun goes down, areas with higher moisture content cool down slower than drier areas. This phenomenon was seen very clearly in the tests done in Finland.

A thermal camera was mounted on Downer's survey van using a similar clamp as for the video camera (figure 2.16). There was no video camera while capturing infrared data because it was night time.

Collected infrared data was analysed and linked to the Road Doctor software for further analysis. The thermal camera survey could not detect wet areas on the roads surveyed. Most likely the difference in temperature between day and night was not great enough to get similar results as those seen in Finland. Error sources like shadows from the trees and parked cars can be seen even hours after the sun has gone down (figure 2.17).

**Figure 2.16 Installation of thermal camera in the survey vehicle**





**Figure 2.17** Thermal camera data from Lyttleton Avenue (D1, L2). Cool anomalous areas, compared with the surroundings, are caused by car parked during the day



## 2.5 Presentation of results

The collected survey data was processed and analysed using the Road Doctor™ software package. The software presents all the data synchronised by distance or by coordinates. After this is done the selected analysed data can be viewed on a single page view which can include video and LIDAR laser survey views. Figure 2.18 presents an example of the basic moisture analysis view used in the integrated moisture analysis. Each data set displayed in figure 2.18 is explained in detail in table 2.1.

For viewing moisture analysis data on a computer, it is possible to download the free Road Doctor viewer from the Roadscanners' web page ([www.roadscanners.com](http://www.roadscanners.com)). The Road Doctor viewer can be used for viewing all the data together with video and LIDAR. The user can change colours, adjust horizontal and vertical axes and rotate the point cloud. Data from the project tree can also be viewed.

**Figure 2.18** Basic Road Doctor software view used in moisture analysis

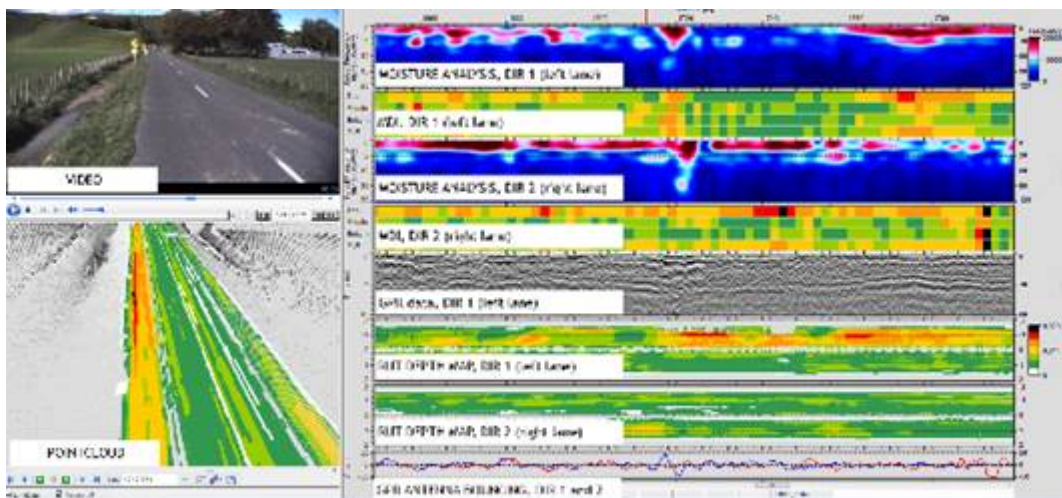
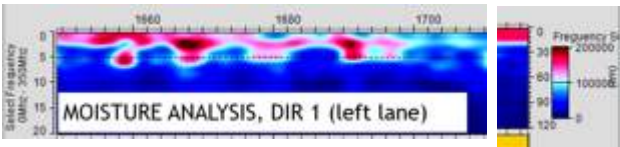

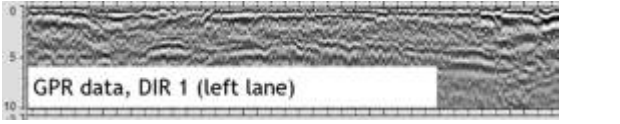



Table 2.2 Data display explanation

Data display item in figure 2.18	Explanation
 <p>MOISTURE ANALYSIS, DIR 1 (left lane)</p>	<p>The top numbers refer to the chainage position along the road.</p> <p>The vertical numbers on the left-hand side (LHS) are nanoseconds of reflection time used to calculate depth as shown on the vertical scale on the right-hand side (RHS) (note 5ns on the LHS vertical scale are shown as 30cm depth on the RHS vertical scale).</p> <p>The colours shown represent dielectric values where red and black colours are the highest values with the highest amount of moisture.</p> <p>DIR 1 (left lane) is the direction of the video picture on the LHS in the increasing chainage direction.</p> <p>DIR 2 (right lane) is in the opposite direction to DIR 1 and is in the decreasing chainage direction or in the direction coming towards us in the video picture.</p>
 <p>MDI, DIR 1 (left lane)</p>	<p>MDI is a unitless relative measure of a combination of saturation level and the materials sensitivity to moisture (eg clay content). If black, then this is the highest MDI of &gt;120 and is generally the only area considered to be wet and of concern. Red is the next highest MDI value from 80 to 120. The other colours are lower levels of MDI and are considered dry.</p> <p>Top is MDI from 0 to 230mm depth from the surface.                  Middle is MDI from 230 to 450mm depth from the surface.                  Bottom is MDI from 450 to 700mm depth from the surface.</p> <p>MDI is the weighted average MDI given by the following formula:</p> $MDI_{TOTAL} = 0.5MDI_{TOP} + 0.3MDI_{MIDDLE} + 0.2MDI_{BOTTOM}$
 <p>GPR data, DIR 1 (left lane)</p>	<p>GPR data shows reflections of the various layers in the pavement and subgrade and the horizontal shaded lines are used to estimate pavement depth. The raw data is shown here and on the vertical scale 5ns are 300mm depth. This raw data allows the user to get an estimate of pavement depth rather than rely on an experienced GPR person to trace the lines to estimate pavement depth. Where the horizontal shaded lines look disrupted as shown on the RHS of the GPR portion of data in this table then this could be a culvert or a pavement patch repair.</p>
 <p>RUT DEPTH MAP, DIR 1 (left lane)</p>	<p>This rut depth map is a view of one side of the road showing where all the surface depressions or ruts are as determined from the laser Lidar point cloud data. The colours represent depression depth ranges which can be set by the user where the colours in order of rut severity are: dark green (nil rutting); light green, yellow, orange, red and black (rutting &gt;26mm). The rutting contour maps are used in conjunction with MDI data as areas showing high depressions and ruts with high MDI readings are considered the worst areas needing treatment first.</p>

## 3 Research results

The collected moisture monitoring survey data was first analysed in several ways and the most promising techniques were selected for the future analysis. That is why thermal camera analysis, for instance, was not continued. Examples of the key findings are presented below.

### 3.1 Moisture damage index analysis results

Because the MDI calibration was made based on the statistical distribution analysis of the survey data it was possible only to draw conclusions from aerial differences from the test areas. A summary of the MDI analysis is presented in table 3.1. This shows the highest amount of potential moisture problems could be found in SH3 Mt Messenger with 63% of the road length having high moisture in the top pavement layers. On a national level this would indicate that drainage funds should be directed to Mt Messenger. However, if drainage funds were limited then the MDI scale for Mt Messenger would need to be adjusted to show the wettest of the wet areas being the worst 10%, for example, to prioritise the spend on drainage improvement.

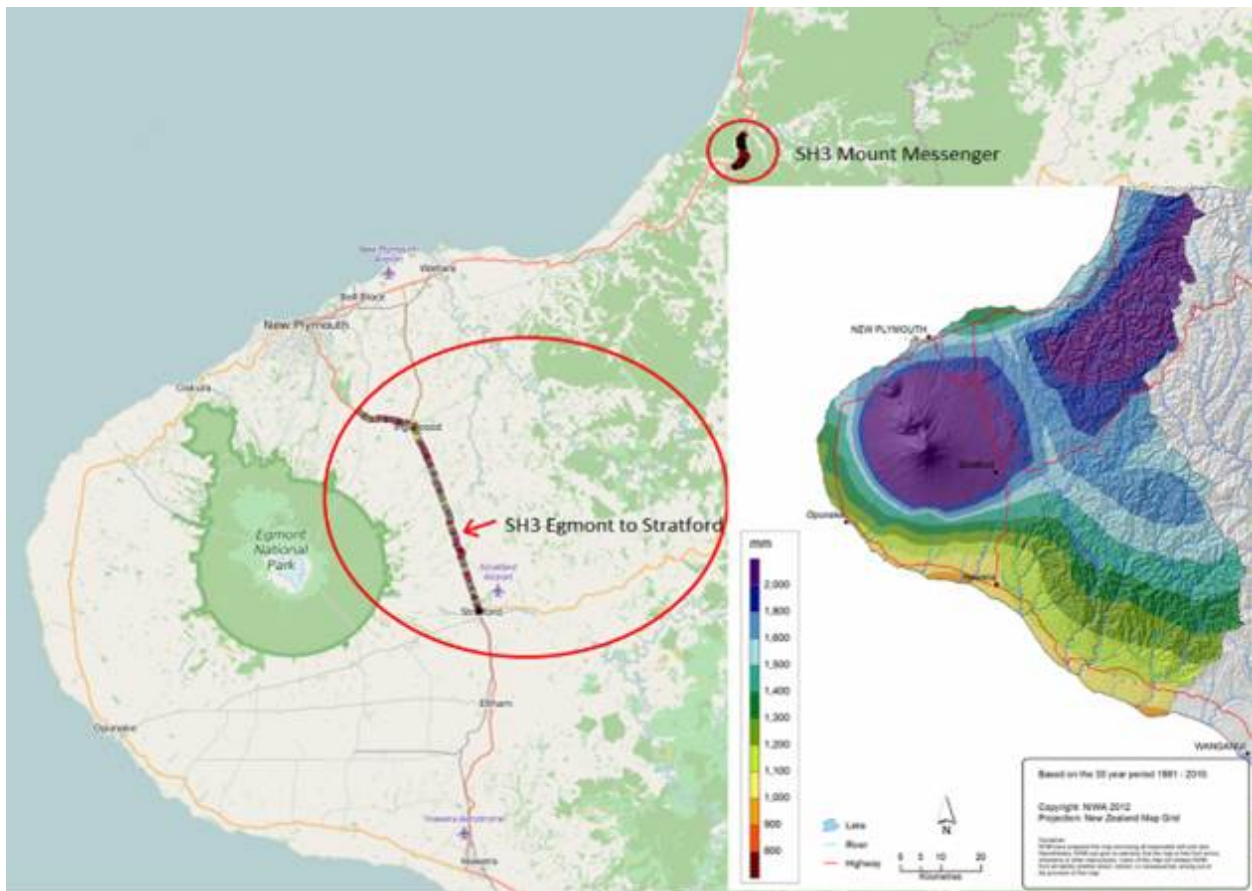
**Table 3.1 The relative amount of moisture problem sections (MDI > 80 and MDI > 120) in test roads in New Zealand**

Road	% of road with MDI top > 80	% of road with MDI top > 120	% of road with weighted average MDI > 80 (includes subgrade)	% of road with weighted average MDI > 120 (includes subgrade)
Brunswick	19	5.0	12	2.1
Carlson St	18	2.5	6.5	0.0
Glasgow St	37	12	24	5.4
Heads Road	62	26	39	6.4
Kaimatira	8.4	3.0	4.4	0.2
Kapiti Road	59	27	31	3.7
London St	47	15	26	3.5
London St part 2	61	26	36	5.9
Lyttelton Avenue	46	11	20	2.3
No. 2 line	15	3.5	16	2.0
No. 3 line	55	16	30	2.4
Otanga Rd	19	6.0	7.0	1.8
Prosser St	6.0	0.3	0.9	0.2
Raiha St	11	1.1	5	0.0
Route 52 0063	34	12	32	6.2
Route 52 0109	18	11	12	4.1
Ruapehu St	67	34	38	4.6
SH2 0678 (6.6–7.5km)	2	0.0	5	0.0
SH2 0678 (9.9–10.2km)	11	0.3	6	0.3
SH2 0691	12	1.0	28	3.0

Road	% of road with MDI top > 80	% of road with MDI top > 120	% of road with weighted average MDI > 80 (includes subgrade)	% of road with weighted average MDI > 120 (includes subgrade)
SH2 0707	2.7	0.8	1.6	0.0
SH2 0743 (0.3–0.5km)	0.5	0.0	1.0	0.0
SH2 0743 (6.0–6.7km)	4.2	0.0	1.7	0.0
SH3 Egmont to Stratford	35	9.8	44	11
SH3 Mount Messenger	81	63	81	55
SH50 0033	34	17	26	8.9
SH50 0049 (10.3–10.58km)	20	8.7	11	4.8
SH50 0049 (4.15–4.6km)	19	5.7	14	2.5
SH50 0079	24	8.5	15	1.2
Springvale Rd	12	3.4	6	0.2
Te Moana	28	6.9	13	1.0
Titahi Bay Road	19	1.5	5.1	0.0
Wicksteed St	14	5.7	10	1.4

An excellent example of the differences from the MDI analysis is the moisture monitoring results of two SH3 road sections in Taranaki area. According to MDI results the moisture content was by far the highest in these roads compared with other test roads. The reason for this can be explained by much higher precipitation in this area compared with other areas, combined with volcanic ash and mudstone absorbing high amounts of water. Annual rainfall in this area can be as high as 2,000mm (figure 3.1).

**Figure 3.1** MDI results from two road sections in SH3 in Taranaki area and annual rainfall map from the same area (courtesy of NIWA)



## 3.2 Integrated moisture diagnosis

Integrated moisture diagnostics (figure 3.2) provided many interesting cases of different types of moisture and drainage-related problems in New Zealand roads.

Figure 3.2 presents a case of a drainage problem on a road located on a side sloping ground. A culvert has most likely been clogged on the embankment side, which has become saturated with water. This has led to a small shear failure than can be seen between 120 and 160m.



Figure 3.2 Example of a moisture problem diagnostics from Route 52 010

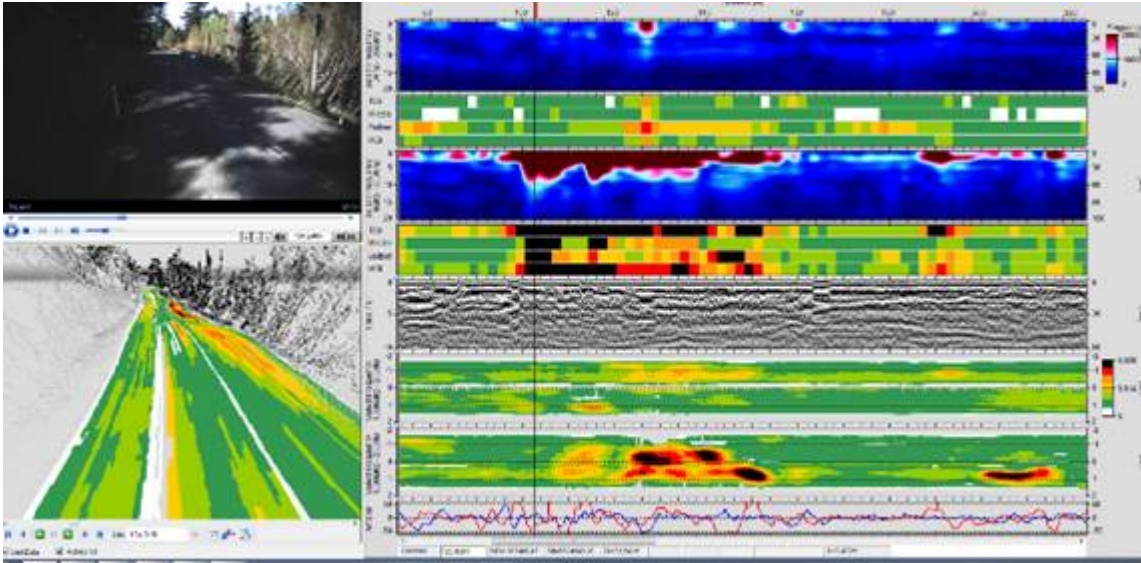


Figure 3.3 presents a possible moisture trap/sandwich structure related problem from no. 2 line. Moisture problems are related to the 'middle' area and results of these problems can be seen as severe shoulder deformation on the road pavement. The sandwich structure refers to a granular overlay on top of an old seal layer, which is assumed to have occurred based on anecdotal data traced by the layer profiles in the GPR (figure 3.3).

Figure 3.3 Example of a moisture trap and sandwich structure related problem

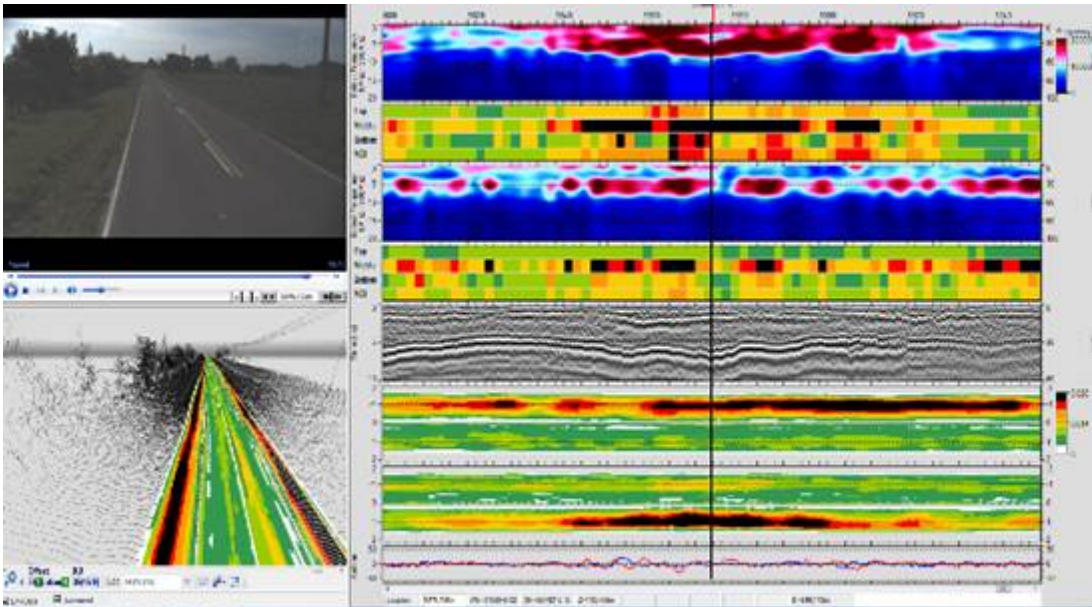
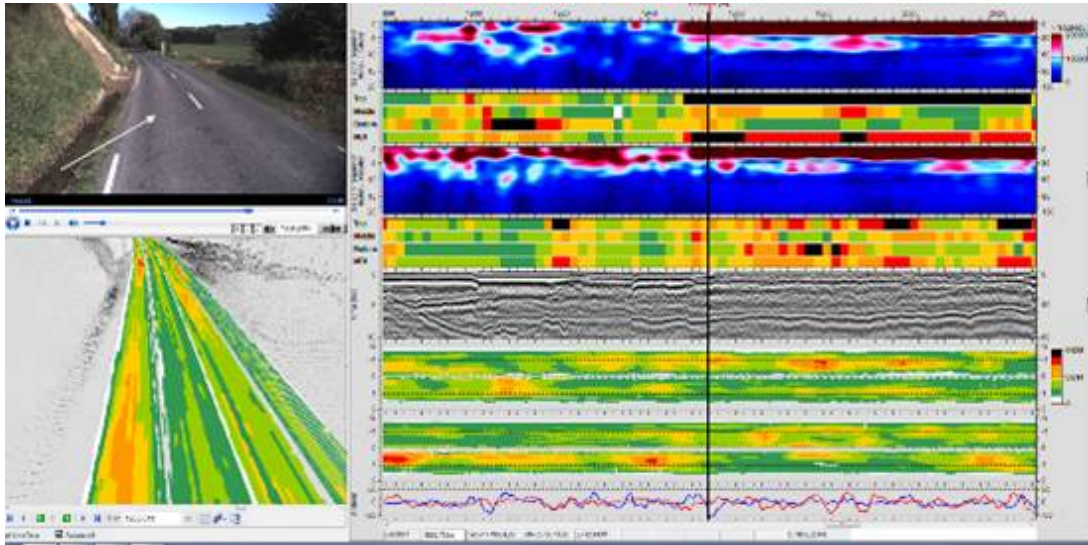


Figure 3.4 presents a typical problem where a slip has blocked the ditch and stopped water flow resulting in water ponding that infiltrates into the pavement structure. This occurred on road no. 3 in the Whanganui area.

**Figure 3.4** Example of a moisture problem caused by an unstable road cut slope that is blocking water flow in the ditch



Finally, figure 3.5 presents an example of a good quality road section in Kaimatira. No high saturation levels could be detected and the road surface is good with no deformations or roughness problems.

**Figure 3.5** Example of a good quality road section with no moisture- related problems (blue areas indicate dry and the LIDAR point cloud is mostly green indicating nil rutting)

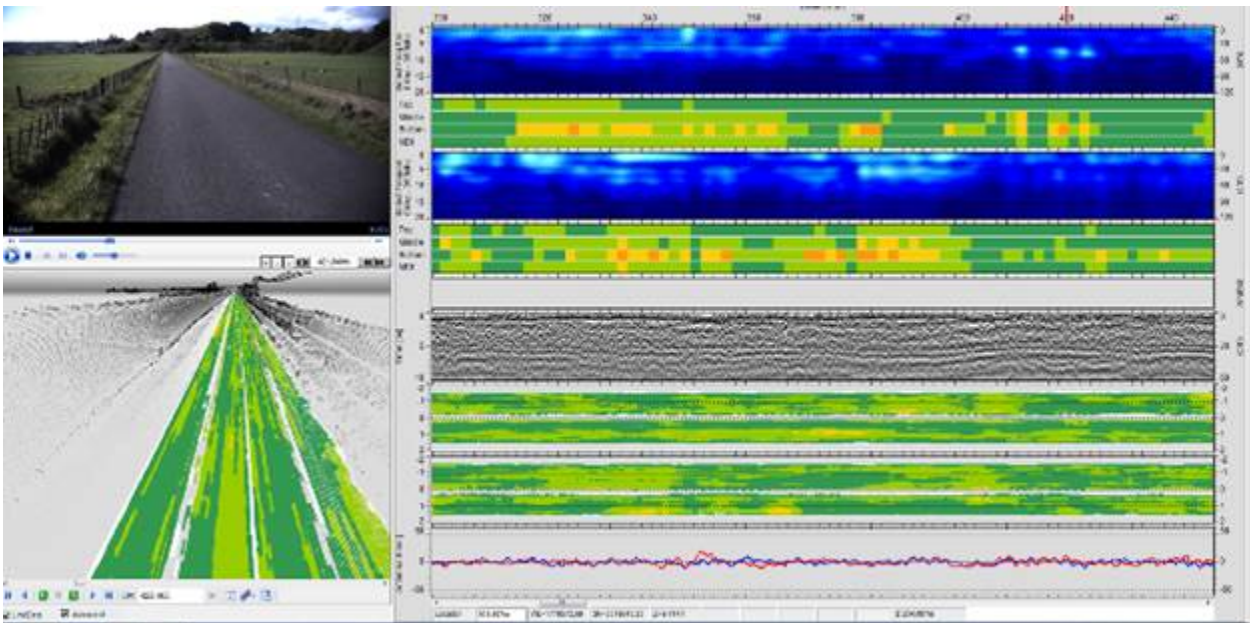
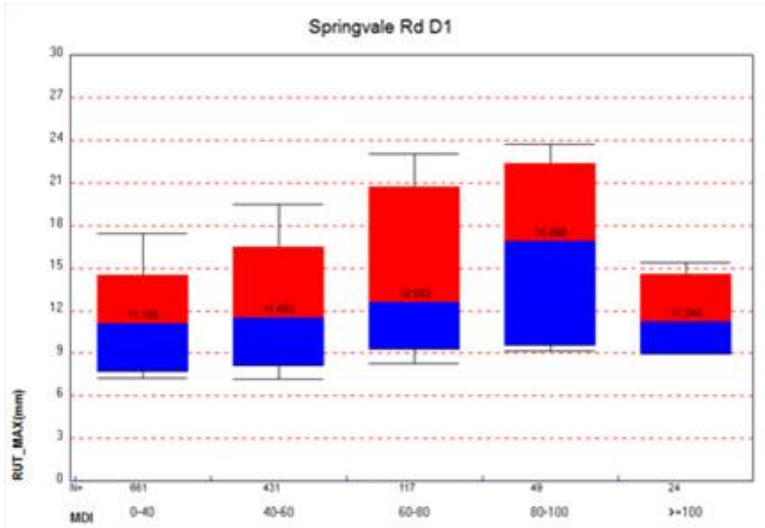


Figure 3.6 presents results of statistical distribution analysis between MDI values and rut depths from Springvale Road, direction 1. Classes in x-axis in figure 3.6 present different MDI values and their numbers at each class. Y-axis presents rut depth distributions at each MDI class. Numbers printed in the middle are median and the coloured area presents 90% of the values and black line 95% of the values. This graph shows that median values with MDI values 0–40 and 40–60 are on the same level but rut depths start to increase when MDI values are higher than 60. And when MDI values are higher than 80 the median rut depths are 50% higher compared with sections where road structures are dry. However, when MDI values are higher than 100 the rut depths are again smaller. This can be explained by the fact these



sections have been already repaired and can have stronger structures. For this reason direct analysis of the correlation between moisture content and deformations (rut depths) cannot be always done.

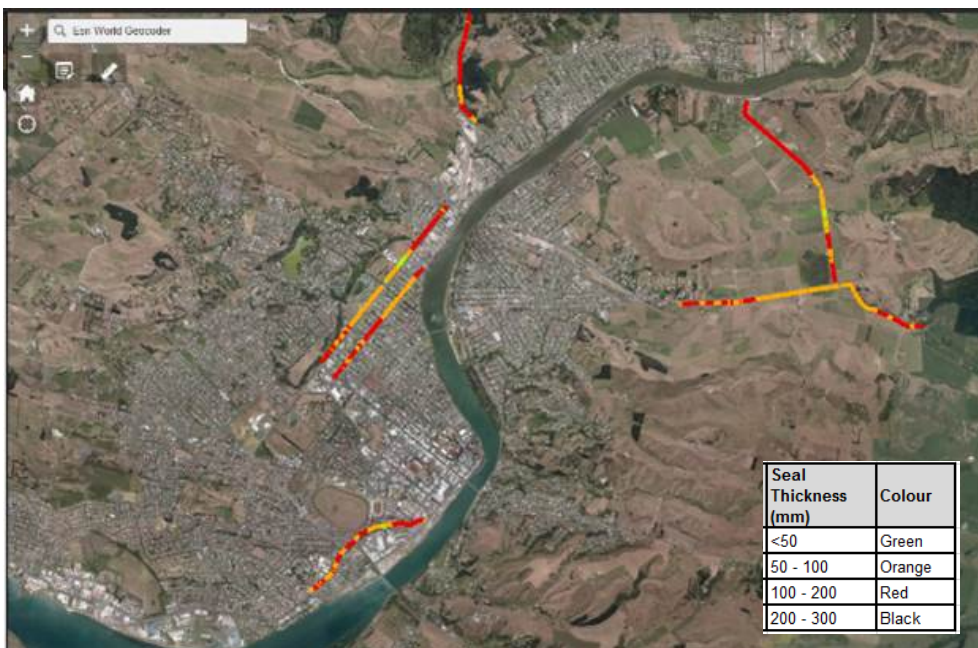
**Figure 3.6 Statistical analysis of the distribution between rut depths and MDI from Springvale road, direction 1**



### 3.3 GPR horn antenna data analysis

The thickness of the bituminous layers was analysed from the GPR horn antenna data. The results showed that in general bituminous layers are very thin but each road had sections with thicker bituminous pavement (generally always multiple chipseal layers). Figure 3.7 presents an example of a GIS map made from the bituminous layer (ie chipseal layers) thickness data.

**Figure 3.7 Colour coding roads in ESRI GIS showing different thicknesses of chipseal or asphalt surfacings in Whanganui area**

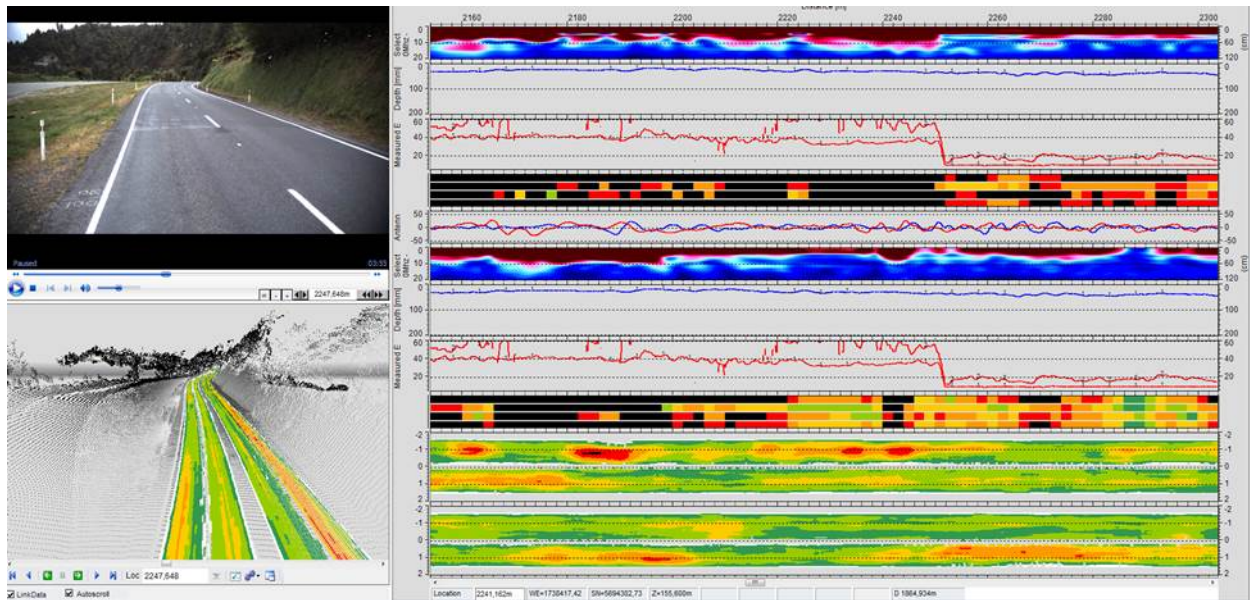




Detailed GPR horn antenna analysis showed also that surface reflection technique could not be used everywhere to provide reliable results from the moisture content of the basecourse surface. There were several reasons for this. First, in a few cases the use of steel slag in the surface layer for improved skid resistance disrupted the dielectric analysis and results were unrealistically high (figure 3.8). Second, cement stabilisation in the basecourse also increased dielectric values and in certain cases the higher basecourse surface dielectric values were due to cement stabilisation or due to high moisture content in basecourse surface. The third reason for unreliable surface reflection results in some road sections was an unclear GPR reflection interface between bituminous pavement and basecourse. This is a well-known problem everywhere the dielectric constant technique is used.

The moisture content in terms of a MDI at three different depths (top, middle and bottom) for the New Zealand trial was calculated from analysis of the ground coupled GPR reflections as this was proven to give the best results as detailed in section 2.2.3 and chapter 4.

**Figure 3.8 SH3 Mt Messenger showing high dielectric value and unrealistic high moisture content (black bars) caused by steel slag surfacing**





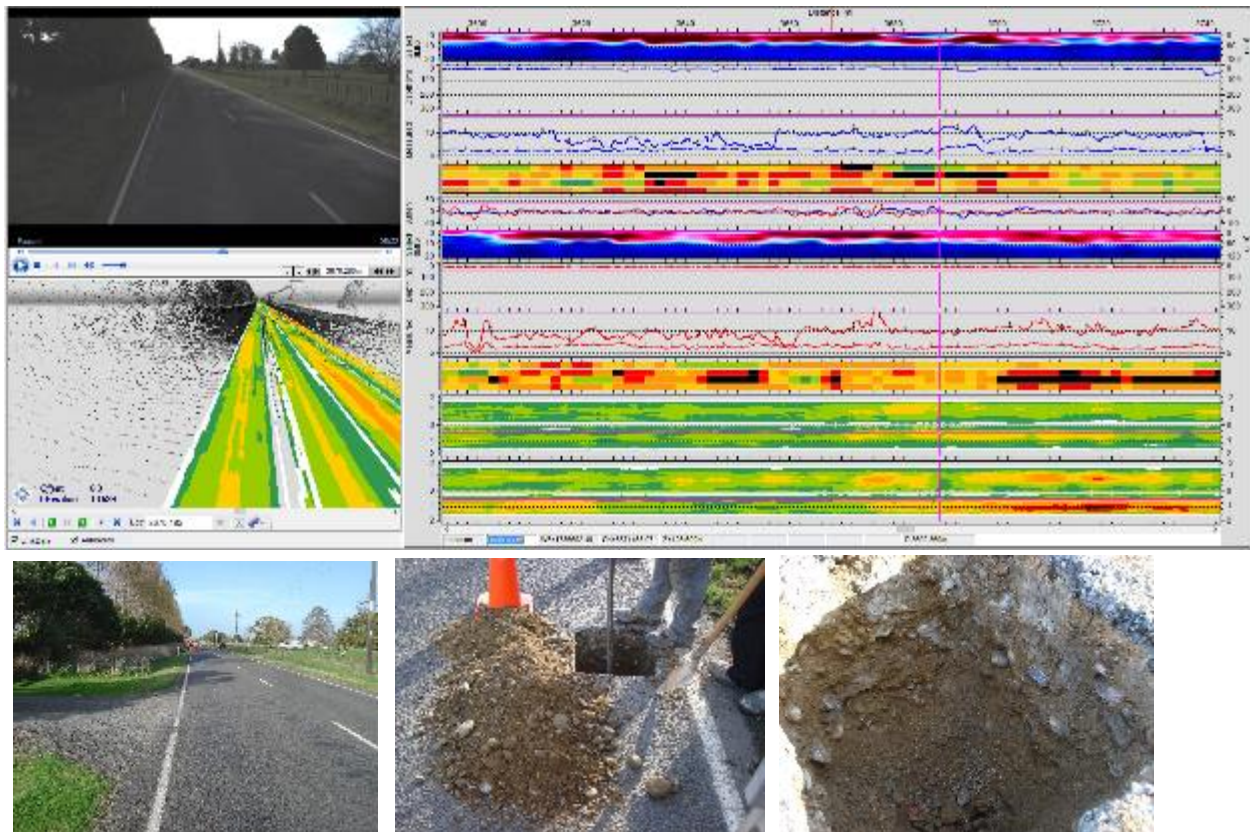


**Table 4.1 Results of test pit log and oven dry moisture contents**

Depth (mm)	Description
0-30	Chipseal lightly flushed.
30-260	Basecourse: sandy GRAVEL to 40mm, some silt, yellowish brown, angular, unbound* shell rock – 6.1% moisture content
260-285	Tar seal
285-500	Sub-base: sandy GRAVEL to 40mm, some silt, greyish brown, rounded – 7.0% moisture content.
500-600+	Subgrade: clayey silty SAND, minor gravel to 20mm, moist, rounded, dark greyish brown, reddish orange streaks, soft – 17.5% moisture content.

### 4.2.2 RP 3690 increasing side

**Figure 4.2 Moisture survey screen output and photos of test pits**



**Table 4.2 Results of test pit log and oven dry moisture contents**

Depth (mm)	Description
0-30	Chipseal – good condition.
30-450	Basecourse: sandy GRAVEL, minor silt, yellowish brown, rounded, dry – moist, unbound – 4.5% moisture content.
450-600	Sub-base: sandy GRAVEL to 20mm, minor silt, yellowish brown, rounded – 5.5% moisture content.

### 4.2.3 RP 5804 decreasing side

Figure 4.3 Moisture survey screen output and photos of test pits

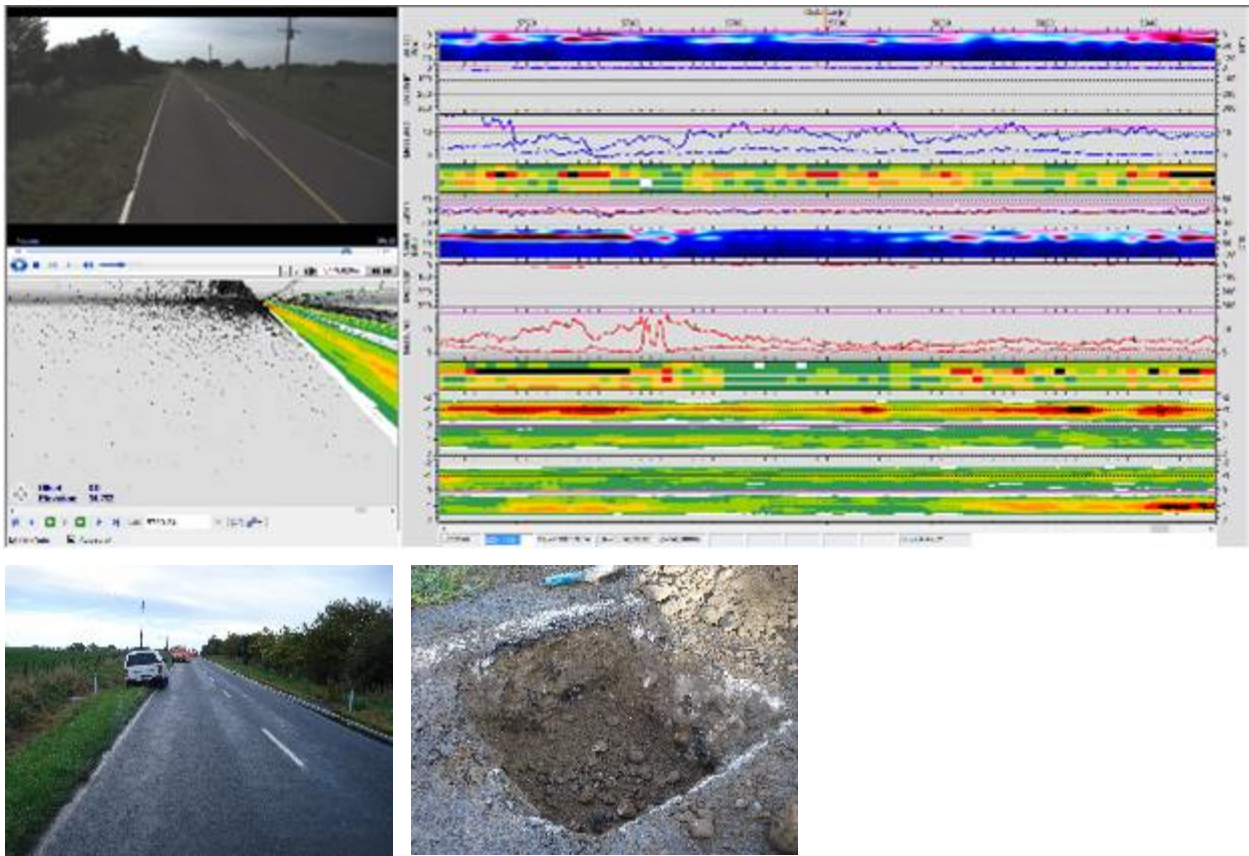


Table 4.3 Results of test pit log and oven dry moisture contents

Depth (mm)	Description
0-30	Chipseal lightly flushed.
30-280	Basecourse: sandy GRAVEL, some silt, greyish brown, rounded, unbound – 8.4% moisture content.
280-600	Subgrade: clayey silty SAND, some gravel, moist, rounded, dark grey – 17.9% moisture content.



#### 4.2.4 RP 5844 increasing side

Figure 4.4 Moisture survey screen output and photos of test pits

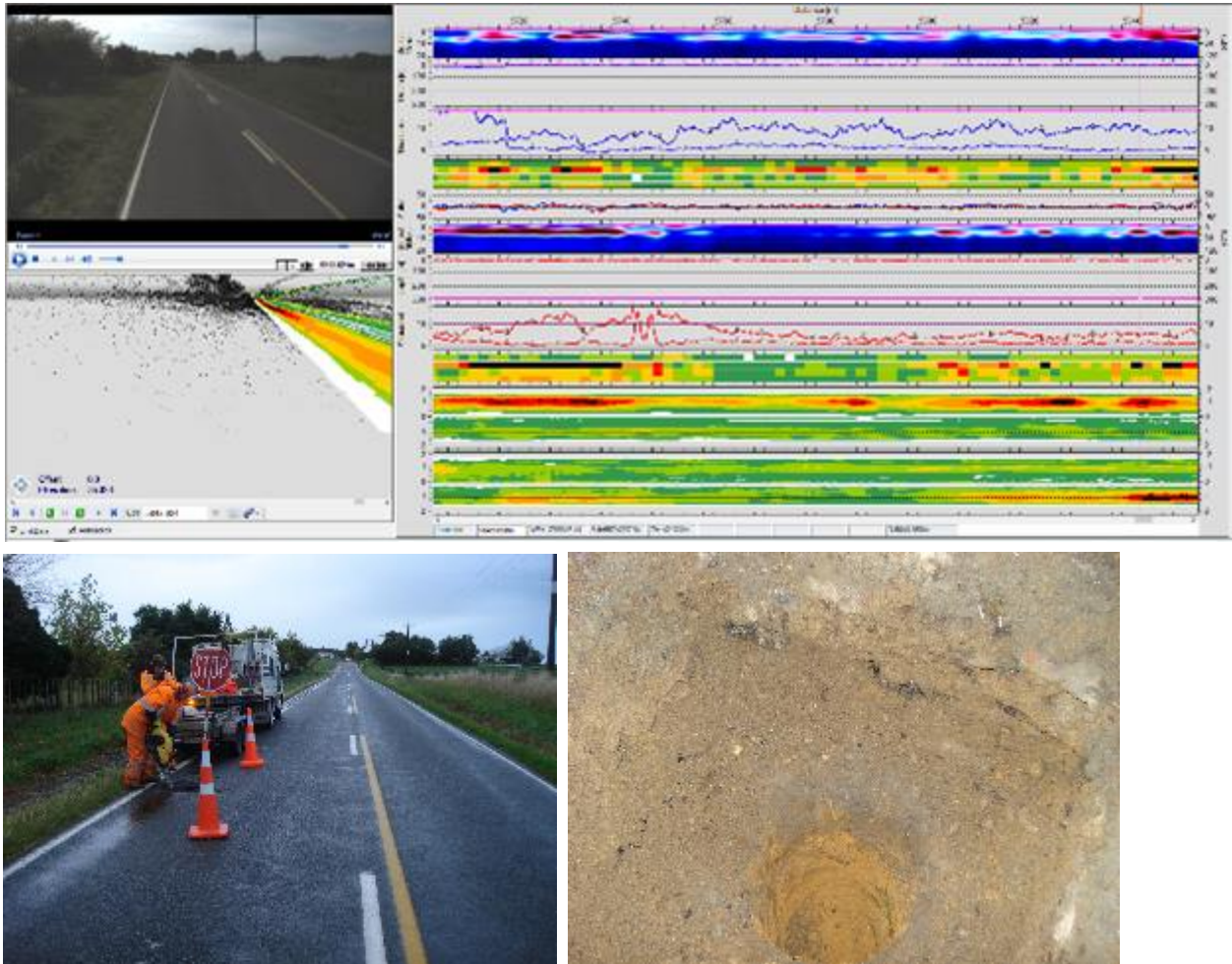


Table 4.4 Results of test pit log and oven dry moisture contents

Depth (mm)	Description
0–30	Chipseal good condition although road rutted.
30–220	Basecourse: sandy GRAVEL, some silt, yellowish brown, rounded to 50mm, moist, unbound – 6.9% moisture content.
220–250	Tar seal
250–380	Basecourse: sandy GRAVEL, some silt, yellowish brown, rounded to 40mm, moist, unbound – 8.4% moisture content.
380–640	Silty CLAY, reddish brown, moist – 38.3% moisture content.

### 4.3 No. 3 line test pits

#### 4.3.1 RP 670m decreasing side (wet location)

Figure 4.5 Moisture survey screen output and photos of test pits

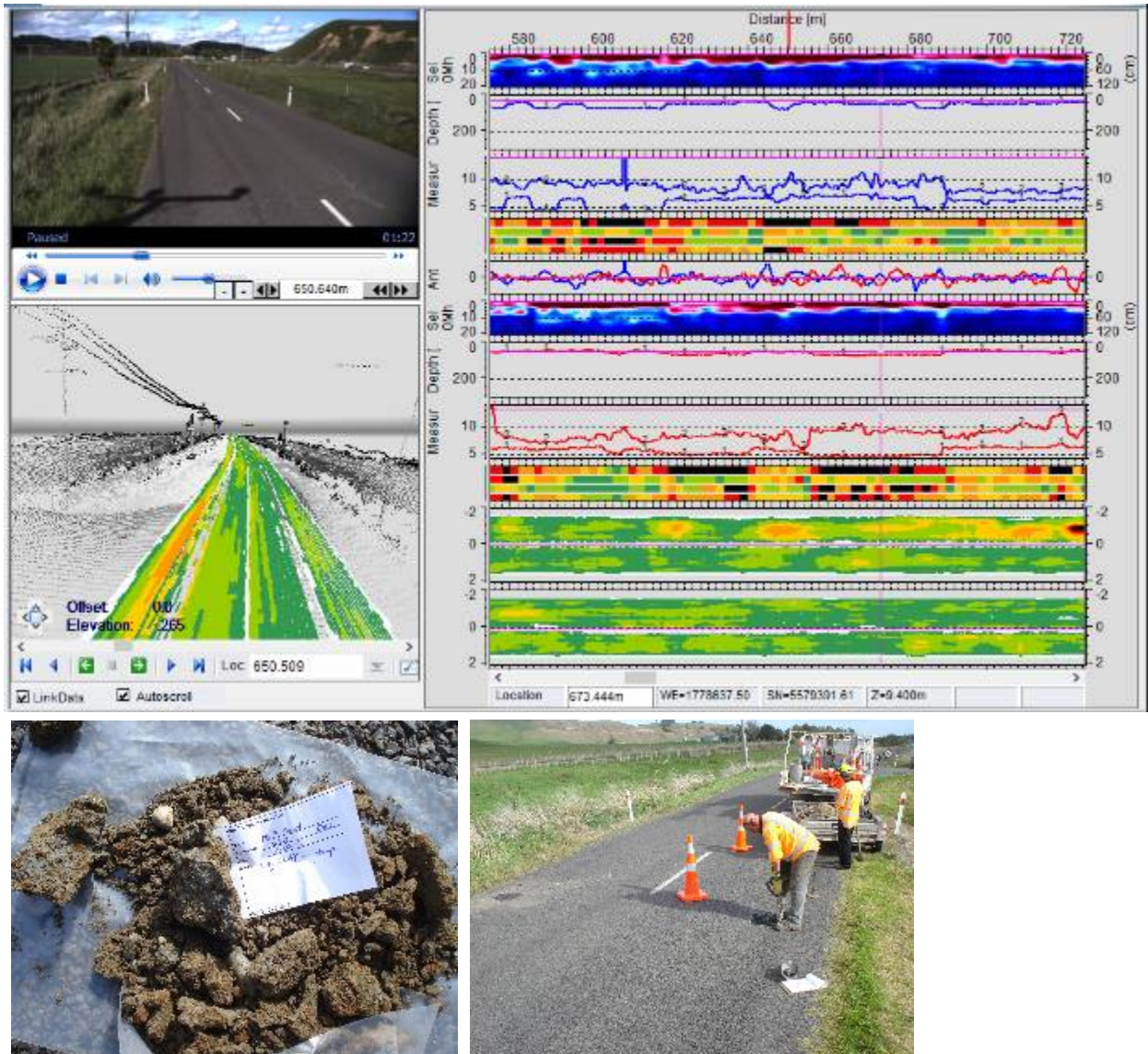


Table 4.5 Results of test pit log and oven dry moisture contents

Depth (mm)	Description
0-40	Chipseal – good condition
40-160	Basecourse: sandy GRAVEL to 65mm, reddish brown, rounded, moist, dense – 3.4% moisture content.
160-185	Tar seal/chipseal
185-440	Basecourse: sandy GRAVEL to 40mm, reddish brown, rounded, moist, dense – 4.9% moisture content.
440-600	Silty CLAY, dark grey, moist – 17% moisture content.



### 4.3.2 RP 670m increasing side (dry location)

Figure 4.6 Moisture survey screen output and photos of test pits

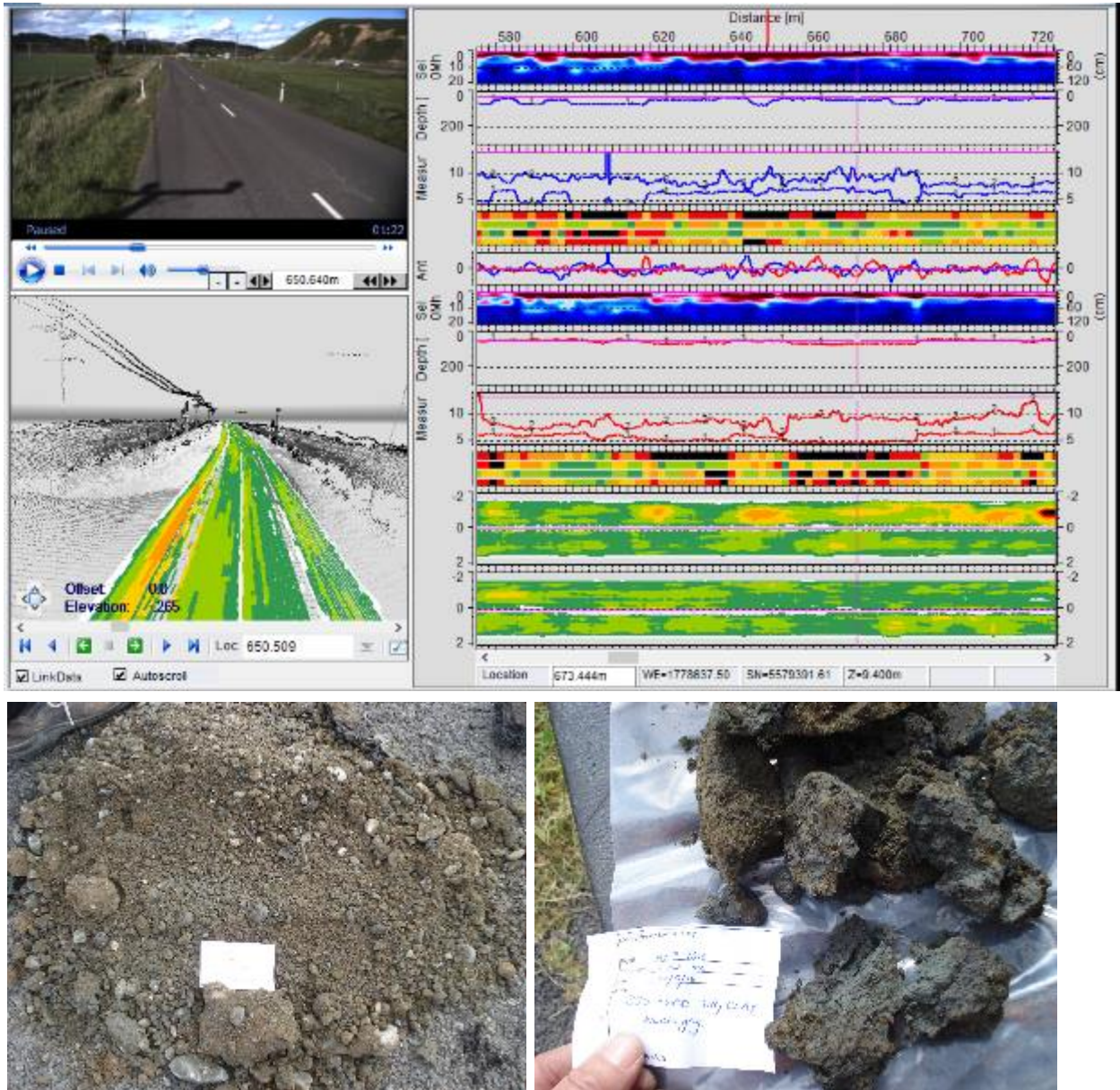


Table 4.6 Results of test pit log and oven dry moisture contents

Depth (mm)	Description
0-50	Chipseal – good condition
50-160	Basecourse: silty sandy GRAVEL to 65mm, reddish brown, rounded, moist, dense – 4.4% moisture content.
160-185	Tar seal/chipseal
185-350	Basecourse: sandy GRAVEL to 40mm, reddish brown, rounded, moist, dense – 5.2% moisture content.
350-600	Silty CLAY, dark grey, moist – 24.8% moisture content.



### 4.3.3 RP 1975m centreline (wet location)

Figure 4.7 Moisture survey screen output and photos of test pits

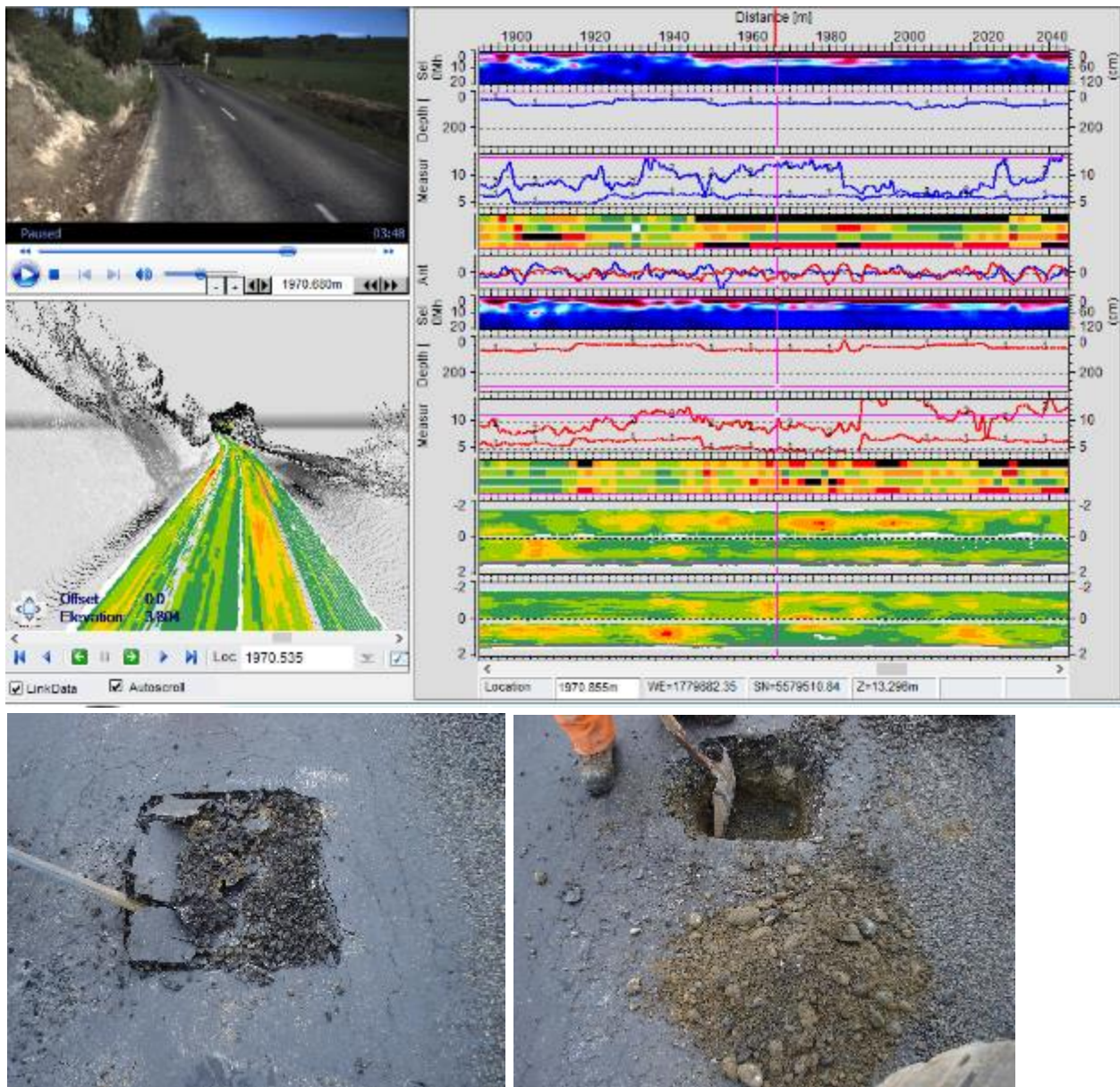


Table 4.7 Results of test pit log and oven dry moisture contents

Depth (mm)	Description
0-10	Bitumen – flushed chip seal, surface cracks, heaved.
10-160	Sub-base: silty sandy GRAVEL AP30mm (all passing 30mm), greenish brown, rounded, moist, dense – 8.1% moisture content. Outer edge of pit is unbound sealing chip.
160-300	Basecourse: sandy GRAVEL AP40mm, greyish brown, rounded, moist, dense – 4.9% moisture content.
300-315	Tar seal/chipseal
315-450, 450-700	Silty GRAVEL, dark grey, 315mm to 450mm depth – 5.9% moisture content, 450 – 600mm+ – 20.4% moisture content.



#### 4.3.4 RP 1970m increasing (wet location)

Figure 4.8 Moisture survey screen output and photos of test pits

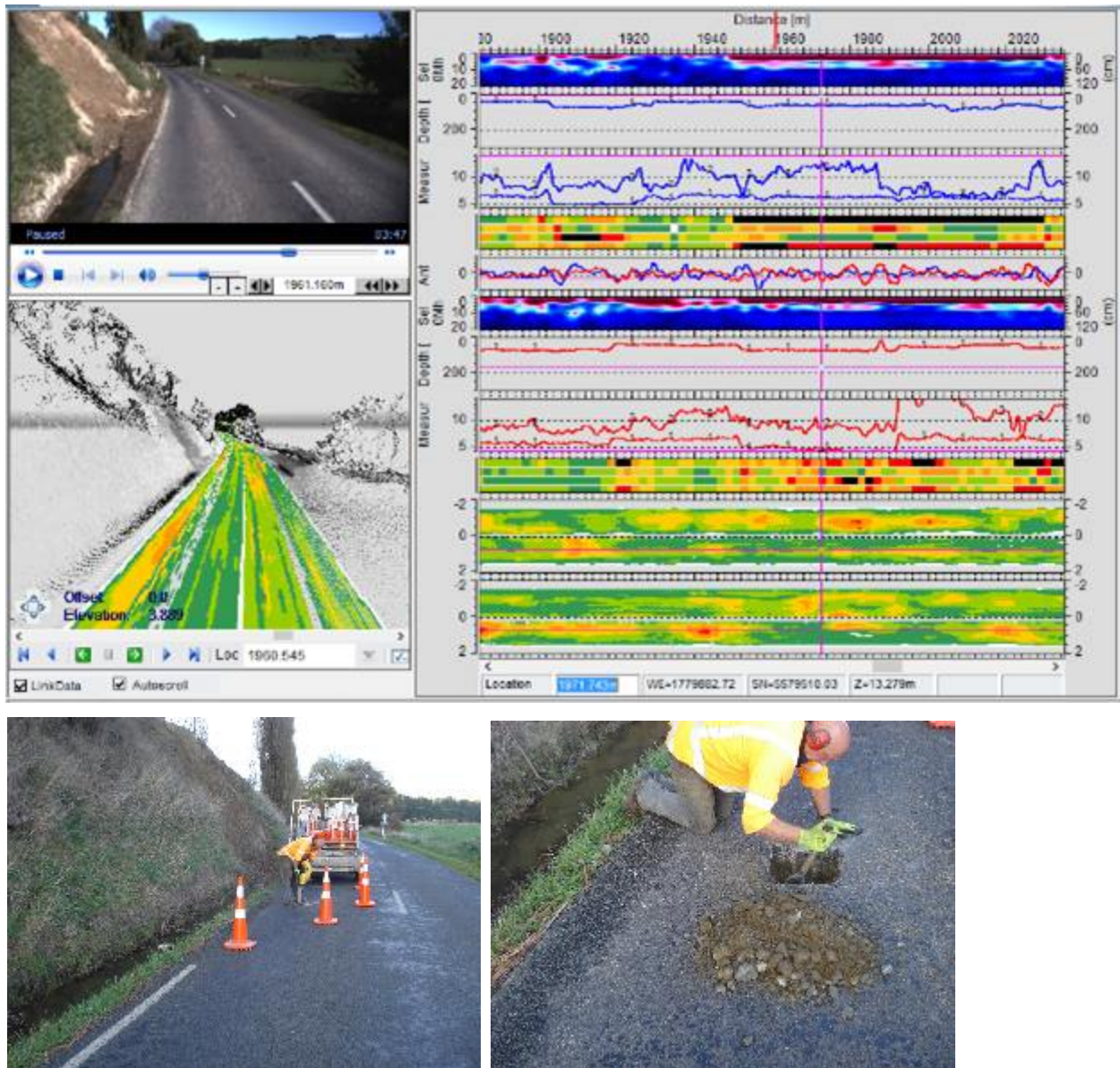


Table 4.8 Results of test pit log and oven dry moisture contents

Depth (mm)	Description
0–50	Chipseal.
50–310	Basecourse: sandy GRAVEL to 40mm, yellowish brown, rounded, moist, unbound – 4.8% moisture content.
310–340	Tar seal
340–450	Sub-base: sandy GRAVEL, some silt, to 65mm, rounded, yellowish brown, moist – 6.3% moisture content.
450–600	Subgrade: silty sandy GRAVEL AP65mm, rounded, yellowish brown, 8.9% moisture content.

## 4.4 London St Pt2 test pits

### 4.4.1 RP 200m increasing side

Figure 4.9 Moisture survey screen output and photos of test pits

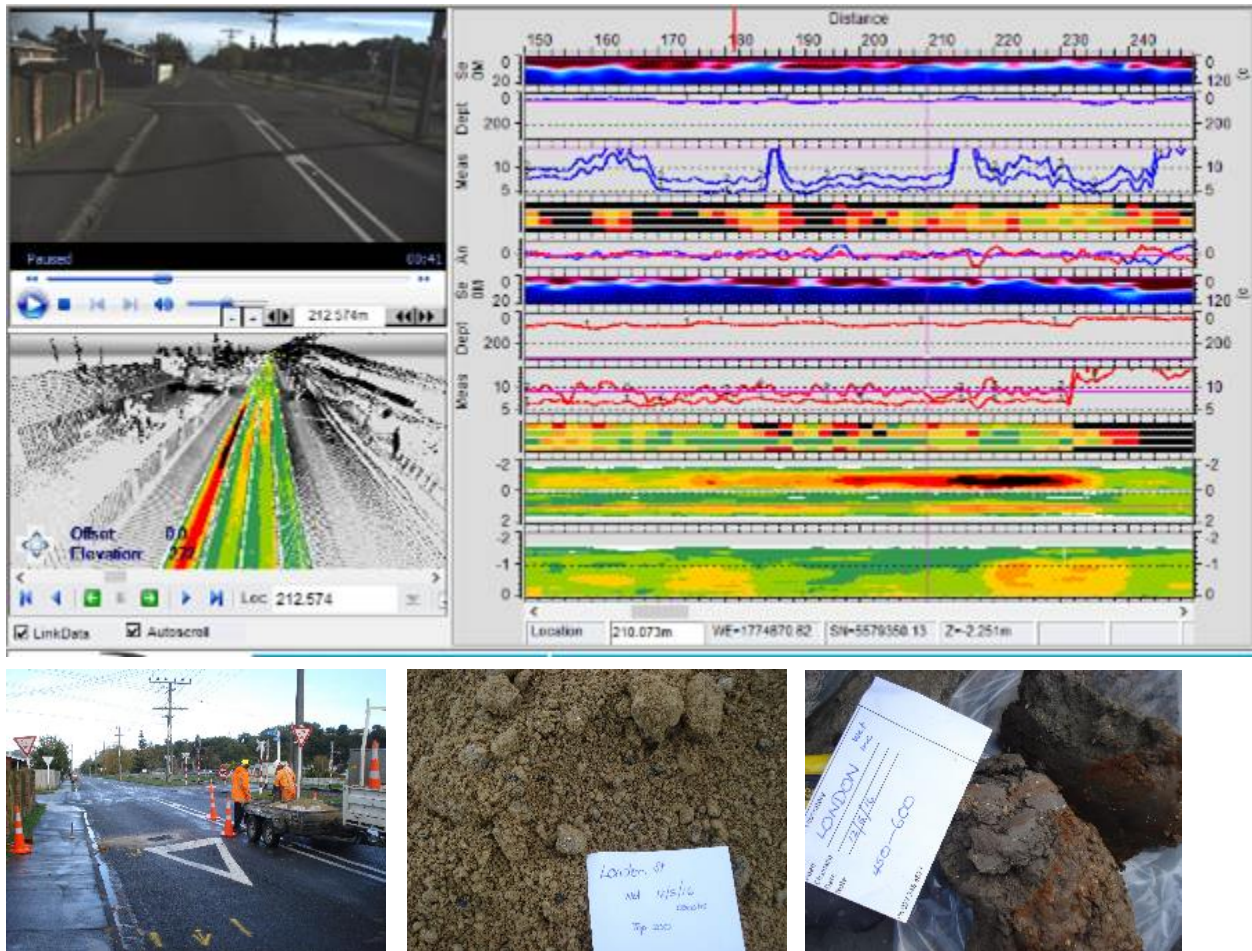


Table 4.9 Results of test pit log and oven dry moisture contents

Depth (mm)	Description
0-20	Chipseal
20-370	Basecourse: sandy GRAVEL AP40mm, some silt, yellowish brown, angular, unbound, shell rock - 6.3% moisture content.
370-450	Subgrade: clayey silty SAND, some gravel, moist, rounded, dark brown, soft, - 44.6% moisture content.
450-600	Subgrade: clayey silty SAND, minor gravel, moist, rounded, dark greyish brown, reddish orange streaks, soft - 36.4% moisture content.



#### 4.4.2 RP 200m decreasing side

Figure 4.10 Moisture survey screen output and photos of test pits

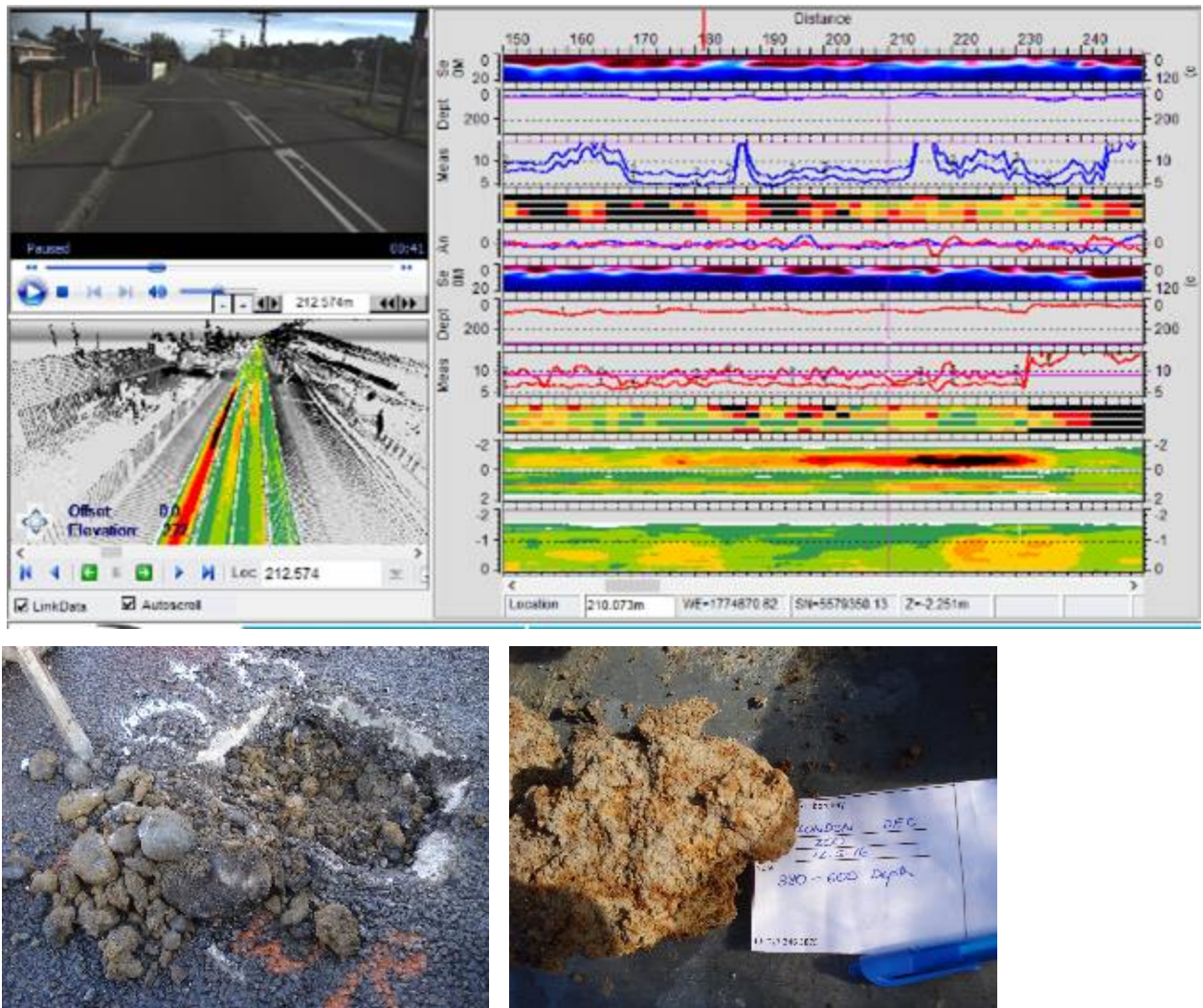


Table 4.10 Results of test pit log and oven dry moisture contents

Depth (mm)	Description
0-70	Chipseal – good condition.
70-200	Basecourse: sandy GRAVEL AP40mm, some silt, yellowish brown, angular, unbound, shell rock – 5% moisture content.
200-380	Subgrade: clayey silty SAND, some gravel, moist, rounded, dark brown, soft – 53.8% moisture content.
280-600	Subgrade: clayey silty SAND, minor gravel, moist, rounded, dark greyish brown, reddish orange streaks, soft – 31.9% moisture content.

## 4.5 Test pit summary

**Table 4.11 Results of test pit log and oven dry moisture contents compared with moisture damage index detection**

Location	Top (0 to 230mm)		Middle depth (230 to 450mm)		Bottom depth (450 to 600mm)	
	Test pits	Survey MDI -	Test pits	Survey MDI	Test pits	Survey MDI
No. 2 line RP 3680 decreasing side	6.1% MC sandy gravel with some silt	Middle	7% MC – 30mm seal layer over sandy gravel with some silt	High	17.5% MC – clayey silty sand	Middle
	Good prediction		Ok prediction – buried seal layer gave a high result.		Good prediction	
No. 2 line RP 3690 increasing side	4.5% MC sandy gravel with some silt	Dry	4.5% MC sandy gravel with some silt	High	5.5% MC sandy gravel with some silt	Middle
	Good prediction		Poor prediction – but possibly estimated wrong RP of test pit.		Poor prediction (although maybe influenced by deeper subgrade)	
No. 2 line RP 5804 decreasing side	8.4% MC sandy gravel with some silt	Dry	17.9% MC – clayey silty sand	High	17.9% MC – clayey silty sand	Middle
	Poor prediction		Good prediction		Good prediction	
No. 2 line RP 5844 increasing side	6.9% MC sandy gravel with some silt	Middle	8.4% MC – 30mm seal layer over sandy gravel with some silt	High	38.3% MC – silty clay	Dry
	Good prediction		Good prediction – buried seal layer gave a high result.		Poor prediction	
No. 3 line RP 670 decreasing side	3.4% MC sandy gravel with buried 30 seal layer	High	4.9% MC sandy gravel	Dry	17% MC – Silty Clay	Middle
	Ok prediction- buried seal layer gave a high result.		Good prediction – no silt		Good prediction	
No. 3 line RP 670 increasing side	4.4% MC sandy gravel with buried 30 seal layer	High	5.2% MC sandy gravel	Dry	24.8% MC – silty clay	Dry
	Ok to poor prediction- buried seal layer gave a high result.		Good prediction – no silt		Ok prediction	
No. 3 line RP 1975 CL side	8.1% MC silty sandy gravel	High	4.9% MC sandy gravel	Middle	5.9% MC – silty gravel	Dry
	Good prediction – silty and high MC		Ok prediction		Good prediction	

Location	Top (0 to 230mm)		Middle depth (230 to 450mm)		Bottom depth (450 to 600mm)	
	Test pits	Survey MDI –	Test pits	Survey MDI	Test pits	Survey MDI
No. 3 line RP 1970 increasing side	4.8% MC sandy gravel	High	6.3% MC – 30mm seal layer over sandy gravel with some silt	Middle	8.9% MC – silty sandy gravel	Dry
	Poor prediction but could be influenced by buried seal layer below		Ok prediction – buried seal layer gave a high result.		Good prediction	
London St Pt2 RP 200 decreasing side	5.0% MC sandy gravel with some silt	Dry	53.8% MC – clayey silty sand	High	31.9% MC – clayey silty sand	Dry
	Good prediction		Good prediction		Poor prediction but high in middle layer – which captures site as needing drainage improvement	
London St Pt2 RP 200 increasing side	6.3% MC sandy gravel with some silt	High	44.6% MC – clayey silty sand	High	36.4% MC – clayey silty sand	High
	Ok prediction		Good prediction		Good prediction	


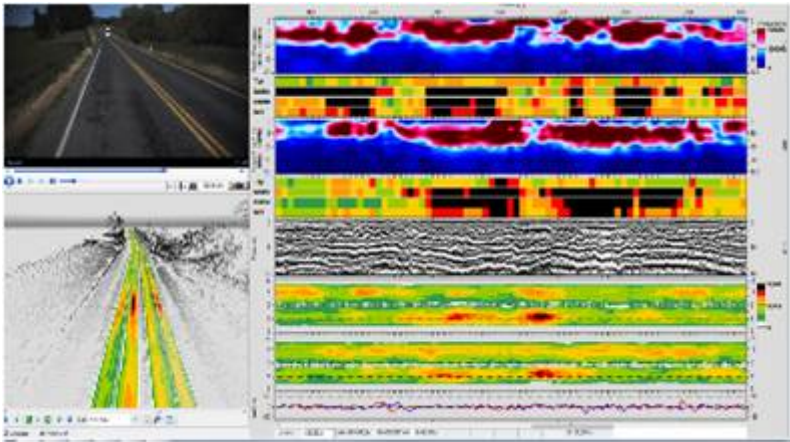

MDI – green = low; yellow and orange = middle; red or black = high

From 30 predictions of MDI, 17 were considered good, 7 OK and 6 poor. Combining the good and OK predictions gives an 80% pass rate. It should be noted the moisture survey was completed in October 2015 while the test pits were completed in May 2016 and the position of the test pits may not be accurate (which causes an error when reading the moisture survey results that could be in the wrong location). Because of these reasons it is expected in some cases the predictions will be poor. Further, the MDI is a measure of both the amount of clay as a measure of moisture sensitivity and moisture content and a high MDI can indicate a clay contaminated basecourse aggregate. Further, the predictions of wet areas show good visual correlation with pavement distress like rutting and flushing which is often a result of water entering the pavement. Reviewing the results it appears high MDI readings can be a result of buried seal layers which form a moisture barrier and trap water in the pavement.

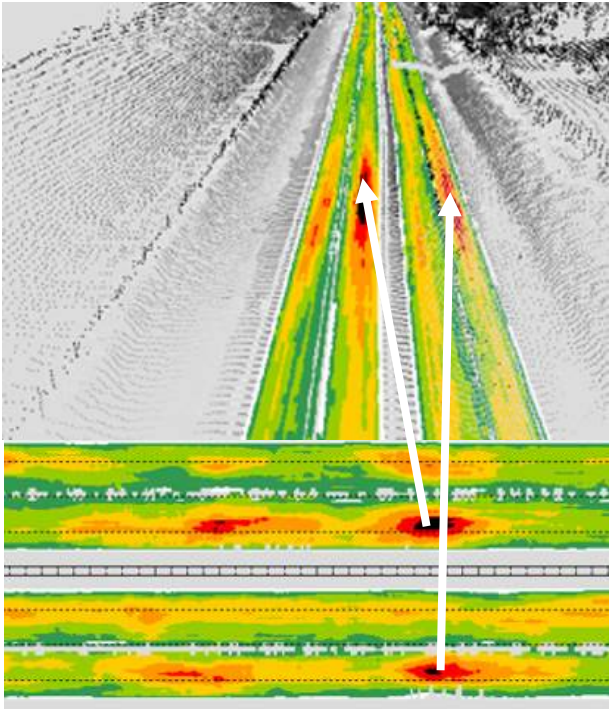
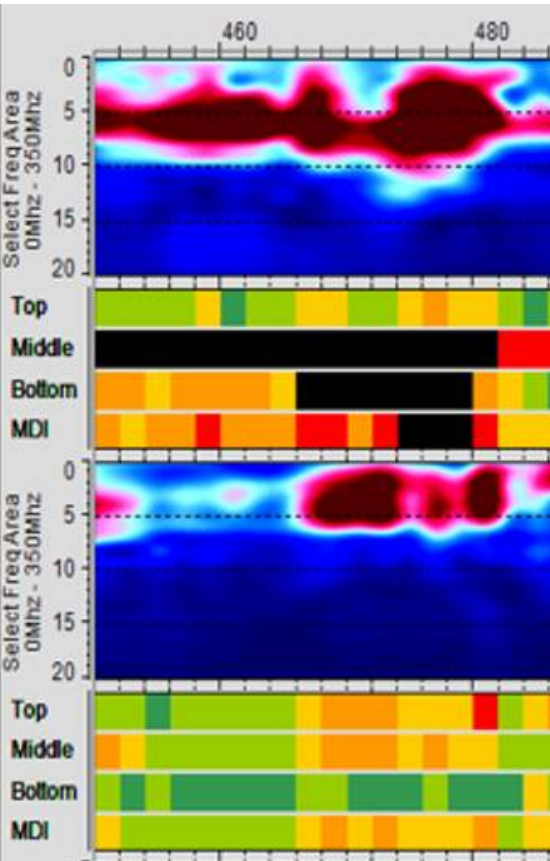
## 4.6 Summary of results

Observations from the moisture survey results in appendix B are detailed in table 4.12.

**Table 4.12 Observations from the moisture survey**

Observations	Result shown	Using the result
<p>Network level or per road</p> 	<p>Results of the moisture survey are displayed in GIS maps to identify the areas of the road marked as black showing the locations with the highest moisture susceptibility.</p>	<p>The data can be exported to quickly determine the length of road with high moisture susceptible areas to estimate the forward works programme for drainage improvements (length and cost).</p> <p>Used to identify road location which may require drainage improvement for further investigation using the Road Doctor viewer software with outputs shown below.</p>
<p>Road Doctor viewer software</p> 		<p>The viewer software is used to give more detail on the condition of the road, moisture and where this occurs, pavement layer thicknesses, and rutting in both road directions.</p> <p>Details of what is shown in the viewer software and its interpretation is shown below</p>
<p>Video</p> 		<p>The video can be expanded to full screen and the picture assists in giving more information to support or otherwise a drainage problem and the type of treatment. Chipseal flushing shown here supports high levels of saturation within the pavement layers.</p>



Observations	Result shown	Using the result
<p>Laser LIDAR – rutting, depressions and cross-sections</p> 		<p>The contour maps derived from the LIDAR laser survey identify localised depressed areas (shown in black) which can and often coincide with sections of the road showing highly moisture susceptible pavement layers. Again this LIDAR data combined with the video is used to assess whether or not the measured high moisture is causing pavement distress and focuses on the area where drainage improvements are needed before further pavement rutting occurs.</p>
<p>Moisture survey results – note shows RP of around 460m to 480m</p> 		<p>Left lane – GPR frequency reflection where red to black identify the wettest areas and/or materials with highest moisture susceptibility</p> <p>Left lane MDI results where black indicates the wettest areas and/or materials with highest moisture susceptibility</p> <p>Top (0–200mm depth) middle (200–400mm depth) bottom (400–600mm depth)</p> <p>Right lane – GPR frequency reflection where red to black identify the wettest areas and/or materials with highest moisture susceptibility</p> <p>Right lane MDI results where black indicates the wettest areas and/or materials with highest moisture susceptibility</p> <p>Top (0–200mm depth) middle (200–400mm depth) bottom (400–600mm depth)</p>

The moisture survey results in table 4.12 show between RP 460 and 480m in the increasing RP direction there is high moisture or materials with high moisture susceptibility at a depth of 200–400mm (middle shown as black shading) and at 400–600mm depth (bottom shown as black shading). This result allows a drainage treatment to target this location and the roadside deeply enough to drain the water from the underlying subgrade soils at depths of at least 600mm. Viewing the LIDAR rutting and video will determine how advanced the pavement distress is and help determine the urgency of the drainage treatment needed for prioritisation.

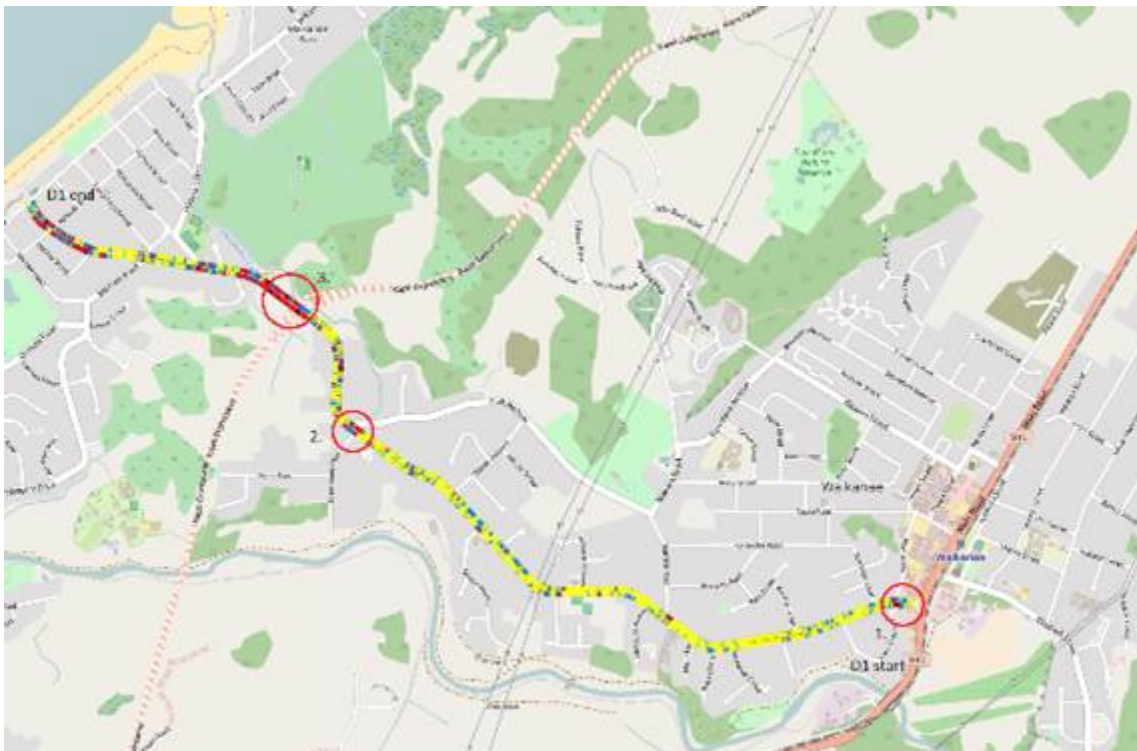
A range of results from the Road Doctor viewer software similar to the results shown in table 4.12 are reported in appendix B. As test pits were not conducted on every road the accuracy of the moisture survey is subjective and based on other pavement distress indicators for poor drainage which includes (chipseal flushing from the video) and rutting from the LIDAR survey. Most locations where high moisture (high MDI results) were determined corresponded with LIDAR rutting and visual pavement distress in the video.



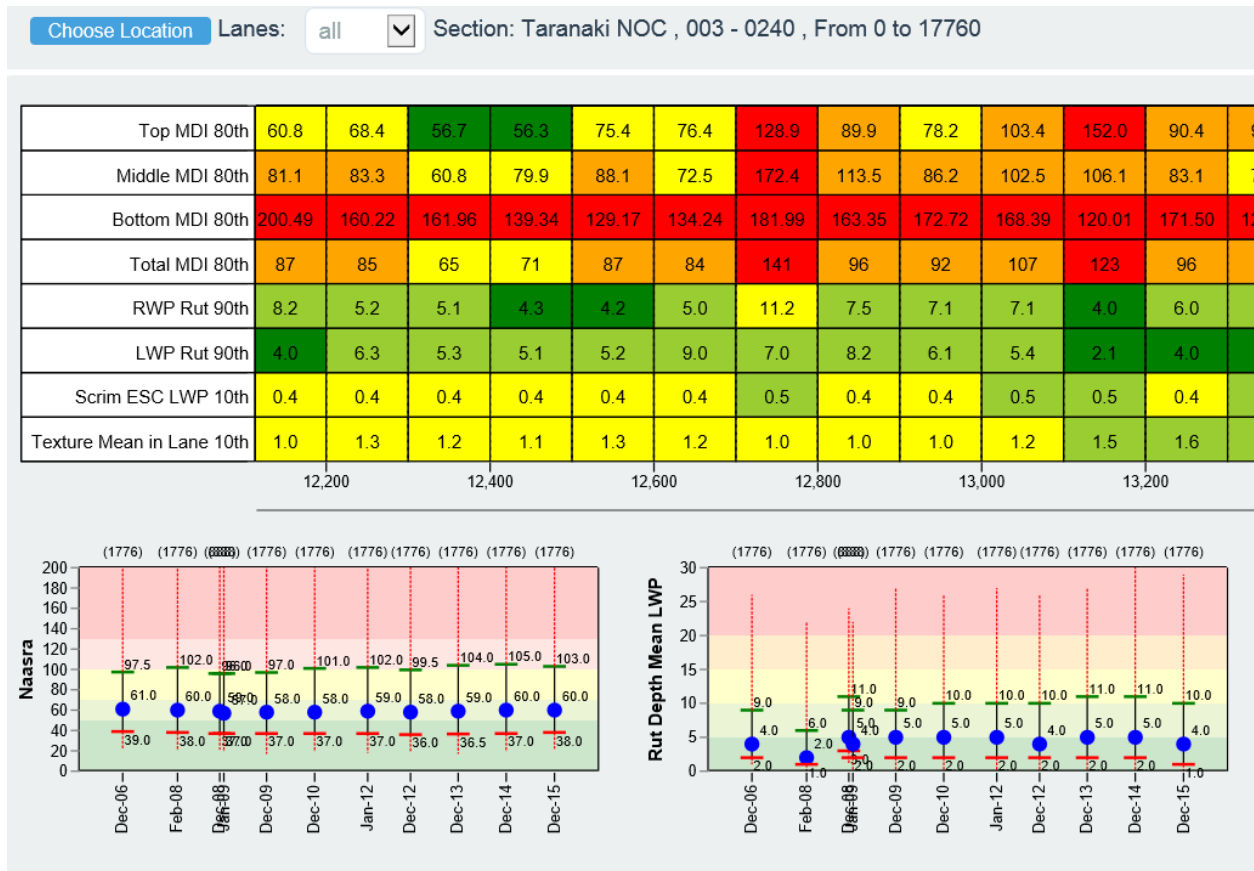
## 5 Use of moisture survey in asset management

The moisture survey data can be used in several ways for managing the asset. At the network level the MDI data can be outputted to GIS or Google maps and colour coded where black indicates the highest MDI values and areas that can be looked at more closely to determine and prioritise appropriate improvements in drainage and surface waterproofness (figure 5.1). Actual raw data from the moisture survey is MDI values at three depths, LIDAR rut depths, roughness, pavement depths (if calculated from GPR) at 2m increments. This data can be imported into any database system and/or post processed to, for example, to be amalgamated into 100m sections and imported into Juno Viewer to display alongside RAMM high-speed data (figure 5.2).

**Figure 5.1** Locations of high moisture on Te Moana Road



**Figure 5.2 Juno viewer strip map displaying MDI 80th percentile values per 100m sections alongside rutting and texture data from RAMM**



Another way to use the moisture survey results is through the Road Doctor viewer software. This viewer software is used at a project level where a particular location is studied more closely to determine whether or not drainage improvement is needed and also the type of drainage improvement at locations scheduled for maintenance patch repairs, reseal, pavement renewal or simply a section prioritised for drainage improvement (from the moisture maps or surface and pavement distress indicating moisture problems). Figure 5.3 has an example screenshot from the viewer software for Springvale Road, which shows a section that has rutted. Moisture in the top basecourse area is indicated by the black strip bars. Conversely, a section on SH3 shows some rutting but in this case the high moisture with black bars is at the bottom at a depth >400mm. The type of drainage improvement for each case will be different dependent on where the water is and the viewer software is an excellent means of determining this. Further, a cross-section view can be obtained from the viewer software to determine whether the ditch depth is adequate and if there is high shoulder lip trapping the water (figure 5.5).

Figure 5.3 Springvale Road site where high moisture was detected (black bars)

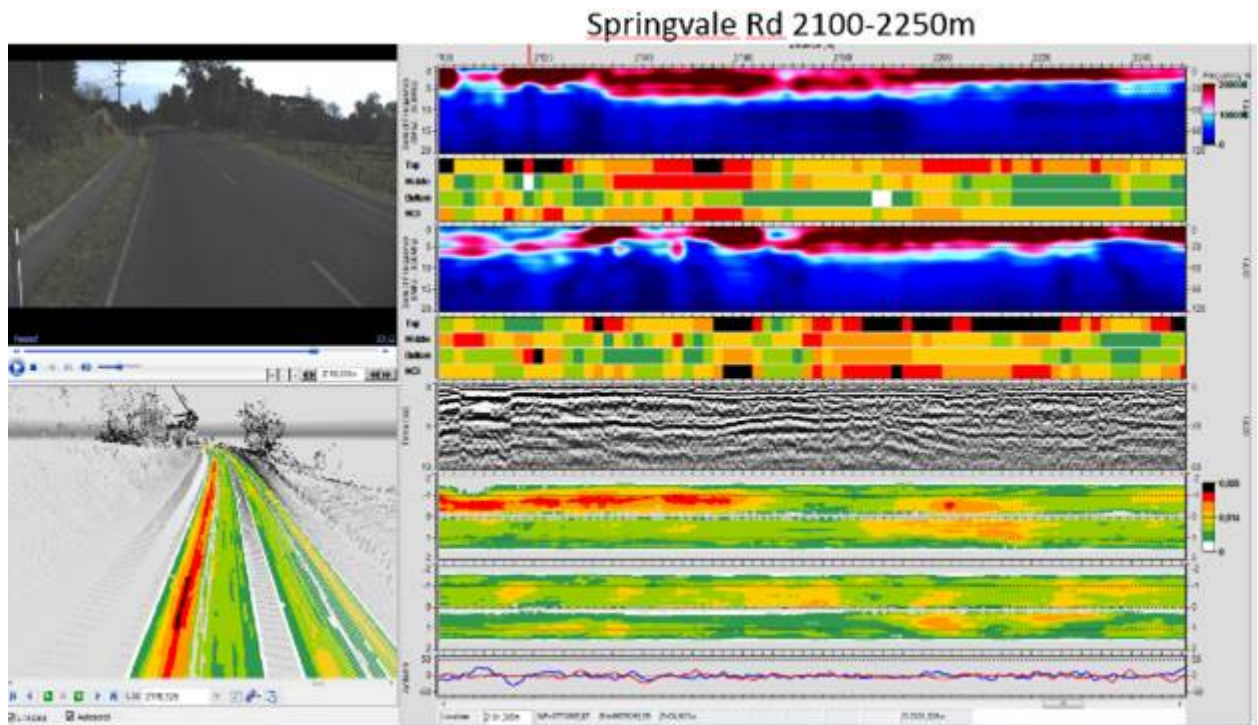
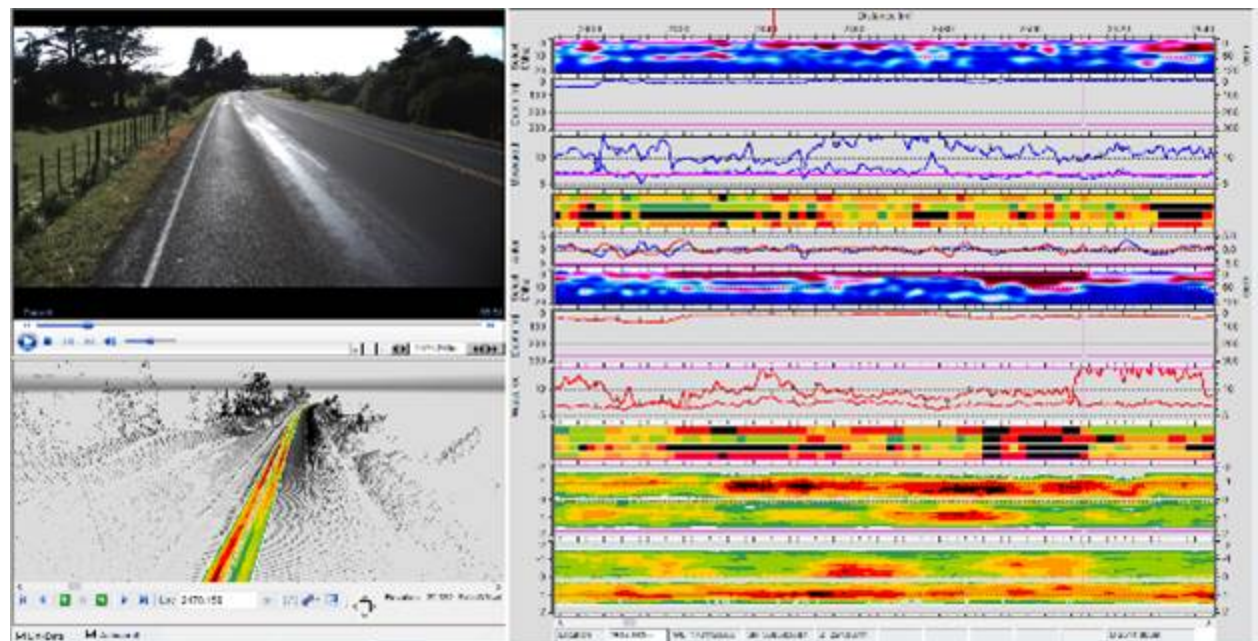
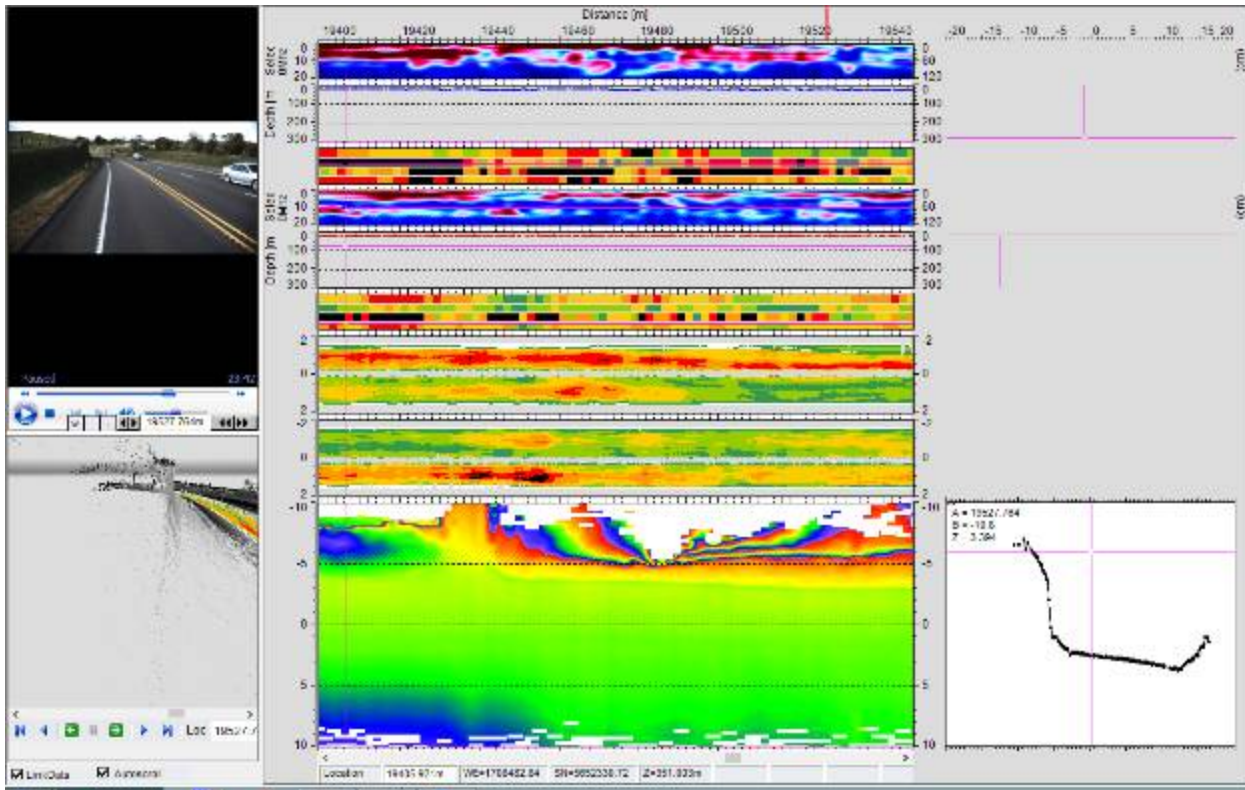


Figure 5.4 SH3 Egmont to Stratford 2,400–2,550m (RP 240/14.48) moisture survey results





**Figure 5.5** Moisture results showing in SH3 Egmont to Stratford 19,300-19,450m (RP 269/2.59) with cross-section information



All asset managers within Downer have a copy of the Road Doctor viewer software installed on their computers along with a 64GB USB flash drive with the survey data. This viewer software is used regularly by asset managers when planning forward works programmes on the network as it allows for a detailed analysis and view of a particular road section to aid in key decisions on drainage improvements required alongside or instead of other treatments planned. Its operation is similar to Road Runner with a video view of the road but the Road Doctor view also gives information on rutting, and moisture at different depths in the pavement. Another advantage of the Road Doctor software displaying the LIDAR rut depth information is small localised areas can be seen showing depressions and problem areas with moisture where the size of these areas is more akin to the common patch size being around 20m in length. The Road Doctor viewer software can be used alongside scheduling patch repairs in the network to determine if any drainage improvements are required alongside the patched areas. Improving drainage alongside patch repairs where needed should extend the life of the patch. The width of the rutting is also an indicator of where the rutting occurs, if the rutting is wide then the rutting is deeper in the subgrade level.

Questions and answers that may be asked about this moisture survey in relation to asset management are given below:

How will this impact on the way contractors currently manage networks?

The survey:

- promotes preventative maintenance
- helps decide where, when and how much to spend on drainage based on data and facts
- drives the most appropriate treatment selection for drainage (either surface swales, deeper subsoil drains or culvert repairs to target specific locations of where the water is detected etc)

- measures effectiveness of the drainage treatment
- allows multi-year planning and monitoring of the network.

How will it impact on the planning of maintenance and long-term modelling of networks?

- Input on moisture is used in network modelling as there will be different pavement and surfacing deterioration rates in locations of poor drainage with high moisture levels measured in the survey.
- Prioritisation and allocation of drainage budget across the networks.
- A higher level of confidence that renewals/rehabs/reseals will likely exceed their design life.

What format does the data comes in – how can this be managed?

- Data can be exported in Shapefile or GIS enabled data and imported into Juno Viewer.
- Maps with moisture contours can also be exported into Google earth format.
- Data is compatible with most GIS systems.

What is the recommended coverage of networks surveys?

- Full coverage on main roads in both directions once a year.
- Full coverage on lower classification roads in both directions every two to three years.

## 6 Conclusions

This report presents the results of moisture detection surveys at high speed (60 to 80km/h or 30 to 50km/h in 50km/h speed zones. Equipment utilised was a transverse LIDAR, ground penetration radar (air and ground coupled) and video camera with analysis and presentation of the results using Road Doctor software. A range of roads were surveyed in the North Island where Downer was the maintenance contractor for ease of in-kind traffic management and asset data. This survey yielded the following conclusions listed alongside the project objectives.

**Objective # 1:** Demonstrate moisture detection equipment can determine saturated pavement areas along the road together with a probable cause (eg the moisture ingress is due to either a cracked seal as found from the thermal imaging camera or inadequate drainage).

- The calibration with boxes of aggregate proved the GPR (air and ground) correlates with increasing saturation/moisture levels.
- The dielectric constant used as an indicator of moisture from the air coupled GPR was found to be a poor indicator of moisture below the surface.
- A New Zealand specific MDI was developed from the calibration boxes and the complete set of moisture survey results using data mostly from ground coupled radar, which allowed the moisture to be detected at three depths below the surface (0 to 200mm; 200 to 400mm and 400 to 600mm)
- The viewing software includes both MDI values at different depths along with video and laser LIDAR rut depths where areas of high MDI values often corresponded to moderate to high rutting.

**Objective # 2:** Investigate and inspect pavement areas of the road network surveyed that were identified as being saturated and in need of drainage improvement to confirm or otherwise the accuracy of the surveys and the accuracy of the probable cause.

- Test pits conducted seven months after the moisture survey confirmed the results of the moisture survey 80% of the time.

**Objective # 3:** Report on the practicality, cost and success or otherwise of the moisture detection equipment trial in New Zealand.

- Despite the high capital cost the moisture survey technique and data analysis routine involved only a few days set up and calibration before the survey could be conducted.
- Results of the moisture survey can be easily outputted to other databases. The results were imported into GIS maps and also into Juno viewer to enable other pavement distress and maintenance history data to be displayed alongside the moisture data.
- The Road Doctor software viewer software allows asset managers to use the moisture survey at a project level where a particular location is studied more closely to determine whether or not drainage improvement is needed and also the type of drainage improvement at locations scheduled for maintenance patch repairs, reseal, pavement renewal or simply a section prioritised for drainage improvement (from the moisture maps or surface and pavement distress indicating moisture problems).
- The technology is applicable to New Zealand roads.
- The technology is a suitable tool allowing the asset owner to understand the effectiveness of road drainage using objective measures.
- The MDI is a suitable measure.
- Multiple data types are captured as part of the survey which is used to determine pavement structure, moisture, rutting and condition of the drainage system.

- The data is transferable to other systems allowing macro and micro analysis.

Benefits of the moisture survey:

- There are significant benefits to proactively improving drainage and surface waterproofness as determined by the moisture survey where studies from the LTPP sites show the life can be extended by 2.5 times.



## 7 Recommendations

There are potential benefits utilising the results of the moisture survey. The first is being able to quantify and prioritise the drainage improvements needed on the road network along with determining the most appropriate moisture mitigation treatment (either deep to remove water from the subgrade or shallow to remove from the basecourse). To maximise this benefit it is recommended that the complete road network is surveyed around the same time to minimise seasonal effects and determine which networks and areas within networks need drainage improvements. These could include deep subsoil drains at locations where the subgrade was identified to have high moisture levels. However, as part of the network survey further test pits should be undertaken soon after the survey to measure moisture and susceptibility to moisture of the pavement materials to further validate and give confidence in the roads. Further full-scale road trials could be constructed with controlled amounts of water added and measurements undertaken to obtain an improved calculation of MDI. This further research should use and build on similar research being conducted by the Finnish Road Agency.

For networks that have been surveyed for moisture it is recommended that the effectiveness of drainage improvements is assessed in terms of moisture detected and the rate of deterioration in relation to different soil types, rainfall, road classification and traffic loading. During the survey period, there should be research into how the results of the survey have changed the way the road network is managed, Also through monitoring rutting with the LIDAR laser and studying maintenance costs, the financial benefits from proactive drainage improvements based on the moisture survey can be determined. As a comparison, moisture surveys should be conducted on local roads also as the moisture technology is transferable between state highways and local authorities.

## 8 References

See also the reference list at the end of the literature review in appendix A.

Henning, T, D Alabaster, G Arnold and W Liu (2014) Relationship between traffic loading and environmental factors and low-volume road deterioration. *Transportation Research Record Journal of the Transportation Research Board*. December 2014.

Matintupa, A and T Saarenketo (2011) *New survey techniques in drainage evaluation – laser scanner and thermal camera*. A ROADEX IV report for task D1'Drainage maintenance guidelines. ROADEX.

ROADEX (2012) e-learning platform. Accessed 25 February 2015. [www.roadex.org/](http://www.roadex.org/)

Saarenketo, T (2006) Electrical properties of road materials and subgrade soils and the use of ground penetrating radar in traffic infrastructure surveys. PhD thesis. Oulu: Oulu University.

## Appendix A: Literature review

This literature review was compiled by G Arnold (Road Science); R Hamrouche, T Herronen, P Maijala, A Matintupa, T Saarenketo, M Silvast, J Wieczorek (Roadscanners Oy); M Middleton (GTK).

### A1 Introduction

Water plays a key role when discussing the mechanical performance and lifetime of any traffic infrastructure. The fact, known for centuries, is that as long as there is no excess water in road structures and subgrade soil the road will perform well. Increased water content reduces the bearing capacity of a soil or aggregate, which under traffic loading will increase the rate of deterioration and shorten the lifetime of the road. In such cases, the road will need maintenance measures and rehabilitation more often than a well-drained road structure. For this reason, road drainage systems need to work effectively over the whole lifetime of the pavement – and not just for a few years. Current predictions of the likely effects of climate change only magnify this issue and modern asset management principles are rightly forcing road owners to consider ways to maximise the use of their available budgets and improve road lifetimes (Matintupa and Saarenketo 2011; ROADEX 2012).

Recent road condition research projects have clearly shown that good drainage maintenance practices are the most effective way to improve road condition, increase road durability, and decrease permanent deformation and spring thaw weakening. A further important matter that directly relates to road drainage is the increasing incidence of flooding as a result of climate change. The frequency and severity of flooding caused by continuous heavy rains have been globally increasing over recent years.

However, one big challenge for road owners is how to monitor the water content in pavement structures and subgrade soils and how to monitor whether the drainage system is effective enough to drain the structures sufficiently to ensure adequate bearing capacity in the road network. Another challenge is how to ensure after flooding that the road sections are safe enough to be opened to heavy traffic.

Over the recent year many new technologies and innovations for monitoring the moisture of pavement structures and subgrade soils have entered the market and some of these techniques have great potential to help road owners and contractors improve their drainage management practices and save money. This is why the Transport Agency funded this research project to test how different moisture monitoring techniques could be applied on the New Zealand road network. This literature review was the first phase of the project and it provides an overview of current technologies available in the market.

### A2 Water and roads

A main cause of road damage, and problems with the serviceability of road networks, is excess water filling the pores of road materials in the road and in subgrade soils. It is generally known that road structures operate well in dry conditions and because of this, roads have historically been built on dry terrain. On those occasions when roads have had to be built on wet terrain, drainage has usually been designed to keep the road structures dry (ROADEX 2012).

The presence of water causes different problems in the road structure that are harmful to both road users and road owners. One example is water on the road surface causing traffic safety problems. Water can pond on the road surface increasing the risk of aquaplaning. This occurs particularly during the rainy seasons. If the road surface is wet, it reduces friction and causes longer braking distances. The water on

the road surface can freeze during the nights in certain seasons, making the surface extremely slippery. Sudden slippery sections can catch drivers unaware and may cause crashes.

If water flows uncontrollably on the road surface or if the drainage system has inadequate capacity, it causes flooding and erosion (figure A.1). The places of high erosion risk are culverts. Clogged or too small culverts steer the water towards the road and saturate it until it is destroyed.

**Figure A.1 Heavy rainfall and an inadequate drainage system can cause flooding and erosion around and under the road pavement. Water infiltrating the pavement structures also reduces the stiffness and bearing capacity of the road and exposes the pavement to permanent deformation**



Poor road drainage and moisture are the main causes of permanent deformations in road structures. If the road suffers from permanent deformation, it directly affects a driver's health and reduces traffic safety (Granlund 2008). The presence of water in the road structure can reduce its bearing capacity and result in higher maintenance costs. According to the results of a ROADEX project, improving the drainage condition in critical sections and maintaining it in good condition is the most profitable and sustainable investment in road asset management. A rule of thumb is that good drainage increases the pavement lifetime by 1.5–2.0 times and contributes to reducing the cost of maintenance.

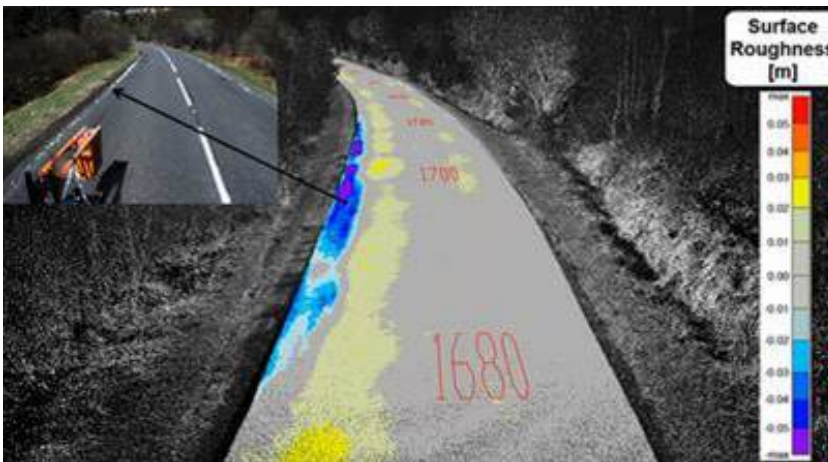
Drainage condition is one of the most critical issues, especially in cold-climate countries, since it can cause frost heaves and permanent deformation during the thawing period. Frost heaves generate unevenness and cracks in the road surface that also decrease traffic safety (figures A.2 and A.3). Frost heave is due to water freezing within the soil and pavement layers, causing them to expand in size until they become bumps in the surface. When this frozen water defrosts the combination of the expansion or the aggregate becoming less dense and the extra water causes significant weakness and ruts.



**Figure A.2** Drainage problems can quite often be related to road cut sections where structures are also thinner and ditches are missing. In such sections water usually infiltrates under the pavement and only a few cold days can cause frost heaves and permanent deformation



**Figure A.3** Grass or soil verges blocking water from flowing away from the pavement are often the main cause of early phase permanent deformation as an example from A83 in Scotland shows



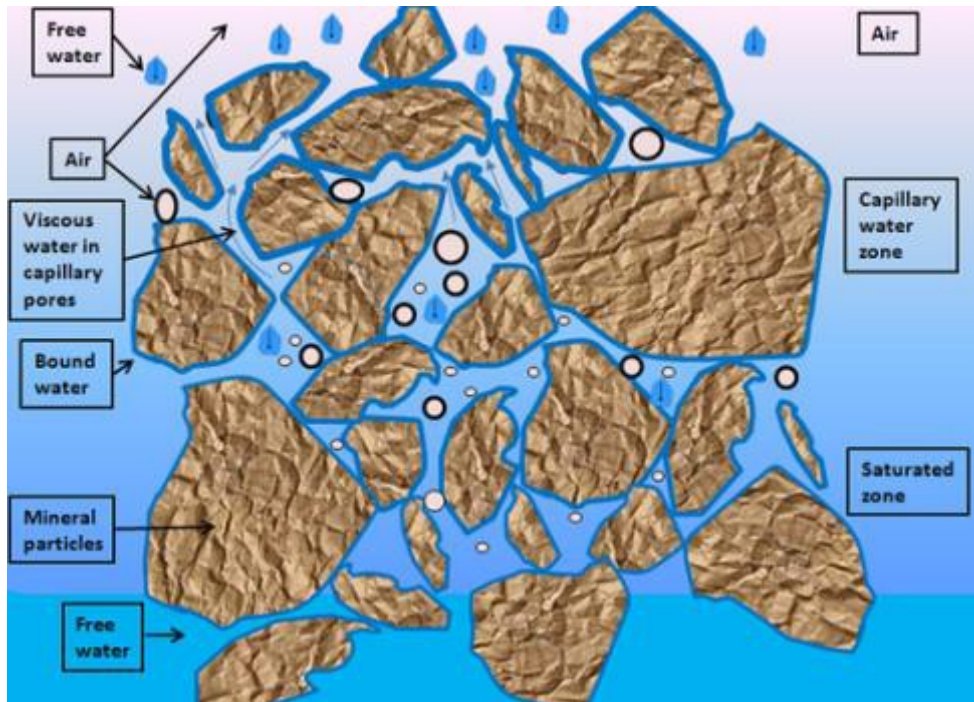
## A3 Water in road materials

### A3.1 General

In road structures and subgrade soils water can occur in all three main states: solid state (ice), liquid state (water) and gaseous state (water vapour). The amount and the state of the water present (ie liquid or frozen) affects the performance of the materials in the road and subgrade soils. Furthermore, the form of the water, the dissolved air content and the content of colloids all have a great effect on the stiffness of materials, their permanent deformation properties and frost susceptibility.

Liquid water in soils and aggregates can be classified as: (1) adsorption water, also called hygroscopic water, (2) viscous water, or capillary water and (3) free water (figure A.4). A simpler classification divides water into two forms (a) bound water and (b) free water.

Figure A.4 Water in soils and road materials (ROADEX 2012)



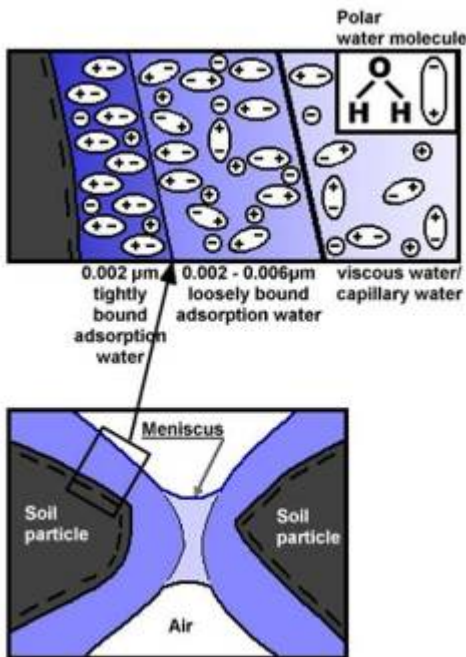
### A3.2 Bound water

Adsorption water can also be referred to as bound water since it can act as a 'binder' between the soil particles producing the tensile strength of the dry material. That is why in some countries dry unbound materials are also called 'water bound' materials. Adsorption water is the first layer around mineral surfaces and it consists of two layers: tightly and loosely bound layers. Adsorption water condenses on the surface of soil particles straight from water vapour in the air. Salt reduces the thickness of this layer, and thus helps compaction of the material. The amount of adsorption water is also controlled by the specific surface area of minerals. The higher the specific surface area, the higher the adsorption water content. However not all the adsorption water is harmful to material performance. For instance, iron oxides can adsorb great amounts of water but this water does not cause performance problems for the aggregates. Even small amounts of organic material adsorb a lot of water but this is not detrimental to the mechanical performance of the material.

The next layer around the adsorption water (water absorbed into the pores of the stone) is usually referred to as viscous water, or capillary water. This water does not respond to gravity. Capillary water can also be divided into 'inner' and 'outer' layers. When compacting aggregates, the optimum water content in road materials is when the inner capillary layer changes to the outer capillary layer. Capillary forces, also known as suction, are also significant factors in the frost heave process in roads.

The air-water interface in soils, referred to as capillary menisci or contractile skin is very important in soil mechanics because of its property of exerting tensile pull. This ability is called surface tension. The magnitude of surface tension depends on temperature; if the temperature increases the magnitude decreases. Menisci also have a great effect on hysteresis behaviour of aggregates and soils, i.e. the fact that materials are stiffer when drying in the same water content compared with when they are wetting.

Figure A.5 Bound water, viscous water and meniscus around mineral surfaces (ROADDEX 2012)



### A3.3 Free water

The water that moves through the aggregate or soil voids under the force of gravity is called free water or gravitation water. The amount of free water has a significant influence in decreasing bearing capacity and that is why road drainage systems should be designed to manage the amount of free water. High free water content also weakens the stability of road edges and causes edge settlements and erosion.

In addition, free water is an important factor in the freeze-thaw process.

The behaviour of material under a traffic load varies greatly based on whether the material is saturated or almost saturated with water compared with when it is unsaturated. In saturated materials the entire pore spaces are filled with water, as is the case for materials under the groundwater table. In unsaturated materials the pore spaces are filled with both water and air. It is important to keep in mind that in these mineral-water-air mixtures the air is the only compressible material, and that under high pressure air can be partly dissolved in water.

Unsaturated soils can be further subdivided into another three groups depending on whether the air phase is 'continuous' or 'occluded'. The classification is made according to the degree of saturation (S).

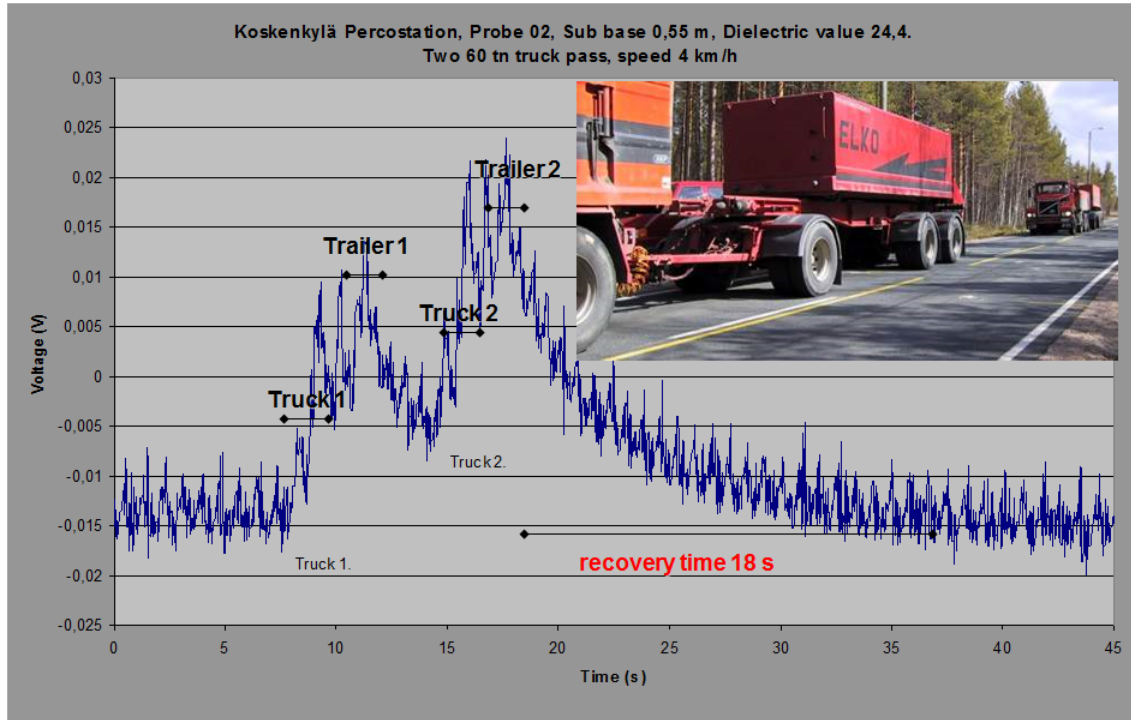
- $S < 80\%$ , unsaturated soil with continuous air phase
- $S > 90\%$ , unsaturated soil with occluded air bubbles
- $80\% < S < 90\%$ , transition zone between continuous air phase and occluded air bubbles.

The 80% limit is an important factor when discussing dynamic loads caused by moving traffic and indicates that road materials do not have to be totally saturated when their performance starts to change.

When a load is applied to a road material or subgrade soil with water filling more than 80% of the voids the air starts to blend with the water. This process of air dissolving into water can be divided into two stages. Initially the air is compressed (Boyle's law) and after that the air is dissolved into the water (Henry's law). The amount of air that dissolves into water is time dependent and when the load is removed

a reverse process takes place that can take a longer time. This process can be used to explain the recovery time and visco-elastic behaviour of road materials (figure A.6).

**Figure A.6 Viscoelastic behaviour of road materials due to air dissolving into water (ROADEX 2012)**



### A3.4 Parameters describing water content in materials

When discussing water and the properties of road aggregates and subgrade soils the most popular term used is 'water content'. Water content is, however, a general term and a clear definition should be always made between whether the discussion is about gravimetric water content or volumetric water content or how the content is measured, ie confined to free water or including bound water. The definitions of gravimetric and volumetric water contents and their measurement techniques are considered in ROADEX (2012).

Lately a third parameter has entered the list of parameters describing water content, especially the mechanical performance properties of the material related to water content. This is a dielectric value of the material, which is also called dielectric permittivity or dielectric constant. Many researchers and engineers with experience of ground penetrating radar (GPR) techniques believe dielectric value is an even better parameter than water content when monitoring strength and deformation properties of pavement structure and subgrade soils and structural performance of the road.

A fourth parameter that has been used to describe water content especially in subgrade soils is electrical conductivity or resistivity. A short description of gravimetric and volumetric water content, dielectric value and electrical conductivity is described in the following.

#### A3.4.1 Gravimetric water content

The gravimetric water content ( $w$ ) of a material is defined as the ratio of the mass of the water to the mass of solid.

The moisture content ( $w$  (%)) is calculated in equation A.1:

$$w (\%) = \frac{M_w \cdot 100}{M_s} \quad \text{(Equation A.1)}$$

where:

$M_w$  – mass of water

$M_s$  – mass of soil solids

This means the mineralogy and density of an aggregate have a great effect on the gravimetric water content, and thus gravimetric water content values cannot be compared between different types of aggregates. Additionally the gravimetric water content does not give any information on the density or degree of saturation of the material. Despite these drawbacks, the gravimetric water content is still the most popular parameter used to describe water content as it is easy to measure.

#### A3.4.2 Volumetric water content

The volumetric water content ( $\theta_w$ ) of a material is defined as the ratio of the volume of water to the total volume (see: equation A.2).

$$\theta_w = \frac{V_w}{V} \quad \text{(Equation A.2)}$$

where:

$V_w$  – volume of water

$V$  – total volume of soil

Volumetric water content ignores the dry density of the minerals involved and is a better parameter for discussing the mechanical behavior of road materials and subgrade soils. This is because volumetric water content can also be presented in terms of porosity, degree of saturation and void ratio (equations A.3 and A.4).

$$\theta_w = \frac{SV_v}{V} \quad \text{(Equation A.3)}$$

where:

$S$  – degree of saturation

$V_v$  – volume of voids

$V$  – total volume of soil

or

$$\theta_w = \frac{Se}{1 + e} \quad \text{(Equation A.4)}$$

where:

$S$  – degree of saturation

$e$  – void ratio

The use of volumetric water content is often more convenient than gravimetric moisture content because it is more directly adaptable to the computation of fluxes, and adding or subtracting water to a soil. These two different ways of calculating moisture content explain the differences between different studies as gravimetric moisture content depends on the bulk density of the material and a rule of thumb is that it is approximately 1.5 to 2 times smaller than volumetric moisture content.



The degree of compaction affects the water content. A compacted material has higher volumetric water content than a loose material. During compaction the volume of the voids (ie pores partly filled with water) becomes smaller as the soil particles are set denser

### A3.4.3 Dielectric value

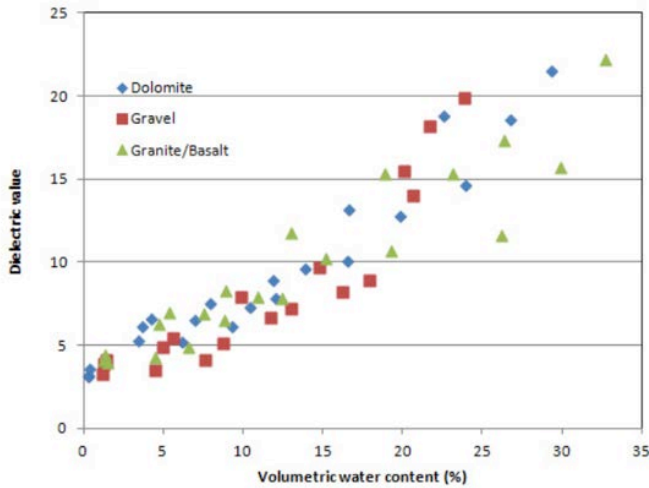
Dielectric value describes a substance's ability to charge or polarise due to the influence of an electric field. After the electric field's effect ends, the substance returns to its initial state. If the material's structure is such that its initial state does not return completely, its polarisation is partly lost. In such cases, dielectric value can be considered a complex quantity, where the real part describes reversible polarisation and loss is in the imaginary part. The most important element in molecular polarisation in road materials and subgrade soil is the water molecule. The extent of dielectric value depends most on how much free water there is in the material because the dielectric value of water is more than 10 times higher than the dielectric value of other road materials. Therefore, increasing water content increases the dielectric value of the material (Saarenketo 2006). Typical dielectric values used in GPR data processing and interpretation are presented in table A.1. Figure A.7 presents the correlation of dielectric value and volumetric water content with different basecourse aggregates.

**Table A.1 Dielectric values air, water, ice and different subgrade soils and road materials normally used in the GPR data interpretation in Nordic countries. Road materials and subgrade soil values, except peat, are those used above the ground water table (Saarenketo 2006)**

Material	Dielectric value
Air	1
Water (fresh)	81
Ice	4
Bedrock (granite)	5-7
Peat (natural)	60
Peat (under road)	40
Clay	25-40
Silt	16-30
Silty sand	7-10
Sand	4-6
Gravel	4-7
Glacial till (moraine)	8-18
Asphalt/other bituminous pavements	4-8 (if slag present 8-15)
Concrete	8-10
Gravel road wearing course	12-14
Crushed base	6-8
Bitumen bound base	6-7
Cement bound base	8-10
Insulation boards (new)	2-2.5
Road structures in average (new/dry)	5
Road structures in average (normal)	6
Road structures in average (wet/old)	7-8
Gravel road structures in average	7-9

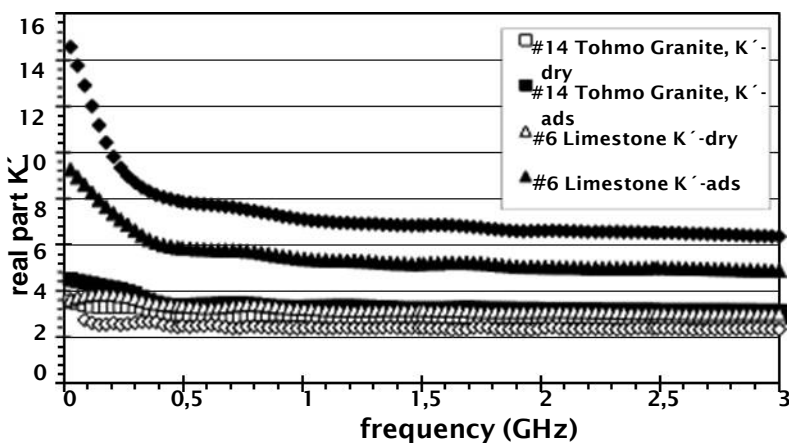
Material	Dielectric value
Frozen road structures (normal)	5
Frozen road structures (wet/old)	6

Figure A.7 Correlation of volumetric water content and dielectric value of Texas basecourse aggregates

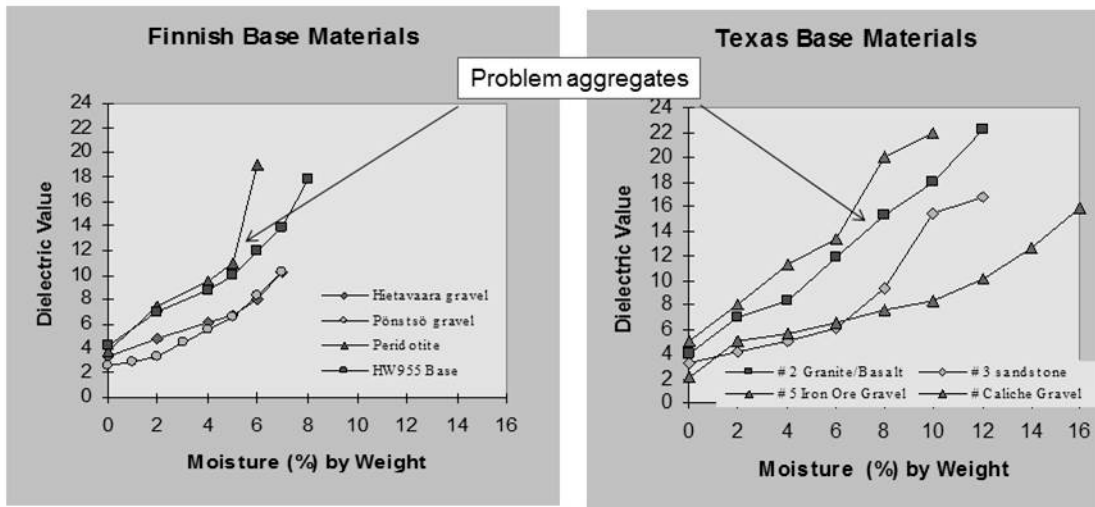


A special feature with the dielectric value of road materials is dielectric dispersion which can be used in locating water susceptible materials and to locate areas with anomalous high water content. Dielectric dispersion means dielectric value on low frequencies is greater than on higher frequencies. Saarenketo (2006) found this dispersion was much higher in problematic materials with high moisture susceptibility than in good quality materials (figure A.8). In this figure Tohmo granite presents a good quality aggregate while granite/basalt aggregate presents a poor quality and extremely water susceptible basecourse aggregate. This means in practice the dielectric value of poor quality basecourse aggregate is higher than well performing aggregates at the same gravimetric water content, as figure A.9 shows. With GPR surveys this feature means low frequency components of a wide band GPR signal return to the receiver antenna a little bit later and this can be seen as wider reflections and ‘ringing’ patterns in the GPR data.

Figure A.8 Real part ( $K'$ ) of the dielectric value of the fines from three different types of basecourse aggregates between measurement frequencies of 30MHz and 3GHz. Measurements with a surface network analyser probe have been made from oven-dried samples and samples balanced with 100% relative air moisture at room temperature (Saarenketo 2006)

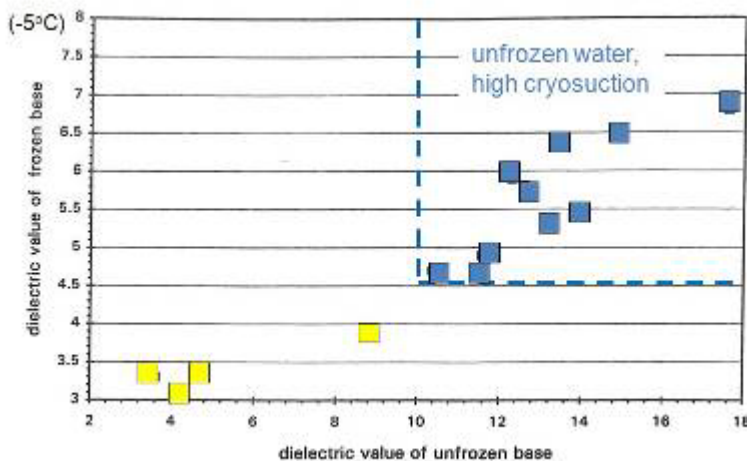


**Figure A.9 Dielectric value of good and poor quality Finnish and Texas basecourse aggregates at different gravimetric water contents**



A special feature of dielectric value is that when free water freezes its dielectric value drops from a value of 81 to a value of 3.8–4.0 and this changes the dielectric properties of frozen material. However not all the water freezes below 0°C temperature. The amount of unfrozen water in frozen ground correlates with cryosuction. This causes negative pore water pressure in the material, which drives water to the freezing front and further leads to formation of segregation ice which can also be called ice lenses. Figure A.10 shows the correlation between dielectric values of frozen and unfrozen aggregates at different moisture contents. Figure A.9 shows high dielectric value relative to moisture % by weight is also an indicator for the high risk of frost susceptibility and risk of permanent deformation during the thawing period of road structures. The critical dielectric value for frost susceptible aggregates is around 9–10.

**Figure A.10 Dielectric value of unfrozen basecourse aggregates and after they have been allowed to freeze at the temperature of - 5°C**



Dielectric value can also be used to measure properties of bound layers. In new hot mix pavements there is no water present and their components are aggregate, bitumen and air. This is why dielectric value of new asphalt depends on the volumetric proportions of asphalt’s components and the degree of compaction. Dielectric value of bitumen is normally 2.8, dry and hot aggregate 5–7 and air 1. In older pavement, water

starts to fill the air voids and then GPR can no longer be used to measure the content of air voids; instead increasing dielectric values provide information about moisture content inside the asphalt.

### A3.4.4 Electrical conductivity

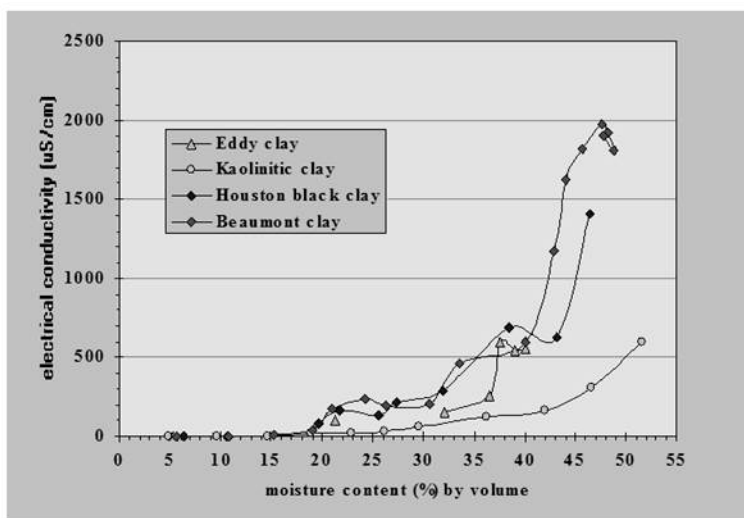
The electrical conductivity of a medium describes the ability of free charges to move within the medium. External electric fields move charges from place to place. Electrical conductivity is mainly a function of water content, mineral quality, ion content and the amount of colloids in the pore water, but also of temperature. Thus, when using electrical conductivity or apparent resistivity to measure water content, it should be kept in mind that it is very material specific and always requires calibration for each material under survey.

Figure A.11 presents electrical conductivity results of Texas soils at different volumetric moisture contents (Saarenketo 2006). The figure shows that in low moisture contents conductivity increases step-wise until free water starts to fill the pores (air voids or air pockets) in the soil. Conductivity does not increase any more once the soils are 100% saturated.

Electrical conductivity is also a good indicator of when a material is frozen. Figure A.16 shows electrical conductivity monitoring results from the Kuorevesi spring thaw monitoring station – when material is frozen the electrical conductivity is very close to zero.

More information about the relationship between electrical conductivity or resistivity and water content are given in this report in section A4.2.6 under *Resistivity-moisture content relationships*

**Figure A.11 Electrical conductivity values of Texas soils as a function of volumetric water content**

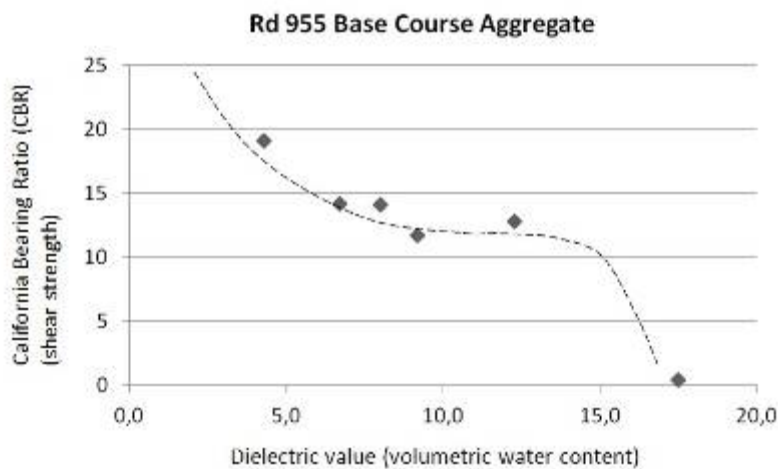


### A3.5 Water and mechanical performance of road structure and subgrade soils

As stated in section A.1, high water content in unbound road materials and subgrade soils always reduces their resilient properties and shear strength. For example, an increase of 1% in moisture content in the most water susceptible materials will reduce the resilient modulus by up to 7.2%. An increase in moisture content of 1% in good quality road materials, on the other hand, will only reduce the modulus by 2.8% (ROADDEX 2012).

Due to matric suction, the stiffness of the materials also increases when they dry. This can be seen for instance in figure A.12 which presents the correlation between the California bearing ratio value and the dielectric value of Rd 955 basecourse aggregate which is known to be a problematic performer.

**Figure A.12 Dielectric value and CBR value, measured using dynamic cone penetrator test, of Rd 955 basecourse aggregate**



## A.4 Water content measurement and monitoring

### A4.1 General

Water content measurement and monitoring is required and should be done in many phases during the lifetime of a road. During the design phase, water content of subgrade soil often defines the compressibility of the soils and also provides information as to what kind of drainage system should be designed. During the construction phase, water content is used for compaction design and control of pavement structure. However, water content should also be monitored during the service life of the road as high water content has an immediate effect on the lifetime costs for road owners. In addition information concerning water content is needed to monitor seasonal changes to support decisions whether or not heavy trucks can use the road network. The same information is also needed after flooding due to heavy rainfall when road structures have been exposed to water.

How water content is monitored depends on what type of information is needed and what kind of measurement or survey techniques are available. In general, water content monitoring methods can be divided into three classes. First class can be referred to as stationary methods and with these methods measurements are made from a previously defined or random selected point or a section. A second category is continuous methods, where data is collected normally from a moving vehicle. The third general class is remote sensing methods where moisture data is collected from aircraft or from satellites. This report will focus mainly on the first two classes and remote sensing methods are described only when discussing hyperspectral methods.

### A4.2 Point methods

#### A4.2.1 Sampling

The Oxford dictionary defines (Oxford University Press 2015) a sample as 'a small part or quantity intended to show what the whole is like'. Consequently, sampling is a process of selection, where the representation of the population is chosen. To achieve high reliability, the process of sampling should be designed. There are many methods described in the literature (eg de Grujiter 2002), but *random* and *systematical* are the most popular ones. In the sampling design the important parameters are layout and



spacing as well as the sample depth. If sampling depths are fixed, the depth is usually set in pairs of 0–15cm, 15–60cm and 0–30cm, 30–60cm (Carter and Gregorich 2007). However, in normal procedures a sample is taken from each representative pavement structure layer, like pavement, basecourse and sub-base. In road diagnostic surveys a special place to take a sample is the top 5–10cm basecourse beneath the pavement because at this depth the material has a high risk of degradation.

No less an important issue is the handling and storage of samples. The types of samples must fulfil the needs of the designed tests. In the case of the road structure investigations the important issues are to ensure that the sample will not dry and not loose small particles on the way to the laboratory. It will ensure the reliability of sieving and water content tests (Carter and Gregorich 2007).

The detailed procedures of sample preparation in the laboratory are dependent on the test type and are described in the respective standards. With respect to water content tests, the variables are the size of the container and the length of the drying. As a primary example, there are water content test standards based on oven drying procedures proposed by ASTM and ISO institutions (ASTM International 2010a; ISO 2004).

**Figure A.13 Sampling of unbound basecourse sample, which is then stored normally in plastic bags**



#### **A4.2.2 Gravimetric method**

Gravimetric method is defined as the mass of water ( $M_w$ ) per mass of dry soil ( $M_{S\ dry}$ ) (Jury and Horton 2004). Mass of air is negligibly small and equal to zero ( $M_a = 0$ ). In the standard procedure, the masses are defined in the process of oven drying thus the calculated moisture content refers only to the 'free' water. In a defined period of time and sufficiently high temperature, the 'free' water is removed. On the contrary, the temperature cannot be too high to prevent the loss of the organic matter and the volatilisation by unstable salts (Pansu and Gautheyrou 2007).

Oven drying test is a procedure where the soil sample is first placed in the standard container ( $m_1$ ), weighed ( $m_2$ ) and dried. The standard temperature is set normally between 105 and 110°C. Exceptions are soils including organic matter and peat where the lower temperature is usually applied to prevent oxidation of organic content (Carter and Gregorich 2007; Jury and Horton 2004). Saline soils are problematic, due to the presence of hygroscopic salts (Pansu and Gautheyrou 2007). After drying, the sample cools down and is weighed again ( $m_3$ ).

The moisture content is calculated from the equation A.5:

$$w = \frac{\text{loss of moisture}}{\text{mass of dry soil sample}} \cdot 100\% \quad (\text{Equation A.5})$$

$$w = \frac{m_2 - m_3}{m_3 - m_1} \cdot 100\%$$

where:

$m_1$  – mass of container

$m_2$  – mass of container and wet soil

$m_3$  – mass of container and dry soil

As an alternative to oven drying, microwave drying might be applied. The procedure is fast, but might produce an uneven temperature inside the material and lead to very high temperatures in some places (Jury and Horton 2004; Topp and Ferré 2002). The differences between oven and microwave drying decrease with the lower value of plasticity of the soil sample (Lade and Nejadi-Babadai 1976). Another method is a sand-bath method used mostly on sites where the oven is not available. Moreover, the calcium carbide  $\text{CaC}_2$  gas pressure meter (known as the speedy moisture tester) method has been developed. One more laboratory procedure is the alcohol method, where the methylated spirit is mixed with the soil and ignites, but due to the high risk of the fire the method is not recommended (Head 1984).

The gravimetric water content (sometimes also called gravimetric moisture content) is highly dependent on the bulk density, thus the different aggregates should not be compared (Jury and Horton 2004). Besides, water content does not provide any information on the density or degree of saturation of the material (Head 1984). The method is also destructive for the road structure due to sampling and does not provide in-situ results.

On the contrary, the gravimetric water content is quite accurate and often used to calibrate the other measurement methods (Dawson 2009). Despite the drawbacks, gravimetric water content is still the most popular parameter used to describe water content as it is so easy to measure. If not stated differently, the gravimetric water content is meant when mentioning *water content* (Dawson 2009).

#### **A4.2.3 Volumetric method**

There are direct and indirect methods of estimating  $\theta_w$ . Direct methods are based on laboratory tests and measuring volumes and masses, while indirect methods are based on certain physical and physicochemical properties of the soil and their relation to the volumetric water content (Yu et al 1993).

The direct methods are thought to be repeatable and give satisfactory results for most soils if the procedures are rigorously respected (Pansu and Gautheyrou 2007). Nevertheless, there might be a need for developing a more precise method for critical soils to limit the uncertainties as argued by Gardner (1986).

The indirect methods of measuring volumetric water content are more common for in-situ tests. Most of them involve measuring some property of the soil that is affected by the soil water content such as electrical conductivity, neutron scattering, or neutron and gamma-ray absorption (Gardner 1986, as cited in Jury and Horton 2004). They represent a wide range of advantages such as in-situ evaluation, minimising the soil disturbance and the possibility of repeatable results. Unfortunately, the methods are highly specialised and require highly trained staff and expensive equipment (Gardner 1986).

#### A4.2.4 Capacitance- based methods

##### *Capacitance*

Capacitance-based methods can also be used in moisture content. Electrodes of capacitance-based sensors form an electrical capacitor, whose impedance depends on the electrical properties of surrounding media. Dielectric value of the material is determined from the change in electrical capacitance due to the influence of the material close to the electrode. Air is normally the reference material used in these measurements.

This report presents the percometer as an example of capacitance-based commercial solutions. There are also many other commercial capacitance-based monitoring techniques such as Soil Scout entering the market.

##### *Percometer and percostation*

A percometer or percostation sensor can be used to measure the dielectric value, electrical conductivity and temperature of a material. In dielectric measurements, the percometer measures the real part of the relative dielectric permittivity. The measurement is based on the change in capacitance caused by the material at the tip of the probe (figure A.14). The capacitance measuring frequency is in the range of 40–50MHz. Conductivity is measured with a dual electrode system using an alternating current of 1–2kHz. The percometer also measures the resistivity between the two electrodes and calculates a specific conductivity value. The measurement is calibrated against standard conductivity solutions. Dielectric measurements, using a tube probe, are reliable when the conductivity of the material being measured is  $<1000\mu\text{S}/\text{cm}$  (Saarenketo and Aho 2005; Saarenketo 2006).

Percostations are used for monitoring seasonal changes and moisture content throughout the year and the results are used, for instance, in deciding the proper time to apply load restrictions and when they can be removed. The percostation differs from the percometer in that it presents the option of measuring the dielectric value, electrical conductivity and temperature through a maximum of eight channels. The measurements are normally repeated at two-hour intervals and the results are saved in the station's memory where they can be read via a wireless modem. Normally the percostation uses solar panels to supply power (figure A.15).

**Figure A.14 Typical percometer sensors: the long tube probe is used for soil measurements, the short tube probe is installed inside the road structure and a surface probe is used to measure dielectric values and electrical conductivity from the material surface**

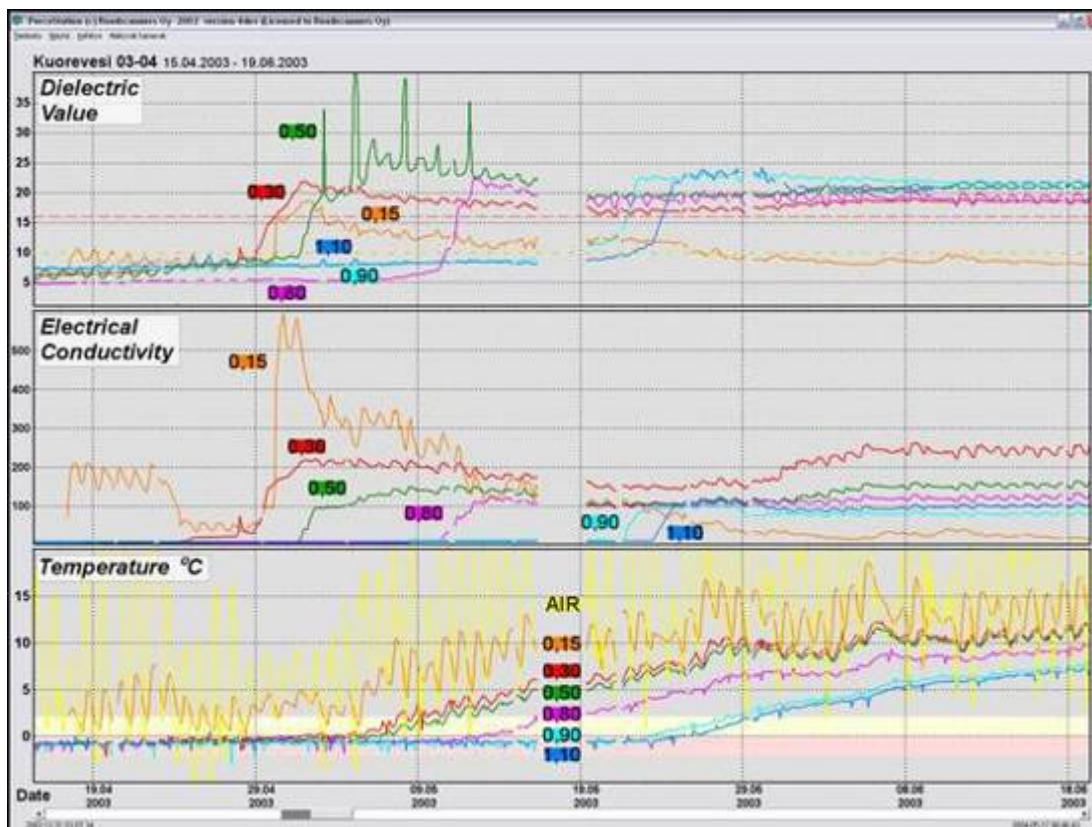


Figure A.15 Percostation installed in road B871 in Scotland



Figure A.16 presents an example of the percystation monitoring results during the spring thaw in 2003 in Kuorevesi, central Finland. The figure shows the dielectric value is highest and above the critical value of 16 immediately after the thawing period starts. At that time electrical conductivity is also very high indicating clay colloids are releasing from particle surface to the pore water and the material is plastic. Soon after that the road surface starts to dry and bearing capacity begins to increase.

Figure A.16 Percystation monitoring results from spring thaw in 2003. The top field presents dielectric value, the middle field presents electrical conductivity monitoring results and the bottom field presents temperature results.



#### A4.2.5 TDR methods

Time domain reflectometry (TDR) has been the most popular method when monitoring moisture content on roads and subgrade soils. The basic principle of TDR is the same as radar as it consists of a radio transmitter that emits a short electromagnetic pulse and the receiver listens to the echo returning from a distant object. TDR systems were originally developed for locating problems with underground cables. When the dielectric value of cable is known, the tester can measure the distance between the break and the measuring point. Conversely, if the distance to the break is known the dielectric value of the cable can be calculated (Hänninen 1997; O'Connor and Dowling 1999). According to Veenstra et al (2005) material properties were measured for the first time with TDR by Fellner-Feldegg (1969), who measured the dielectric properties of various liquids. In 1980, Topp et al (1980) used TDR to measure the permittivity of a wide range of agricultural soils and developed an empirical equation relating TDR measured apparent permittivity to volumetric moisture content. A later innovation was to use TDR to measure soil conductivity simultaneously with soil moisture (Dalton et al 1984).

A TDR measurement is done by first installing two or parallel electrodes, normally steel rods, into the soil or road structure (figure A.17) so they comprise a wave guide. When an electromagnetic pulse is sent to the end of electrodes the voltage between them begins to increase as the pulse reaches the electrode tip. If the lengths of the electrodes are known, the time interval between transmission of the pulse and the instant in which the voltage starts to increase can be used to calculate the mean dielectric value of the material around the electrodes (figure A.18).

Figure A.19 presents an example of moisture monitoring using TDR. However, a mistake with many moisture monitoring publications is the presentation of volumetric water content when the material is frozen. This model does not take dielectric value of ice into account and the volumetric water values presented in these publications are far too high.

The most popular commercial TDR systems used in roads are Campbell scientific systems, TRASE by Soilmoisture equipment Corporation and Tektronix systems. Recently numerous new and cheap systems have also entered the market.

**Figure A.17 Installation of a typical TDR probe in road structure (Hänninen 1997)**





Figure A.18 Basic principle from TDR surveys (O'Connor and Dowling 1999)

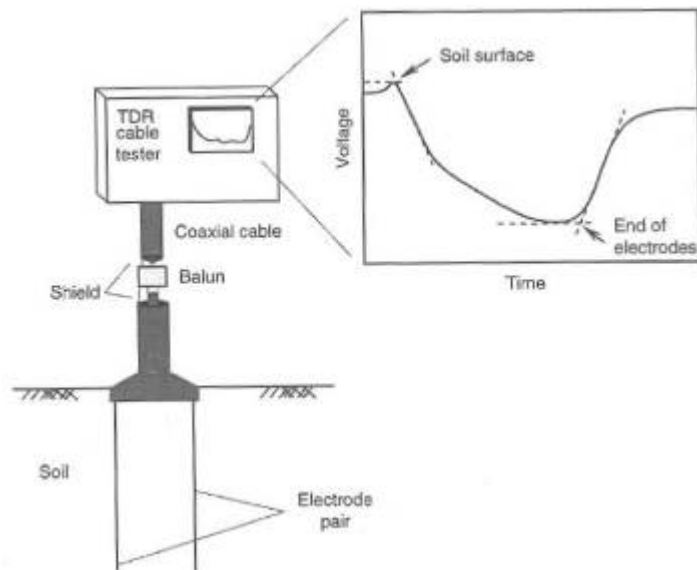
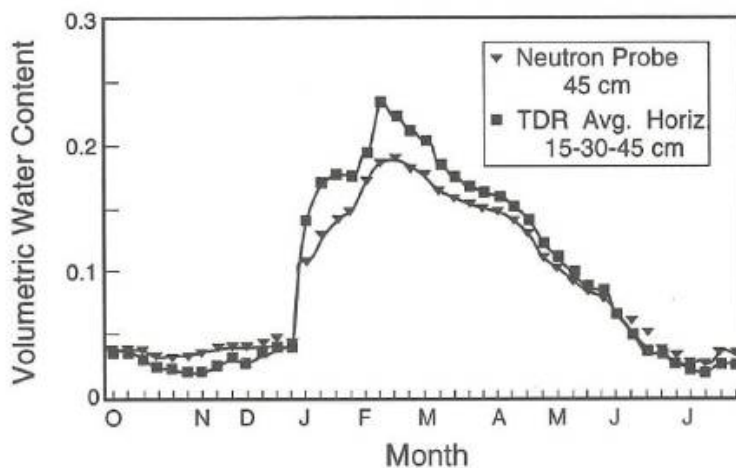


Figure A.19 Example of moisture monitoring data using TDR and neutron probe data (O'Connor and Dowling 1999)



#### A4.2.6 Resistivity- based methods

The purpose of electrical surveys is to determine the subsurface resistivity distribution by making measurements on the ground surface. From these measurements, the true resistivity of the subsurface can be estimated. The effective parameter is resistivity (Ohm-m) or its inverse, conductivity (S/m). The ground resistivity is related to various geological parameters such as the mineral and fluid content, porosity and degree of water saturation in the rock. Electrical resistivity surveys have been used for many decades in hydrogeological, mining and geotechnical investigations. More recently, it has been used for environmental surveys (Loke 2001).

The resistivity method is based on the ground's response to the flow of electrical current. Resistivity is measured in the field using a four-electrode array consisting of two current (I) injection electrodes using either direct current (DC) or low frequency alternating current (AC) and two potential electrodes measure

the resultant potential difference ( $\Delta U$ ). Resistance [Ohm] is calculated applying Ohm's law that directs the flow of current in the ground.

$$R = \frac{\Delta U}{I} \tag{Equation A.6}$$

An apparent resistivity  $\rho_a$  [ohm-m] of the subsurface can be calculated when the potential difference is measured and the geometric factor K is known.

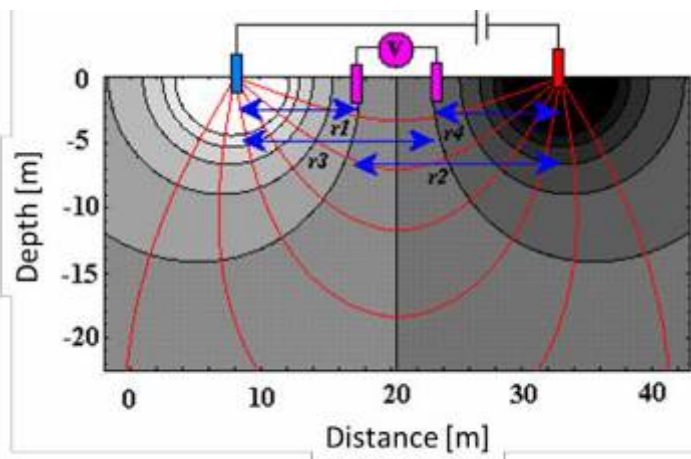
$$\rho_a = K \frac{\Delta U}{I} \tag{Equation A.7}$$

Geometric factor depends on electrode position and is defined using equation 4.4.

$$K = 2\pi \left[ \frac{1}{r_1} + \frac{1}{r_2} + \frac{1}{r_3} + \frac{1}{r_4} \right] \tag{Equation A.8}$$

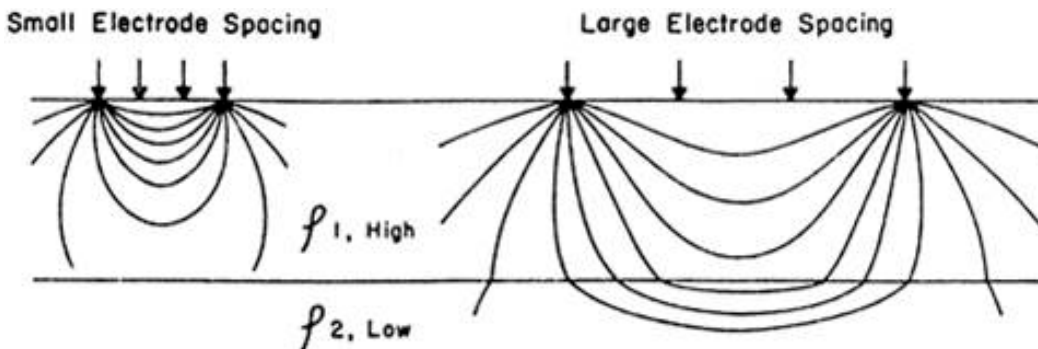
where  $r_1, r_2, r_3$  and  $r_4$  are electrode distances (figure A.20)

**Figure A.20** Definition of geometric factor K in symmetric four electrode system (Boyd 1999, as cited in Silvast 1999)



The depth penetration depends on electrode spacing as presented in figure A.21. As the spacing of the electrodes is increased, there is an increase in the depth and volume of material measured.

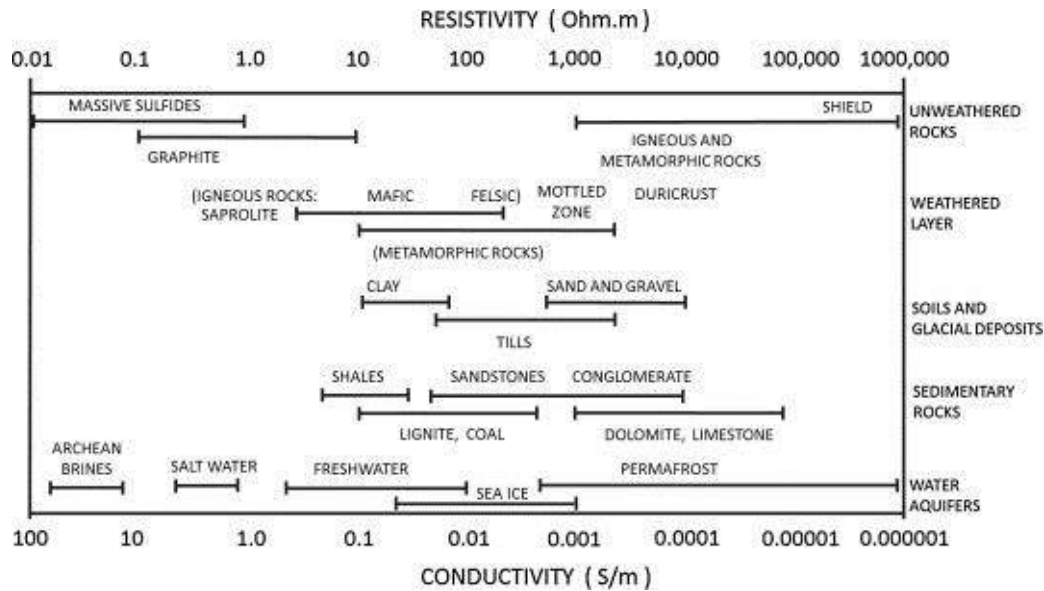
**Figure A.21** Increased electrode spacing samples = greater depth and volume of earth (ASTM International 2010b)



The resistivity of the overburden can vary a lot depending on soil type. Soil is an electrolyte conductor and ground water affects the resistivity value. The resistivity decreases when material gets finer and water content increases. The greatest resistivity values of the overburden in Finland have been documented with

dry gravel and coarse sand (3,000 – 30,000Ωm). Solid (not weathered) bedrock has similar resistivity values. In water-saturated gravel and sand the resistivity value changes between 300 – 2,000Ωm. Silt and clay have the lowest resistivity values that change between 2 – 200Ωm.

Figure A.22 Resistivity ranges for surface waters, rocks and soils (Gunn et al 2015)



### Resistivity-moisture content relationships

In sands and gravels, the current flows around non-conducting grains via ionic migration within the saturating fluid. A clear relationship has been established between resistivity in sands and gravels and various other factors, so an accurate measure of resistivity can lead to the calculation of key soil parameters, particularly pore water saturation, and therefore moisture content. This relationship is often termed Archie's equation (see equation A.9), where the soil resistivity  $\rho_s$  is related to the resistivity of the fluid in the pore space,  $\rho_w$  by the degree of saturation,  $S$ , ie the proportion of the pore space that is filled by the fluid, where  $S = 0$  represents completely dry soil (air filled pores) and  $S = 1$  represents fully saturated soil (fluid filled pores). Archie's equation also shows soil resistivity increases with greater compaction (via the compaction factor,  $\alpha$ , but decreases with increased porosity,  $n$ , where the value of the exponent  $m$  is related to the grain morphology and how it affects current flow (Gunn et al 2015).

$$\rho_s = \frac{\alpha \rho_w}{n^w S^p} \quad \text{(Equation A.9)}$$

where:

$\alpha$  – compaction constant

$n$  – porosity

$S$  – saturation ( $0 < S < 1$ )

$m$  – cementation factor

$p$  – saturation factor

### 2D resistivity imaging

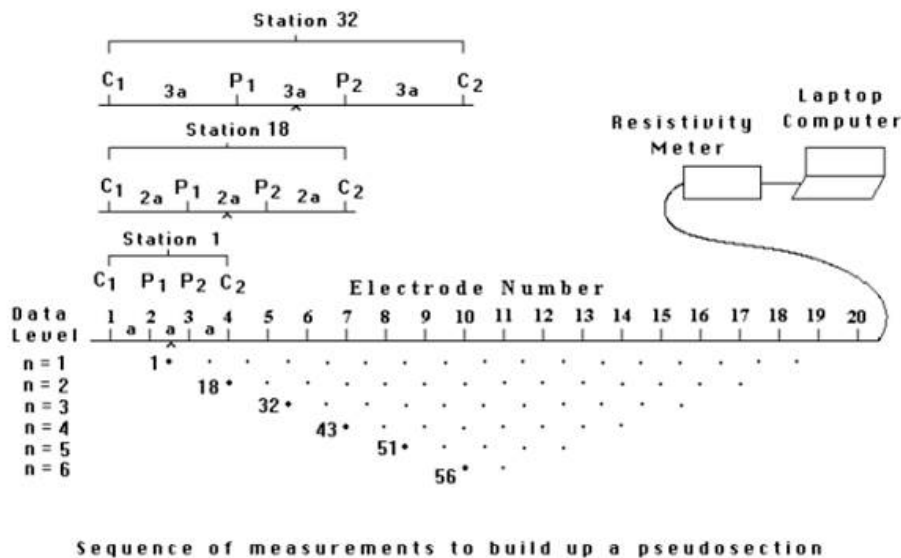
In an application of 2D resistivity imaging, a series of measurements is made between a variety of current electrode pairs and potential electrode pairs. In general, as the distance between the two electrodes increase, the apparent resistivity  $\rho_a$  is measured at greater depths and across increasing volumes of

ground. 2D resistivity imaging produces resistivity information from varying depths in the ground and thus different layers with different electrical properties can be distinguished from the results. Figure A.23 presents the basic arrangement of a multi-electrode 2D resistivity setup.

The typical system consists of a computer-controlled electrode selector, resistivity meter, field laptop, electric cables and steel electrodes (figure A.23). The measurement process is controlled by laptop.

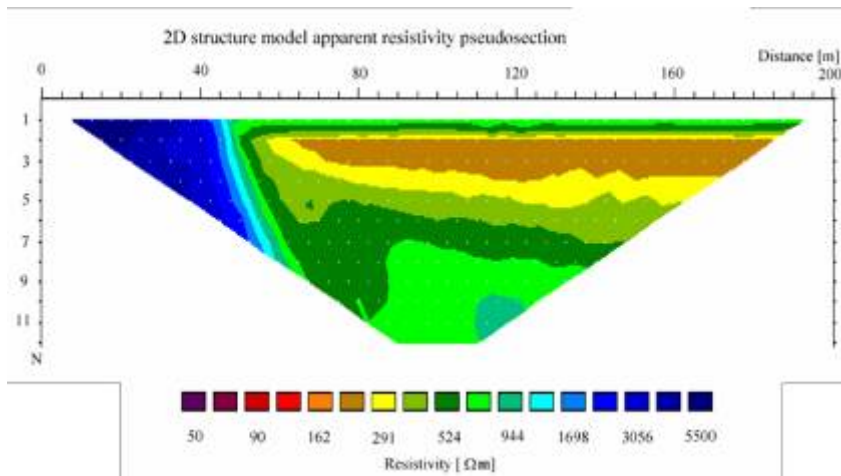
In a multi-electrode survey the measurements are conducted in equal electrode spacing (usually 1–60m) along the survey line. The measuring software activates certain electrodes as potential electrodes and certain electrodes as current electrodes. The software also activates the resistivity meter and saves the result to hard drive. Electrode separation is changed every time a line has finished. The apparent resistivity of the measurement points in different depths can be calculated from results.

**Figure A.23 The arrangement of electrode for a 2D resistivity survey and sequence of measurements used to build up a pseudosection (Loke 2001)**



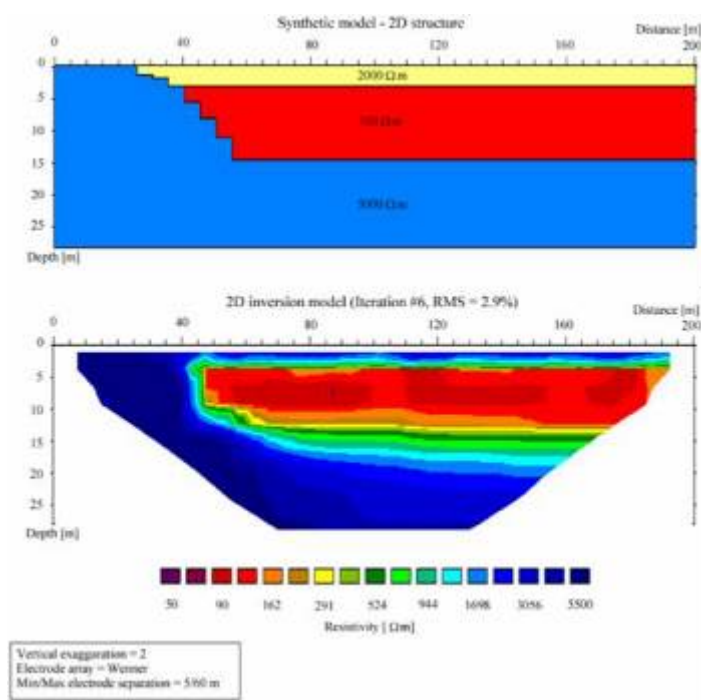
To plot the data from a 2D imaging survey, the pseudosection contouring method is normally used (figure A.24). In this case, the horizontal location of the point is placed at the mid-point of the set of electrodes used to make that measurement. The vertical location of the plotting point is placed at a distance that is proportional to the separation between the electrodes. The pseudosection gives a very approximate view of the true subsurface resistivity distribution. However, the pseudosection gives a distorted picture of the subsurface because the shapes of the contours depend on the type of array used as well as the true subsurface resistivity.

**Figure A.24** The apparent resistivity pseudosection from 2D imaging survey



To define the true resistivity of the ground, the apparent resistivity results have to be modelled using forward modelling and inversion algorithms, the latter being more common in modern resistivity data analysis. Figure A.25 shows the inversion result from the model in figure A.24 (Silvast 1999).

**Figure A.25** Resistivity model above and inversion results below



Resistivity measurements can be done using different electrode arrays (figure A.26). These have advantages and disadvantages, which have to be taken into account when determining the aim of the measurement. Table A.2 shows a comparison between the most typical electrode arrays.



Figure A.26 Electrode arrays used to measure resistivity (Wightman et al 2003)

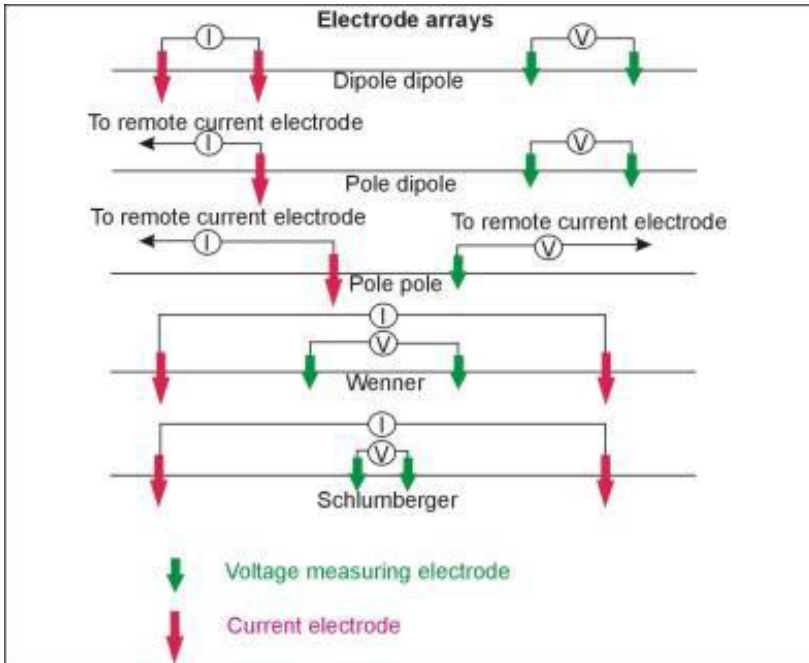


Table A.2 Comparison of most typical electrode arrays. (+ low, ++ moderate, +++ good)

Criteria	Wenner	Schlumberger	Dipole-dipole
Resolution of horizontal layers <sup>(a)</sup>	+++	++	+
Resolution of vertical structures <sup>(c)</sup>	+	++	+++
Depth penetration <sup>(a)</sup>	+	++	+++
Sensitivity to inhomogeneity perpendicular <sup>(a)</sup>	large	moderate	moderate
Sensitivity to near surface inhomogeneity <sup>(b)</sup>	moderate	moderate	large

<sup>(a)</sup> Reynolds (1997)

<sup>(b)</sup> Barker and Moore (1998)

<sup>(c)</sup> Loke (2001)

Over the last 20 years, there has been a steady growth in the number of commercial companies offering systems for resistivity imaging surveys, such as ABEM Instruments from Sweden (ABEM Instrument AB), Advanced Geophysical Instruments from USA (Advanced Geosciences), Geometrics from USA (Geometrics), Iris Instruments from France (IRIS Instruments), Pasi Geophysics from Italy (PASI srl) and Scintrex from Canada (Scintrex).

For resistivity imaging there are two types of systems available: static and dynamic systems. The more common static system enables measurement of multi-electrode array, in which the electrodes are connected to a multi-electrode cable and planted into the ground during the survey (figure A.27). Static measurement is relatively slow and demands a large number of electrodes to get dense data coverage.

**Figure A.27** Example of static multi- electrode array with IRIS Syscal unit

#### A4.2.7 Nuclear method

##### *Neutron scattering method*

The neutron scattering (sometimes also called *neutron attenuation*) method is based on radioactive decay. It is applied in many types of in-situ neutron moisture meters (NMM), especially in widely used moisture-density gauges. The primary application of the method is continuous soil monitoring for agricultural irrigation purposes (Hillel 1980). The topic is widely discussed in the literature by, for example, Hignett and Evett (2002); Gardner (1986); Gardner and Kirkham (1952) and Van Bavel et al (1956).

The gauge is constructed from the source placed in the end of the rod and a detector. The most popular radioactive sources are radium-beryllium and americium-beryllium. They emit a high energy, around 5MeV, neutrons (Jury and Horton 2004). Usually, the rod is placed in a pre-driven hole with the access tube installed at a 150–300mm depth (Dawson 2009). The other device utilising neutron scattering is surface NMM with a back-scatter method (Veenstra et al 2005). These methods are presented respectively in figures A.28 and A.29.

Both methods require correlation, which should be conducted as advised by the equipment producer. Mostly, they require double correlation. First, an external one to the drum count, where the source is lowered down a tube placed in the centre of a drum full of water. The second one is correlation with a soil by a two-point linear regression of volumetric water content. The regression is counted from soil cores and compared with the NMM reading (Charlesworth 2005). For typical applications the correlation recommended by the manufacturer is usually accurate enough.

Neutrons emitted from the source collide with the surrounding soil atoms. Most of these collisions will not affect the initial energy of neutrons, since they are lighter than the surrounding nuclei. The situation changes when neutrons hit the hydrogen nuclei – they can either be absorbed or scattered. After a few collisions, the neutrons lose their energy and reach the velocities characteristic of hydrogen atoms in the soil (Jury and Horton 2004). The process is called neutron thermalisation. As Troxler Electronic Laboratories (2011) reports, the neutron thermalisation requires around 19 collisions with hydrogen.

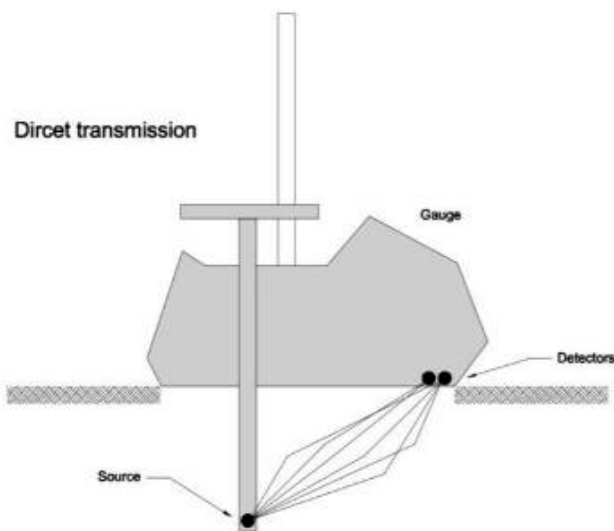
Sensitivity to water content makes this method particularly suitable for water content testing and monitoring (see also figure A.19). The water content is calculated directly on the volume of mass and a large volume of soil can be tested at the same time. The volume of measured material is dependent on its

density and moisture (figure A.30). In dry soils the radius of 0.5m from the emitter might be achieved, when the wet surrounding would limit it to 0.15m radius (Veenstra et al 2005). The most important advantage is the high accuracy (sometimes greater than 0.1%) achieved by the big volume of tested material. With the repeated measurements it is also possible to minimise sampling errors (Hillel 1980).

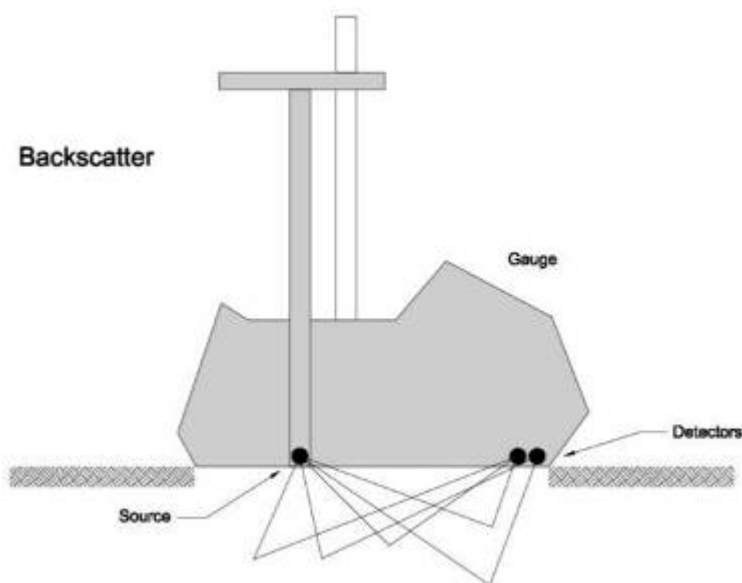
Most of the disadvantages are connected to the radioactive source. Staff must be trained and prepared to work with radioactive elements. Additionally, the equipment cannot be left without surveillance thus the method is not suitable for automated monitoring programmes (Veenstra et al 2005; Dawson 2009). The radioactive source is also costly to maintain (regulation, licensing) and due to its construction makes the devices particularly heavy. The last aspect is the cost of the installation and maintenance of the access tubes (Veenstra et al 2005).

Among others, the commercial manufacturers of NMM are Berthold Technologies GmbH & Co KG; CPN, Inc; Humboldt Mfg Co; ICT International; Seaman Nuclear Corporation and Troxler Electronic Laboratories.

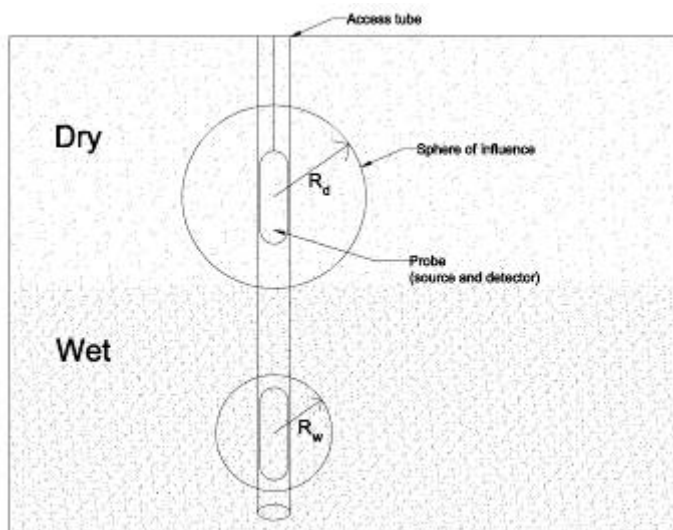
**Figure A.28 Radioactive rod placement in a pre- driven hole**



**Figure A.29 Utilising of backscatter method in the moisture- density gauge**



**Figure A.30** Effect of moisture on measurement sphere of influence. The dry soil allows to test a larger volume of soil (radius,  $R_d$ ) and wet soil smaller ( $R_w$ ). Figure adapted after Charlesworth (2005)



### *Gamma-ray attenuation*

This method utilises the narrow beam of rays sent from the gamma-ray emitter. The source of the radioactive rays is usually the isotope of caesium (Dawson 2009). The gamma-ray attenuation method and neutron scattering are often applied together and provide data about respective density and moisture.

The gamma-ray source is lowered into a pre-drilled tube and the rays are sent through the sample of a known thickness to be received by the detector located at the soil surface (Veenstra et al 2005). On the way, the neutrons are either absorbed or scattered by hydrogen atoms. The amount of scatter is proportional to the total unit weight of sample's material (Dawson 2009). To reach the desired reliability the method requires correlation. The volume of measured soil is about 0.0062m<sup>3</sup> (Veenstra et al 2005). This procedure is true for the soils that do not swell. It is also possible to use the method in swelling soils, but two beams with different energies must be used (Reginato 1974, as cited in Jury and Horton 2004). The main disadvantage of the method is related to the substantial errors due to the surface roughness. Consequently, the method is not recommended for soil testing, but might be used for asphalt construction. As with the neutron scattering method, it has costly licensing and regulations are needed. Despite the drawbacks, the gamma-ray is one of the most established non-destructive methods on the market (Veenstra et al 2005).

Commercially, the method is applied together with neutron scattering in neutron gauges. The manufacturers are listed on the previous page.

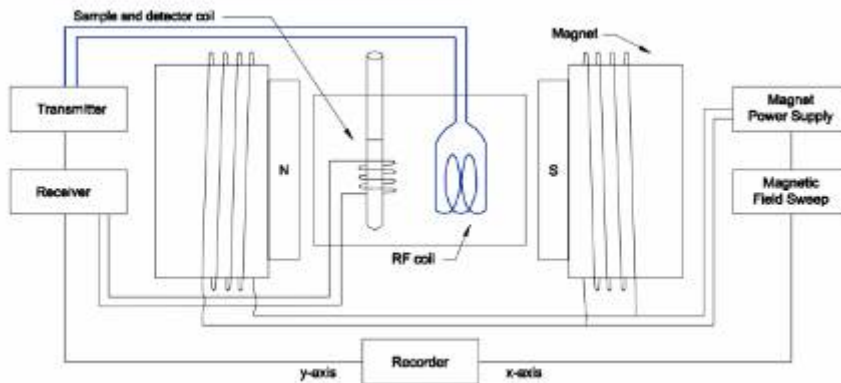
### *Nuclear magnetic resonance*

Although nuclear magnetic resonance (NMR) is mostly associated with medical applications, it has also been used in civil engineering. The method is based on the detection of nuclear species that have a magnetic spin or moment, causing interaction with magnetic fields (Veenstra et al 2005).

The most widely used in NMR applications is hydrogen ( $^1H$ ). It has a nucleus spin of  $\frac{1}{2}$ , large nuclear magnetic moment and the highest natural sensitivity. These make it easy to detect when the spins relax and return to the lower energy state. There are also other soil components as  $^{13}C$ ,  $^{15}N$ ,  $^{27}Al$ ,  $^{29}Si$  and  $^{31}P$ , which can give the NMR response, but they are mostly not used (Veenstra et al 2005).

The method is illustrated in the figure A.31. The sample is placed together with the radio frequency (RF) coil in the constant magnetic field, where the magnetic moment of nuclei rotates. At the same time, the coil produces an oscillating magnetic field, which at certain frequencies can induce a transition between spin states. During that transition some of the spins are placed at their higher energy state. When the RF is switched off the spins return to the previous energy states which causes the response signal. The signal decays in time and this is called the free induction decay (Veenstra et al 2005, Nave 2014).

**Figure A.31 The principle of the NMR method. Source: Becker 1969, as cited in Nave 2014)**



Free induction decay is used in soil moisture content measurements, when its maximum signal height is detected. After that it is necessary to determine the moisture content based on the calibration curve on the same soil (Veenstra et al 2005).

As reported by Wolter et al (2003) the NMR might also be used to determine the properties of water storage and transport in the material and detailed information about its porous microstructure. The application possibilities are numerous, including even the studies of water content in plants and food (Ruan and Chen 1997; Nygren and Preston 1993). From the civil engineering perspective, the most popular applications are connected with the early-stage concrete monitoring, water tightness of building structures and soil moisture content analysis (Wolter et al 2003). In the above cases, the equipment is used in situ and differs significantly from the NMR equipment used in the laboratory, which due to the scope of the research has been excluded from this appendix.

The in-situ instruments may be applied from one side or lowered into a borehole (so called logging). The choice of instrumentation depends on the intended use. The main advantage of the NMR is obtaining fast results. The method is non-destructible and may be used for quality control.

If the samples are uniform, the results are really accurate and precise (Wolter et al 2003).

On the contrary, the NMR cannot be used on the non-heterogeneous samples, which makes it impossible to obtain the most reliable results. In this way the method is not recommended for soil studies. The additional problems according to soil investigation are occurrence of iron and bound water. Iron generates additional errors and must be taken into account during calibration. Bound water cause problems for dry soils where a lot of moisture is absorbed by the fine soil particles. In this case the water nuclei do not respond equally to the RF pulse. To achieve reliable results, it is necessary to determine the moisture content based on the calibration curve prepared on the same soil with different moisture contents (Veenstra et al 2005). All these steps make the method costly and difficult to repeat with a high certainty.

It is very hard to find well-established instruments using NRM that are intended especially for network road surveys. Paetzold (1986) reported the possibility of continued NMR measurements of volumetric



water with 17km/h speed. No further studies have been found using this technique and commercially available instruments needed for this technique have not been developed. The possible options for NMR moisture monitoring are mostly linked with ground water level detection instruments, eg the *Discus* instrument from Vista Clara Inc and *NUMIS Lite* from IRIS Instruments.

### A4.3 Continuous method

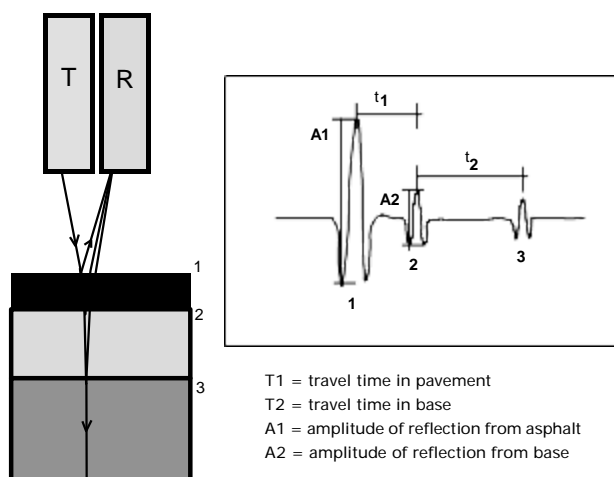
#### A4.3.1 GPR methods – general

GPR systems use discrete pulses of radar energy with a central frequency varying from 10MHz up to 2.5GHz to resolve the locations and dimensions of electrically distinctive layers and objects in materials. Pulse radar systems transmit short electromagnetic pulses into a medium and when the pulse reaches an electric interface in the medium, some of the energy will be reflected back while the rest will proceed forwards. The reflected energy is collected and displayed as a waveform showing amplitudes and time elapsed between wave transmission and reflection (figure A.32). When the measurements are repeated at high frequencies (currently up to 1,000 scans/second) and the antenna is moving, a continuous profile is obtained across the target (Saarenketo 2006). In addition to pulse radar GPR systems, stepped frequency radar systems are also entering the road survey markets.

The propagation and reflection of the radar pulses is controlled by the electrical properties of the materials, which comprise 1) magnetic susceptibility, ie magnetism of the material, 2) relative dielectric permittivity and 3) electrical conductivity. The magnetic susceptibility of a soil or road material is regarded as equal to the value of the vacuum, and thus does not normally affect the GPR pulse propagation. The most important electrical property affecting GPR survey results is dielectric permittivity and its effect on the GPR signal velocity in the material and, as such, it is very important to know precisely how to calculate the correct depth of the target (Saarenketo 2006).

**Figure A.32 Basic principle of GPR and surface reflection technique**

*Horn antenna pair scan*

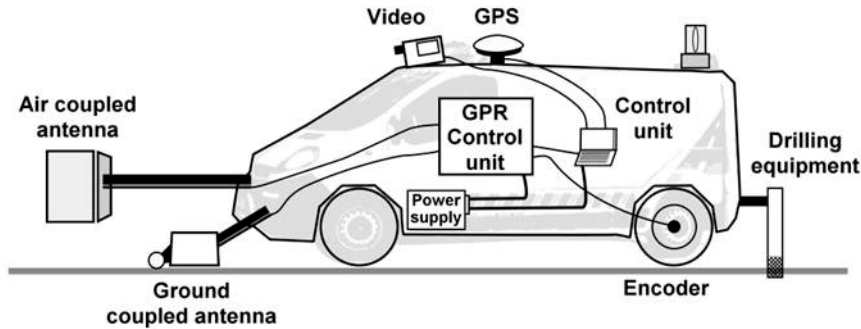


GPR equipment for road investigations consists of several components (figure A.33). Antennas consist of a transmitter, which transmits the pulse into the medium and a receiver that receives the reflected signals. The antennas are controlled by a control unit, where the wavelength and strength of pulse are regulated. In digitisers, the received pulses are converted into digital format. A digitiser can be located in the antenna or in the control or central processing unit. The data collection setup is controlled with data collection software. Some setup parameters include scans per time or distance unit (for instance scan/sec, scan/m), measuring time window (ns), the number of the samples per scan (for instance 512, 1024

samples/scan) and the data format (for instance 16, 32, 64 bit). Calibrated optical encoders (distance measuring instruments) are used to trigger the control unit as the system moves over a distance.

Nowadays, GPS is also an essential part of GPR data collection and this also applies with digital video and the still image capture process. A power supply is of course necessary for operation of the equipment.

**Figure A.33 Typical instrument configuration of the ground penetrating radar survey vehicle**



GPR antennas can be divided roughly into two categories: air coupled antennas and ground coupled antennas. These in turn can be either monostatic, when the same antenna is a transmitter and a receiver, or bistatic, when transmitter and receiver are different antenna units. Most road survey antennas are bistatic, but the antenna elements are built into the same box.

The frequency of ground coupled antennas in road rehabilitation surveys varies from 50MHz to 2500MHz. Their advantage compared with air launched antennas is better depth penetration, though ringing (caused mainly by strong coupling) may cause interference. The ground coupled antennas have better resolution of individual objects than air launched antennas. The depth penetration of 400MHz ground coupled antennas, usually used in road surveys, is normally 1–3m. In highly resistive subgrade soil, GPR signal penetration can be 10–30m with 100MHz antennas.

Air coupled antennas are mainly horn antennas, but lately other antenna types have also been developed. Frequencies vary from 400MHz to 2.5GHz, but the most commonly used central frequency is 1.0GHz. Air coupled 2.0–2.2GHz antennas are also available on the market. These antennas have proven to be effective, for instance, in detecting individual layers in bitumen bound layers, in gravel road wearing course thickness surveys and in locating steel nets. Normally the depth penetration of air coupled antennas is 0.5–0.9m and that is why they are mainly used in pavement structure surveys. During the measurements, air coupled antennas are typically 0.3–0.5m above the pavement surface. Since pulse radar air coupled antennas are suspended in the air, the antenna's coupling does not change when electrical properties of the road surface change. That is why these antennas can also be used in repetitive measurements, where the GPR data quality should not change if and when the properties of the road surface are changing. This makes it possible to calculate quality parameters on the basis of reflection amplitude and frequency response. In addition, air coupled antenna data collection can be done using survey speeds up to 80–100km/h and thus without interruption to the other traffic.

Currently, there are several device manufacturers, which produce GPR equipment suitable for road surveys. The biggest ones are Geophysical Survey Systems Inc (USA), IDS (Italy), Mala Geoscience (Sweden), 3d-Radar A/S (Norway), Sensors & Software (Canada), Utsi Electronics (UK), Penetradar (USA), Radarteam Sweden Ab (Sweden), Geoscanners AB (Sweden). In addition, there are also several smaller companies involved in the business.

### A4.3.2 Air coupled GPR methods

#### *Air coupled reflectivity method*

An accurate estimation of layer dielectric values or signal velocities is a key issue in successful traffic infrastructure GPR data processing. An interpreter, analysing traffic infrastructure data, needs information concerning the dielectric properties of structures and subgrade soils in order to a) calculate the correct layer thickness of structural layers and subgrade soil layers, b) calculate the moisture content, c) calculate the asphalt air voids content, d) estimate the moisture susceptibility and sensitivity which is directly related to permanent deformation of unbound materials, e) estimate the frost susceptibility of subgrade soils, f) estimate the compressibility of subgrade soils, g) estimate the homogeneity and fatigue of bound layers (Saarenketo 2006).

A very popular method for measuring dielectric values of top two surface layers is the surface reflection method (Maser et al 1991), which can be used with air coupled antenna systems. In this method the reflection amplitude from the pavement surface is compared with the metal plate reflection representing a total reflector. By calculating the amplitudes, it is possible to calculate the dielectrics of both layers (figure A.34). Equation A.9 presents the algorithm for the surface dielectric value calculation and equation A.10 for second layer (basecourse) surface dielectric value.

$$\epsilon_a = \left[ \frac{1 + A_1/A_m}{1 - A_1/A_m} \right]^2 \quad (\text{Equation A.9})$$

$\epsilon_a$ - the dielectric value of the asphalt surfacing layer

$A_1$  - the amplitude of the reflection from the surface

$A_m$ - the amplitude of the reflection from a large metal plate (100% reflection case).

$$\sqrt{\epsilon_b} = \sqrt{\epsilon_a} \left[ \frac{1 - \left[ \frac{A_1}{A_m} \right]^2 + \left[ \frac{A_2}{A_m} \right]}{1 - \left[ \frac{A_1}{A_m} \right] + \left[ \frac{A_2}{A_m} \right]} \right] \quad (\text{Equation A.10})$$

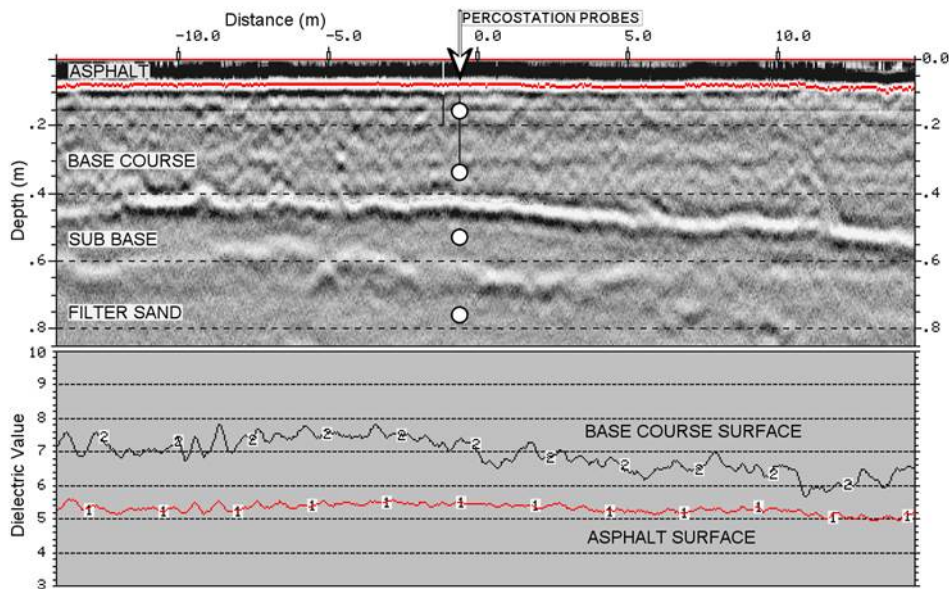
where

$\epsilon_b$  - the dielectric of the layer 2 (base layer)

$A_2$  - the amplitude of reflection from the top of layer 2

These equations have proven to work well for estimating dielectric values for the first layer in homogenous asphalt pavement and most concrete pavements. Equation A.10 assumes that no attenuation of the GPR signal occurs in the surface layer. This assumption appears to be reasonable for asphalt pavements and also provides reasonable dielectric values for the base layer, if the asphalt is thicker than 60mm and there are no thin layers with different dielectric properties (figure A.34).

**Figure A.34** An example of measuring moisture content of unbound basecourse. The measured dielectric values from the basecourse surface (2) are lower where the basecourse is thicker above a very moist sub base layer. This demonstrates the effect of capillary rise. According to measurements from the percystation (see section 4.2.4) the dielectric values of the basecourse at the time of the GPR measurements were about 7–8 and the dielectric value of the sub-base was 16–18. The depth scale of the GPR data has been calculated using a dielectric value of 6 (Saarenketo 2006)



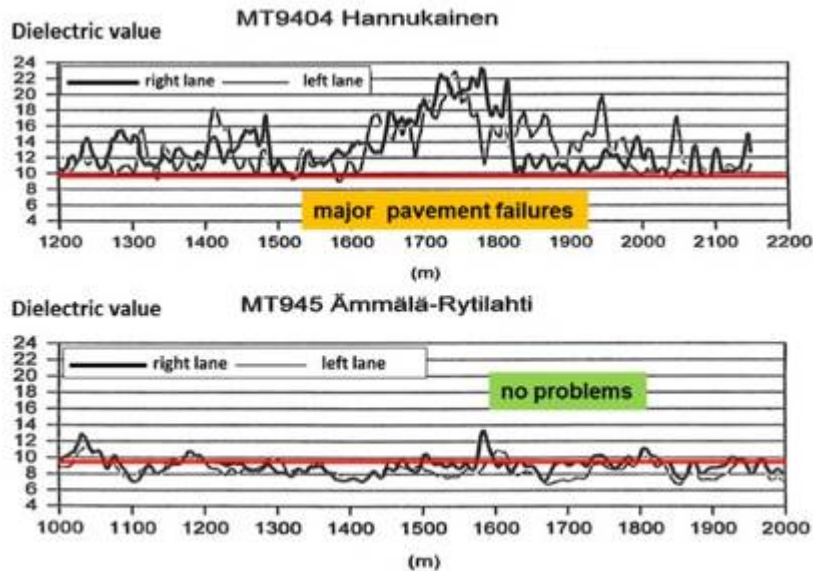
In the USA and in Nordic countries surface reflection methods have been used for years in measuring free water content in unbound base and base in the laboratory tests and as a result of years of experience a general classification of basecourse quality has been made (table A.3).

**Table A.3** Classification of basecourse materials according to their dielectric properties. The limit value for problem base in the USA is 10, while in Finland it has been 9 (Saarenketo 2006)

Dielectric value	Interpretation
<5	Dry and open graded basecourse material with low water adsorption and large voids ratio. Low tensile strength, might be sensitive to permanent deformation
5–9 (10)	Dry base with low water adsorption properties, optimum dry strength properties, non-frost susceptible, non-water sensitive
9 (10)–16	Moist basecourse, still high shear strength due to suction, hysteresis has great effect on strength value, frost susceptible especially if drainage is not working, sensitive to permanent deformation on higher stress levels especially after freeze-thaw cycles
>16	Wet or almost water saturated basecourse, low shear strength above the ground water table, sensitive to plastic deformation under dynamic load, extremely frost susceptible

Figure A.35 presents a longitudinal profile of two road sections in northern Finland. Road 9404 has basecourse built with poor quality base and dielectric values are mainly higher than 10. In sections with poor drainage these values are even higher than 20 and have failed within one year of construction. The other road, Road 945, has a relatively good quality basecourse and dielectric values are above 10 only in sections with poor drainage.

**Figure A.35 Dielectric values of unbound basecourse surfaces from two roads in Finland. The first road, 9404, had major pavement failures shortly after construction and the second road, 945, has a basecourse of adequate quality**



When several survey lines are measured from a road it is possible to prepare maps presenting the dielectric value of the basecourse surface from the whole road cross section as figure A.36 shows. From this map it is possible to evaluate where increased water content can be related to poor drainage along the road shoulder (section 300–1,000m), where poor drainage is affecting basecourse water content throughout the cross section (section 1,000–2,300m) and where water infiltrates to the basecourse through leaking pavement joints (section 3,100–4,200 left and right).

Because water content in the basecourse can have substantial changes during different seasons it is often useful to measure water content two to three times a year to develop a more reliable understanding of how water content leads to permanent deformations in pavement structure. Figure A.37 presents a good example of the results of such surveys. Here a GPR survey was made on road 3662 during the frost thaw phase in spring and another time in summer. In addition the figure shows rut depth maps from both lanes made from laser scanner data. The figure shows that deformation on the edge of the wheelpath (shoulder deformation) has been high in sections where dielectric value is high during the spring thaw period.



Figure A.36 A map of dielectric values of basecourse surface on Highway 6 in south eastern Finland (Roadscanners Oy 2015)

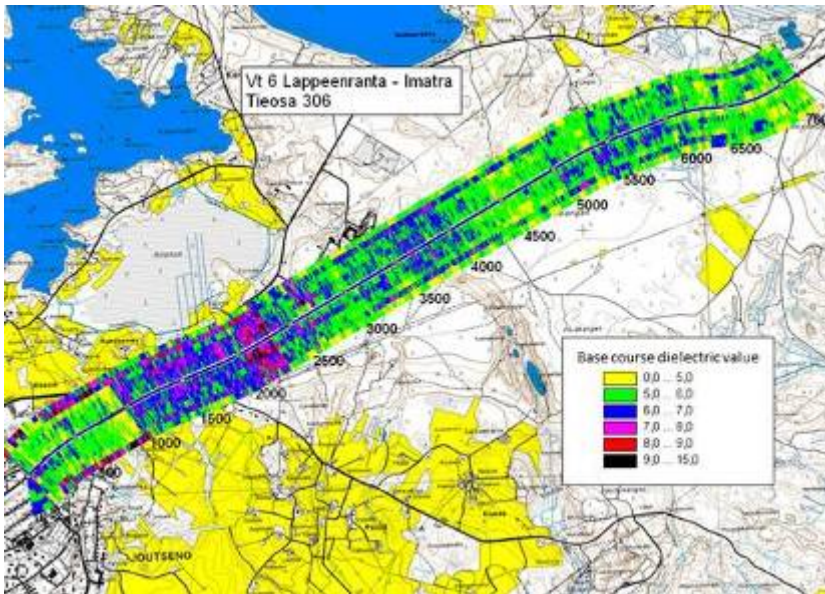
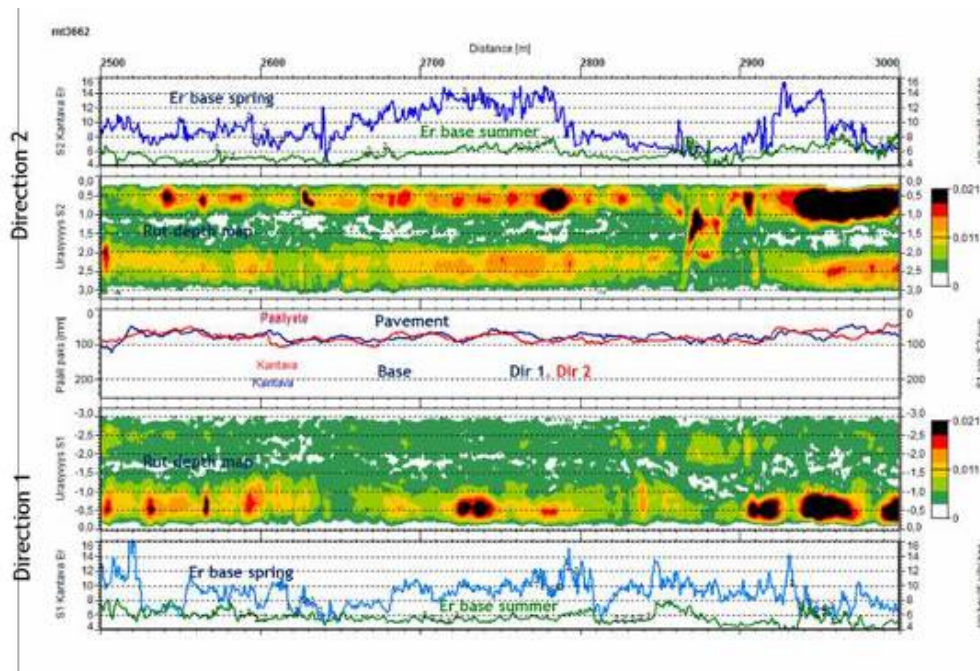
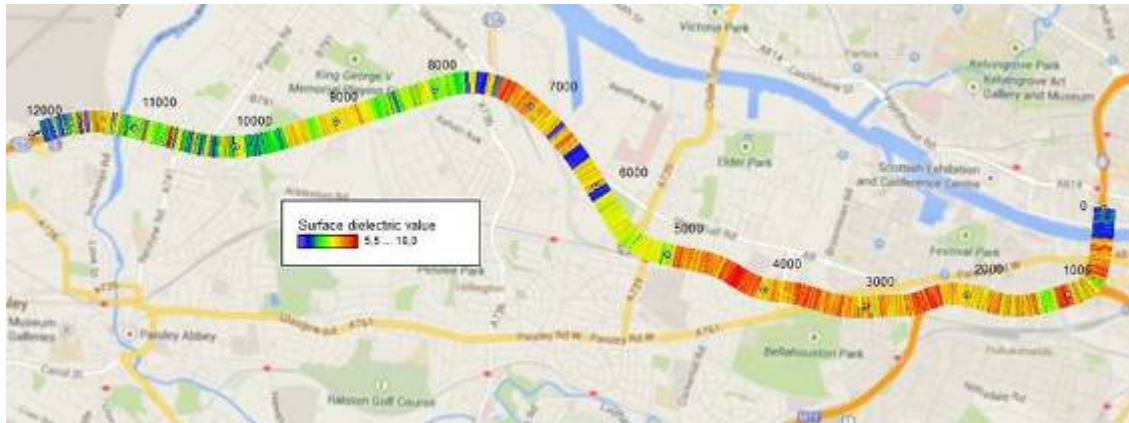


Figure A.37 A Road Doctor diagnostics profile from Road 3662. Uppermost and lowermost fields present results of basecourse surface dielectric measurements during spring thaw periods (blue line) and during dry summer (green line). The coloured maps present rut depths from each direction and the centre area presents pavement thickness calculated from GPR data



Finally dielectric value from old asphalt surface or from concrete road surface can also tell about water content and anomalies and distress in asphalt surface. Figure A.38 presents a map of dielectric value of the asphalt surface of the M8 motorway in Scotland. High dielectric value can mean high water content in asphalt but it can also indicate a special asphalt mixture. Low dielectric values always mean low water content.

**Figure A.38** A map of surface dielectric value of motorway M8 in Scotland (Roadscanners Oy 2015)

#### *Coreless GPR method (two air coupled antennas)*

The problem with the surface reflection method presented above is that it measures the dielectric value only from the asphalt surface and basecourse surface. The thickness of the surface layer, where the information is measured, is roughly 25–40mm depending on the antenna's frequency. This causes problems especially with thicker asphalts and basecourse built with different materials. That is why, in the EU funded TRIMM project, a special coreless GPR method was developed to measure average dielectric value through the whole pavement layer (Hamrouche and Saarenketo 2014).

Coreless GPR is based on measurements using a multi-receiver GPR. The travel time shift of the electromagnetic wave between reflections recorded at each receiver from a specific boundary is determined. This time shift leads to calculation of the road layer thickness and the wave velocity. In addition, the average dielectric value ( $\epsilon_r$ ) of full layer thickness can be calculated without the need for empirical estimation.

This technique is already used in seismic surveys (wide-angle reflection and refraction (WARR) (Vallina 1999). It has been applied with GPR for instance in permafrost sounding (Annan and Davis 1976) or for measuring soil water content (Du and Rummel 1994).

The WARR method gives reasonably accurate wave velocity calculation between the minimum and the maximum antenna offset (Huisman et al 2001; Galagedara et al 2003).

Using the air coupled antennas, the thickness of asphalt and its dielectric value is unknown and the known information is: a) fixed antenna offsets (figure A.39a), b) height of the antennas from each surveyed point (bottom of the antenna to asphalt surface), c) time delay from the receivers on the asphalt layer bottom from each surveyed point (figure A.39b).

The processing of the coreless GPR data is described in figure A.40.

Figure A.39 (a) General schema of dual receiver air coupled (horn) antenna. (b) Scans recorded on receivers 1 and 2 showing time delay of the reflected wave on the bottom of the first layer

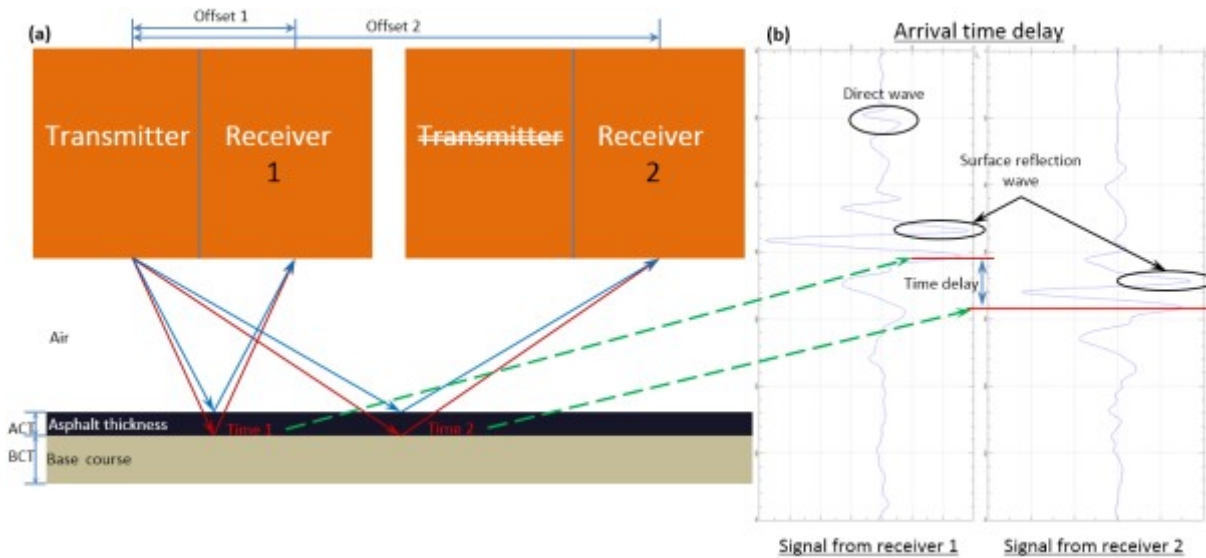
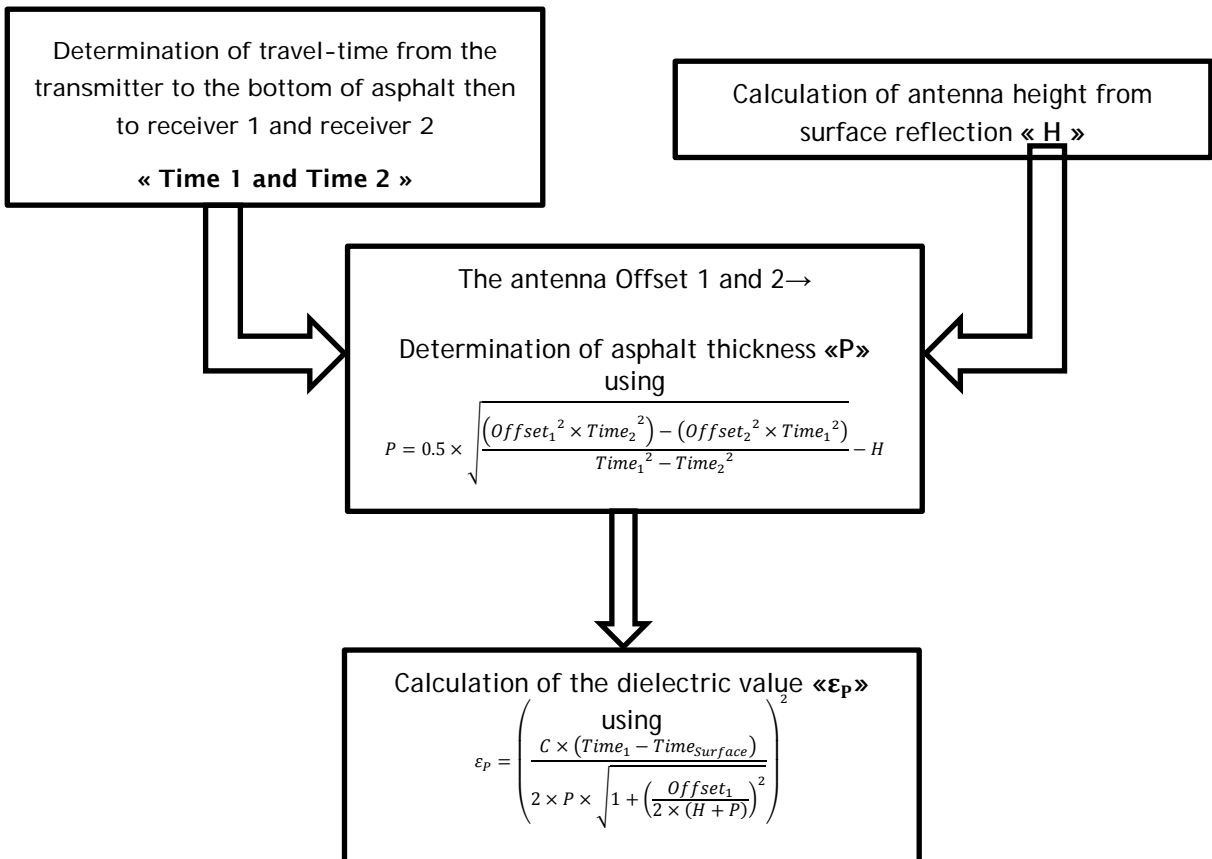


Figure A.40 General description of the dual receiver calculation processing (Hamrouche and Saarenketo 2014)





The coreless GPR method (two air coupled antennas) using a WARR configuration provides accurate thickness information and gives the corresponding variation of the average dielectric value throughout the surveyed road section. A dedicated test field in Finland and results from a road survey in Portugal provided very accurate results. The layer thickness accuracy from the Portuguese data is 3.2% without using ground truth samples (drill core reference data), which represents a substantial improvement on the commonly used technics (Wright et al 2014).

However currently coreless GPR configuration requires the use of two high frequency (2GHz) horn antennas and a modern high resolution GPR unit to guarantee the needed data accuracy for the proposed dual receiver calculations. In addition, the data interpretation is still not 'automated', which means a skilled GPR operator is needed to correctly analyse the data.

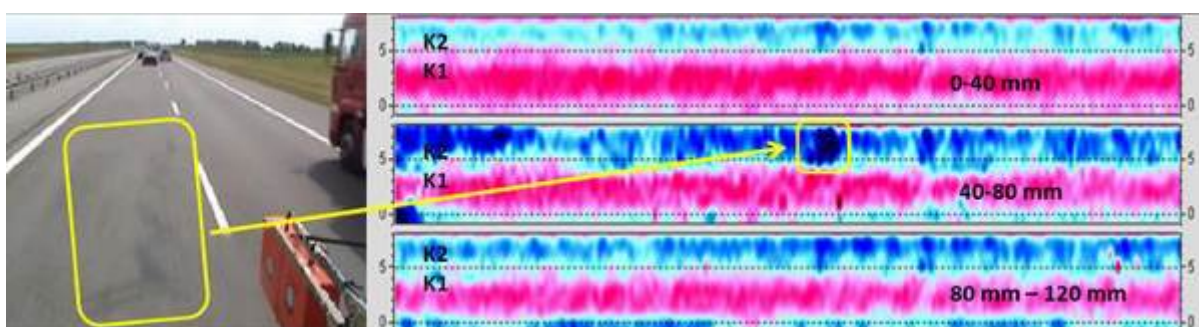
Currently the dielectric value and moisture content can only be measured from the bound pavement layer. In the future additional studies are needed to expand the calculation to the underlying layers. This can be done by combining complex refraction effects and travel time to determine the thicknesses and the specific dielectric proprieties for each layer below the asphalt.

#### *Air coupled amplitude analysis*

When the surface reflection method measures dielectric value from the layer interface and coreless GPR measures the average dielectric value of the whole pavement the amplitude analysis of air coupled antenna data can be used to detect relative moisture anomalies inside certain pavement layers. A good example for such an application is detecting moisture traps inside asphalt or detecting moisture anomalies in a concrete slab. This method cannot be used for measuring absolute water content in the material but for finding areas and depths where water content is higher than average. Amplitude analysis can be made visually from a single survey line but the most useful information is received when time slices are made from several passes.

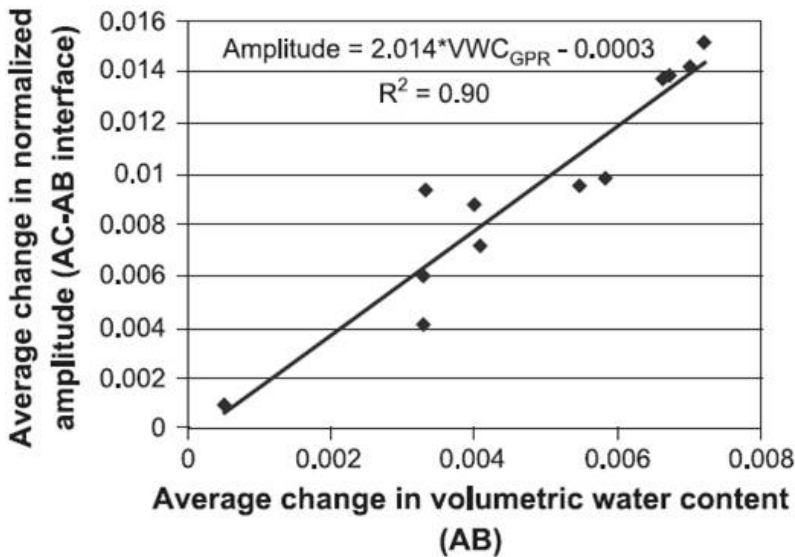
Figure A.41 presents a case where air coupled amplitude analysis using time slices has been used to detect moisture related damages on a motorway passing lane K2. The problem in this case is related to open graded porous asphalt (OGPA) pavement between two dense graded asphalts (moisture trap).

**Figure A.41 GPR air coupled antenna time slices asphalt amplitudes from two lines (K1 and K2) of a motorway. Circled moisture anomaly in passing lane K2 has already caused pavement failures**



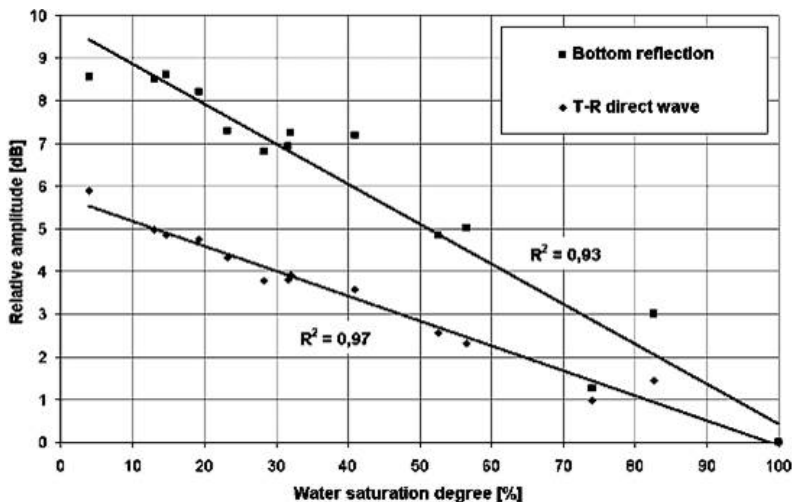
GPR data has been used for water content estimation in pavement materials where GPR amplitude data was used to qualitatively monitor the infiltration of saline water injected alongside a highway (Saarenketo and Scullion 1994). The response of the GPR relative to the water content is visible in figure A.42 by the strong positive correlation between the changes in water content and amplitude.

Figure A.42 Average change in normalised amplitude per survey for the reflection from the AC-AB interface in the undrained pavement, plotted as a function of the average change in water content of the AB (Grote et al 2005)



The same observation can be made when the GPR is used on concrete slab at different water saturation level. Figure A.43 shows the relation between the amplitudes of the two recorded signals and the moisture state of the concrete. Amplitude values are normalised in relation to amplitudes measured on the saturated slab in order to highlight the contrasts between different moisture states. A linear increase in the amplitudes of the two signals associated with the decrease in the degree of pore saturation can be observed. Linear regressions indeed present good determination coefficients ( $R^2 = 0.97$  for the T-R direct wave and  $0.93$  for the bottom reflection). Moreover, differences of 6dB for the T-R direct wave and 9dB for the bottom reflection are quantified between dry and saturated states (Laurens et al 2003).

Figure A.43 Effect of the degree of saturation upon signal amplitude (Laurens et al 2003)



Nevertheless, amplitudes are easily affected by different factors, such as scattering, geometric spreading, transmitter-receiver coupling, radiation patterns and transition/reflection effects. This makes it difficult to estimate a reliable attenuation from time-domain data (Liu et al 1998).



### *Air coupled frequency analysis*

The electromagnetic wave propagation in a loose medium broadens the pulse because of absorption and dispersion due to dielectrically dispersive materials. This leads to a decay of the lower frequency components of a GPR pulse. As the GPR records the arrival times of electromagnetic waves and their amplitudes, the intrinsic attenuation is observed in the signal amplitude from the surveyed material. One of the important factors that cause the attenuation is the presence of moisture in the medium.

Figure A.44 shows the relation between the spectral content of the signal reflected by the bottom of the slabs and the degree of saturation of concrete. The central frequency decreases from approximately 1.18GHz (saturated concrete) to 1.4GHz (dry concrete) as water content increases. This behaviour is explained by the electromagnetic dispersion of concrete due to the presence of water. In concrete, high frequencies are generally more attenuated than low frequencies and the importance of this phenomenon is amplified by the presence of water (Laurens et al 2003).

**Figure A.44** Effect of saturation on the spectral content of the bottom reflection (Laurens et al 2003). The sample presents good quality concrete

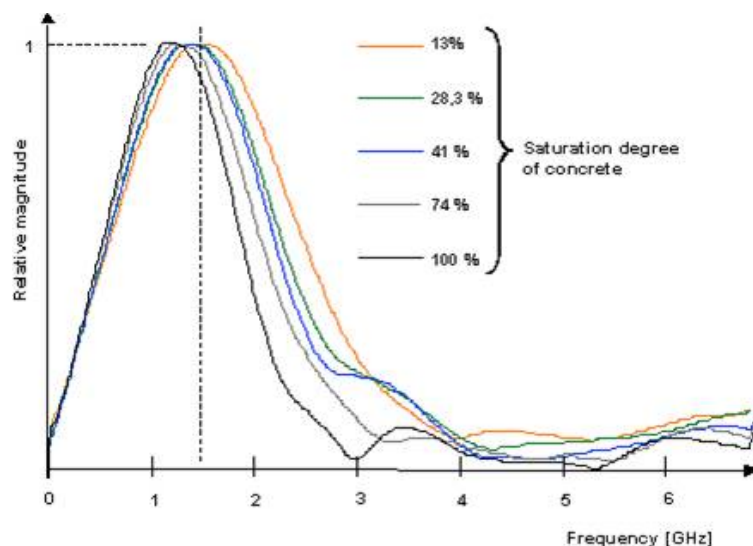
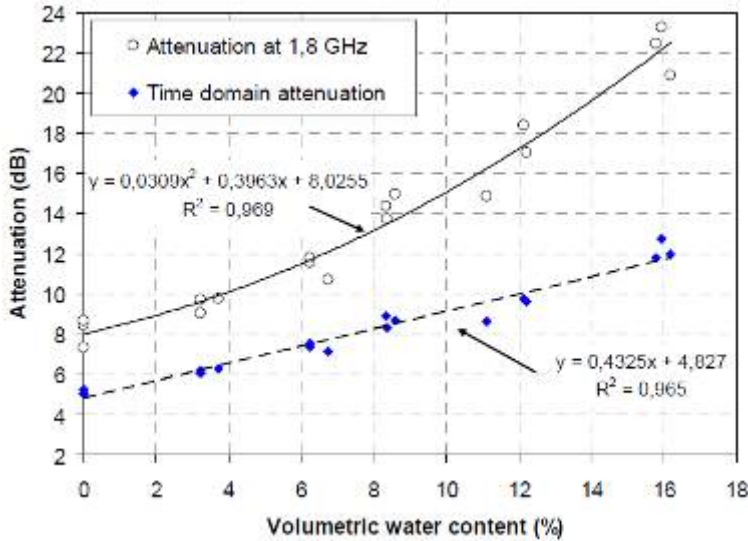


Figure A.45 shows a comparison of two empirical models relating direct wave attenuation and volumetric water content. The first model corresponds to the spectrum attenuation at 1.8GHz that presents the highest sensitivity to moisture. The second model has been reported by Sbartai et al (2006), which correlates the attenuation in the time domain to concrete volumetric water content. The time domain attenuation was calculated from the peak-to-peak amplitude of the direct signal. It can be seen that the frequency attenuation at 1.8GHz is more affected by concrete moisture than the time domain attenuation. Between the extreme saturation states, the 1.8GHz attenuation varies about 14dB whereas the time domain has only 7dB of variation. Finally, despite an accuracy range slightly higher for a frequency attenuation model ( $\pm 1.2$ dB) compared with a time domain attenuation model ( $\pm 1$ dB), the information provided by frequency attenuation regarding concrete moisture is more relevant (Sbartai et al 2009).

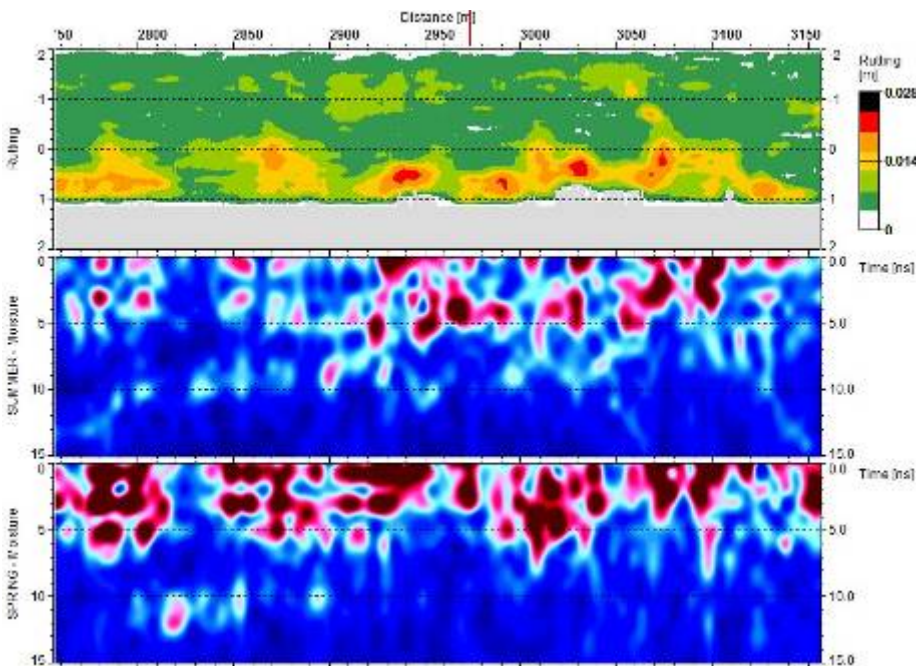
Figure A.46 presents an example of the use of frequency analysis in moisture monitoring of the upper part of the pavement structure. In this case the road was surveyed two times, during the spring and during summer, with 2GHz air coupled antenna. Moisture anomalies were detected using a Fourier transform (used to smooth the data and remove spikes or outliers) to the data and analysing the ratio between high frequency and low frequency components on the data.

Results show a clear correlation between moisture anomalies and deformations in the outer wheelpath where the GPR survey was also conducted.

**Figure A.45 Attenuation function of volumetric water content. Comparison of time and frequency domain attenuation (Sbartai et al 2009)**



**Figure A.46 Rut depth map (top) and moisture analysis using air coupled frequency technique from summer (middle) and spring (bottom) season from road 3662, direction 1 in Finland**



### A4.3.3 Ground coupled GPR methods

#### *Ground coupled WARR method (wide-angle reflection and refraction)*

This technique comes from seismic surveys (Vallina 1999) and is primarily used to define the propagation velocity. It uses a fixed transmitting antenna while the receiving antenna is moved along the survey track and a trace is recorded at each position (the inverse is also possible). The resulting radar diagram provides the travel time as a function of the antenna separation (figure A.47). The linear relationship between the

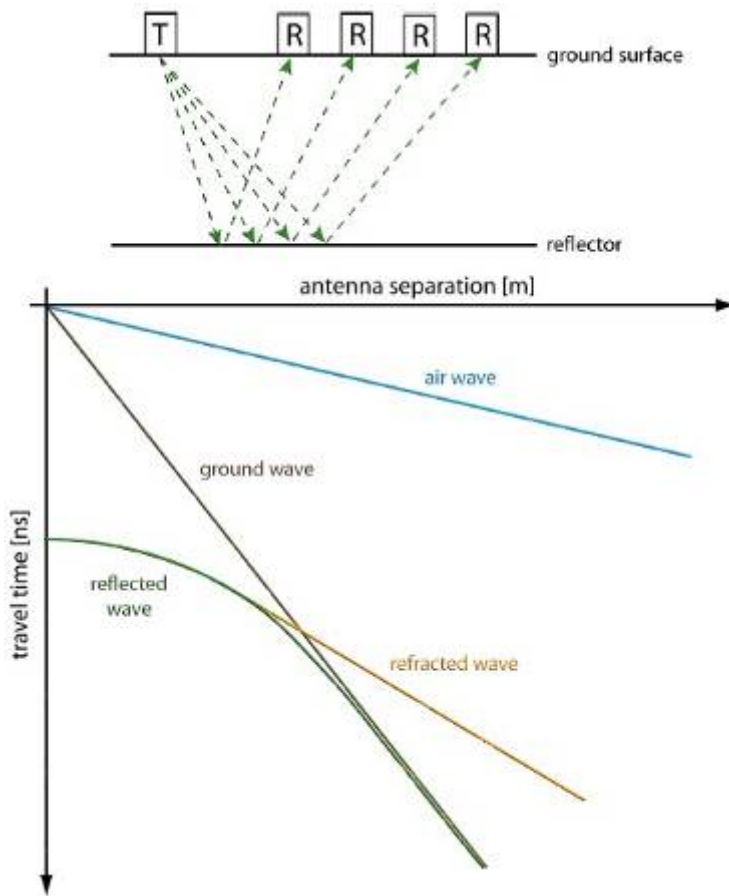
travel time of the ground wave and the antenna separation allow the calculation of wave propagation velocity through the soil.

Once the velocity is calculated, the dielectric propriety of the soil can be calculated using equation A.11:

$$V = \frac{C}{\sqrt{\epsilon_r}} \quad \text{(Equation A.11)}$$

The specificity of the WARR measurements is that the reflection point moves along the reflector by following the moving antenna.

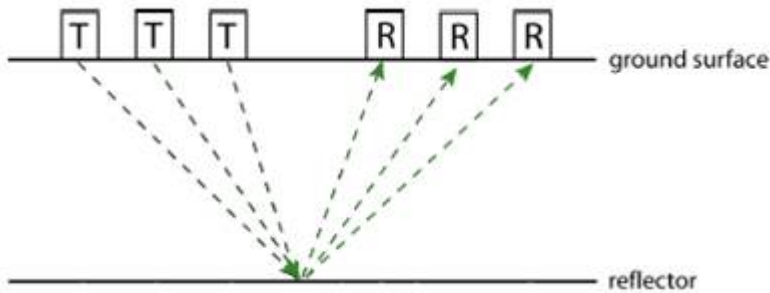
**Figure A.47 Wide- angle reflection and refraction**



*Ground coupled common-midpoint method*

This method is, like the WARR, used primarily to define the propagation velocity. In this method the transmitter and the receiver are moved simultaneously in the opposite direction of each other (figure A.48, JoI 2009).

Figure A.48 Common- midpoint



At each position a trace is measured and the velocity of propagation follow the same principle as for the WARR method. The difference here is that the reflection point is fixed.

*Radar surface arrival detection*

Radar surface arrival detection (RSAD) is a special GPR antenna array developed by the Geological Survey of Finland in 1990. The GPR transmitter and receiver antennas are fixed at a certain distance apart and the first arrival (refraction from the ground) is recorded and examined. Because the wave propagation depends on the dielectric value of the surface, the changes in material properties will be notified in the first arrival time when the antenna array is dragged along the profile. The system was developed for inspection of the properties of topsoil.

In general it can be stated RSAD has proved to be an effective method for numerically characterising and classifying soil materials with variable moisture contents. It is at its best with soils with high fines content (with  $13 < \epsilon_r < 20$ ) (Hänninen 1997). On the road, application of the RSAD method could be used to rapidly locate wet or saturated surface structures after flooding where there is a high potential for permanent deformations or stability problems. Yet the method has not been widely tested on road structures.

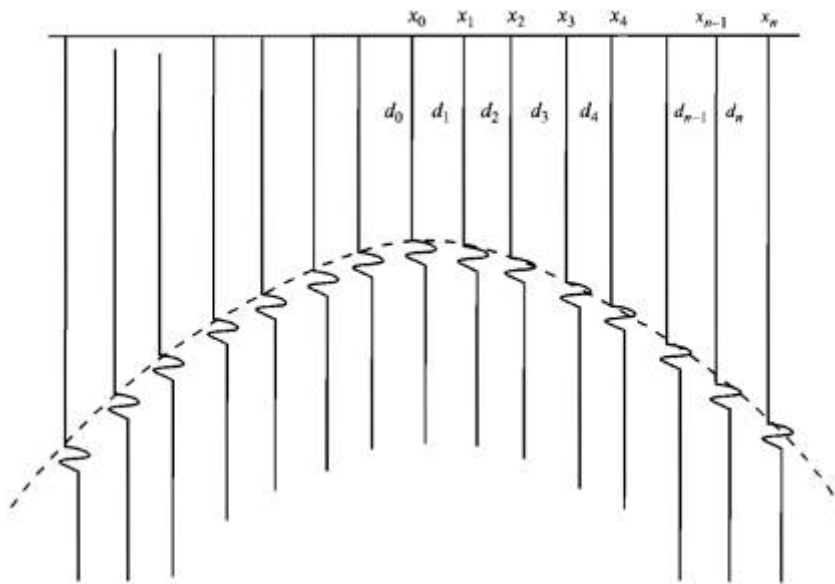
*Velocity calculation from hyperbolas*

The time to depth conversion is a necessary step for a realistic interpretation and for recognising the internal structure with accurate dimensions. One of the methods for estimating the average subsurface propagation velocity, or dielectric value, is the hyperbolic velocity matching (hyperbolic spreading function) (Jol 2009).

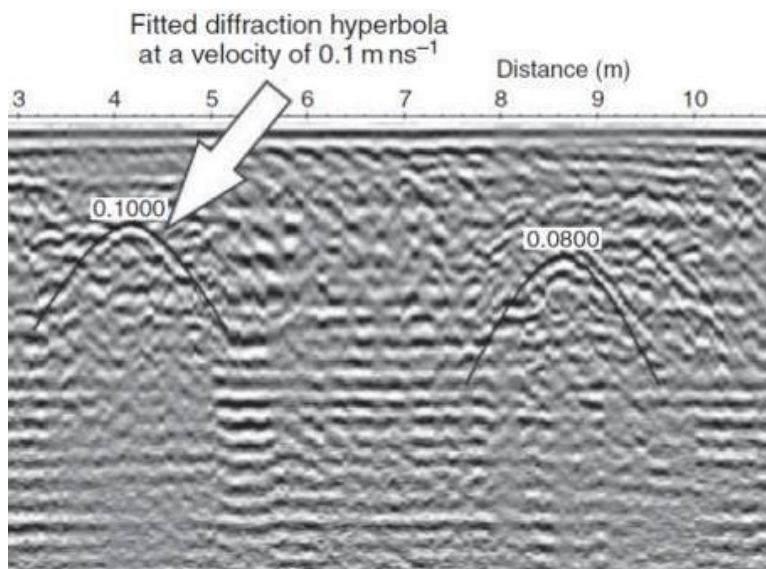
The hyperbolic function (figure A.49) can be fitted and the velocity calculated using equation A.12 (Daniels 2004):

$$V_r = 2 \sqrt{\frac{x_{n-1}^2 - x_0^2}{t_{n-1}^2 - t_0^2}} \tag{Equation A.12}$$

The dielectric value  $\epsilon_r$  can be directly calculated using equation A.11.

**Figure A.49 Hyperbolic spreading function (Daniels 2004)**

Hyperbolic matching can be performed on any section that contains diffraction or reflection hyperbola and is achieved by matching the ideal form of a velocity specified hyperbolic function to the form of the observed data (Jol 2009). Figure A.50 presents an example of two hyperbolic functions fitted to diffraction hyperbola.

**Figure A.50 Example of hyperbolic velocity matching (Jol 2009)**

#### *Ground coupled amplitude analysis*

As with air coupled GPR amplitude analysis, ground coupled amplitude analysis is an easy way to locate moisture anomalies under roads. The idea of the analysis is to highlight bigger or lower amplitudes in the 2D GPR profiles, in 3D GPR surveys through single survey line analysis or using horizontal time slice analysis. In most cases higher amplitudes in homogenous structure can represent higher moisture content. However, with high chloride content this can be vice versa. That is why the analysis has to be made carefully judging whether there are other possible sources of increase in amplitude levels, such as actual structural or material changes.



Figure A.51 presents an example of a 3D GPR survey tracking the anomalous water flow under the road structure. The site is a major road in Sweden, crossing a city. The environment is an underpass, a road cut that has had problems with bumps and pavement distress. The survey was made using a 3D stepped frequency radar and multi-channel antenna. The whole width of the road was surveyed with 7.5cm antenna spacing. Amplitude maps were made to evaluate areas with anomalous moisture and moisture flow under the road (yellow arrows). The reason for the problems was found to be a leaking water pipe in the upper left side of the survey area.

**Figure A.51 Amplitude map from a major road in Sweden. The red colour represents stronger reflections, which has been interpreted here to indicate high moisture. Yellow arrows show the estimated water flow in the road structure. The surrounding terrain supports the idea of the suggested water flow.**

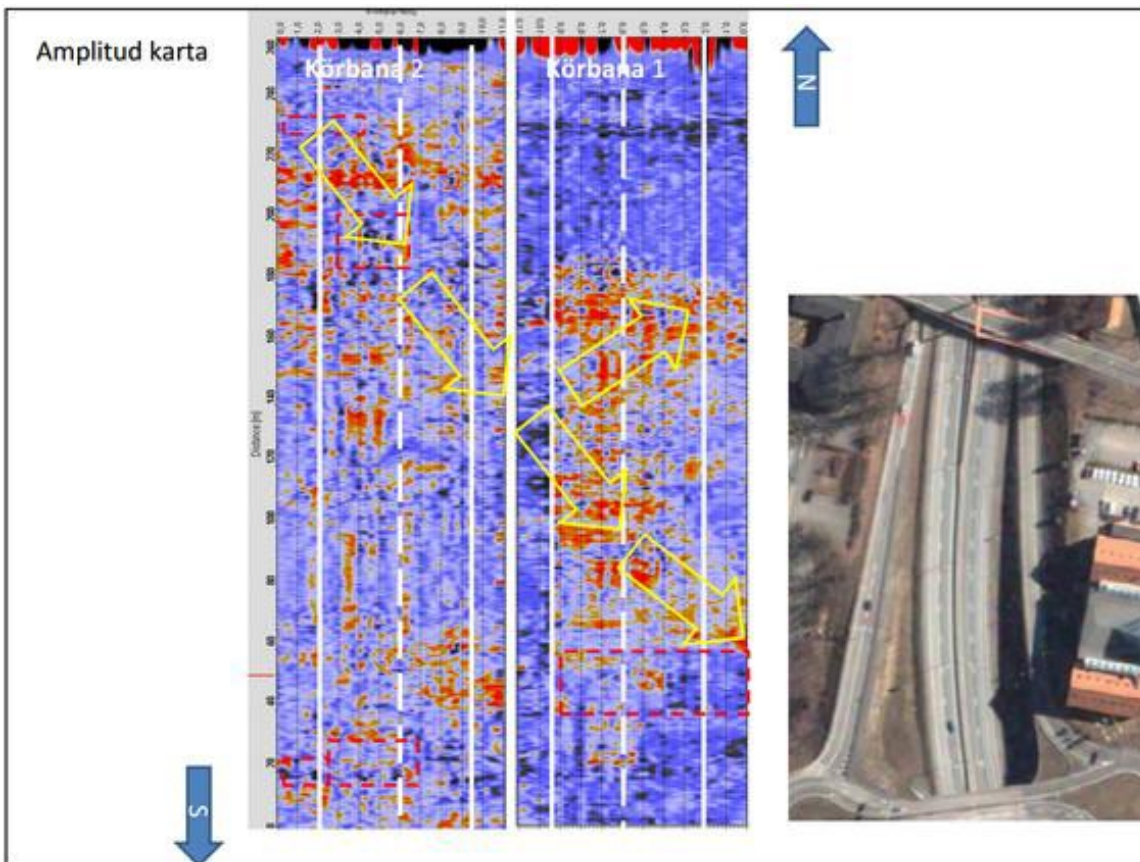
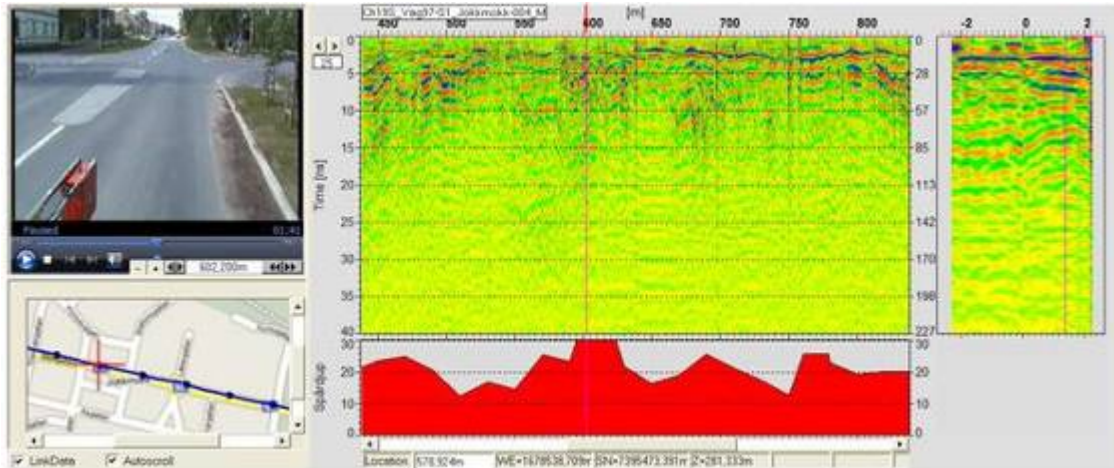


Figure A.52 presents another case from a small Swedish municipality. The pavement close to the street crossing suffered from rapid deterioration, fast rut growth and increased roughness. The moisture analysis was made using same type of 3D GPR setup as in figure A.51. The results clearly show the correlation between increased amplitude levels indicating high moisture and high rutting values. The 3D radar cross section, as seen on the right in figure A.52, clearly shows moisture accumulated in the right edge of the road. This shows the longitudinal gradient of the pavement on the right edge is not big enough to ensure water flow to the closest rainwater well.

**Figure A.52** Road Doctor view of a road in Jokkmokk in Sweden with moisture problems. The GPR view above shows a single longitudinal line (left) and shorter GPR data (right) presents a cross section from point 600m (red line). The lowest red data presents measured rut depths.



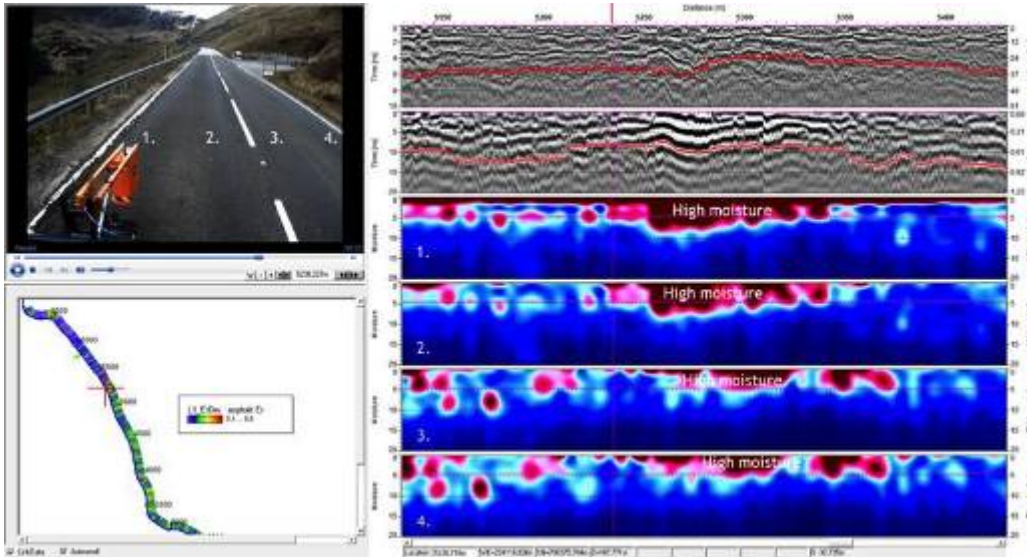
#### *Ground coupled frequency analysis method*

The theory behind frequency analysis method with ground coupled antenna has already been explained. However, this methodology is even more suitable for ground coupled antennas because their frequencies are normally lower and they more easily measure the dielectric dispersion effect below 400MHz frequency bands. In addition, depth penetration of ground coupled antennas is generally greater and thus information from the moisture anomalies can be collected and analysed even from deeper road structures and subgrade soils.

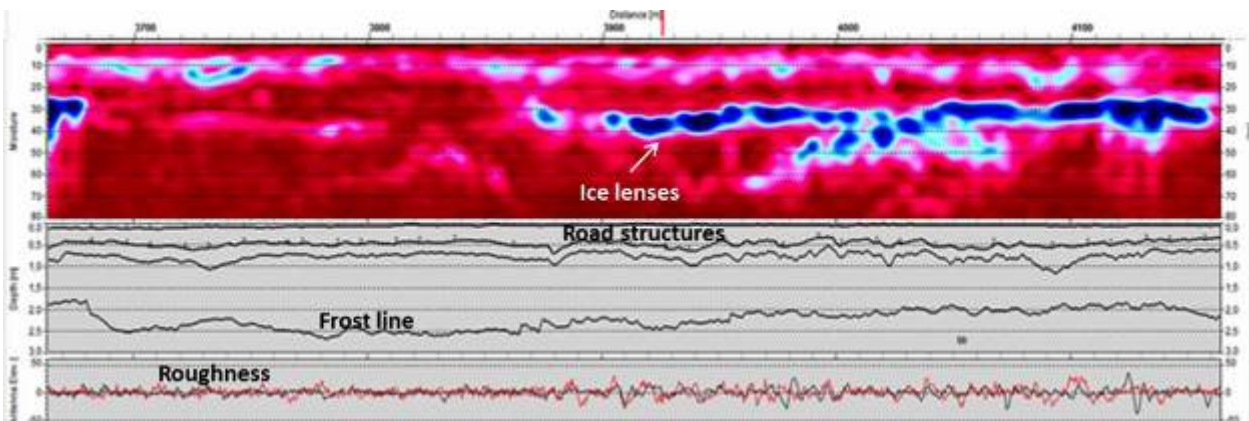
Figure A.53 presents an example of the use of ground coupled GPR antennas in detecting moisture anomalies that can be related to slope stability problems. In this case a clogged main road culvert has resulted in the road structures around the culvert becoming saturated with water, which has reduced the shear strength of the road and caused further shear failures in the road embankment built on the side sloping ground.

Another popular application where this frequency analysis method has been used is in the detection of segregation ice, ie ice lenses in frozen ground, which indicate potential frost action damages and permanent deformation problems of the road structure under heavy trucks during the spring thaw period when these ice lenses are thawing (figure A.54). The frequency response of unfrozen water in frozen material differs substantially from the totally frozen or unfrozen material and thus can be clearly seen in the data. The correlation of the roughness data is very good in the presence of ice lenses.

**Figure A.53** Example of moisture analysis and diagnostics. In this case a damaged or clogged main road culvert is causing water to infiltrate the road structure. The top field shows the 2.0GHz air coupled GPR data (pavement bottom interpreted), the second field shows the 400MHz ground coupled GPR data (total structure thickness interpreted). The last four fields present the relative moisture content of the road on different survey lines calculated from 400MHz ground coupled data.



**Figure A.54** Example of detection of ice lenses in frozen road structure and subgrade soil. The top field present frequency analysis data based on 400MHz antenna, the middle field presents interpretation of road structures and frost line and the bottom field presents roughness information of the road collected using GPR horn antenna ‘bouncing’ data.



*Dielectric value back calculation from ground truth*

Back calculation of dielectric value and moisture content has been one of the most common GPR calibration techniques. It uses drill cores or other ground truth calibration data from the surveyed road to calculate the dielectric value of different layers. These values are then used in the interpretation of the GPR data. Drill cores can be taken at some specific locations or at a regular interval along the surveyed road.

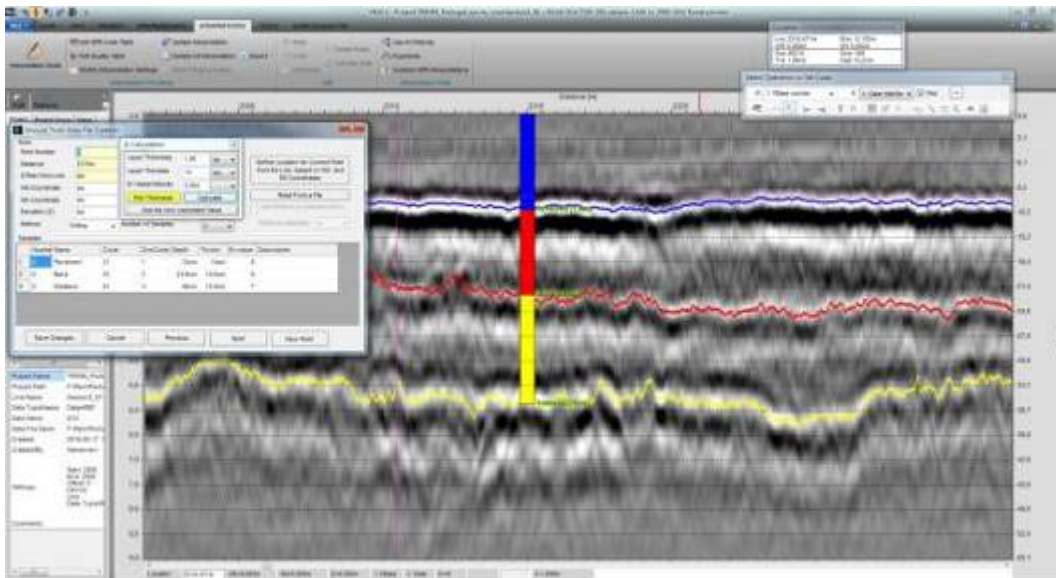
The basic principle of this method is very simple. GPR measures the propagation time of the electromagnetic wave reflected on the interfaces between the different road layers and the thickness information from the drill cores enable calculation of the wave velocity  $V$  at each layer. The speed of light dielectric value and moisture content can be calculated.



This GPR calibration method provides accurate results if the electromagnetic properties of the road layer are constant. On the other hand, drill cores can be very useful to calibrate and clarify suspicious locations already identified in the GPR data and because of that this method also provides very limited information about the moisture changes in the road structure. However, if water content is analysed from ground truth samples the system can be used to calibrate the data collected using other GPR methods.

Figure A.55 shows the calculation of the dielectric value  $\epsilon_r$  and the incorporation of drill core data into the GPR data using RoadDoctor® software.

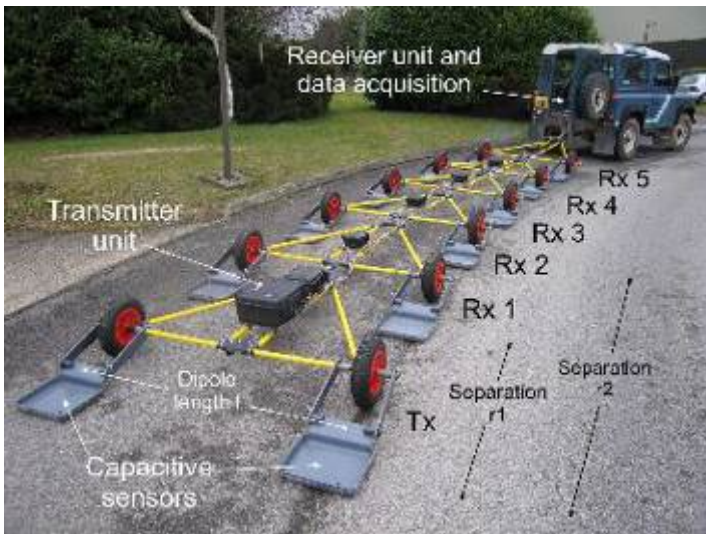
**Figure A.55** Calculation of the dielectric value ( $\epsilon_r$ ) and the incorporation of drill core data using RoadDoctor® software



#### A4.3.4 Pulled array continuous electrical profiling technique (PA- CEP)

The PA-CEP technique is a resistivity-based method (see section A4.2.6) and was developed to perform high density survey coverage with high productivity (Sørensen et al 2005). Figure A.56 shows the towed resistivity system in which one dipole acts as a current electrode while five of the dipoles are used for potential measurements. The electrodes are capacitive sensors and the coupling type does not require direct ground contact, thus they can be used in many areas where normal resistivity surveying systems cannot be used (for example in built-up areas). However, this method has problems with limited penetration depth due to the limited amount of current that can be induced into the ground compared with direct contact systems. In addition, the rapidly changing soil environment and metal potential electrodes is a source of important noise (Møller et al 2006).

**Figure A.56** Plate- wire capacitive sensors (electrostatic quadruple) arranged in a towed array (courtesy of British Geological Survey, Kuras et al 2007)



The productivity depends on the configuration and the equipment used for the survey. Normally two technicians, with the PA-CEP technique, can survey 10–20km/day at a speed of 3km/h using eight electrode arrays (Møller et al 2006). Figure A.57 presents a photo of electrical resistivity meter (a) and six capacitive coupled carpets pulled on the surface behind a towing vehicle (b).

**Figure A.57** (a) Electrical resistivity meter, (b) capacitive coupled carpets pulled on the surface behind a towing vehicle (source: IRIS Instruments)



#### A4.3.5 Thermal camera methods

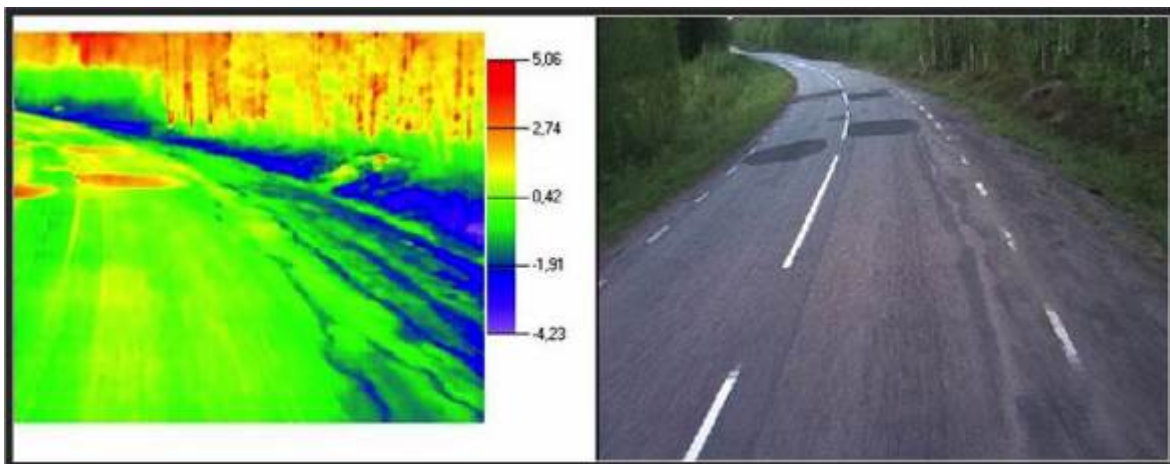
The use of a thermal camera in drainage monitoring has been tested in some research projects over the last few years. Thermal camera analysis is very efficient when done in spring or fall when there are big changes in day and night temperatures. During the frost thawing period in spring, the thermal camera also shows where the cold water, released from the melting ice, is flowing (figure A.58).

Thermal cameras have also been successfully used in detecting where water from thawing unbound basecourse is 'pumping' through the pavement. This can be seen as a colder temperature on asphalt wheel paths when normally wheel path temperatures are slightly higher since passing tyres heat the surface (figure A.59).

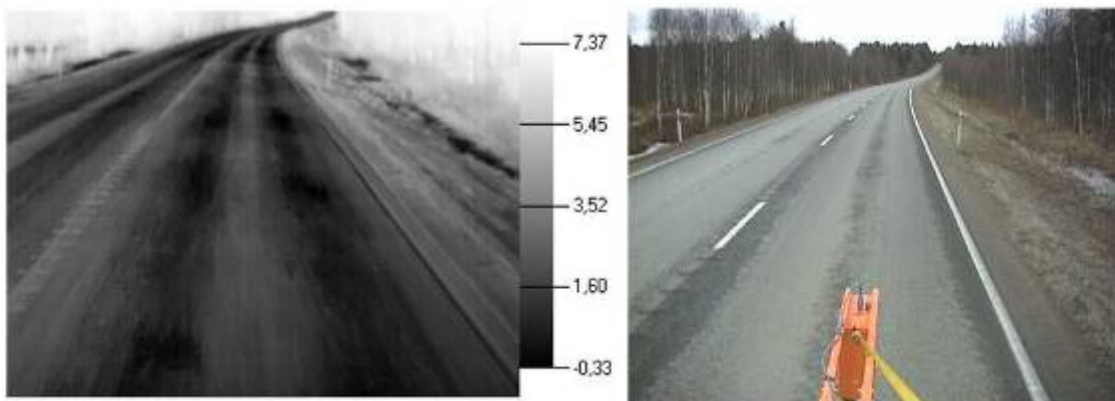


There are also other moisture-related applications for thermal cameras. In the EU-funded ROADDEX project one of the goals was to check the condition of access road culverts and thermal cameras proved to be helpful in detecting their quality (Matintupa and Saarenketo 2011). In most cases it was difficult to observe access road culverts and their condition (working well or clogged) from video, but it is easy to observe culverts from thermal camera images. Usually the culvert stands out from thermal camera image as a warmer point than the surroundings. An example of a good quality access road culvert using both a digital video still image and a thermal camera image is presented in figure A.60.

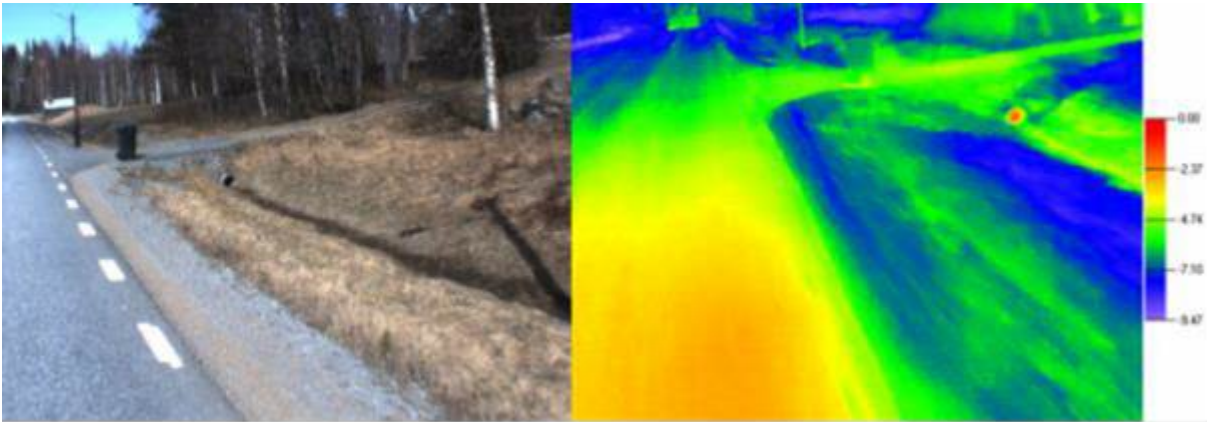
**Figure A.58 Thermal image and digital image from a road measured during the spring thaw weakening season. Cold water released from frost can be seen as blue colour in thermal image.**



**Figure A.59 Thermal camera image and digital video still photo of an asphalt during spring thaw period in HW in Rovaniemi, northern Finland. Pumping of cold water released from the basecourse can be seen as colder spots in the asphalt surface. The dynamic loading effect can also be clearly seen on the asphalt surface.**



**Figure A.60** Access road culvert is in good condition (sufficient size and open, not clogged). The access road culvert can be observed from both digital video and thermal camera image (red spot).



## A4.4 Hyperspectral close-range and remote sensing methods

### A4.4.1 General

Spectroradiometry is the technique of measuring the spectrum of radiation emitted by a source in the visible and infrared part of the spectrum (350–2,500nm). Imaging spectrometry, ie hyperspectral imaging is considered as simultaneous acquisition of spatially co-registered images, in many narrow, spectrally continuous bands, measured in calibrated radiance units, from a remotely operated platform. This technique has also shown some promising results when monitoring soil surface properties and it has also great potential in the future in monitoring the moisture of roads and their surroundings.

Currently one problem with the implementation of these techniques is the high price of the instruments but as they are becoming more popular the prices are coming down.

Hyperspectral sensing is capable of identifying and quantifying road surface materials because of its high spectral resolution (tens to hundreds of spectral bands) at the visible, near-infrared and short-wave infrared wavelength ranges from 350nm to 2,500nm. However, currently the literature on quantification of asphalt surface moisture is scant or non-existent. Road surface conditions, eg road surface snow, ice and water cover can be mapped with an infrared camera (Jonsson et al 2015, see also section 4.5). Andreou et al (2011) claim that the reflectance spectra of new asphalt surface (mineral aggregates sealed completely with bitumen) and wet asphalt surface are identical, which means surface moisture mapping of new asphalt might be difficult. Greater changes of successful surface moisture detection can be predicted for aged pavement with higher overall reflectance.

Based on the knowledge gained from the surface of mineral soils, wetting causes lowered reflectance throughout the spectral range but especially at water absorption bands at 1,400 and 1,900nm (eg Middleton et al 2004). Another fundamental water absorption band is centred at 2,800nm and an OH-combination band at 3,100nm. These are located beyond the short-wave infrared range range outside the regular spectrometers but have a wing effect on the spectra at  $\lambda < 2,500\text{nm}$  (Bishop et al 1994). These water absorption bands cannot be exploited in field conditions because of atmospheric water vapour interference. However, the moisture content of soils can be quantified using atmospheric windows between the absorption bands as reflectance decreases non-linearly with increasing moisture content until approximately 27% volumetric water is reached. With wetter soils quantification becomes impossible because no further decrease in reflectance can be observed at a high water content (>27%).

Although no reported results can be found on the asphalt or concrete moisture prediction with spectra the behaviour can be expected to be similar as with the pavement material. At least, spectral separation between wet and dry surfaces should be possible with hyperspectral spectroscopy within a similar pavement material and ageing class. Moisture prediction of gravel roads should be even more straightforward as the hydrocarbons of bitumen are missing. Field calibration, eg with dielectric methods, for model calibration is needed for accurate predictions. A multivariate regression model, ie chemometric model to predict water content from spectra or a non-linear classification can then be constructed.

In addition to the road pavements, surface moisture of exposed road shoulders, ditch slopes and ditches can be similarly detected. In the presence of vegetation cover, the visible and near-infrared rays are blocked by plant species meaning that information on moisture can be only indirectly retrieved. It may be acquired through the abundance and distribution of plant species that are indicative of soil moisture. Such work related to road infrastructure is not common but applications for forestry purposes are developed at least in cool humid subarctic environments (Middleton et al 2011). Open water at the bottom of drainage ditches is also detectable at visible and infrared wavelengths.

To estimate subsurface moisture, weather conditions need to be optimal for surveys. Post-rain periods should be avoided and sunny conditions are needed for quality data. Specular reflectance from the road surface might be an issue, especially at low sun angles. Shadowing from nearby objects will cause decreased reflectance. Light shadowing may be compensated in data processing but the presence of dark shadows equals data loss.

Hyperspectral imaging is generally divided into two classes a) hyperspectral proximal sensing methods and b) hyperspectral remote sensing methods.

#### **A4.4.2 Hyperspectral proximal sensing methods**

Proximal hyperspectral sensing is a suite of techniques carried out in the field in situ with the instrumentation in close range to the target. Proximal measurements can be conducted point-wise with a spectroradiometer or surfaces can be mapped with a hyperspectral camera. These instruments measure the intensity of the reflected energy per unit area which is called radiance. Radiance is normalised to reflectance by calibrating the instrument with a perfect diffuse reflector panel. The following techniques can also be conducted in laboratory conditions for ex-situ samples where the term close-range spectroscopy is most suitable.

Spectroradiometers can be considered most useful in the research state when the scientific background of phenomena has been established. However, rugged field spectrometers are also available which could be mounted on vehicles with the option of artificial illumination with lamp configurations. Well known examples of such instruments are by Analytical Spectral Devices (eg Field Spec, USA), Spectral Evolution (eg PSR, USA) and Integrated Spectronics (eg PIMA, Australia). An example of mobile automated near-infrared spectrophotometer (Hamamatsu Photonics) mounted behind a tractor for agricultural soil measurements is presented by Schirrmann et al (2013). Naturally, these systems provide spectral data along the driven path only across a narrow strip.

Data from imaging spectrometers is across a wider field-of-view and is therefore more readily applicable for mapping of road surfaces. Present pushbroom imaging spectrometers cover the wavelength ranges from 350–2,500nm and 8–12 $\mu$ m and are programmable to allow adjustment of the bandwidths and wavelength ranges. Andreou et al (2011) mounted a CASI (Itres, Canada) sensor on a van roof to create a terrestrial mobile imaging system. Other compact commercially available pushbroom sensors are AISA (Specim, Finland) and HySpex (Norsk Elektro Optikk, Norway). A wide range of more inexpensive

lightweight hyperspectral cameras with varying data qualities are also available (eg Resonon, USA, Rikola, VTT, Finland).

#### **A4.4.3 Hyperspectral remote sensing methods**

In this context, hyperspectral remote sensing is considered as imaging techniques operated on airborne or satellite platforms. Hyperspectral imaging spectrometers are most commonly carried on airplanes because of their substantial size. With the emergence of the lightweight hyperspectral cameras they can be now carried on UAVs (Saari et al 2012), producing more affordable data. Hyperspectral satellite missions (ASTER, Hyperion, EnMap to be launched in the future) produce data that is too coarse in spatial resolutions (>10m) for practical applications but commercial very high resolution optical satellite data (Ikonos, GeoEye, Quickbird, Worldview) might have some applicability on road infrastructure, although they are multispectral with a few wide spectral bands usually in the visible and near-infrared ranges.

#### **A4.4.4 Spectroradiometry in moisture monitoring**

According to current knowledge and experience proximal sensing methods are most feasible hyperspectral methods for moisture detection of road infrastructure. From the wavelengths the short wave infrared (1900-2500nm) might be most appropriate for moisture detection because the reflectance decrease is more progressive on the longer wavelength than on the shorter wavelengths (Weidong et al 2002). Also long-wave infrared spectroscopy (8-15 $\mu$ m) might offer additional information with regards to moisture. However, cool weather is needed for measurements. The vertical moisture gradient might be disrupted on highways by coarse grained pavement structure layers but the surface moisture might be indicative of the basecourse moisture on gravel roads. The bidirectional reflectance properties might be an issue when natural lighting is used. New asphalt is a strong forward scattered but aged surfaces are more diffuse (Puttonen et al 2009). Shadowing of the road surface might become an issue, especially at low sun angles.

As with any proximally sensed sensor data, simultaneous collection of data with a few techniques might produce the best synergy for road infrastructure management. For instance, a laser scanner might have the best spatial resolution for crack mapping but hyperspectral data might increase the accuracy of the classification. Unlike most other sensing techniques, with hyperspectral proximal methods several road properties can be estimated from a single scan. This multi-attribute feature of reflectance spectroscopy relies on a single spectrum holding information about multiple pavement constituents. Based on this literature research most of these capabilities are still undiscovered.

## **A5 Laser scanner as indirect moisture and drainage system monitoring method**

In addition to direct methods there are also new survey methods that allow indirect evaluation of the road drainage system. The best example of such a system is the laser scanner, also known as LIDAR, which has been successfully tested in many drainage related surveys.

Laser scanning is a technique where distance measurement is derived from the travel time of a laser beam from the laser scanner to the target and back. When the laser beam angle is known, and beams are sent to a range of directions from a moving vehicle with a known position, it is possible to make a 3D surface image, a 'point cloud', of a road and its surroundings. The point cloud can have millions of points, with every point having x, y and z coordinates and additional reflection or emission characteristics. The accuracy of a laser scanner survey can be affected by factors that reduce visibility, such as dust, rain, fog or snow. High roadside vegetation can also prevent the capture of information from the hidden ground surface.

A laser scanner is composed of three parts: a laser canon, a scanner and a detector. The laser canon produces the laser beam, the scanner circulates the beam and the detector measures the reflected signal and defines the distance to the target. The distance measurement is based on the travel time of light, or phase shift, or a combination of both. Laser scanner systems can be classified into two types of system: 3D laser scanners, which are used for mobile mapping and 2D laser, which is designed to be used in basic pavement engineering projects (figure A.61). A 3D laser scanner system normally uses two powerful and accurate laser scanners which map the road and its surroundings up to 200m both sides of the road. The price range for these systems varies from US\$0.5–1 million. A 2D laser scanner system normally has one laser scanner that measures a cross section of the road and its surroundings about 20m both sides of the road. The price for a 2D laser scanning system is less than US\$100,000. There are numerous laser scanner systems on the market and some of the most popular used in road surveys are: Carl Zeiss, Optech, Riegl, Sick, TopCon and Trimble.

**Figure A.61 2D (left) and 3D laser scanning systems (right) for road surveys**



The great advantage of laser scanner data compared with, for instance profilometer data, is that the data is collected outside the pavement area and shows the connection of different drainage deficiencies to the pavement failures. Figure A.62 presents a case of 3D laser scanner data analysis showing how a main road culvert that is too small and/or partly clogged causes saturation of the road structure on the upper side of the hill and further permanent deformation problems. Figure A.63 presents a case from 2D laser scanner data analysis showing how clogged and/or poorly constructed access road culverts cause infiltration of water into the road structure and further pavement deformations. The greatest benefits of 2D and 3D laser scanning systems are gained when they are used together with other NDT pavement systems. Examples of such analysis have already been shown earlier in this appendix in figures A.37 and A.46.



Figure A.62 3D laser scanner data showing deformations around the main road culvert. The smaller map presents runoff analysis, where blue lines show the water paths.

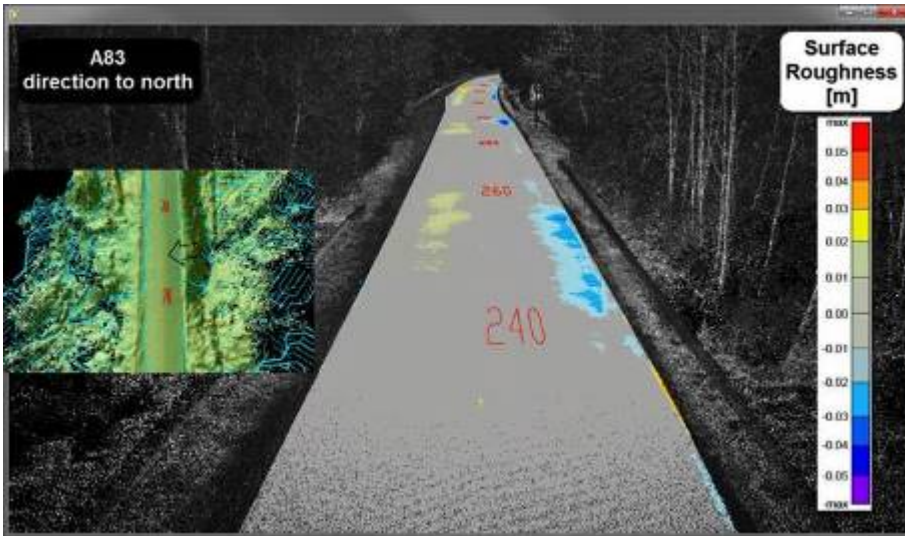
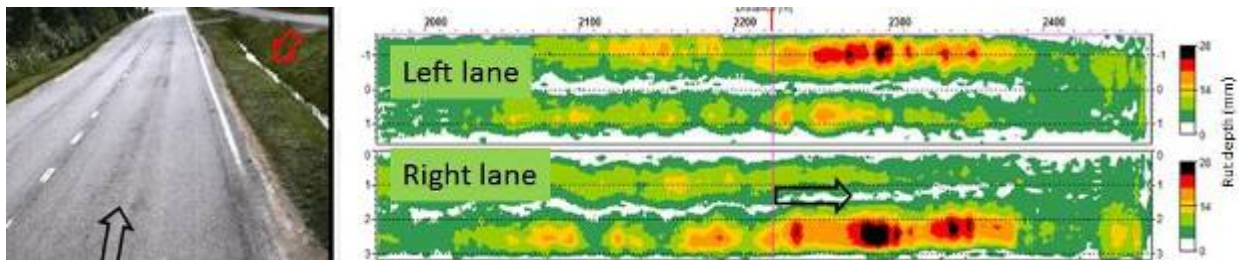
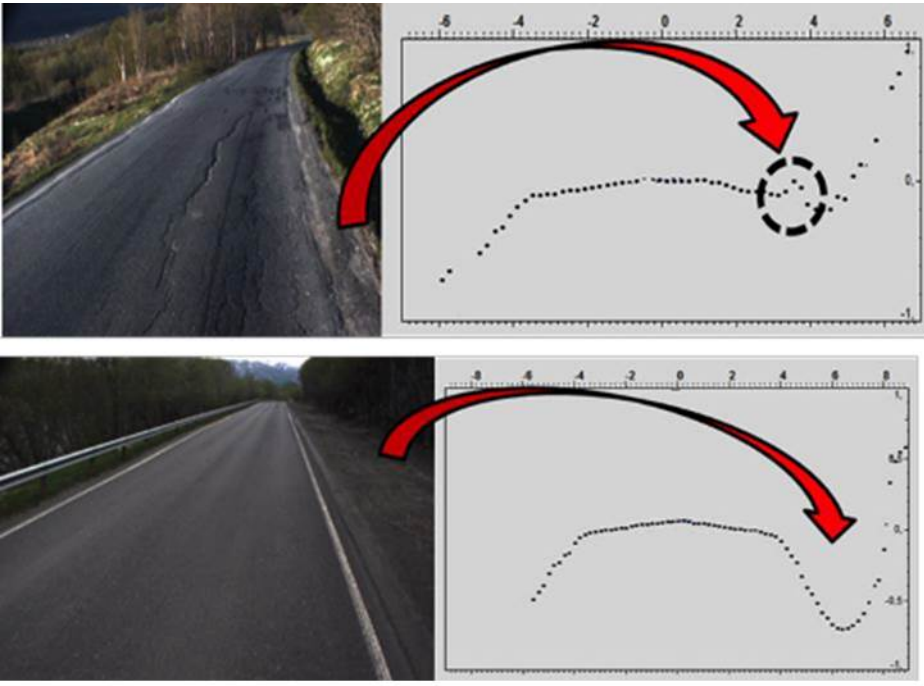


Figure A.63 Example of the effect of 2D laser scanner data in moisture- related diagnostics. Rut depth maps made from 2D laser data indicate severe shoulder deformations. The video on the left can give an indication of the reason for these rutting problems, eg poor drainage (red arrow showing water in the ditch) is causing shoulder deformation in the road structure. The black arrow shows the viewing point.

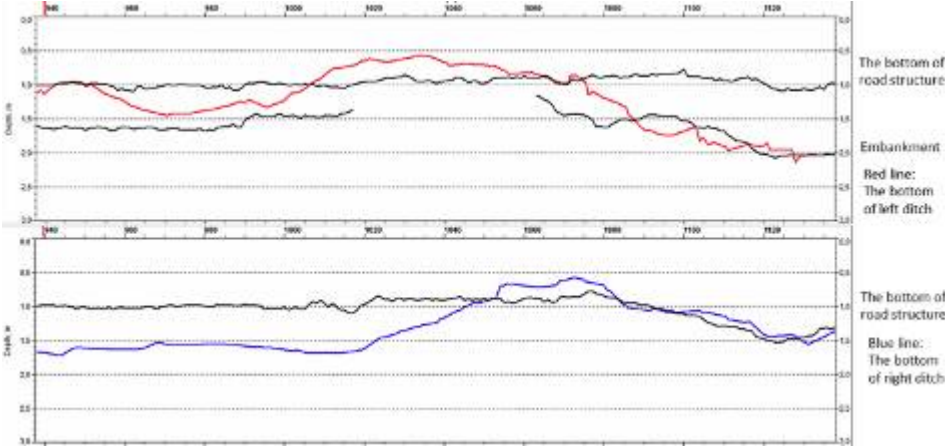


Laser scanners are also excellent methods for checking drainage systems around the road and one important parameter is the ditch depths. ROADDEX project research in different countries has shown clearly that when ditches are deep enough and in good shape the condition of the road pavement is also okay (figure A.64). If GPR data is available laser scanner data can be used to check if the ditch bottom level is deeper than the bottom of the pavement structures. Figure A.65 provides an example of such analysis in Finland.

**Figure A.64** Video still photo and laser scanner cross sections of road with poor drainage (above) and good drainage system (below) from Norway.



**Figure A.65** GPR analysis presenting the bottom of a pavement structure and embankment and presenting the ditch bottom level. Road pavement had problems in places where the ditch bottom was higher than the bottom of the road structure.



## A6 Conclusions and recommendations

Investing in a drainage system that performs well will, in the future, be the most profitable investment in road asset management. However, this can be done only if there is an efficient and reliable moisture monitoring system to support decisions needed for drainage management.

This report presents numerous water content measurement and moisture and drainage monitoring techniques that can be used either in a stationary manner or from a moving vehicle. Where and how these methods should be used depends on whether the purpose of the moisture monitoring is:

- water content measurement in rehabilitation design projects
- general monitoring and follow up of the drainage system in maintenance contracts
- monitoring seasonal changes in order to provide information for deciding if load restrictions should be used
- after heavy rains and/or after flooding to determine if a road can safely be opened to traffic.

In rehabilitation design projects the focus should be on the problem diagnostics, ie if the current problems are related to missing or poorly performing drainage structures or if the road materials are water or frost susceptible. Information concerning water content is needed for geotechnical design. In these surveys most of the technologies presented in this literature review can be used, especially GPR and laser scanning, which when properly used and analysed, are the most useful techniques for basic analysis. GPR methods in rehabilitation projects are also useful for guiding where to take samples.

In maintenance contracts the main need is to get information regarding the general condition of drainage to ensure the maintenance crew can react to drainage deficiencies in time to prevent pavement damage or problems with traffic safety. This can be done most efficiently by applying continuous survey methods such as laser scanners and GPR technique. Laser scanners especially have great potential in finding early phase drainage-related damage.

Stationary methods are most suitable for monitoring seasonal changes and these results can be used for guidance where and when load restrictions should be applied and when they can be removed. Continuous systems, such as thermal cameras, can also be used to monitor the effects of heavy trucks.

Finally, after heavy rains or flooding both continuous and stationary moisture monitoring methods can be used when measuring water content to evaluate whether bearing capacity is high enough to allow heavy trucks to use the flooded road section. Continuous methods should be used if there is a risk of dangerous cavities and washouts under the pavement.

This literature review provides a summary of road moisture monitoring technologies. However, it should be kept in mind when designing these systems, data management systems should be designed at the same time.

## 7 References

- Andreou, C, V Karathanassi and P Kolokoussis (2011) Investigation of hyperspectral remote sensing for mapping asphalt road conditions. *International Journal of Remote Sensing* 32, no.21: 6315–6333.
- Annan, AP and JL Davis (1976) Impulse radar sounding in permafrost. *Radio Science* 11, no. 4: 383–394.
- ASTM International (2010a) *ASTM D2216-10, Standard test methods for laboratory determination of water (moisture) content of soil and rock by mass*. West Conshohocken, PA: ASTM International.
- ASTM International (2010b) *ASTM D6431-99 Standard guide for using the direct current resistivity method for subsurface investigation*. West Conshohocken, PA: ASTM International.
- Barker, R and J Moore (1998) The application of time-lapse electrical tomography in groundwater studies. *The Leading Edge* 17, no.10: 1454–1458.
- Becker, ED (1969) *High resolution NMR: theory and chemical applications*. First ed. Academic Press.
- Bishop, JL, CM Pieters and JO Edwards (1994) Investigation of hyperspectral remote sensing for mapping asphalt road conditions. *Clays and Clay Minerals* 42, no.6: 702–716.

- Boyd, TM (1999) *Introduction to geophysical exploration*. Homepage of the Society of Exploration Geophysicists.
- Carter, R and EG Gregorich (2007) *Soil sampling and methods of analysis*. 2nd ed. Canada: CRC Press. 1262pp.
- Charlesworth, P (2005) Soil water monitoring. *Irrigation Insights 1*.
- Dalton, FN, WN Herkelrath, DS Rawlins and JD Rhoades (1984) Time-domain reflectometry: simultaneous measurement of soil water content and electrical conductivity with a single probe. *Science* 224: 989–990.
- Daniels, DJ (2004) *Ground penetrating radar*. 2nd ed. Bodmin, Cornwall: Institution of Engineering and Technology.
- Dawson, A (2009) *Water in road structures: movement, drainage and effects*. Dordrecht: Springer Netherlands.
- de Gruijter, JJ (2002) Sampling. Pp 45–80 in *Methods of soil analysis: part 4 – physical methods*. JH Dane and GC Topp (Eds). Madison, WI: Soil Science Society of America.
- Du, S and P Rummel (1994) Reconnaissance studies of moisture in the subsurface with GPR. In *Proceedings of the Fifth International Conference on Ground Penetrating Radar*. Kitchener, Ontario, Canada, Waterloo Centre for Groundwater Research, 12–16 June 1994.
- Fellner-Feldegg, H (1969) Measurement of dielectrics in the time domain. *The Journal of Physical Chemistry* 73, no.3: 616–623.
- Galagedara, LW, GW Parkin and JD Redman (2003) An analysis of the ground-penetrating radar direct ground wave method for soil water content measurement. *Hydrological Processes* 17, no.18: 3615–3628.
- Gardner, W and D Kirkham (1952) Determination of soil moisture by neutron scattering. *Soil Science* 73, no.5: 391–402.
- Gardner, WH (1986) Water content. Pp 493–544 in *Methods of soil analysis: part 1– physical and mineralogical methods*. A Klute (Ed). Madison, WI: American Society of Agronomy and Soil Science Society of America.
- Granlund, J (2008) *Health issues raised by poorly maintained road networks*. ROADEx.
- Grote, K, S Hubbard, J Harvey and Y Rubin (2005) Evaluation of infiltration in layered pavements using surface GPR reflection techniques. *Journal of Applied Geophysics* 57, no.2: 129–153.
- Gunn, DA, JE Chambers, S Uhlemann, PB Wilkinson, PI Meldrum, TA Dijkstra, E Haslam, M Kirkham, J Wragg, S Holyoake, PN Hughes, R Hen-Jones and S Glendinning (2015) Moisture monitoring in clay embankments using electrical resistivity tomography. *Construction and Building Materials* 92: 82–94.
- Hamrouche, R and T Saarenketo (2014) Improvement of a coreless method to calculate the average dielectric value of the whole asphalt layer of a road pavement. Pp 899–902 in *Proceedings of 15th International Conference on Ground Penetrating Radar (GPR)*, Brussels, Belgium, 30 June – 4 July 2014.
- Hänninen, P (1997) *Dielectric coefficient surveying for overburden classification*. Espoo: Finland Geological Survey of Finland.
- Head, KH (1984) *Manual of soil laboratory testing, vol 1: soil classification and compaction tests*. London: Pentech Press. 339pp.

- Hignett, C and SR Evett (2002) Neutron thermalization. Pp 501–520 in *Methods of soil analysis: part 4 – physical methods*. JH Dane and GC Topp (Eds). Madison, WI: Soil Science Society of America.
- Hillel, D (1980) *Applications of soil physics*. New York: Academic Press.
- Huisman, JA, C Sperl, W Bouten and JM Verstraten (2001) Soil water content measurements at different scales: accuracy of time domain reflectometry and ground-penetrating radar. *Journal of Hydrology* 245, no.1–4: 48–58.
- IRIS Instruments (nd) IRIS Instruments [Homepage of IRIS Instruments]. Accessed 24 February 2015. <http://www.iris-instruments.com/>.
- ISO (2004) *ISO 17892-1:2014 Geotechnical investigation and testing – laboratory testing of soils – part 1: determination of water content*.
- Jol, HM (2009) *Ground penetrating radar theory and applications*. 1st ed. Elsevier.
- Jonsson, P, J Casselgren and B Thörnberg (2015) Road surface status classification using spectral analysis of NIR camera images. *IEEE Sensors Journal* 15, no.3: 1641–1656.
- Jury, W and R Horton (2004) *Soil physics*. 6th ed. Hoboken, NJ: John Wiley.
- Kuras, O, PI Meldrum, D Beamish, RD Ogilvy and D Lala (2007) Capacitive resistivity imaging with towed arrays. *Journal of Environmental & Engineering Geophysics* 12, no.3: 267–279.
- Lade, PV and H Nejadi-Babadai (1976) Soil drying by microwave oven. Pp 320–335 in *Proceedings of Soil specimen preparation for laboratory testing: a symposium 7*. Annual Meeting American Society for Testing and Materials, Montreal, 22–27 June 1975, ASTM International, Baltimore.
- Laurens, S, JP Balayssac, J Rhazi, G Klysz and G Arliguie (2003) Non-destructive evaluation of concrete moisture by GPR technique: experimental study and direct modelling. *International Symposium NDT-CE*, Berlin, 16–19 September 2003.
- Liu, L, JW Lane and Y Quan (1998) Radar attenuation tomography using the centroid frequency downshift method. *Journal of Applied Geophysics* 40, no.1–3: 105–116.
- Loke, MH (2001) *Tutorial: 2-D and 3-D electrical imaging surveys*.
- Maser, KR, T Scullion and RC Briggs (1991) *Use of radar technology for pavement layer evaluation*. USA: Texas Transportation Institute.
- Matintupa, A and T Saarenketo (2011) *New survey techniques in drainage evaluation – laser scanner and thermal camera*. A ROADX IV report for task D1'Drainage maintenance guidelines. ROADX.
- Middleton, M, P Närhi and R Sutinen (2011) Imaging spectroscopy in soil-water based site suitability assessment for artificial regeneration to Scots pine. *ISPRS Journal of Photogrammetry and Remote Sensing* 66, no.3: 287–297.
- Middleton, M, A Teirilä and R Sutinen (2004) Response of reflectance to dielectric properties of bare tills. *International Journal of Remote Sensing* 25, no.3: 627–641.
- Møller, IB, K Sørensen and E Auken (2006) Geoelectrical methods. Pp80–81 in *Groundwater resources in buried valleys*. BurVal Working Group. Hannover, Germany. Leibniz Institute for Applied Geosciences (GGA-Institut).
- Nave, CR (2014) *HyperPhysics* [homepage of Georgia State University]. Accessed 19 February 2015. <http://hyperphysics.phy-astr.gsu.edu/hbase/hph.html>.



- Nygren, N and CM Preston (1993) Determination of seed moisture content in *Pinus contorta* (L.) by low resolution pulsed NMR. Dormancy and barriers to germination. In *Proceedings: International Symposium of IUFRO Project Group P2.04-00 (seed problems)*. DGW Edwards (Ed). Victoria, BC: Forestry Canada, Pacific Forestry Centre.
- O'Connor, KM and CH Dowling (1999) *Geomeasurements by pulsing TDR cables and probes*. USA: CRC Press LLC.
- Oxford University Press (2015) *Oxford university dictionary*. Accessed 17 February 2015. [www.oxforddictionaries.com](http://www.oxforddictionaries.com) [2015, 02/17].
- Paetzold, RF (1986) NMR instrument for soil moisture ground-truth data collection. In *Proceedings of Working Group on Remote Sensing for Soil Survey, Symposium*, Wageningen and Enschede, Netherlands, 3–8 March 1985.
- Pansu, M and J Gautheyrou (2007) *Handbook of soil analysis: mineralogical, organic and inorganic methods*. New York: Springer.
- Puttonen, E, J Suomalainen, T Hakala and J Peltoniemi (2009) Measurement of reflectance properties of asphalt surfaces and their usability as reference targets for aerial photos. *IEEE Transactions on Geoscience and Remote Sensing* 47, no.7: 2330–2339.
- Reginato, RJ (1974) Gamma radiation measurements of bulk density changes in a soil pedon following irrigation. *Soil Science Society of America Journal* 38, no.1: 24–29.
- Reynolds, JM (1997) *An introduction to applied and environmental geophysics*. Wiley.
- ROADDEX (2012) e-learning platform. Accessed 25 February 2015. [www.roadex.org/](http://www.roadex.org/)
- Roadscanners Oy (2015) Roadscanners Oy [Homepage of Roadscanners Oy]. Accessed 2015. [www.roadscanners.com/](http://www.roadscanners.com/) .
- Ruan, RR and PL Chen (1997) *Water in foods and biological materials. A nuclear magnetic resonance approach*. Lancaster: Technomic Publishing Company.
- Saarenketo, T (2006) Electrical properties of road materials and subgrade soils and the use of ground penetrating radar in traffic infrastructure surveys. PhD thesis. Oulu: Oulu University.
- Saarenketo, T and S Aho (2005) Monitoring and classifying spring thaw weakening on low volume roads in northern periphery. In *Proceedings of the 7th International Conference on the Bearing Capacity of Roads, Railways and Airfields*. Trondheim, Norway, 27–29 July 2005.
- Saarenketo, T and T Scullion (1994) *Ground penetrating radar applications on roads and highways*. College Station, Texas: Texas Transportation Institute.
- Saari, H, I Pölönen, H Salo, S Tuominen, J Kaivosoja, J Heikkilä, J Mäkynen and C Holmlund (2012) UAS Summer 2012 UAV flight campaign results for forest and agriculture applications. *Finnish Remote Sensing Days 2012*. Helsinki: Helsinki University, Department of Geosciences and Geography. 25–26 October 2012.
- Sbartai, ZM, S Laurens, J Balayssac, G Arliguie and G Ballivy (2006) Ability of the direct wave of radar ground-coupled antenna for NDT of concrete structures. *NDT & E International* 39, no.5: 400–407.
- Sbartai, ZM, S Laurens and D Breyse (2009) Concrete moisture assessment using radar NDT technique – comparison between time and frequency domain analysis. *NDTCE'09 Non-Destructive Testing in Civil Engineering*. Nantes, France.

- Schirrmann, M, R Gebbers and E Kramer (2013) Performance of automated near-infrared reflectance spectrometry for continuous in situ mapping of soil fertility at field scale. *Vadose Zone Journal* 12, no.4.
- Silvast, M (1999) *Sähköiset monielektrodimitaukset maa- ja kallioperätutkimuksissa*, Oulu, Finland: University of Oulu.
- Sørensen, K, E Auken, N Christensen and L Pellerin (2005) An integrated approach for hydrogeophysical investigations: new technologies and a case history. Pp585–606 in *Near-surface geophysics*. DK Butler (Ed). Society of Exploration Geophysicists.
- Topp, GC, JL Davis and AP Annan (1980) Electromagnetic determination of soil water content: measurements in coaxial transmission lines. *Water Resources Research* 16, no.3: 574–582.
- Topp, GC and PA Ferré (2002) Methods for measurements of soil water content. Pp 422–427 in *Methods of soil analysis: physical methods*. A Klute and AL Page (Eds). Madison, WI: Soil Science Society of America.
- Troxler Electronic Laboratories (2011) *Manual of operations and instructions. 3400-B series moisture density gauge*. 4th ed. 107pp.
- Vallina, AU (1999) Refraction and wide-angle reflection. Pp155–156 in *Principles of seismology*. 1st ed. Cambridge, UK: Cambridge University Press.
- Van Bavel, CHM, N Underwood and RW Swanson (1956) Soil moisture measurement by neutron moderation. *Soil Science* 82, no.1: 29–42.
- Veenstra, M, DJ White, VR Schaefer and Iowa Department of Transportation (2005) Synthesis of nondestructive testing technologies for geomaterial applications. Iowa, USA: Center for Transportation Research and Education, Iowa State University.
- Weidong, L, F Baret, G Xingfa, T Qingxi, Z Lanfen and Z Bing (2002) Relating soil surface moisture to reflectance. *Remote Sensing of Environment* 81, no 2–3: 238–246.
- Wightman, WE, F Jalinoos, P Sirles and K Hanna (2003) Application of geophysical methods to highway related problems. *Federal Highway Administration, Central Federal Lands Highway Division publication no.FHWA-IF-04-021*. 742pp.
- Wolter, B, F Kohl, N Surkowa and G Dobmann (2003) Practical applications of NMR in civil engineering. *International Symposium Non-Destructive Testing in Civil Engineering (NDT-CE)*. Berlin, 16–19 September 2003.
- Wright, D, V Baltazart, N Elsworth, R Hamrouche, J Krarup, ML Antunes, S McRobbie, V Merecos and T Saarenketo (2014) Monitoring structural and surface conditions. *Forum of European National Highway Research Laboratories collaborative project FP7-285119*.
- Yu, C, C Loureiro, J-J Cheng, LG Jones, YY Wang, YP Chia and E Faillace (1993) *Data collection handbook to support modeling the impacts of radioactive material in soil*. Argonne, IL: Argonne National Laboratory (ANL).

# Appendix B: Field test results in New Zealand October 2015

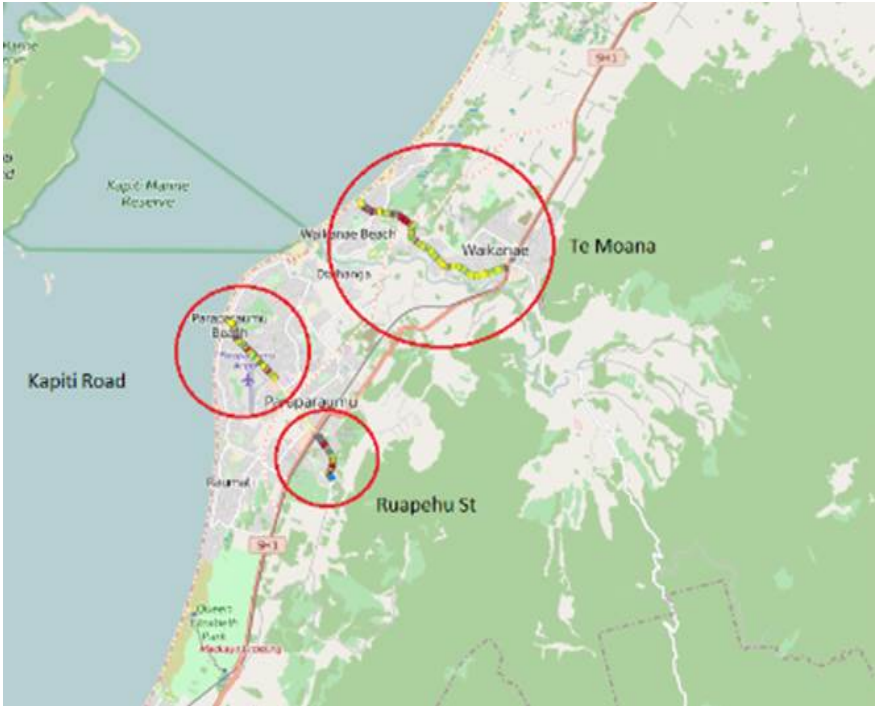
## B1 Introduction

The validation of results was based on examining sites where the moisture survey identified higher levels of moisture and compared this with rutting and visual inspection data that supports or otherwise that water has likely damaged the pavement. For some of the Whanganui roads, test pits were also dug and moisture content measured to confirm the presence or not of water.

## B2 Kapiti Coast

Three streets (Kapiti, Ruapehu, Te Moana) were surveyed within the Kapiti Coast maintenance contract with the locations shown in the map in figure B.1. Each street was examined to find locations with the highest moisture levels.

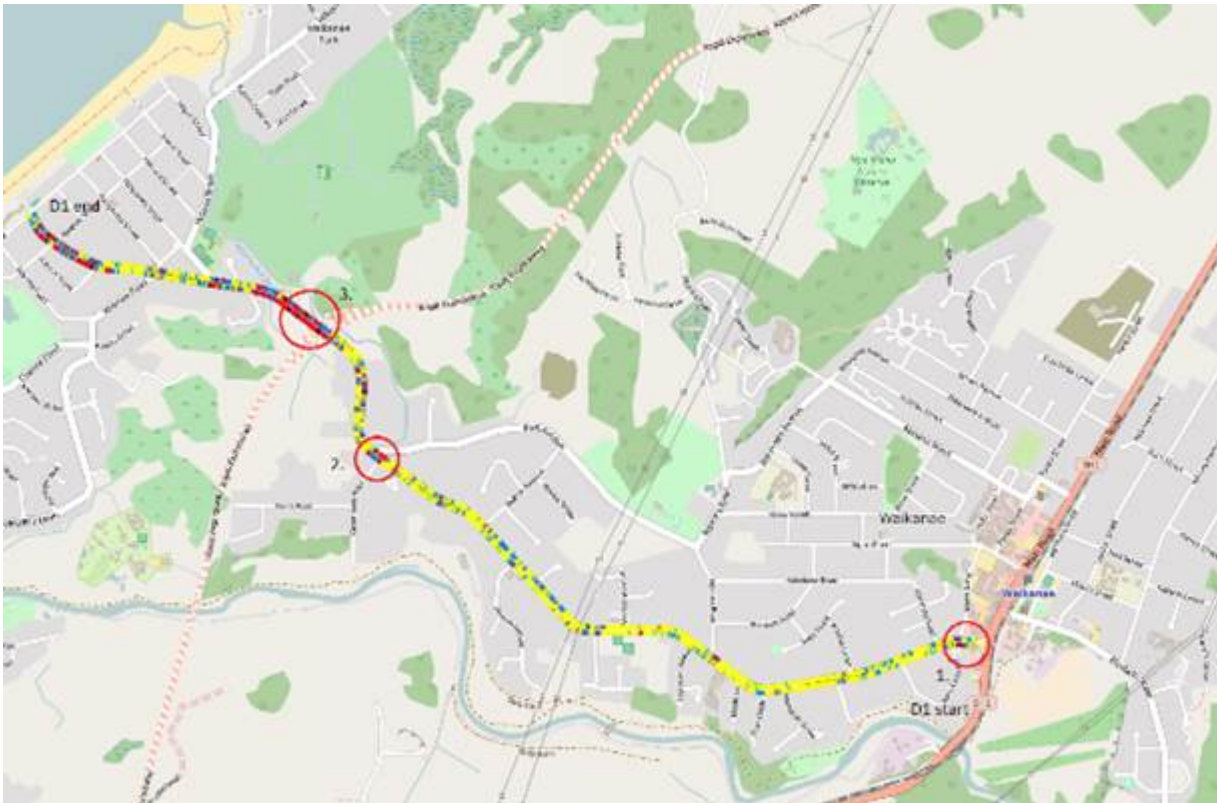
Figure B.1 Survey locations on the Kapiti Coast



## B2.1 Te Moana Road

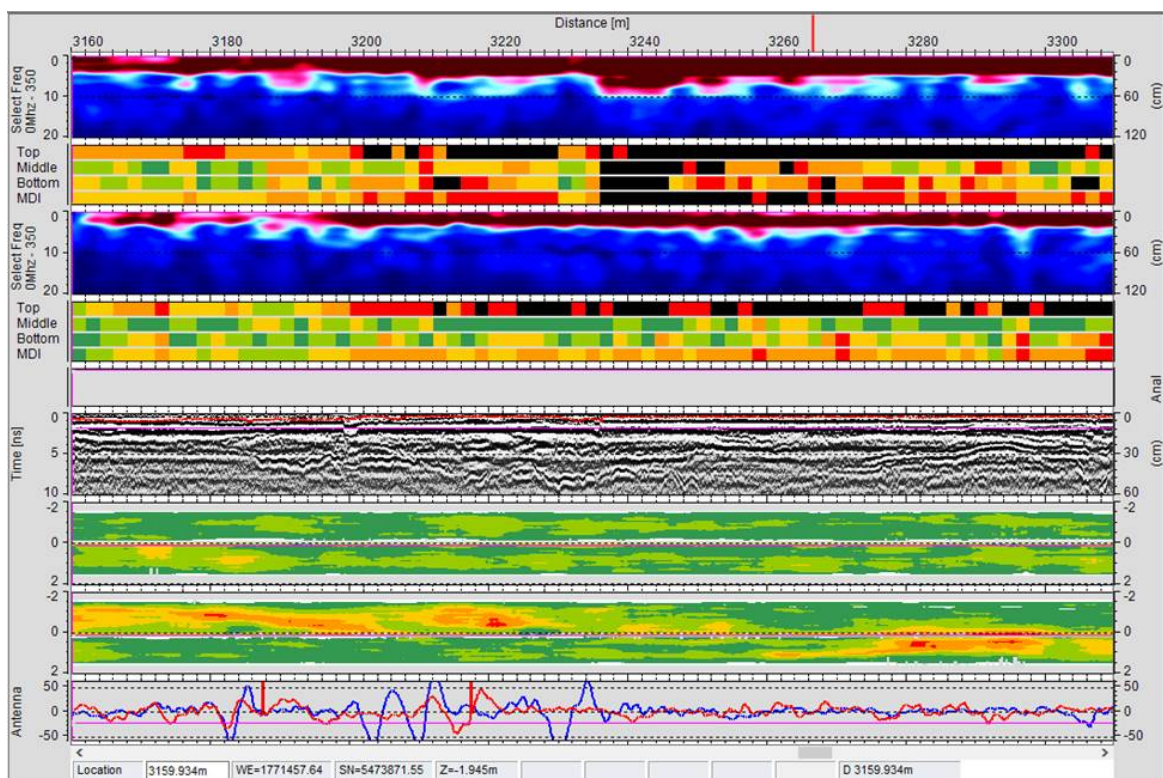
Three locations on Te Moana Road with high moisture were selected for further examination as shown in figure B.2

**Figure B.2** Locations of high moisture on Te Moana Road



Spot number 3 (figure B.2) was examined further using the Road Doctor viewer software with a screen shot shown in figure B.3. As can be seen at this location (RP 3220 to RP 3300) there are high levels of saturation in the top pavement layer indicated as a black shade in figure B.3. Reviewing the video photo of the site it can be seen that the shoulders pond water which could be the reason for the high moisture content.

Figure B2.3 Moisture survey results on Te Moana Road spot # 3 (RP approx 3,220m) – black shade indicates highest level of saturation or MDI

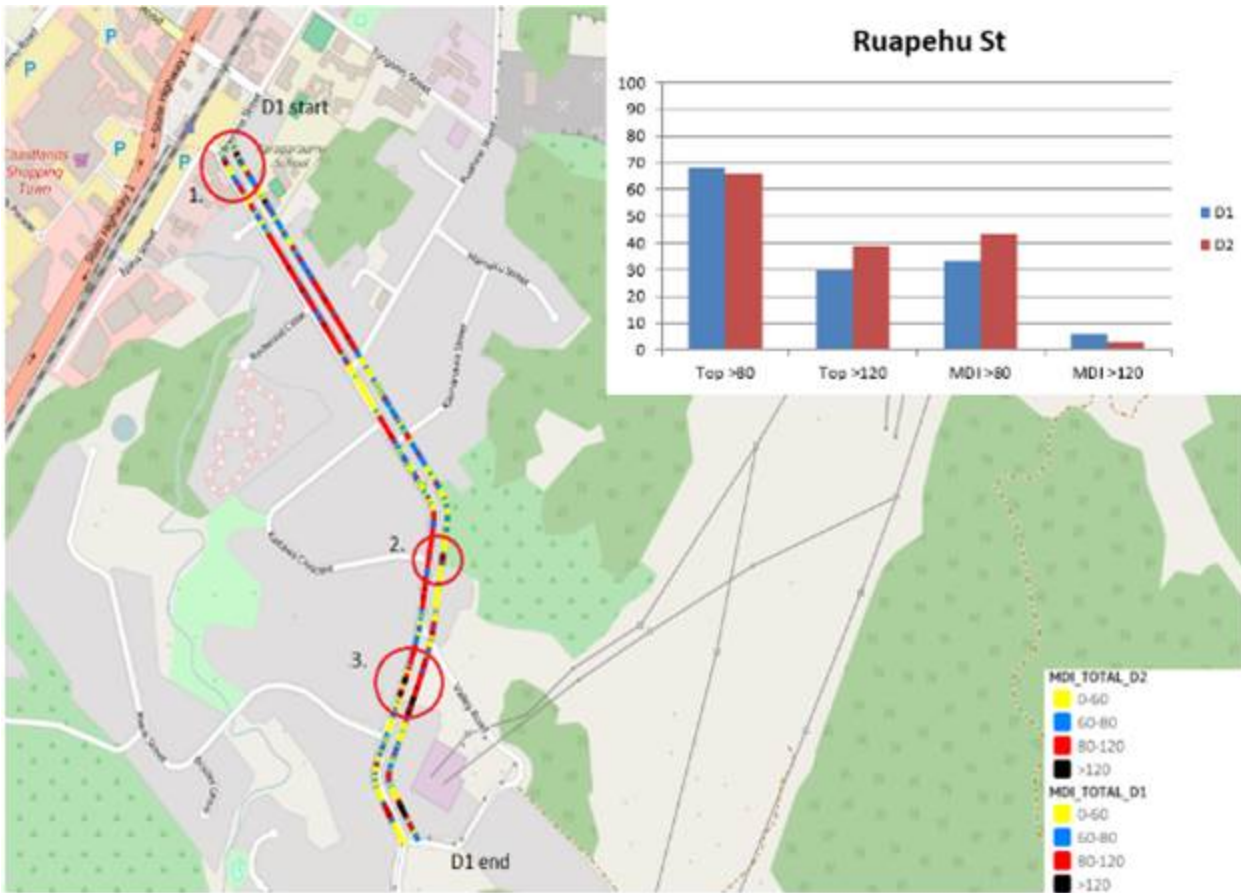


## B2.2 Ruapehu Street

Three locations on Ruapehu Street with high moisture were selected for further examination as shown in figure B.4.

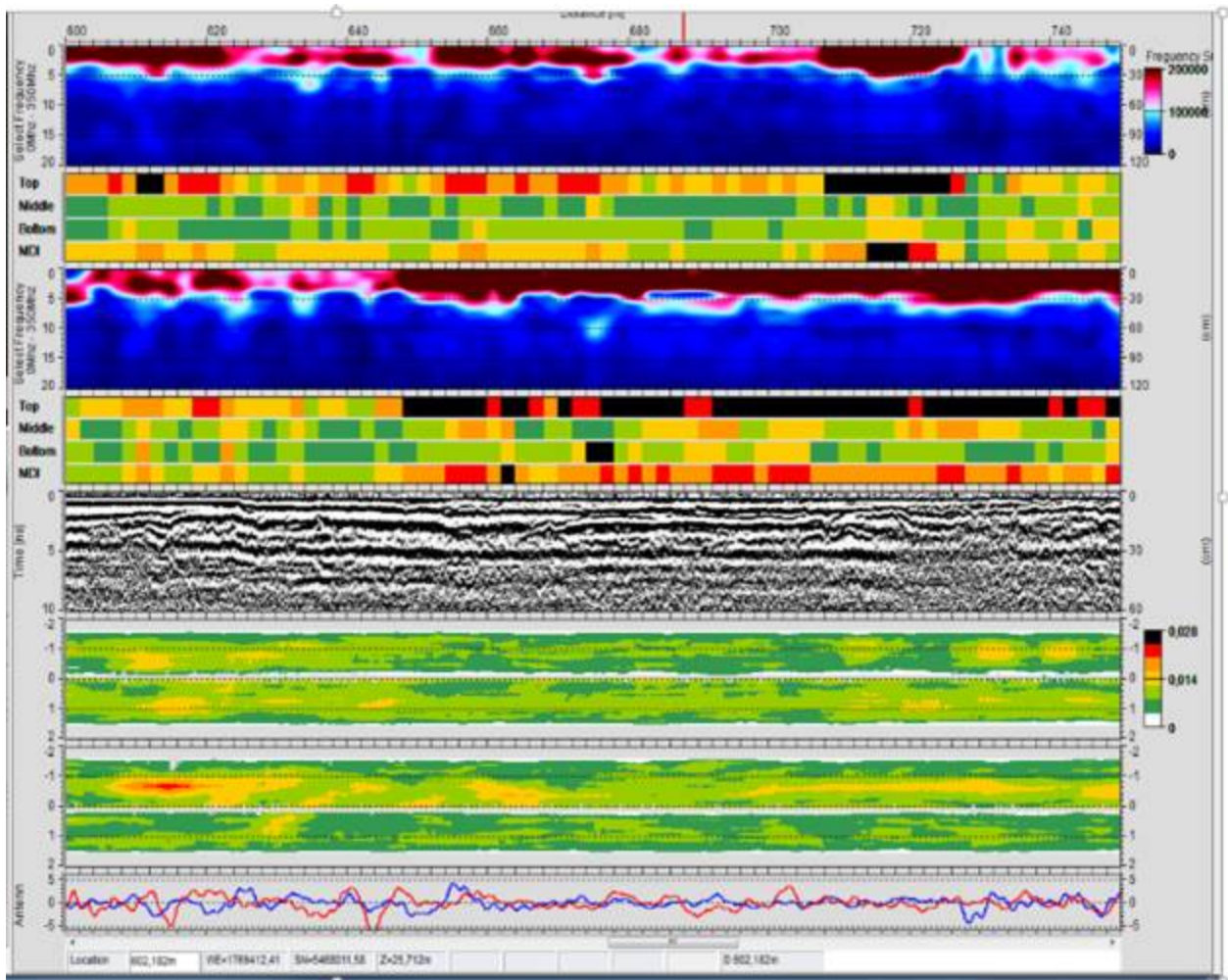


Figure B.4 Locations of high moisture on Ruapehu Street



Spot number 3 (figure B.4) was examined further using the Road Doctor viewer software with a screen shot shown in figure B.5. As can be seen at this location (RP 3220 to RP 3300) there are high levels of saturation in the top pavement layer indicated as a black shade in figure B.5. Reviewing the video photo of the site has many patches possibly replacing pipes which could be an indication of high moisture in the pavement layers.

Figure B.5 Moisture survey results on Ruapehu Street spot # 3 (RP approx 688m) - black shade indicates highest level of saturation or MDI



## B3 Porirua

Several urban streets were surveyed in the Porirua area and the maps showing locations of high moisture are shown in figures B.6 to B.9.

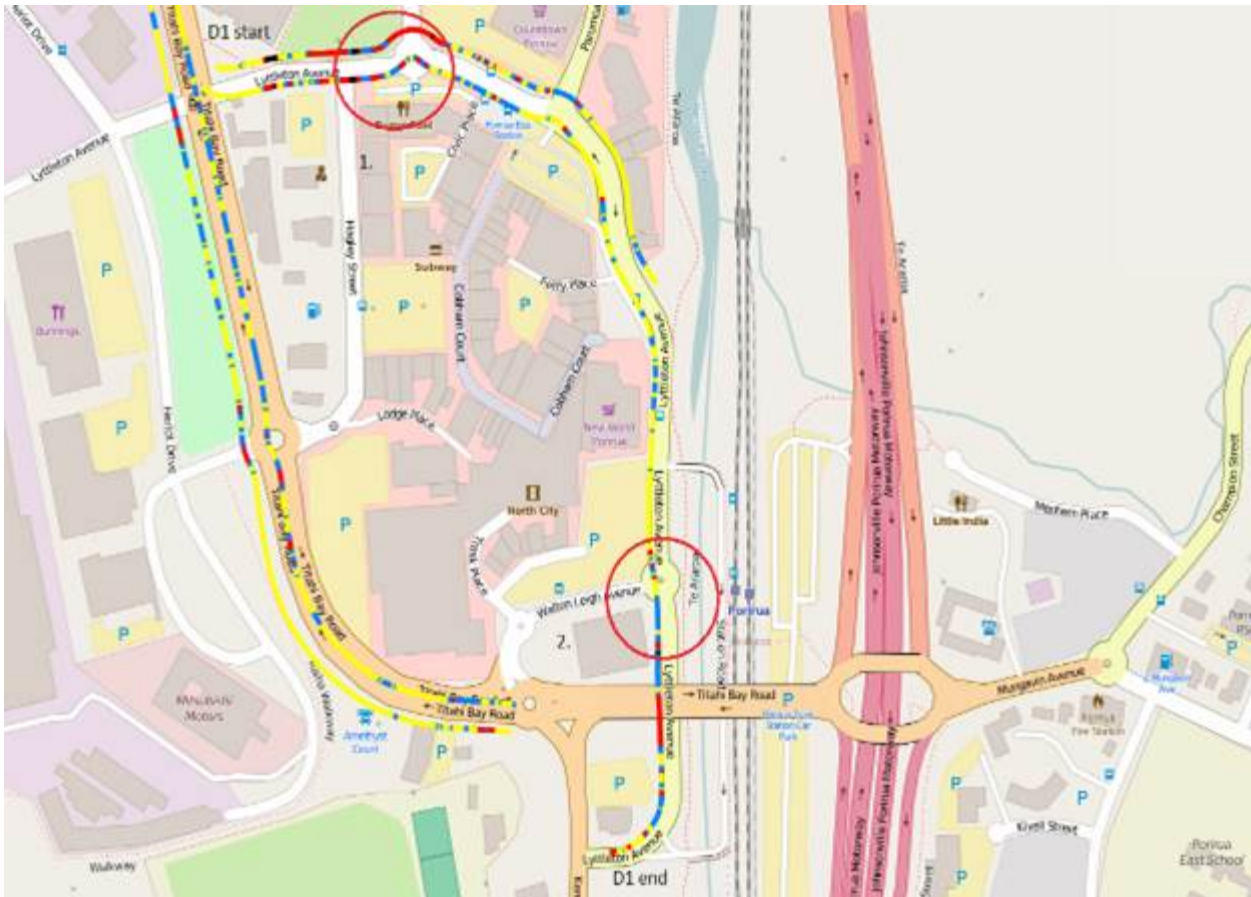


Figure B.6 High moisture locations on Lyttelton Avenue in Porirua



Figure B.7 High moisture locations on Titahi Bay Road in Porirua

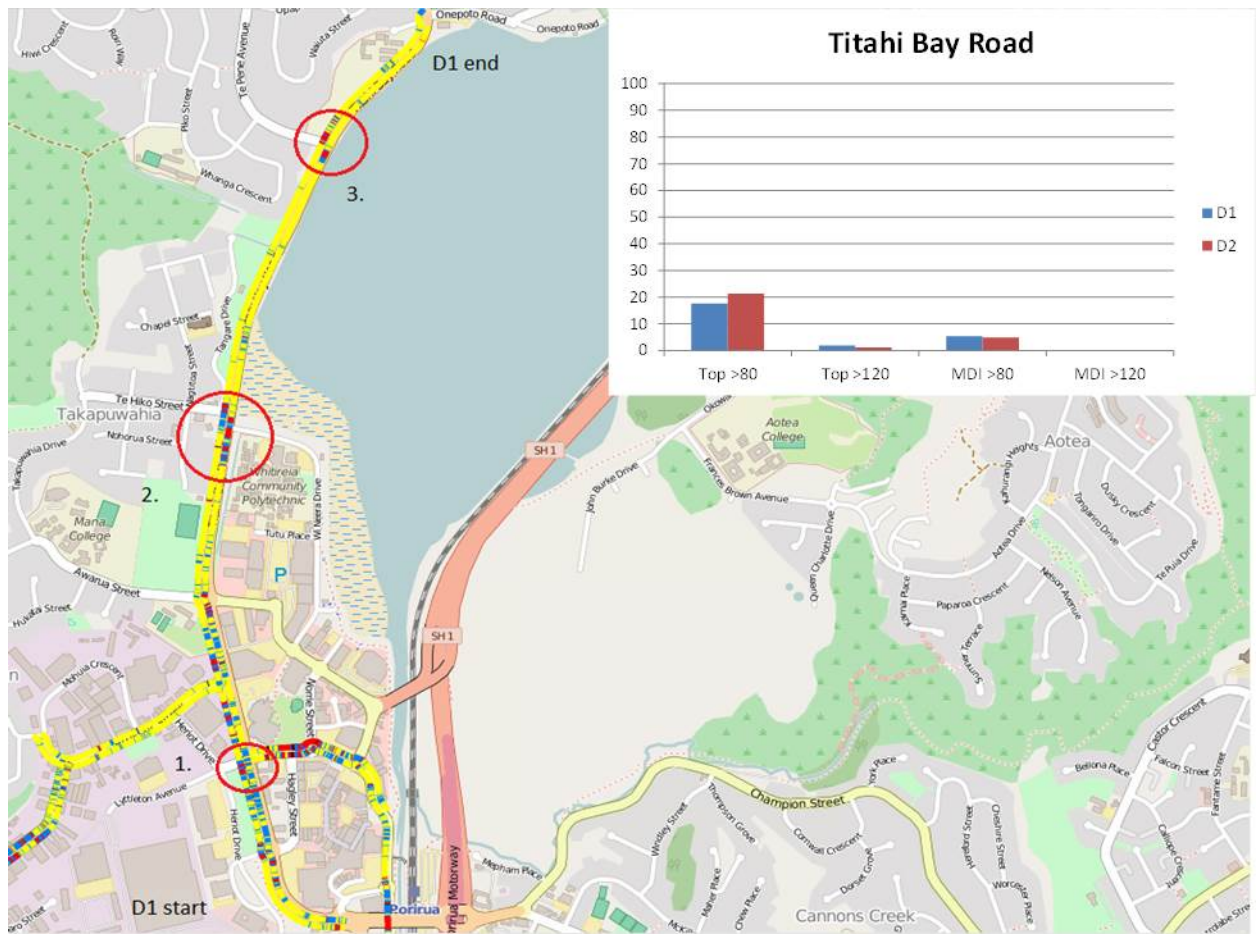


Figure B.8 High moisture locations on Prosser Street in Porirua

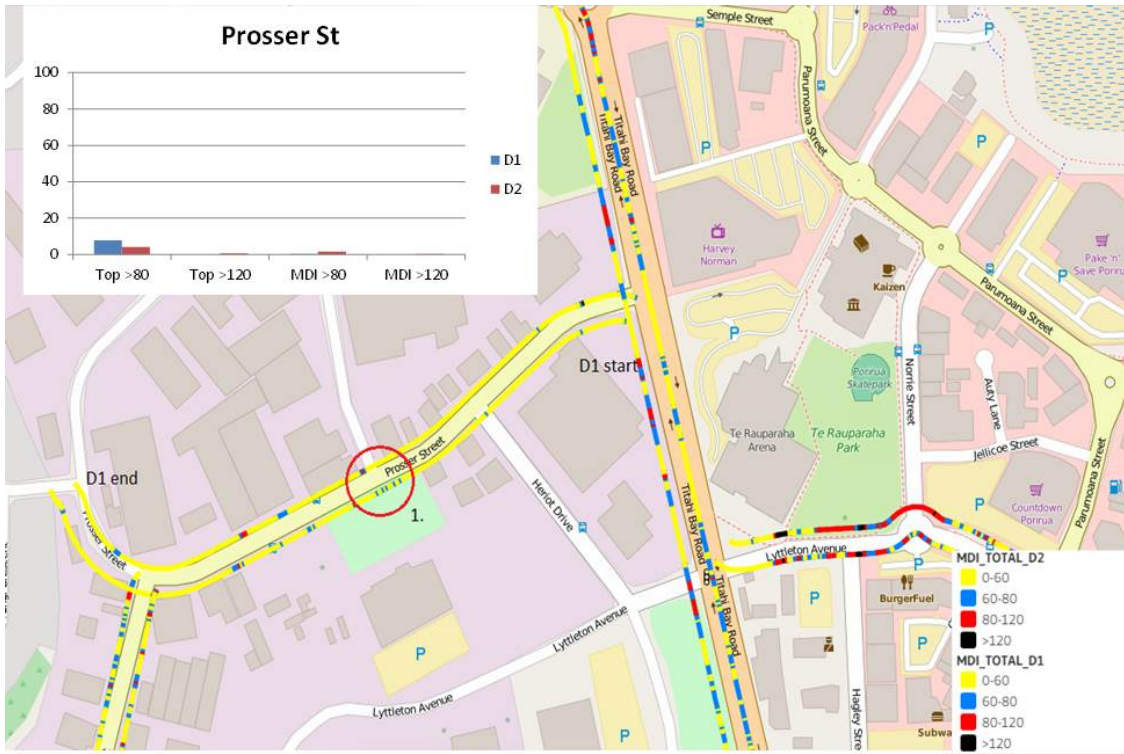


Figure B.9 High moisture locations on Raiha Street in Porirua

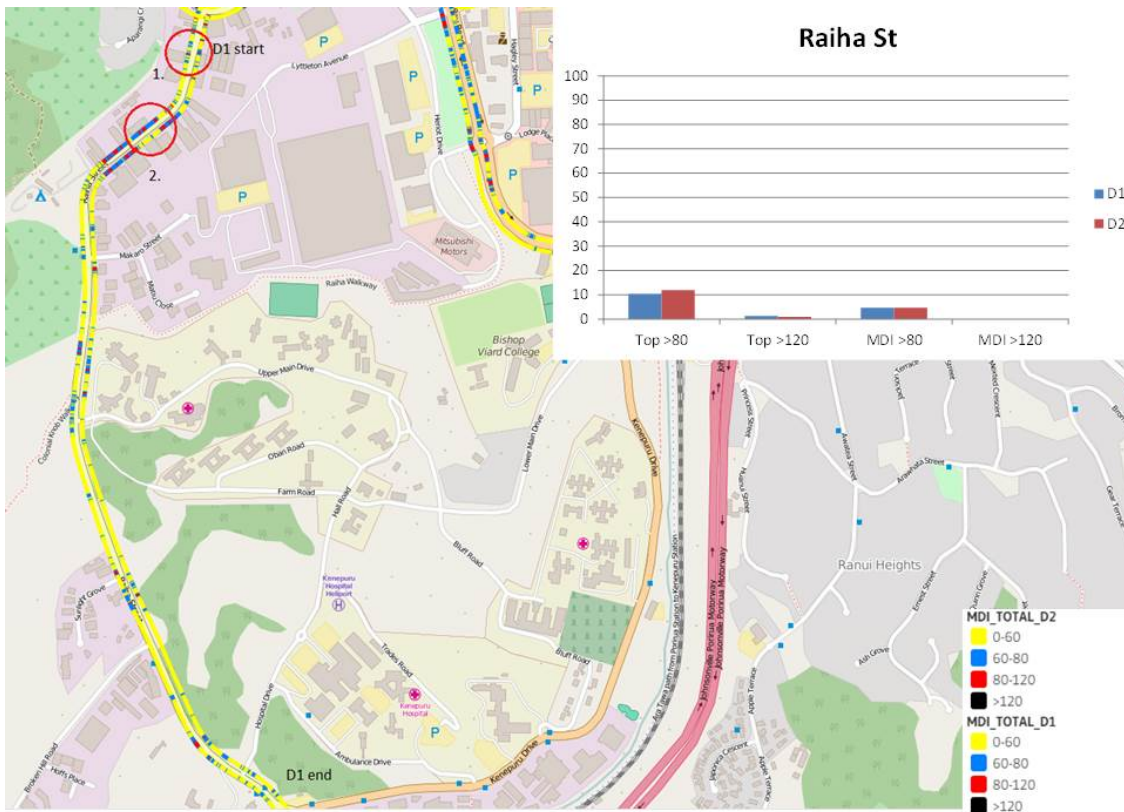




Figure B.10 High moisture locations at point 2 (274m) on Raiha Street in Porirua



Figure B.10 shows a location on Raiha Street where high moisture was recorded (black bars shown in top layer being the top 250mm of the pavement). From the photograph there is flushing in the wheel track and the LIDAR survey does show some rutted areas which further supports an area of high flushing.

## B4 Hawkes Bay

Figure B.11 High moisture locations on SH 50 RS0033 in Hawkes Bay

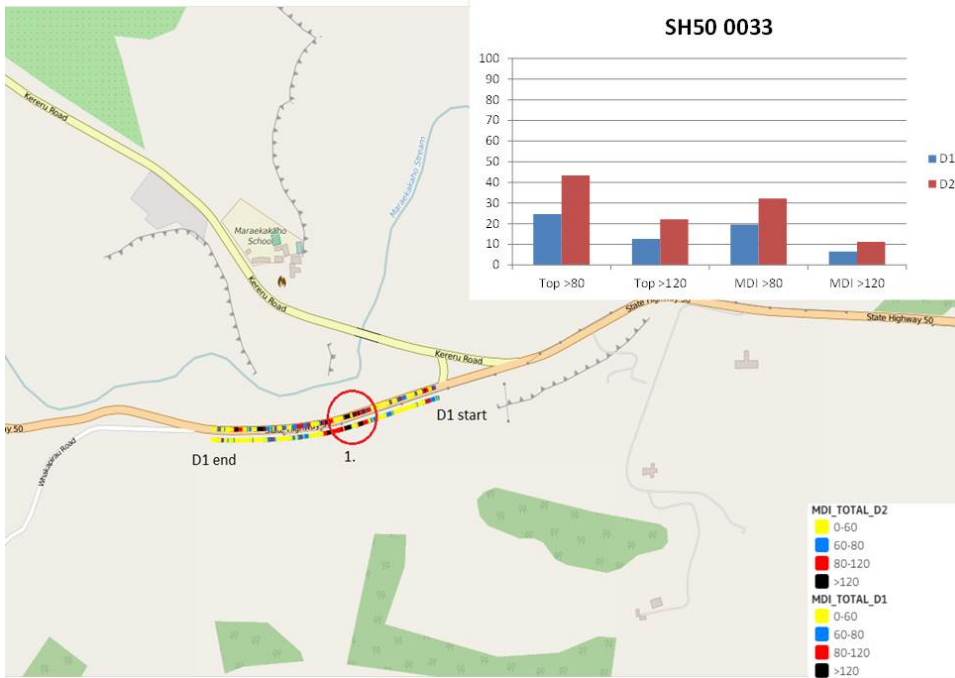


Figure B.12 High moisture locations on SH50 RS0049 (RP 4.15 to 4.6km) in Hawke's Bay

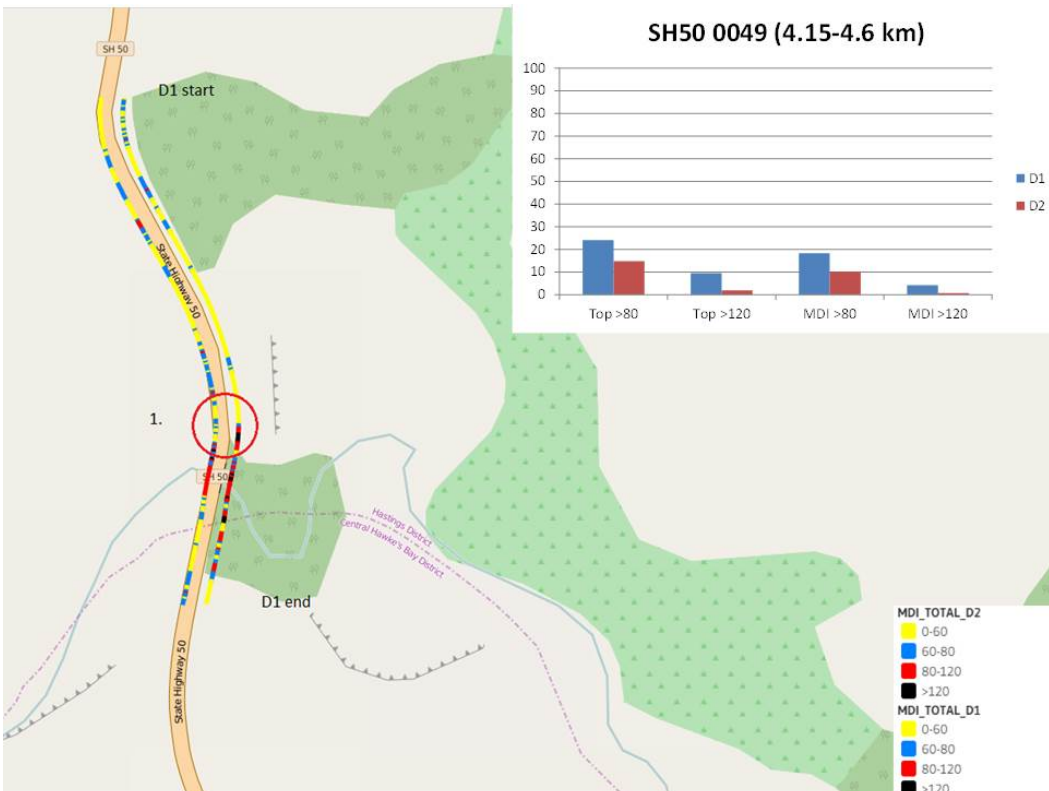


Figure B.13 High moisture locations on SH 50 RS0079 in Hawke's Bay

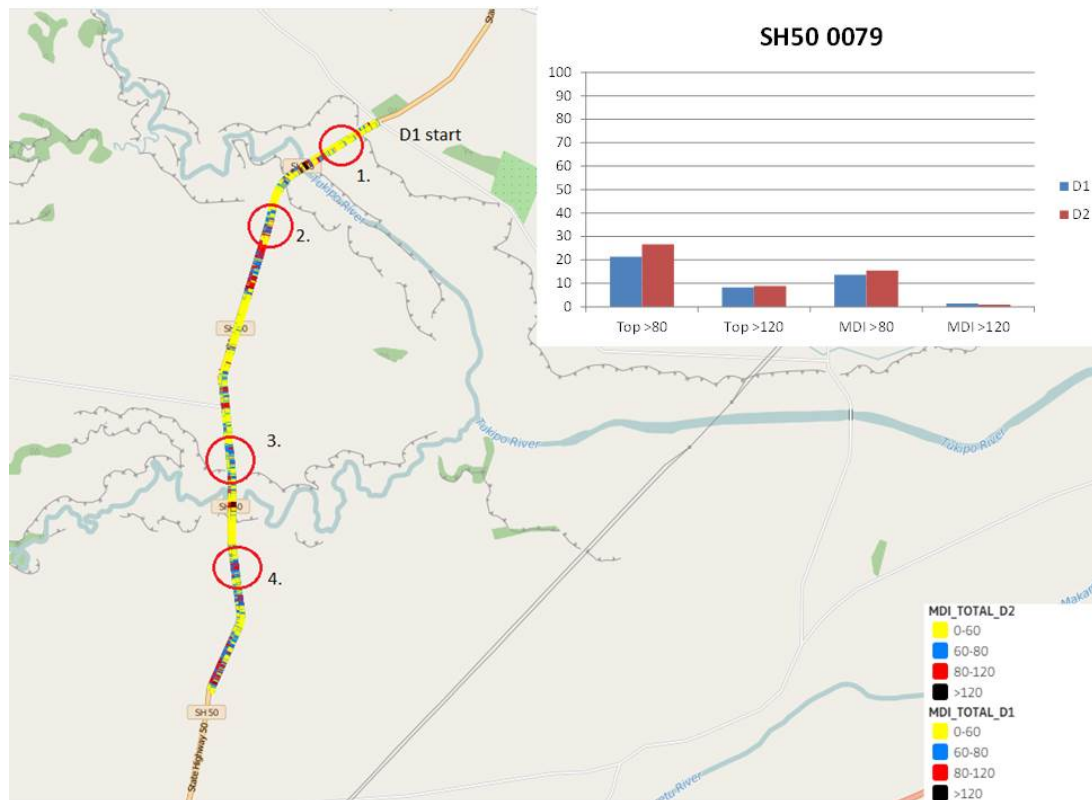


Figure B.14 High moisture locations on SH 2 RS0678 in Hawke's Bay

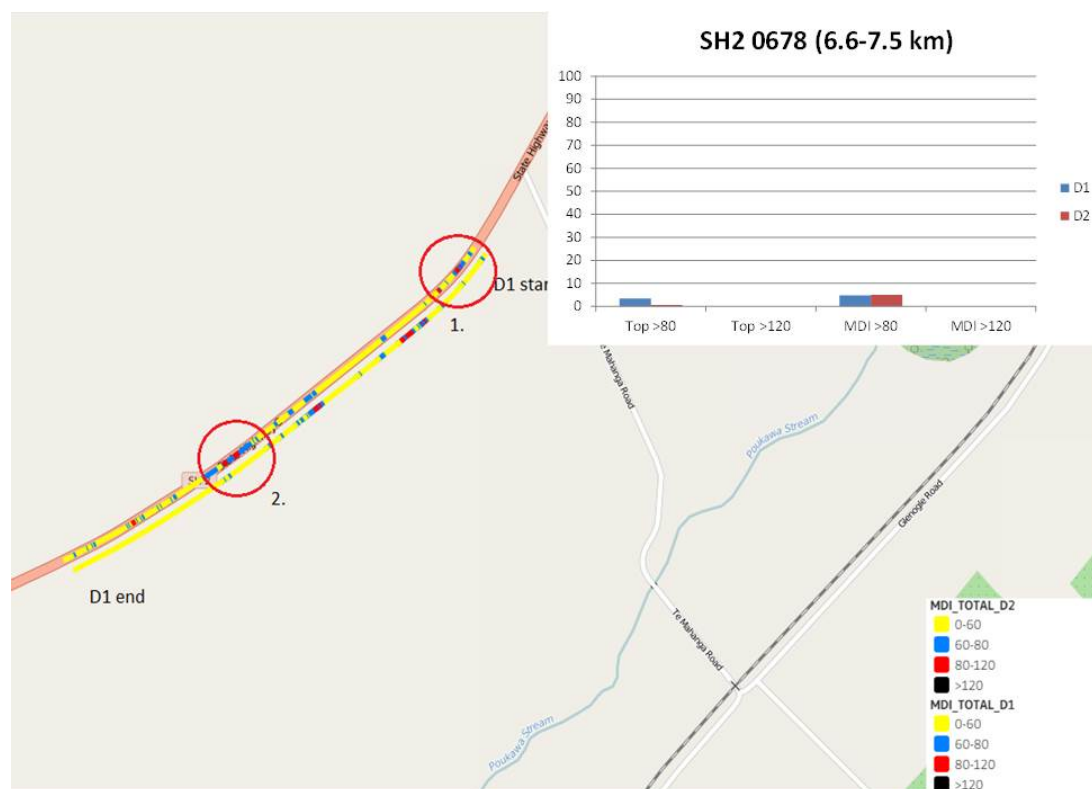


Figure B.15 High moisture locations on SH2 RS0691 in Hawke's Bay

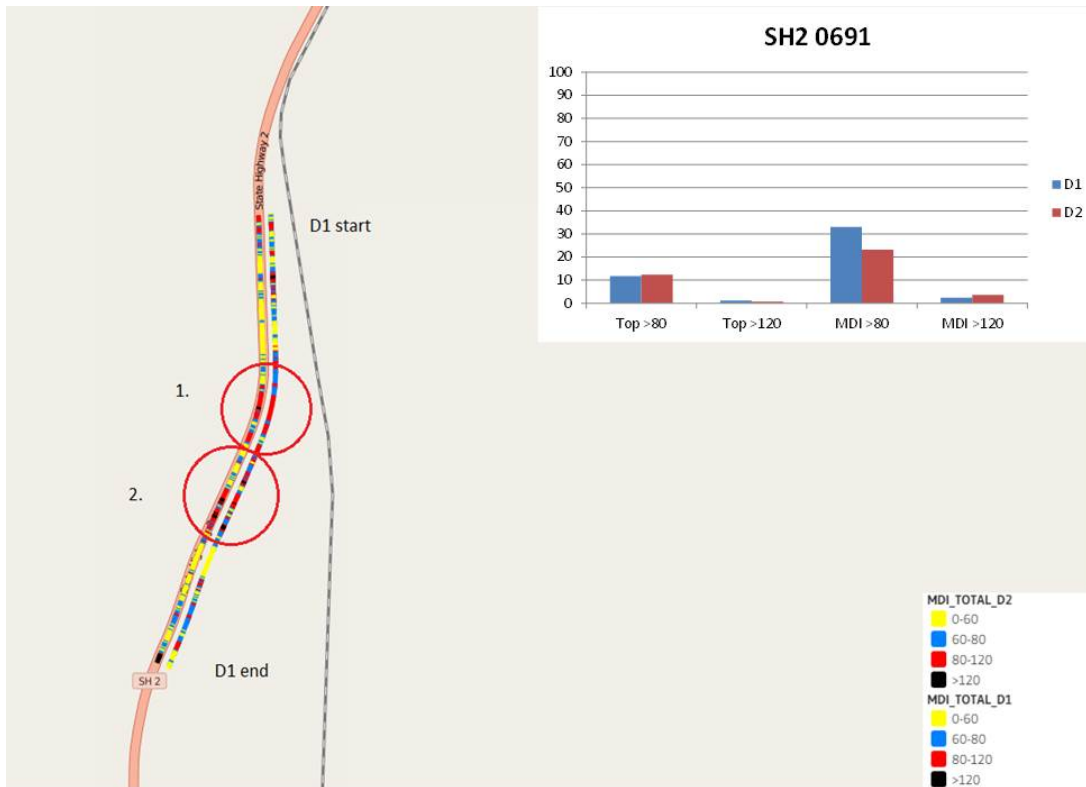




Figure B.16 Moisture location on SH2\_0691 450-600m in Hawke's Bay

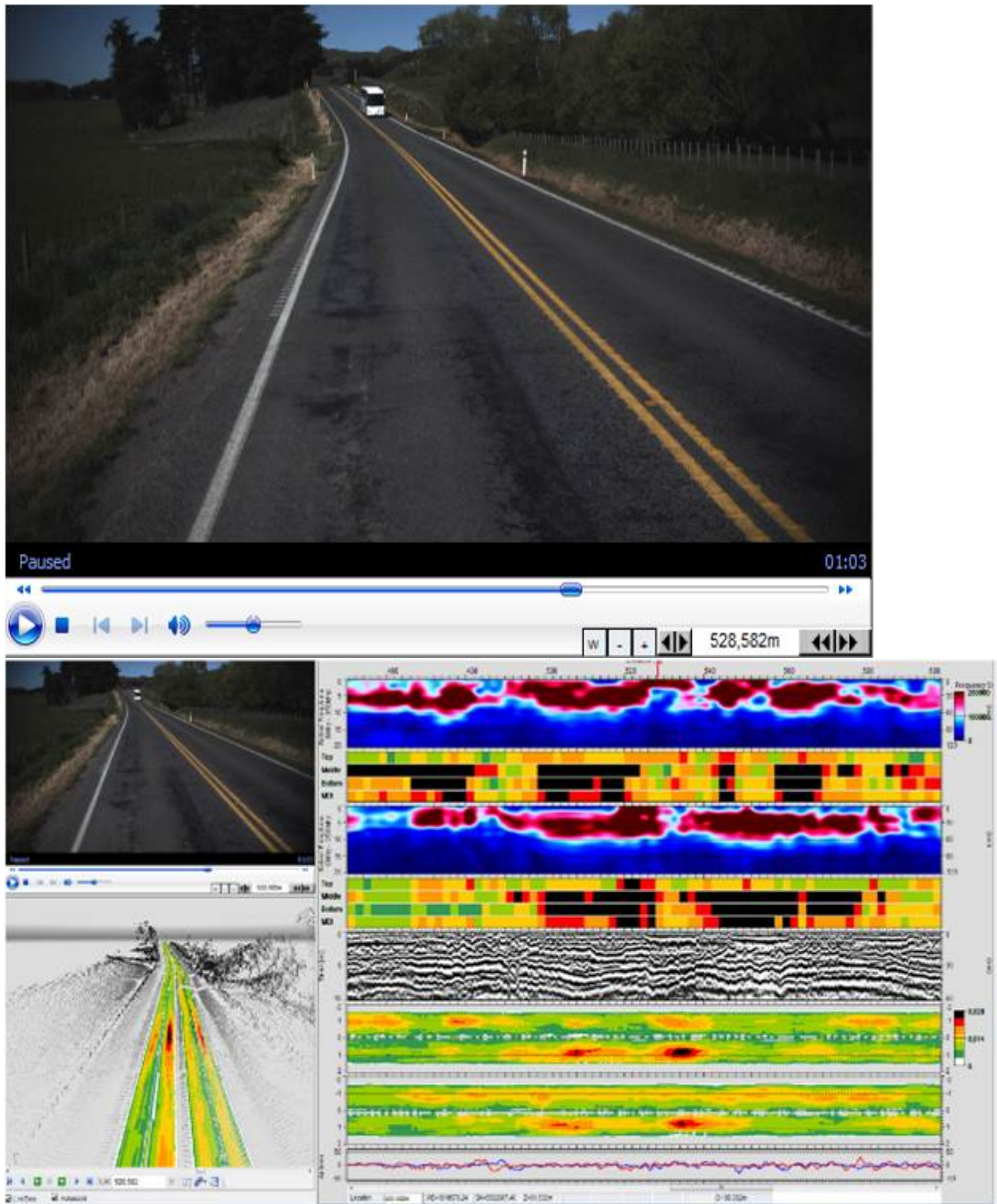


Figure B.16 is an example of where high moisture was measured in the subgrade (depth >250mm) as shown in the black shaded bars. From the photo and LIDAR survey rutting can be seen in this location. This example shows the deformation is likely due to saturation of the fill subgrade rather than the top pavement aggregate layers.



## B5 Tararua

A few sites were surveyed in the Tararua alliance contract with the sites shown in figure B.17.

Figure B.17 Sites locations surveyed in Tararua

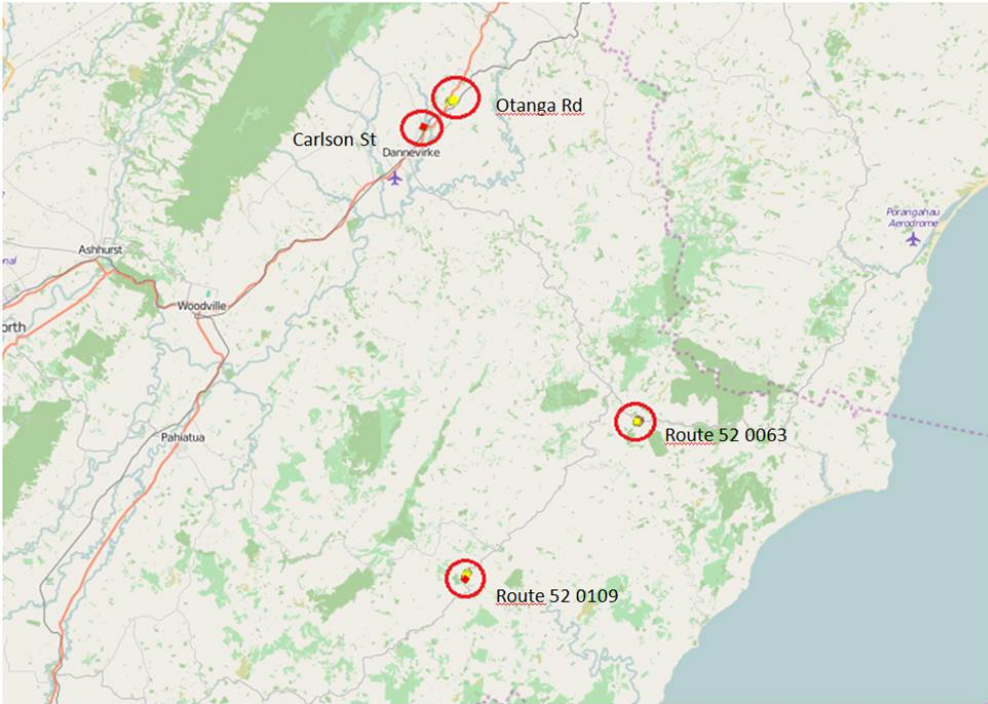


Figure B.18 High moisture locations surveyed in Tararua (Carlson Street, Route 52 and bottom shown is Otonga Rd)

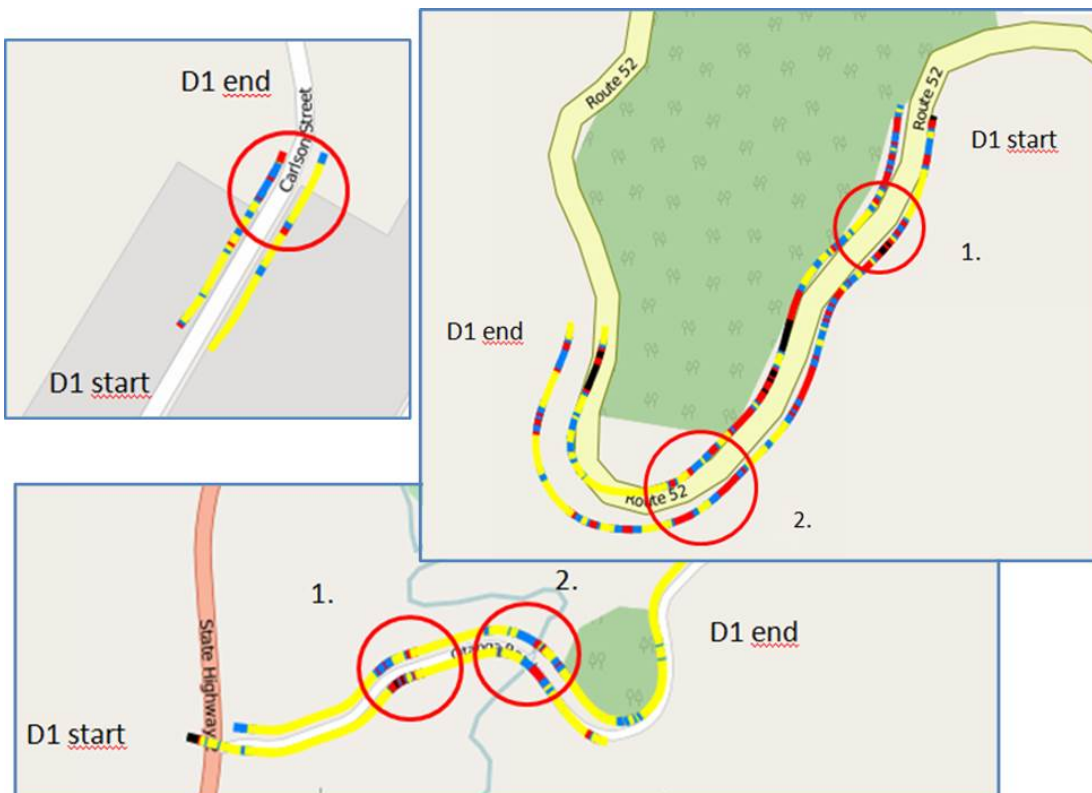
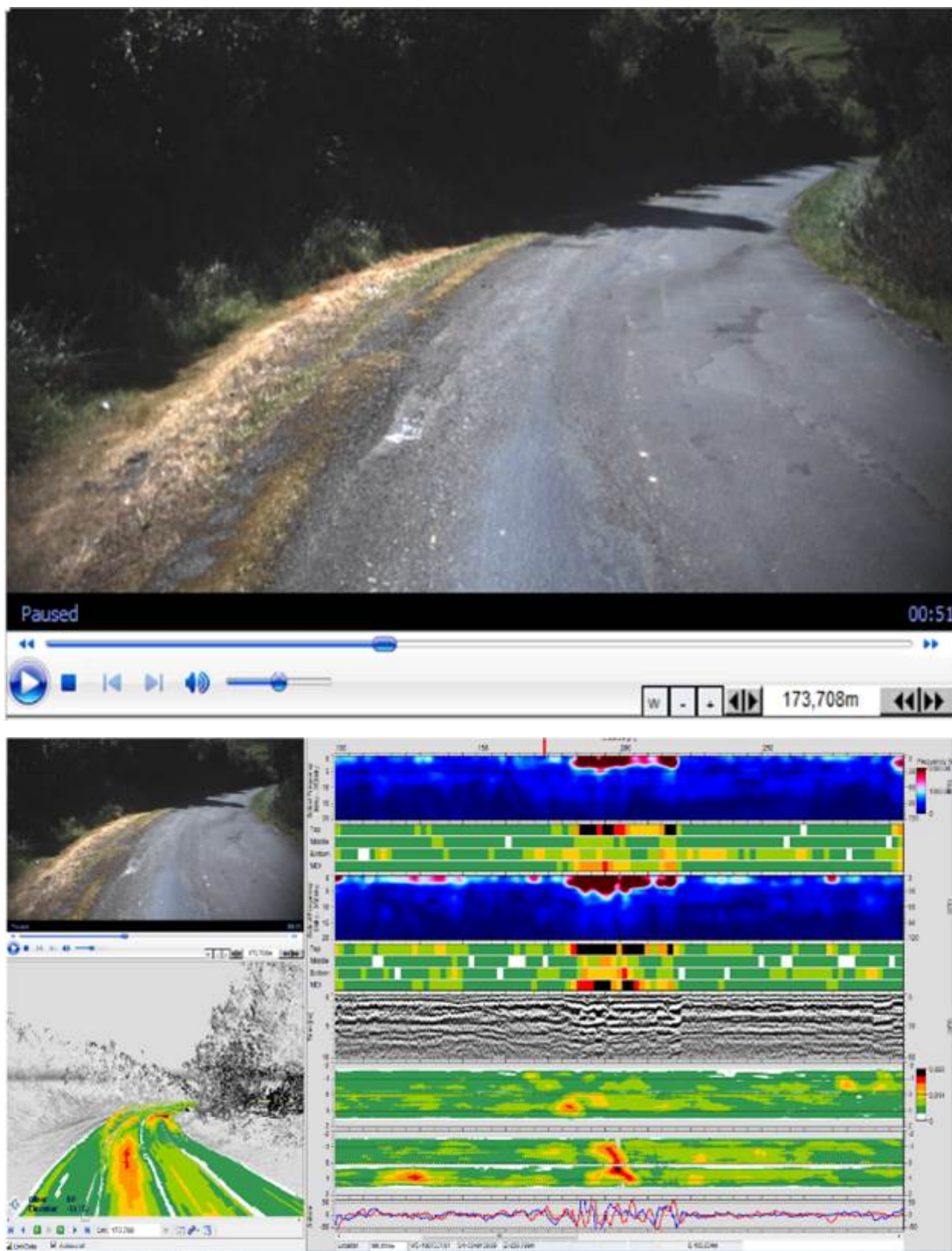


Figure B.19 Otonga Rd RP 174m

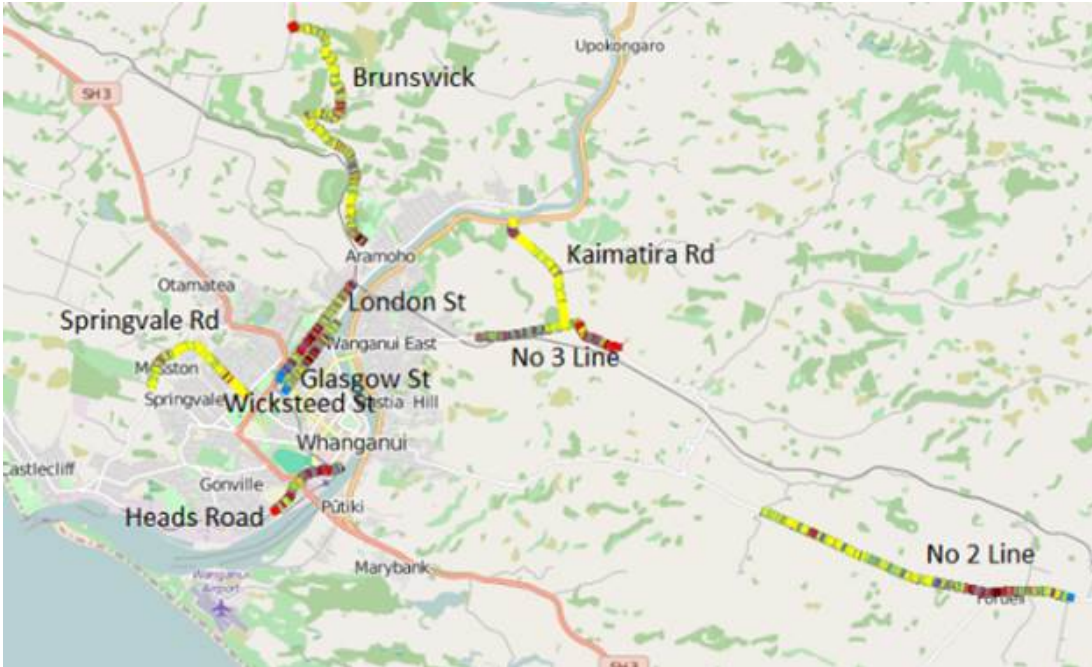


On Otonga Rd RP 174m shows an output from the moisture detection survey where the photo and LIDAR survey show high deformation. At this location high moisture is detected near the top of the pavement in a small area where there is deformation.

## B6 Whanganui

Figures B.20 to B.24 show MDI maps of where the moisture surveys were undertaken in Whanganui.

**Figure B.20** Site locations surveyed in the Whanganui district



**Figure B.21** No. 2 and 3 line sites where high moisture was measured in the Whanganui district





Figure B.23 Sites where high moisture was measured in the Whanganui district

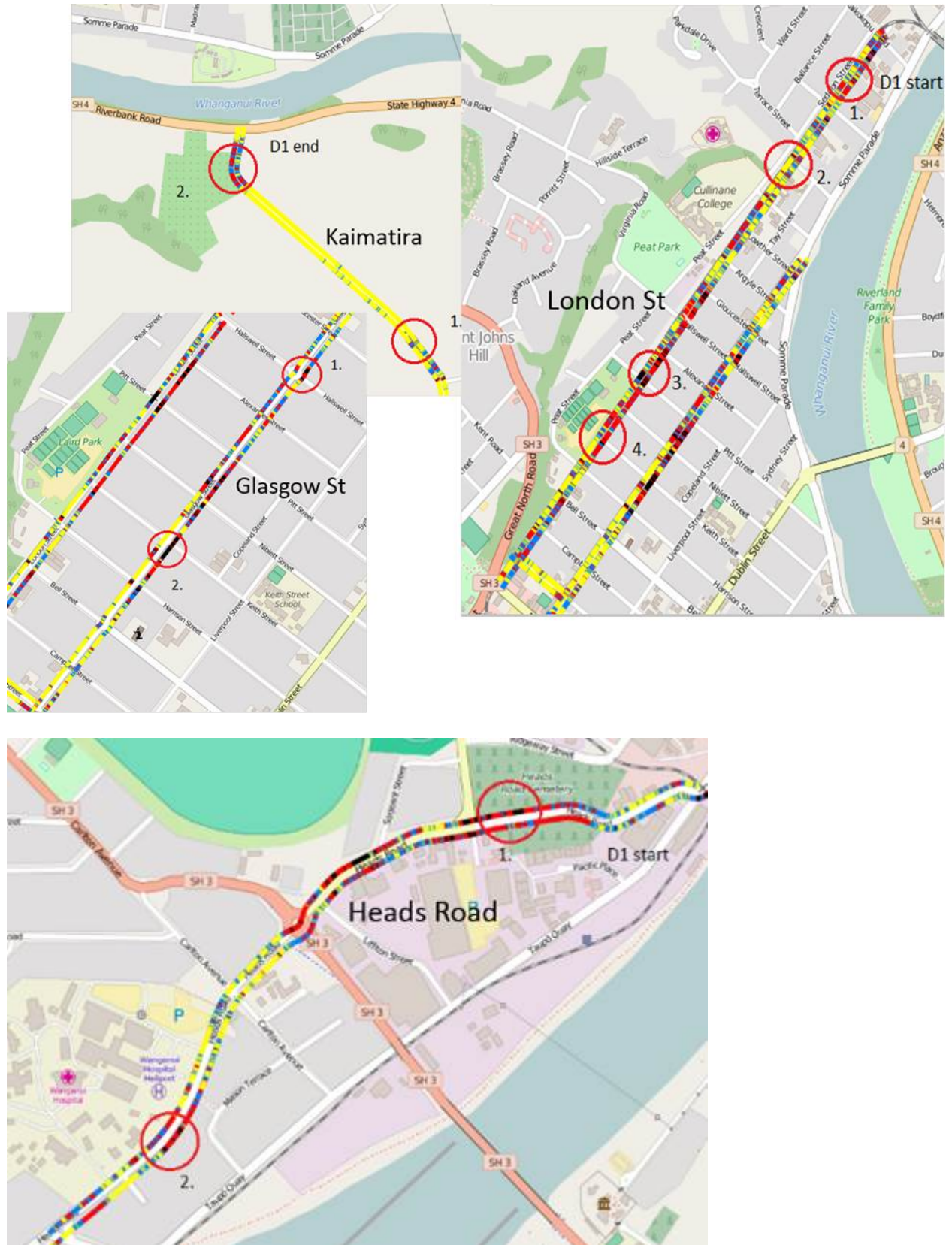


Figure B.24 Sites where high moisture was measured in the Whanganui district

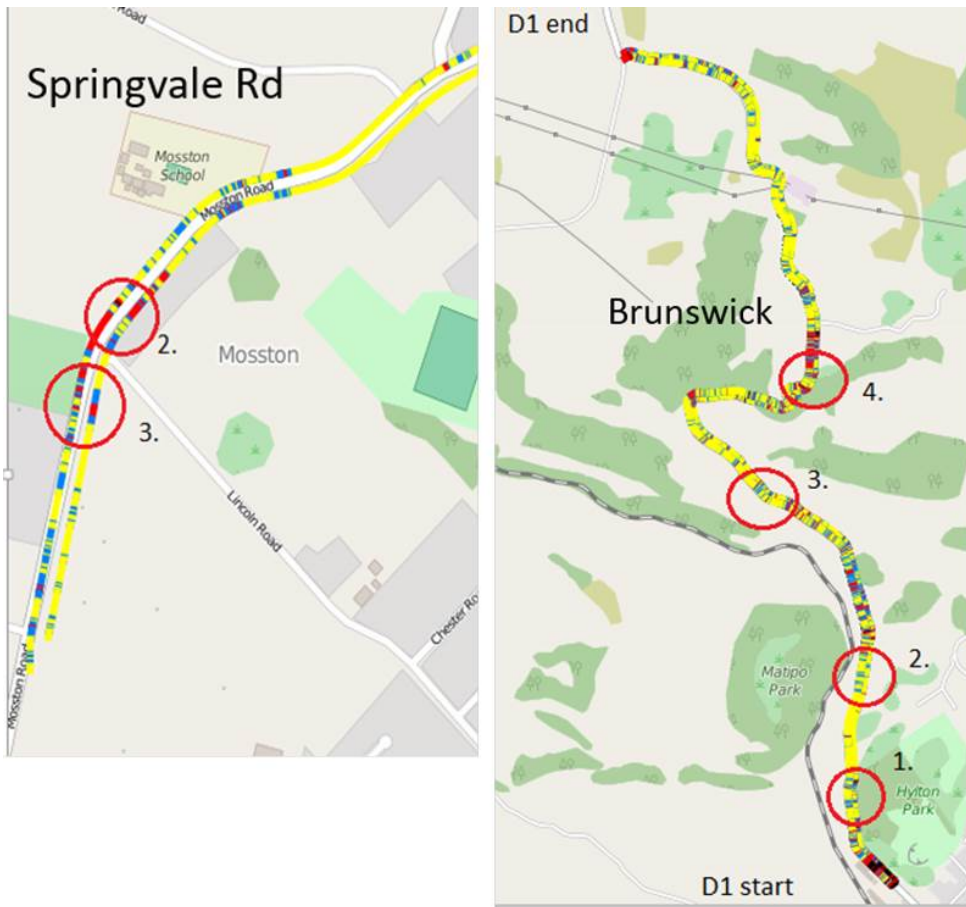




Figure B.25 Springvale road site where high moisture was detected (black bars)

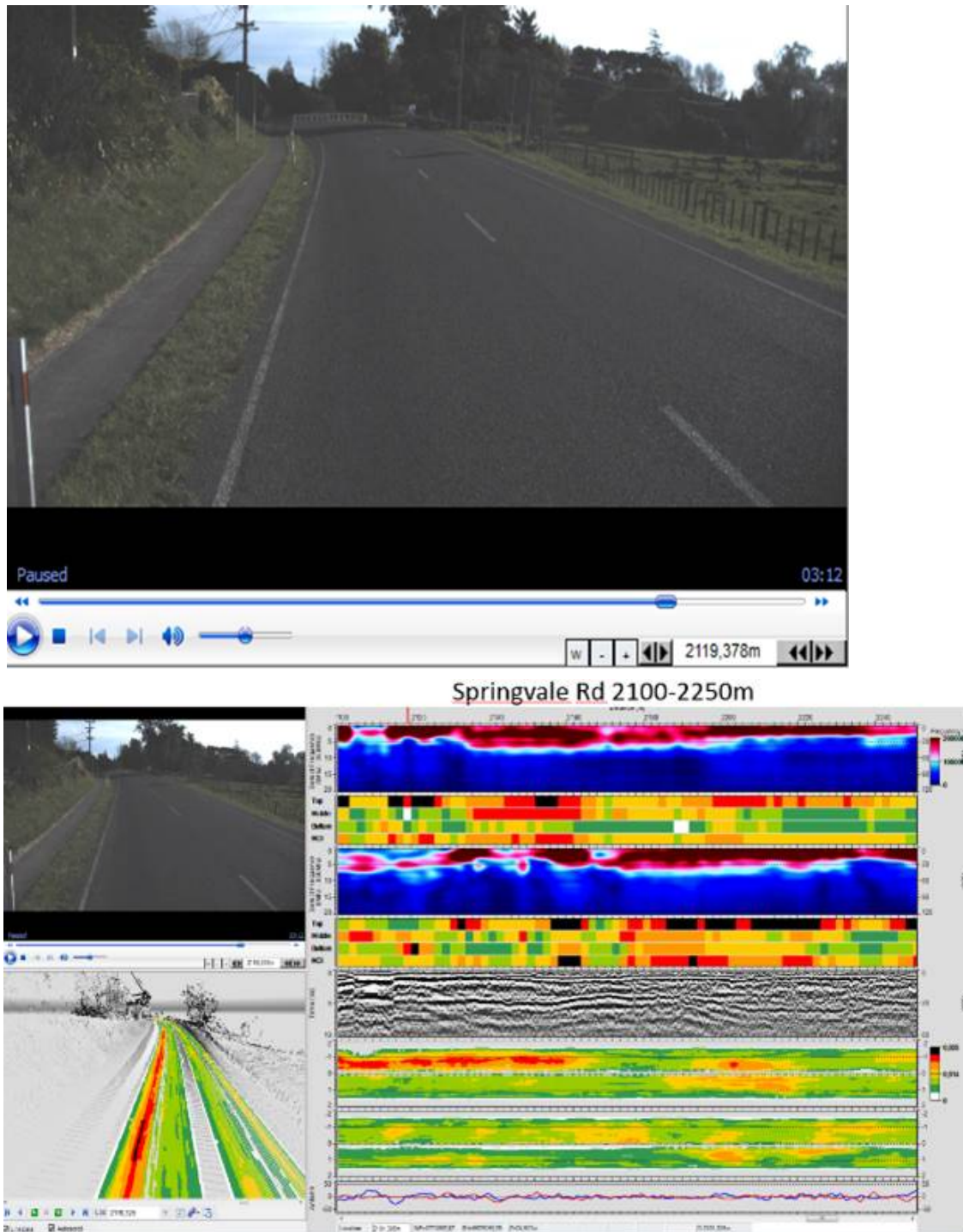


Figure B.25 shows a site with high moisture on Springvale road where the LIDAR laser shows rutting in the outside wheel track near the footpath. Interestingly both sides of the road show high moisture and not just the side nearest the footpath. Viewing the photo of this site on Springvale road shows a lack of drainage on the left-hand side next to the footpath which supports the reason for the high moisture detected.

## B7 Taranaki

Figure B.26 Locations in Taranaki surveyed for moisture

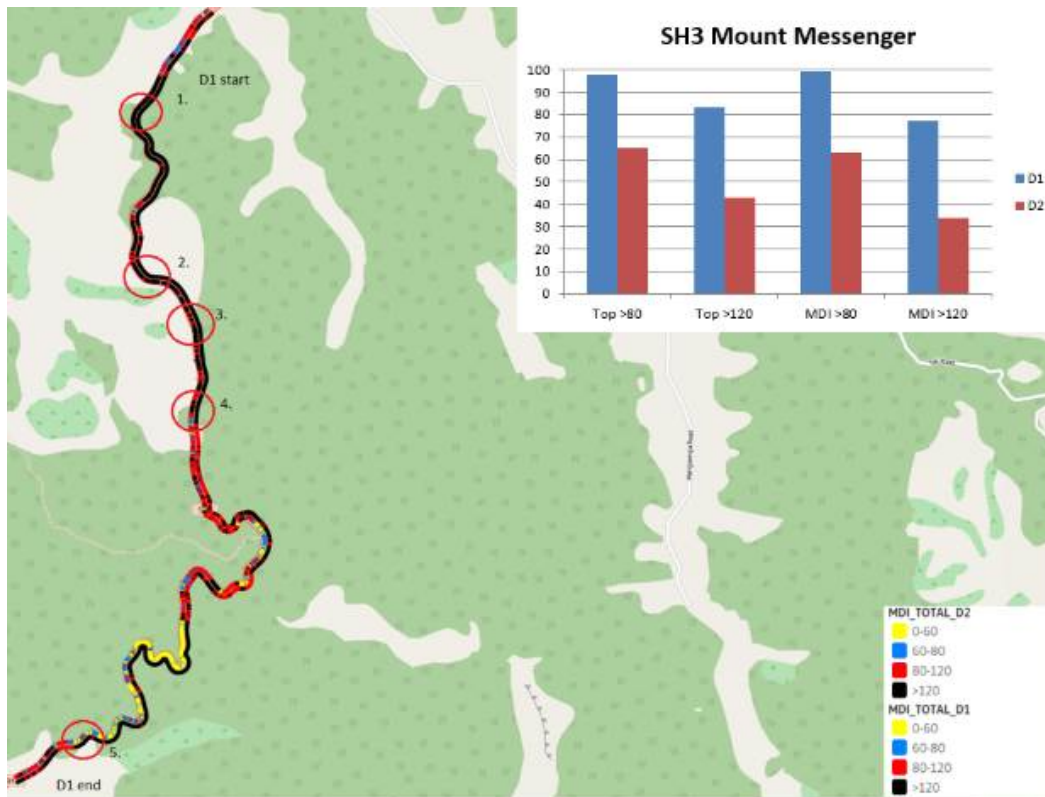


### B7.1 SH3 Mount Messenger

The section of SH3 known as Mt Messenger is a windy mountainous area. The geology of the area is largely papa mudstone, which may have resulted in high moisture being detected by the GPR survey. Many sections along this road have a kerb and channel on at least one side of the highway and where this exists there are also subsoil drains.

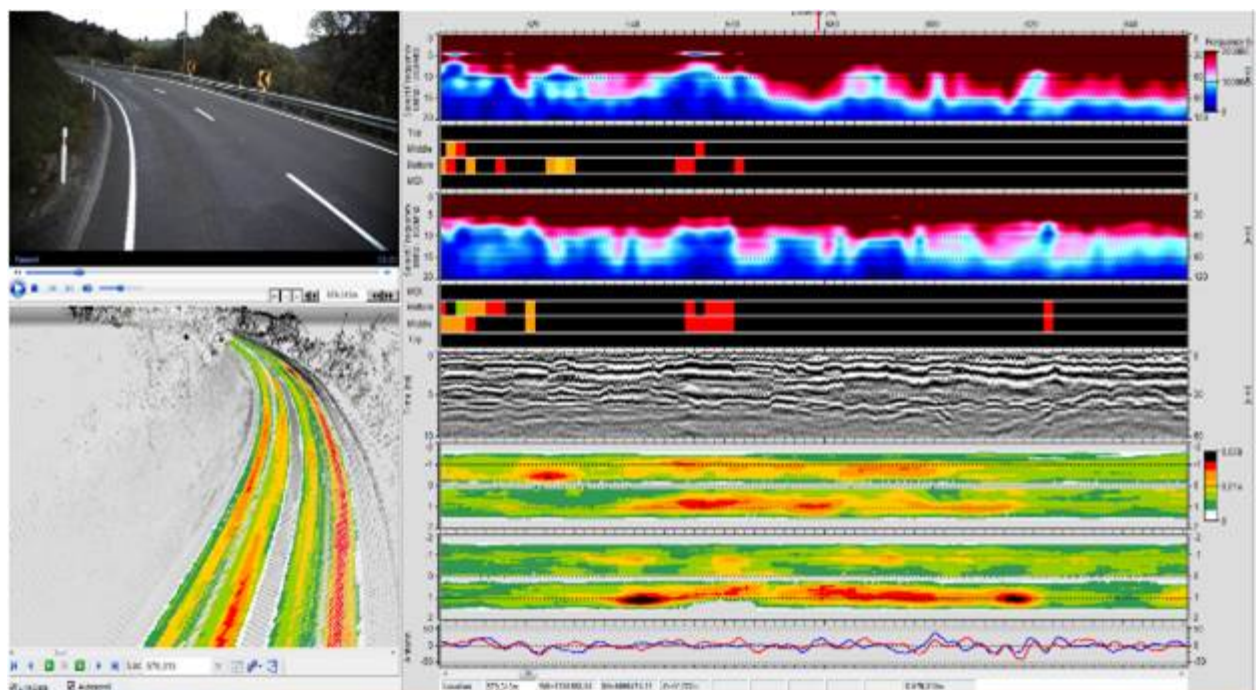
Melter slag, because it is electrically conductive, affects the GPR moisture values and results in high moisture reading everywhere. Melter slag was used along the surveyed route as a surfacing material in both 2011 and 2013 at route positions 4.025 to 4.166 (two-coat seal) and at 4.750 to 6.590 (SMA). This is very roughly displacements 2400 to 2500 and 3100 to 4900 in the survey data.

**Figure B.27 Results of moisture survey on SH3 Mt Messenger (note large areas show black or high moisture which is likely due to measurement error caused by steel slag in the surfacing and heavy cement stabilisation)**



**B7.1.1 SH3 Mount Messenger 500–650m (RP 176/2.15)**

**Figure B.28 Results of moisture survey on SH3 Mt Messenger (580m) (note large areas show black or high moisture which is likely to be caused by measurement error due to steel slag in the surfacing and heavy cement stabilisation)**



This site has good drainage with a kerb on the left and a drop off on the right behind the guard railing, and sits as the transition between two super elevated curves on an uphill climb. Any movement of moisture through the pavement layers therefore is not likely to follow a simple path from one side to another.

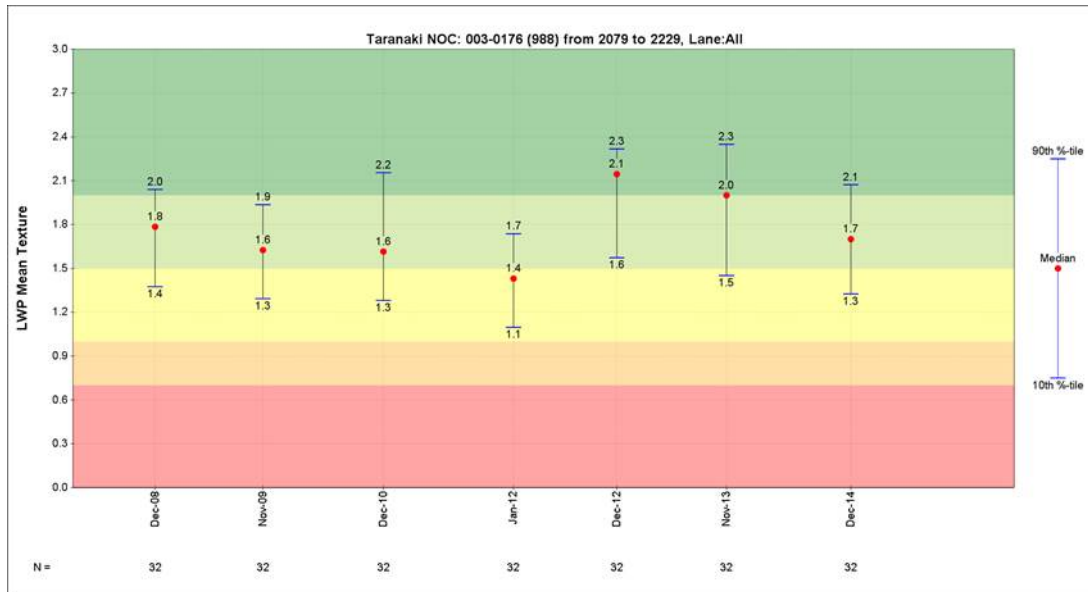
The most recent rehabilitation occurred here in 2011 and the site currently has two seal layers. This rehabilitation had issues as it required holding through the winter, and even though it is only five years old, it looks a lot older.

Since the 2011 rehabilitation, RAMM shows (within a 300m area) there has been cyclic cleaning of culverts and water channels, some 110m<sup>2</sup> of crack sealing due to alligator cracking, 36m<sup>2</sup> of pavement repairs due to depressions/deformations and a massive number of recorded pothole repairs numbering 260 over five years (many due to reworking the same spots). It is also noted that as this is the start of the Mt Messenger Eastern climb, it is often subject to effluent dumps/spills both on the road surface and sometimes (as observed in the field inspection) directly into the drainage channels/sumps.

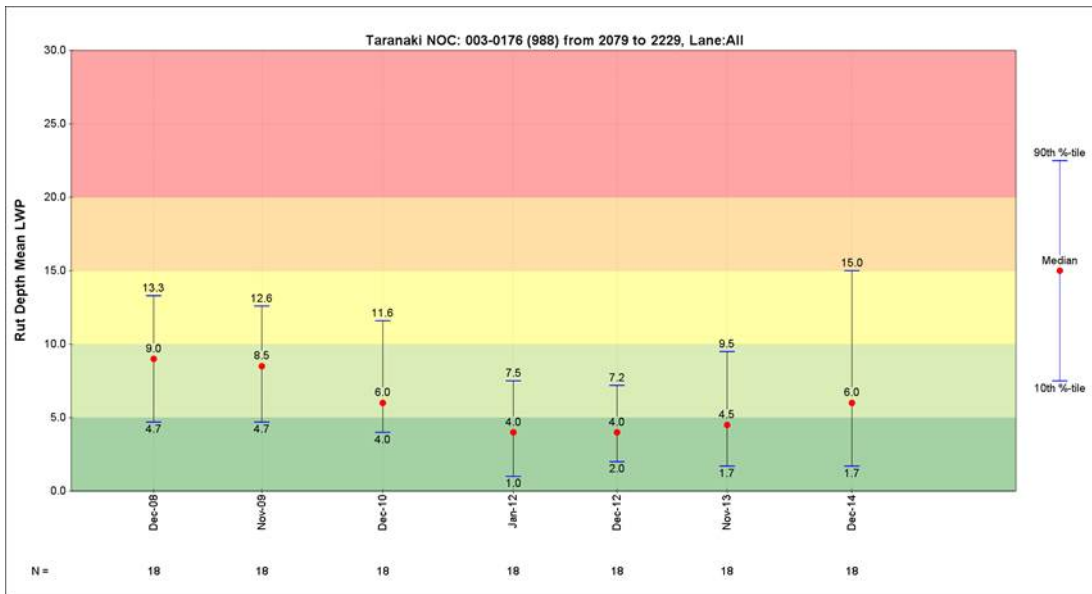
There is both rutting and flushing developing along this section with, at one point, fines being pumped through the seal which supports the high moisture measured for this site. The loss of texture at this site has triggered both a 200m SCRIM seal as imminent as well as some water cutting.



Figure B.29 SH3 Mount Messenger 500-650m: rutting and texture measurements from 2008 to 2014



Texture deterioration

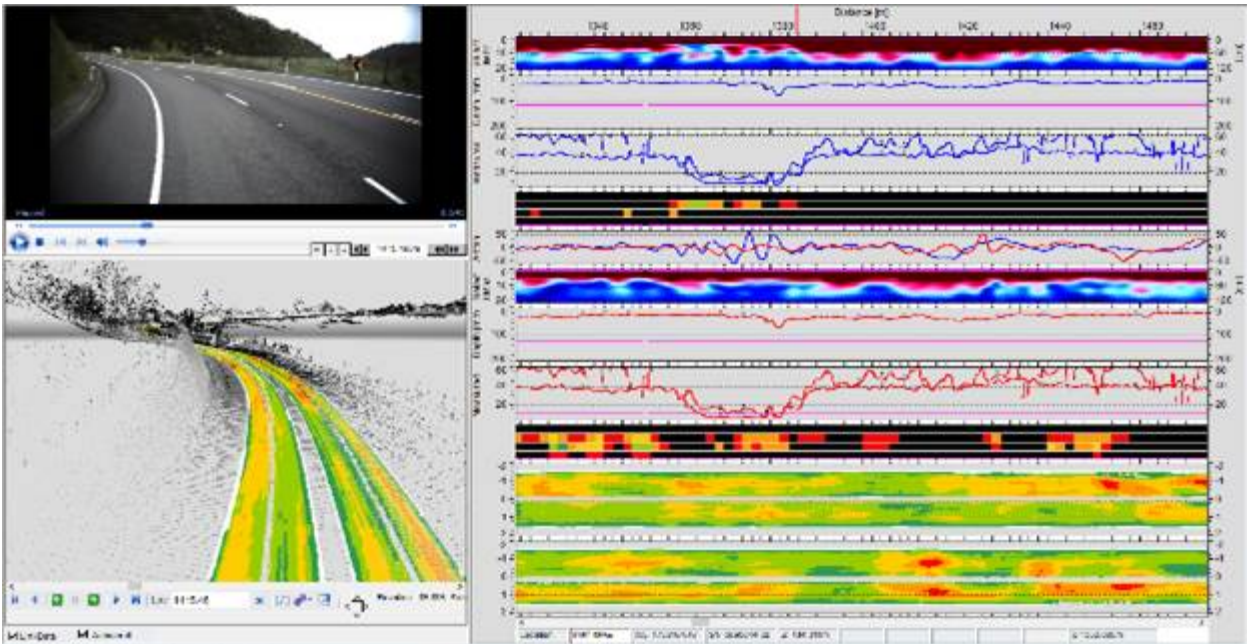


Rutting deterioration



**B7.1.2 SH3 Mount Messenger 1,400-1,550m (RP 176/3.04)**

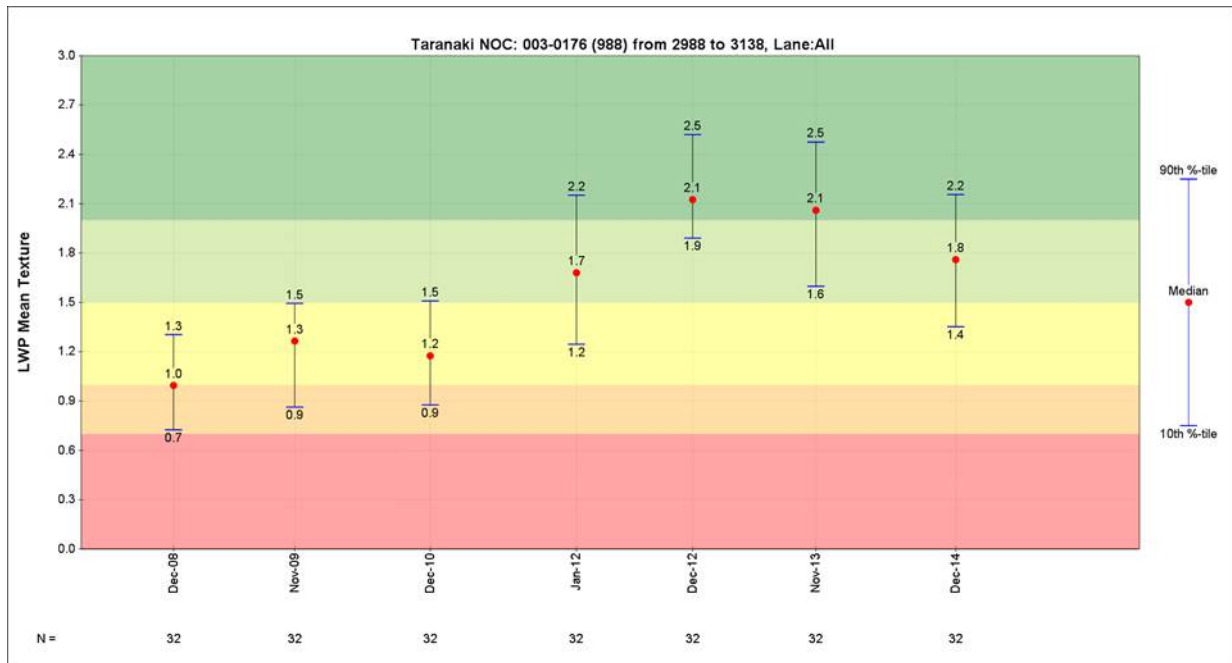
**Figure B.30 Results of moisture survey on SH3 Mount Messenger 1,400-1,550m (RP 176/3.04)**



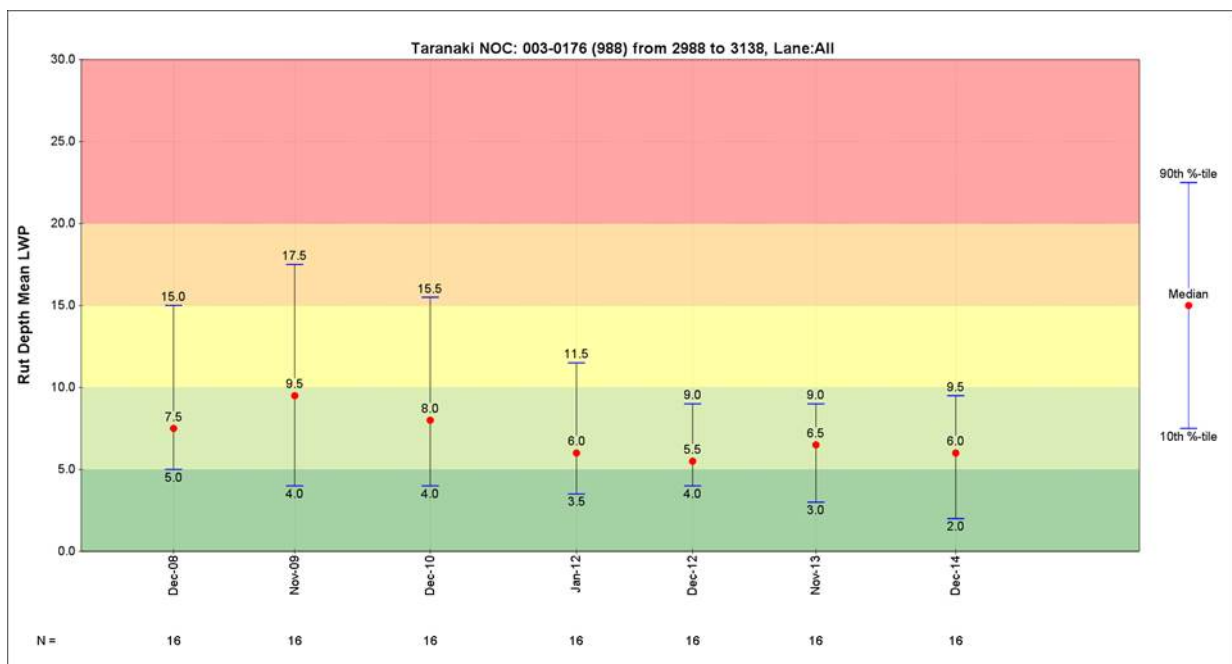
Results from the moisture survey on SH3 Mount Messenger show very high moisture (black areas) and dielectric values >40 which is well in excess of normal dielectric values in the range of 5 to 15. These unusually high values indicate there is surfacing and/or pavement materials that have high electrical conductivity like steel slag aggregate or possibly volcanic ash. The RAMM database shows the steel slag does not start until 2,400m (RP 176/4.025); however, these high dielectric values indicate there is steel slag present as there is no other explanation.

This site has a well-drained top surface on an inclining site with a kerb and channel both sides. The most recent rehabilitation occurred in 2011 and the site currently has two seal layers. This appears to be a stable site with little maintenance needed since the rehabilitation other than normal water channel clearing. No further treatment is planned in the forward works programme (FWP) over the next five years.

Figure B.31 SH3 Mount Messenger 1,400-1,550m: rutting and texture measurements from 2008 to 2014



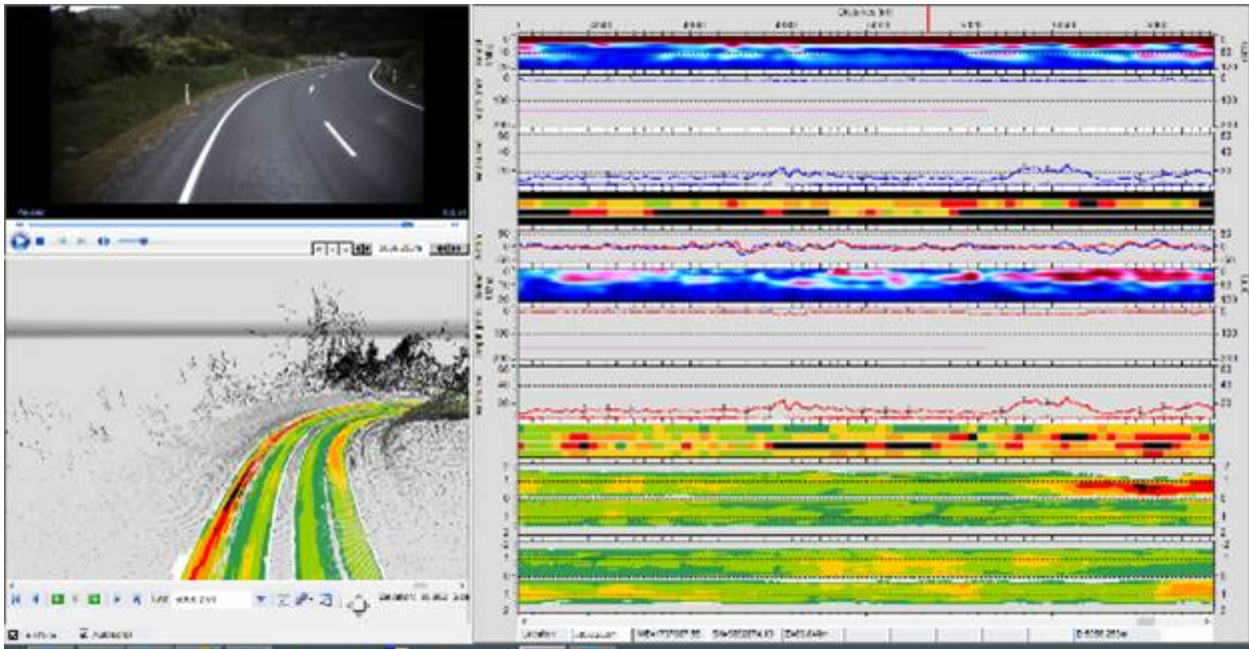
Texture deterioration



Rutting deterioration

### B7.1.3 SH3 Mount Messenger 5,000–5,150m (RP 176/6.63)

Figure B.32 Moisture survey outputs

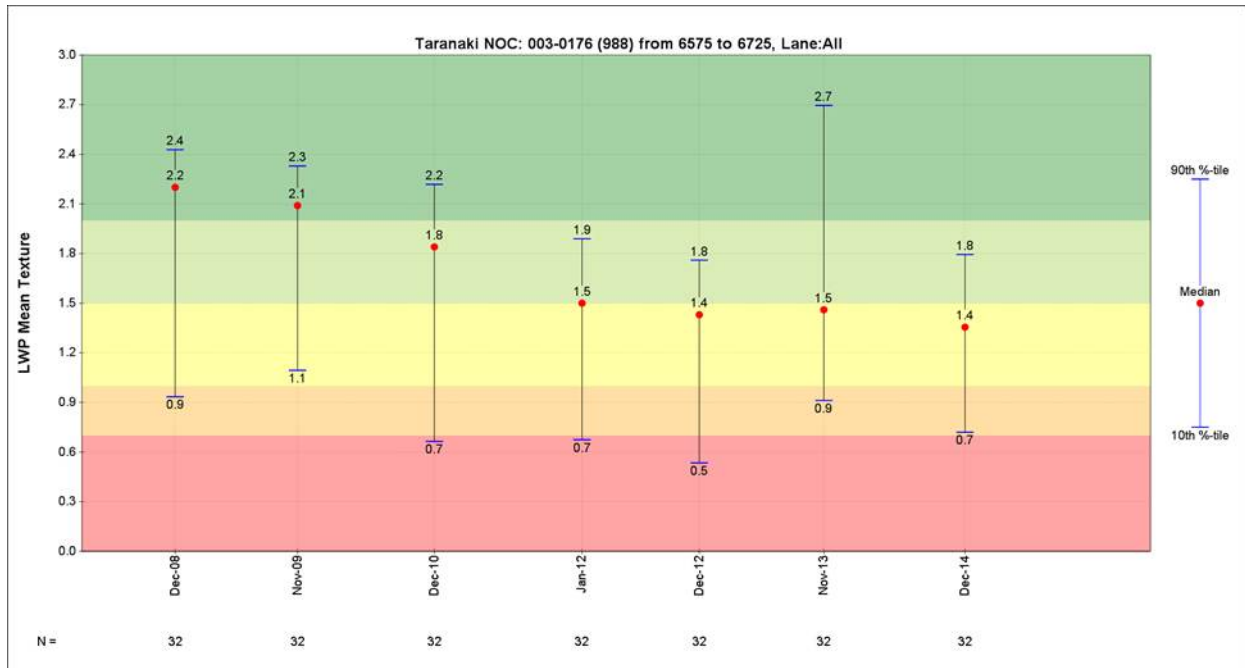


This section of Mt Messenger has surfacing challenges due to the steepness and torturous curves, coupled with a high percentage of heavy vehicles. It is at the western extent of the mountain and has largely been constructed over a papa fill.

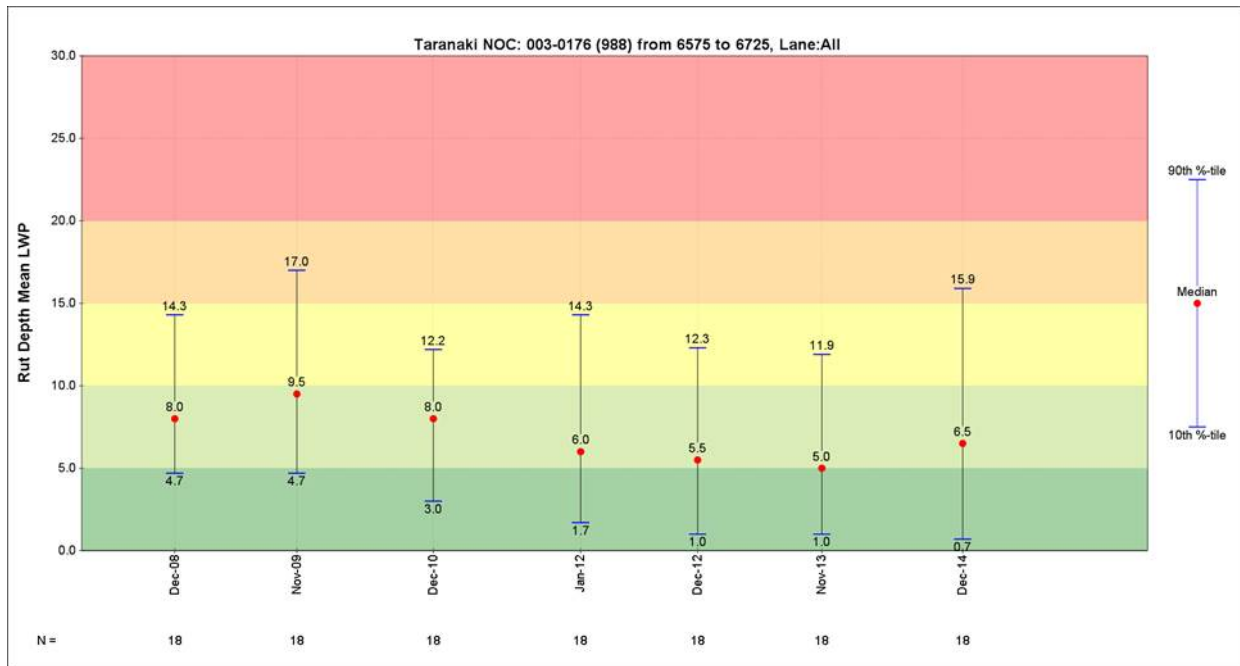
There is constant dampness beyond the kerbs on the right-hand side as moisture leaches from the adjoining landscape (cuttings and bushed area). Existing drainage comprises intermittent kerb and channel on the inside of the curves with little on the opposing high sides (open channel between), complemented by frequent culverts crossing the carriageway to move the water from the higher right side to the left where it can flow away naturally.

The most recent rehabilitation seems to have been in 1990. Our records show four seals present with the most recent incorporating melter slag and laid early 2016 (post survey); this was a result of cracking, flushing and rutting. Current defects are blocked culverts, but prior to reseal (ie at time of survey) there were numerous fatigue cracking, and the occasional blocked culvert and deformations. This is consistent with previous years' maintenance activities of crack filling, pothole repairs and culvert clearing.

Figure B.33 SH3 Mount Messenger 5,000-5,150m: rutting and texture measurements from 2008 to 2014



Texture deterioration

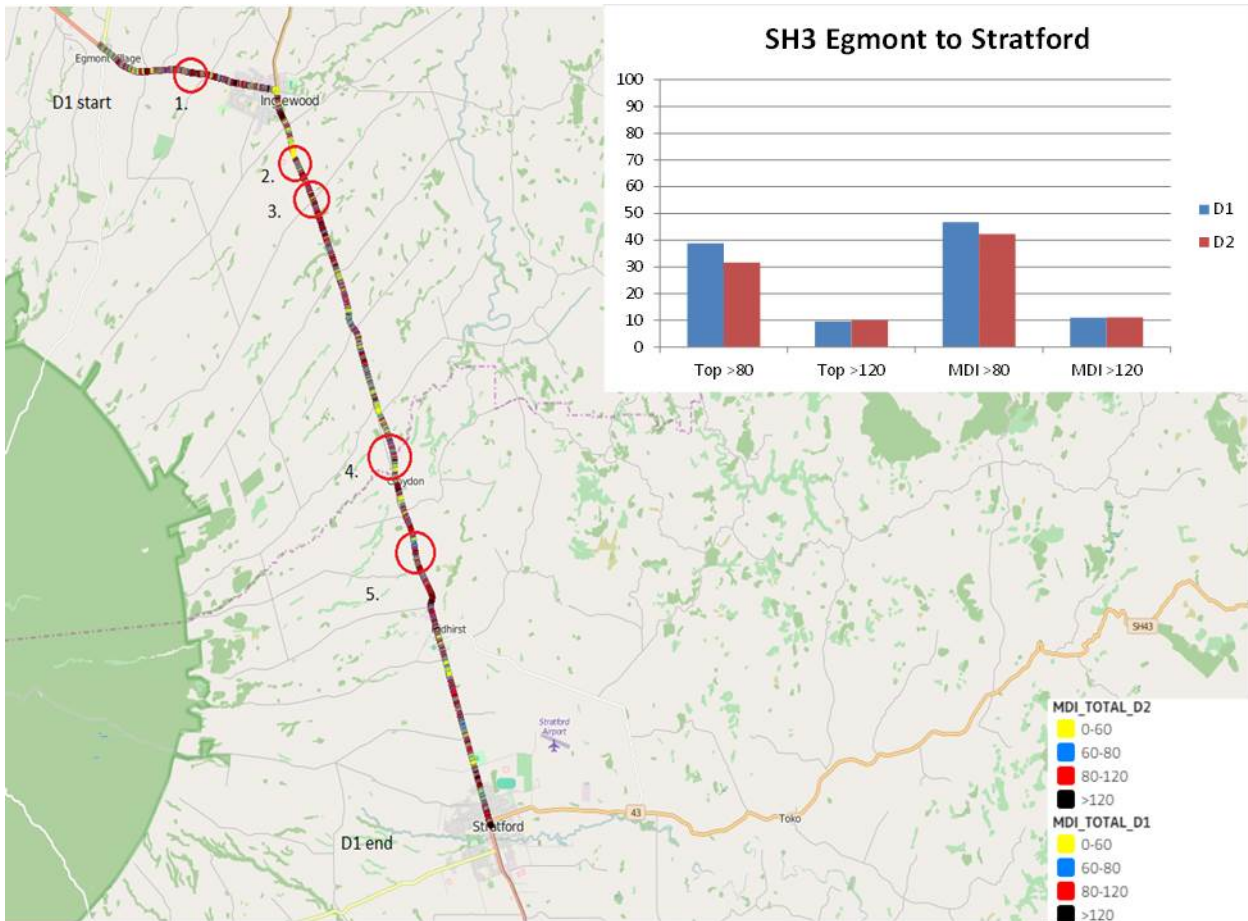


Rutting deterioration

## B7.2 SH3 Egmont to Stratford

This section of SH3 is largely sited on Taranaki ash. It has a few tight curves, but is not unduly steep. The road does, however, cross numerous water paths as it skirts around the base of the mountain with the flow generally crossing under the highway in a right to left direction. There is no record of melter slag currently being used along the surveyed route.

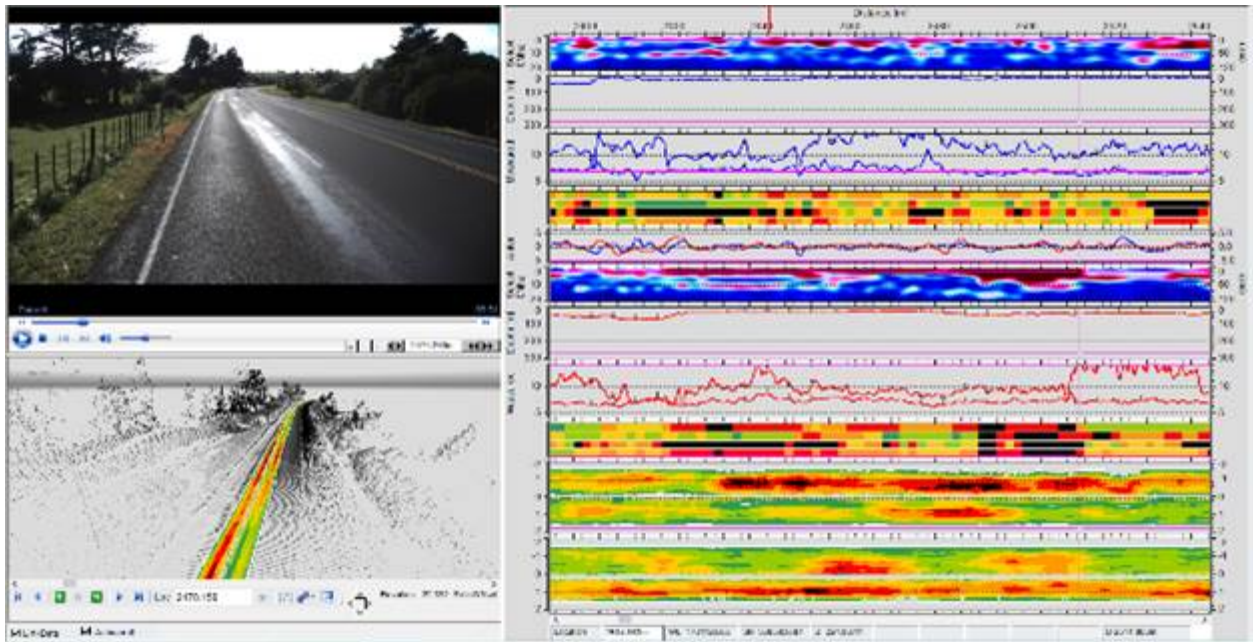
Figure B.34 Results of moisture survey on SH3 Egmont to Stratford





**B7.2.1 SH3 Egmont to Stratford 2,400–2,550m (RP 240/14.48)**

**Figure B.35 SH3 Egmont to Stratford 2,400–2,550m (RP 240/14.48) moisture survey results**

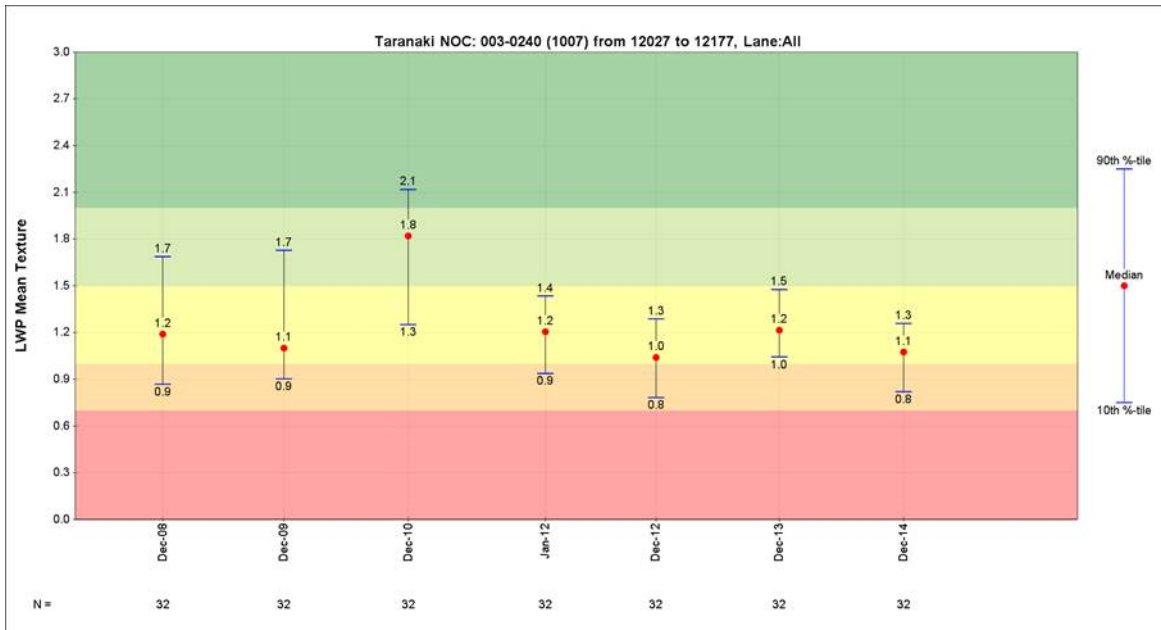


This site shows high moisture mostly in the middle and bottom (depth >250mm) from the survey and this is supported by the wheel track rutting and flushing.

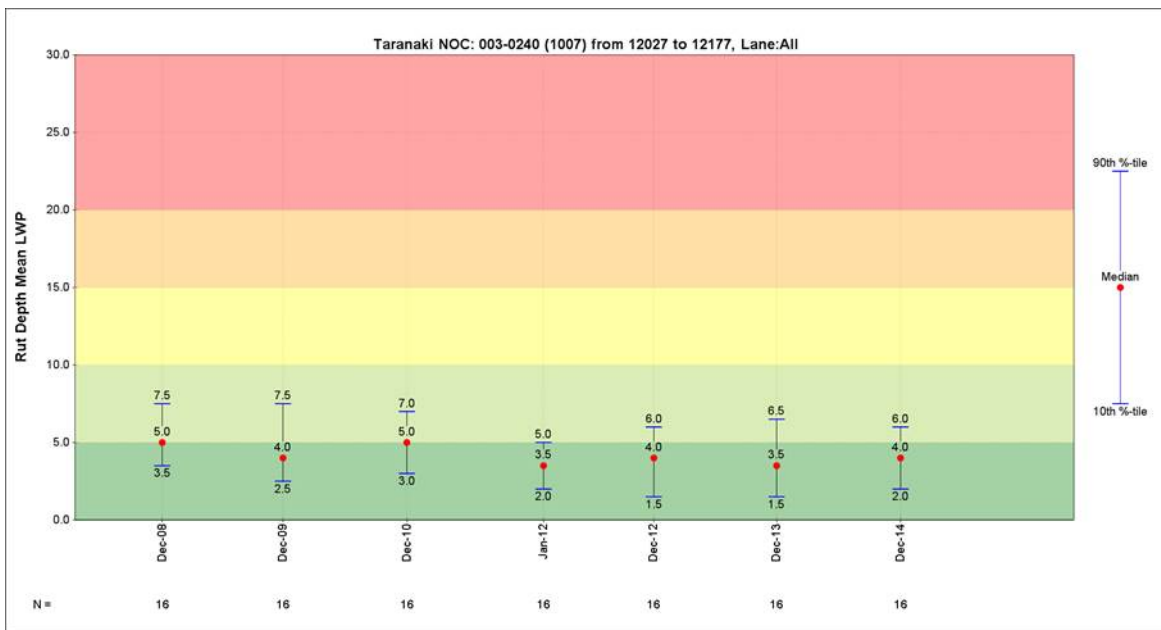
No actual water channels exist at this point; however, just beyond it, at its limits, there is a drainage channel down to a nearby waterway. Apart from this, water is able to escape from the grassed shoulder onto nearby farm land.

The most recent rehabilitation occurred in 1987 and the site now has five seal layers with the most recent being laid in 2013. 900m<sup>2</sup> pre-reseal pavement repairs were carried out in 2012 but little has been needed since other than 450m<sup>2</sup> of water blasting due to flushing. No further treatment is planned in the FWP for the next five years.

Figure B.36 SH3 Egmont to Stratford 2,400–2,550m: rutting and texture measurements from 2008 to 2014



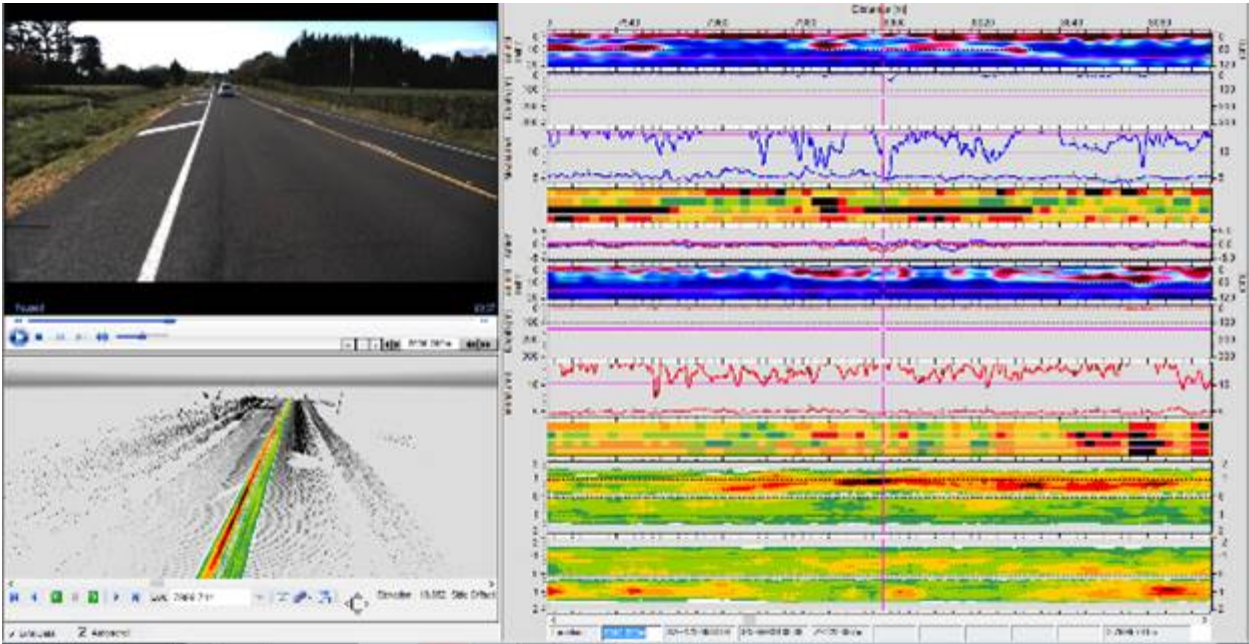
Texture deterioration



Rutting deterioration

**B7.2.2 SH3 Egmont to Stratford 7,950–8,100m (RP 258/2.24)**

**Figure B.37 Moisture survey results for Egmont to Stratford 7,950–8,100m (RP 258/2.24)**



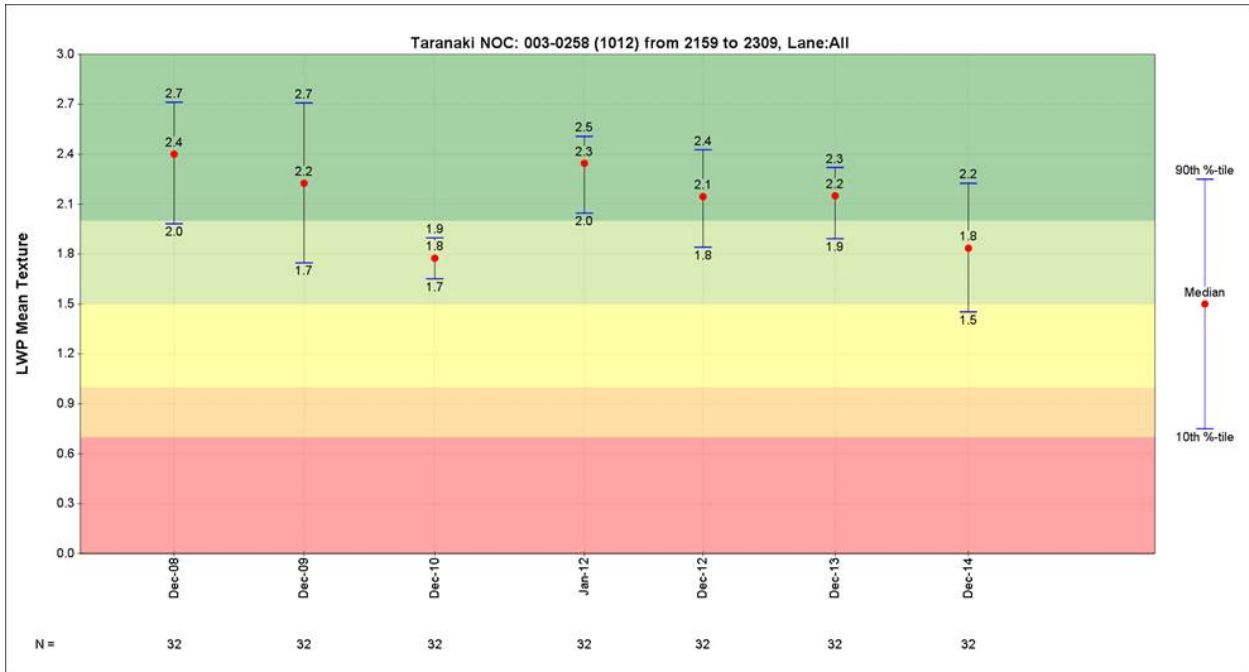
The moisture survey results for this section show high moisture (black bars in MDI calculation) and the laser survey has identified some rutting.

This road is bounded by rail on one side and slightly higher farm land on the other; however, shallow water channels exist along the section which runs between the Ngatoro and the Ngatoro-iti stream bridges.

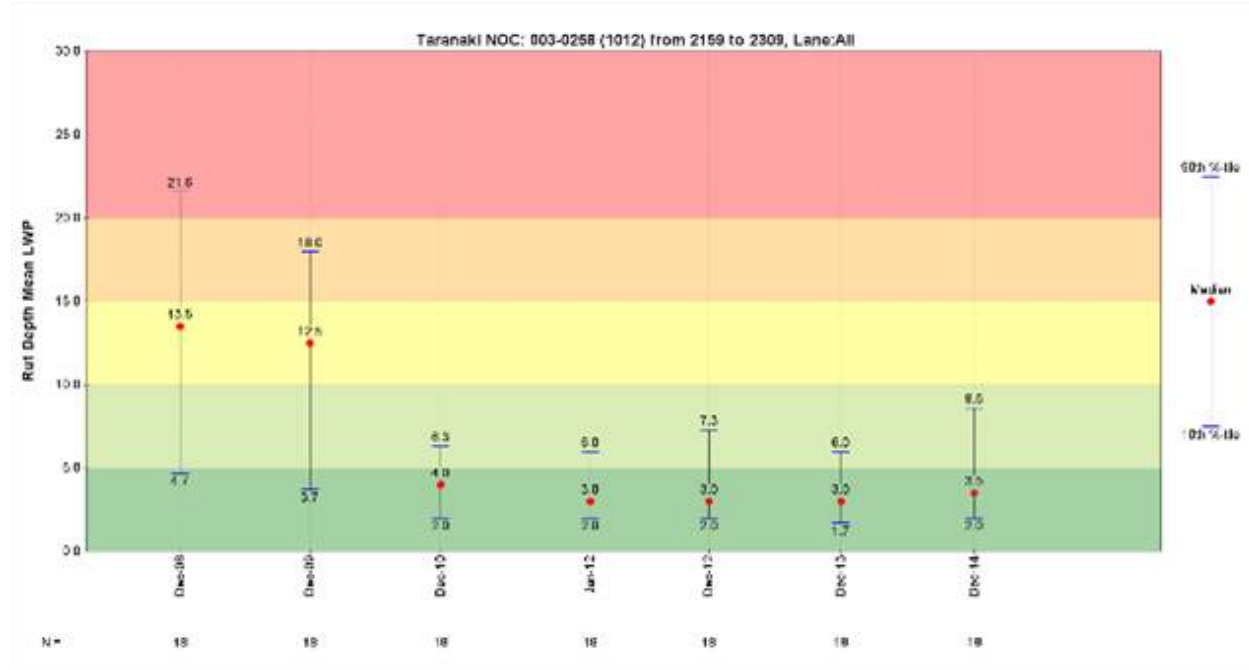
This site was last rehabilitated in 2000 and only has the two seal coats recorded. Maintenance history shows numerous pot hole repairs in the last two years but these are not evidenced in the field. There has, however, been bad potholing leading up to both bridge abutments so these are probably the potholes shown in the maintenance data. Little in the way of shoulder/drainage work has been carried out (or needed) since 2009. It is noted that cracking is also present along some of this section and visually there is also isolated shallow rutting along the left wheel path of the left lane.

No area rehabilitation or reseal treatment is identified in the FWP for the next five years.

Figure B.38 SH3 Egmont to Stratford 7,950-8,100m: rutting and texture measurements from 2008 to 2014



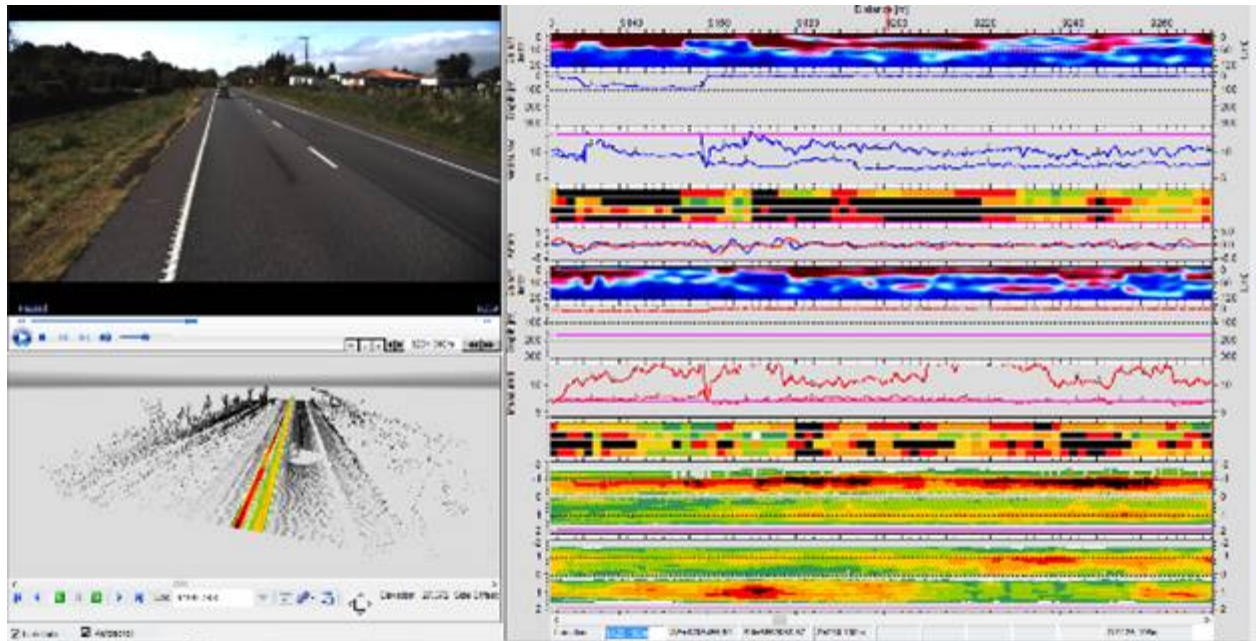
Texture deterioration



Rutting deterioration

### B7.2.3 SH3 Egmont to Stratford 9,150–9,300m (RP 258/3.39)

Figure B.39 Moisture survey results for SH3 Egmont to Stratford 9,150–9,300m (RP 258/3.39)



High moisture is detected at this site and high rutting in the wheel tracks is shown.

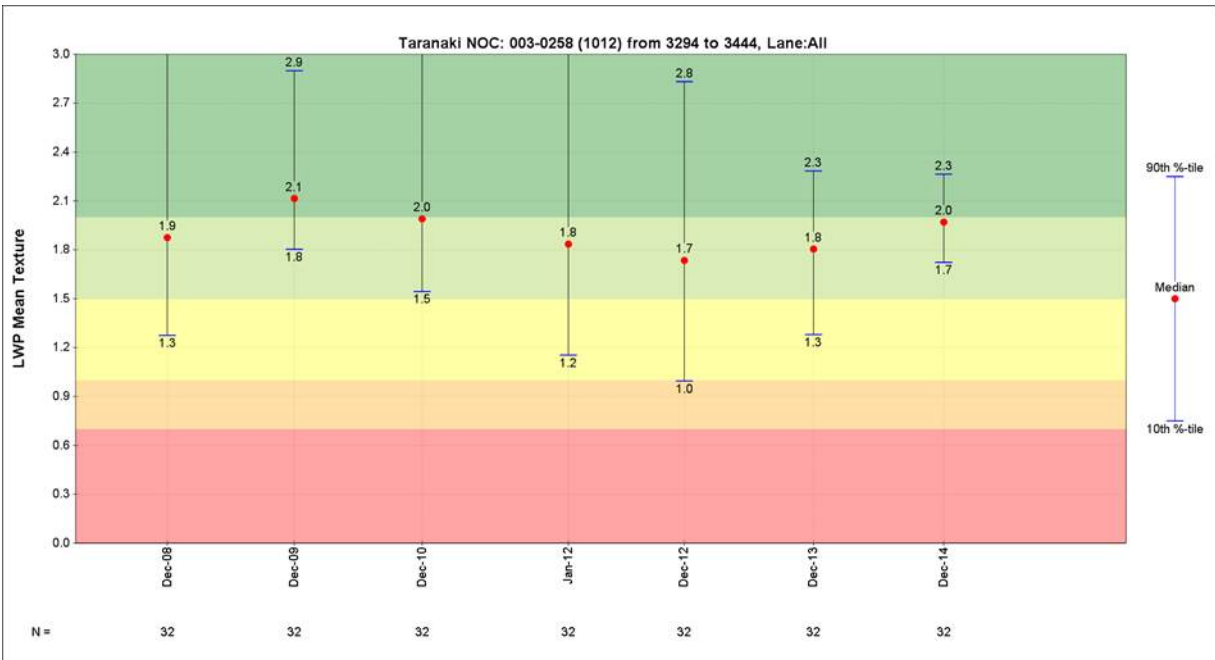
A shallow swale runs along the left of the highway while a reasonable drainage path exists along the right (a length of this has a culvert – it is uncertain if this presents a problem for the free drainage from the adjacent pavement). This carriageway does, however, traverse a slight vertical hump so little surface water should exist here other than the direct runoff from the road. It is unclear how old the pavement is but it is possible/likely that it was reconstructed in 2004 and currently has just two seal layers. If the 2004 treatment was just a resurface, then this site would have at least five layers present.

Since 2004 the only noteworthy maintenance has been low shoulder work which is once again about to be carried out.

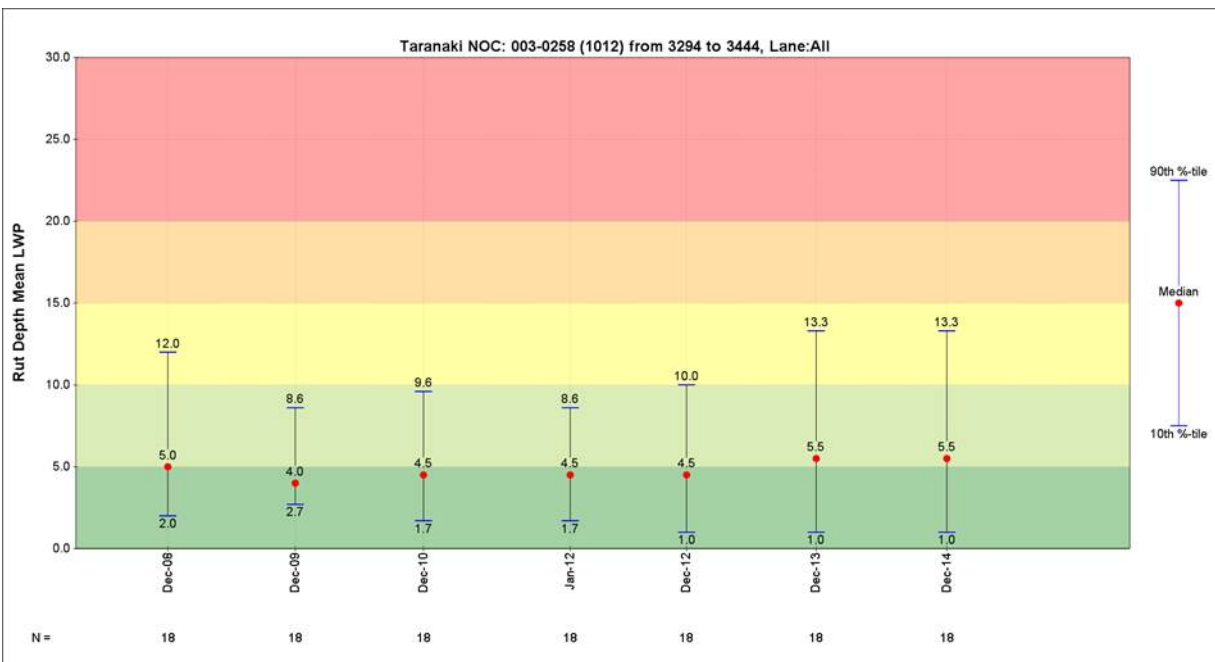
The next entry in the FWP for this site is a resurface in another three years and it is entirely possible this may be pushed out further closer the time.



Figure B.40 SH3 Egmont to Stratford 9,150-9,300m: rutting and texture measurements from 2008 to 2014



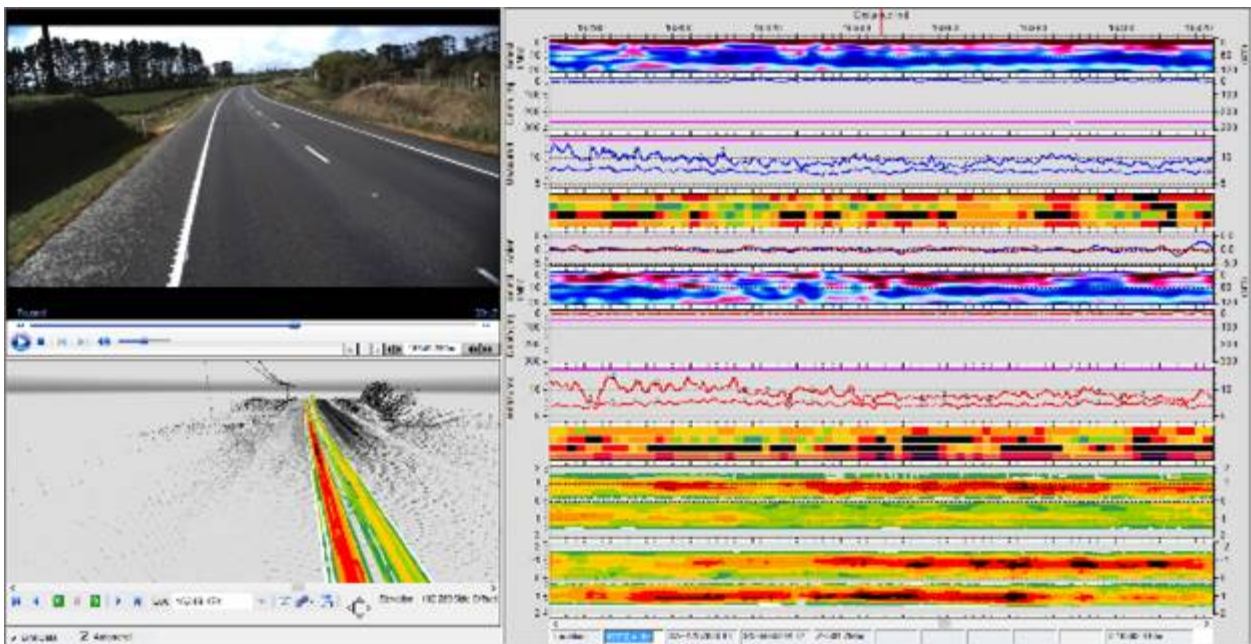
Texture deterioration



Rutting deterioration

### B7.2.4 SH3 Egmont to Stratford 16,300–16,450m (RP 258/10.57)

Figure B.41 Moisture results for SH3 Egmont to Stratford 16,300–16,450m (RP 258/10.57)



This section shows some moisture at depths of >250mm but not as bad as other sites. There is also some rutting.

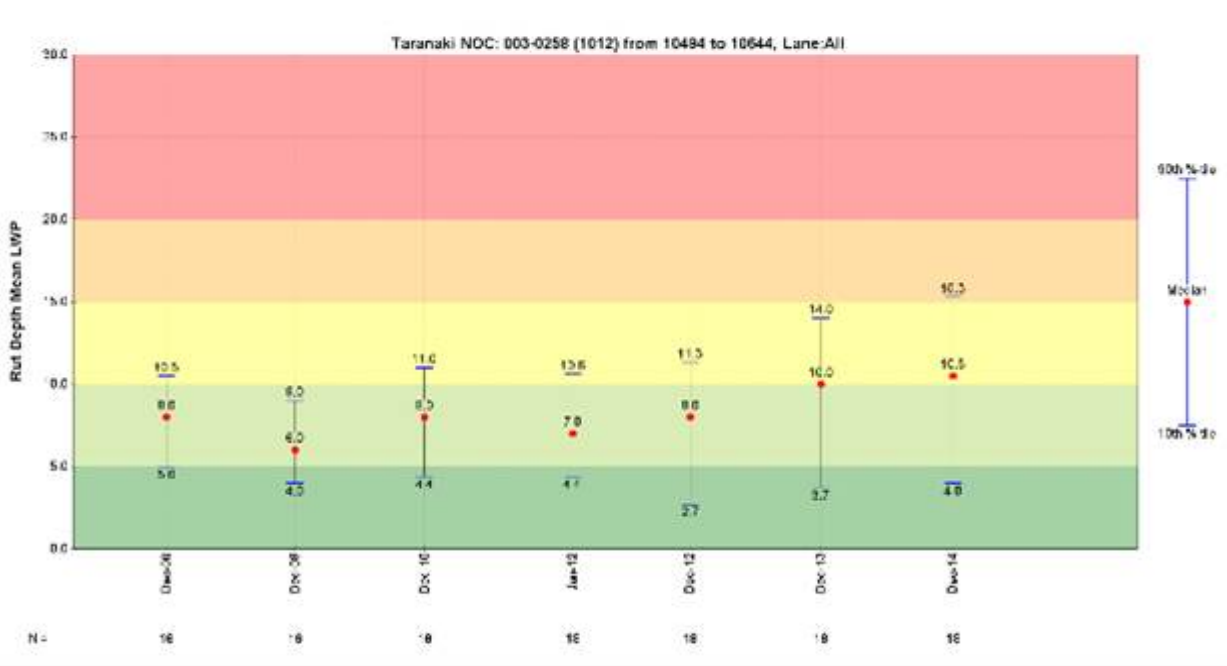
Good side drains exist along both sides of this carriageway. The platform has been made through a slight cut but the channels lead down toward the Waipuku stream some 300m south of the site.

Again the data is unclear as to when this site was last rehabilitated but it is likely to have been 1987 with either four of five seals being present today (most recently 2006).

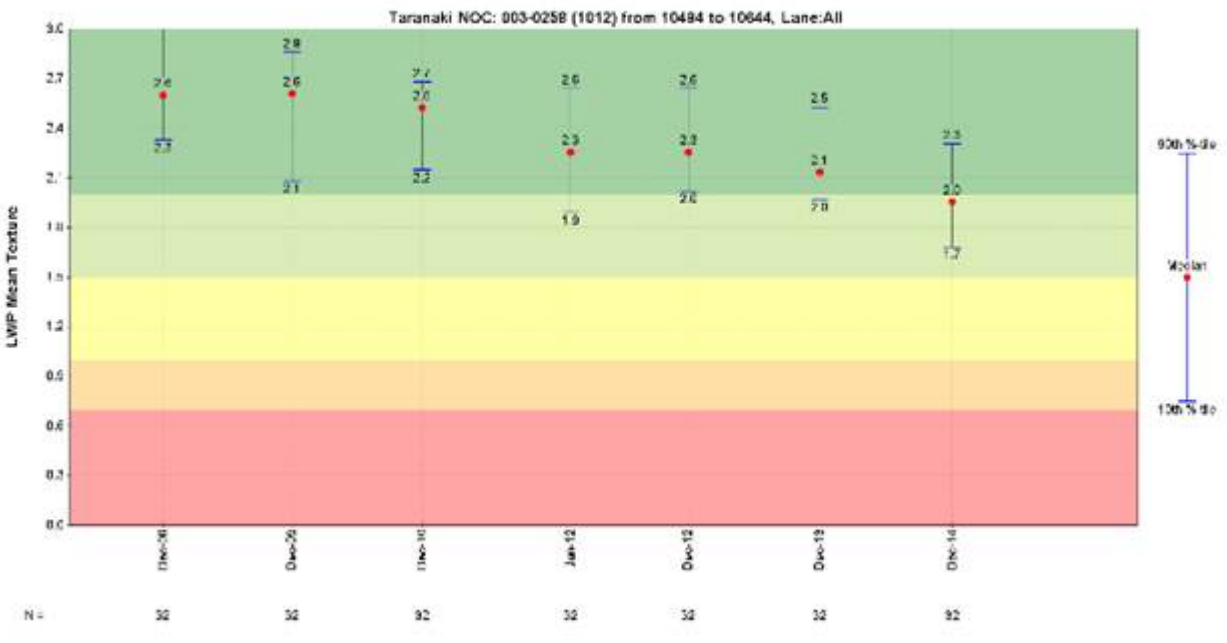
No significant pavement or drainage maintenance has occurred here since 1987, and no defects are recorded in the all faults programme. Shallow rutting is, however, visible in the wheel paths of both lanes, but this is not inconsistent with a pavement of this age. The section of highway leading up to the site has undergone recent water blasting to treat flushing.

The next planned renewal is in the FWP for three years' time and although flushing has been noted in NOMAD as the indicative driver, there is no visible indication of this on site. It will be evaluated and possibly even deferred closer to the proposed renewal time.

Figure B.42 SH3 Egmont to Stratford 16,300-16,450m: rutting and texture measurements from 2008 to 2014



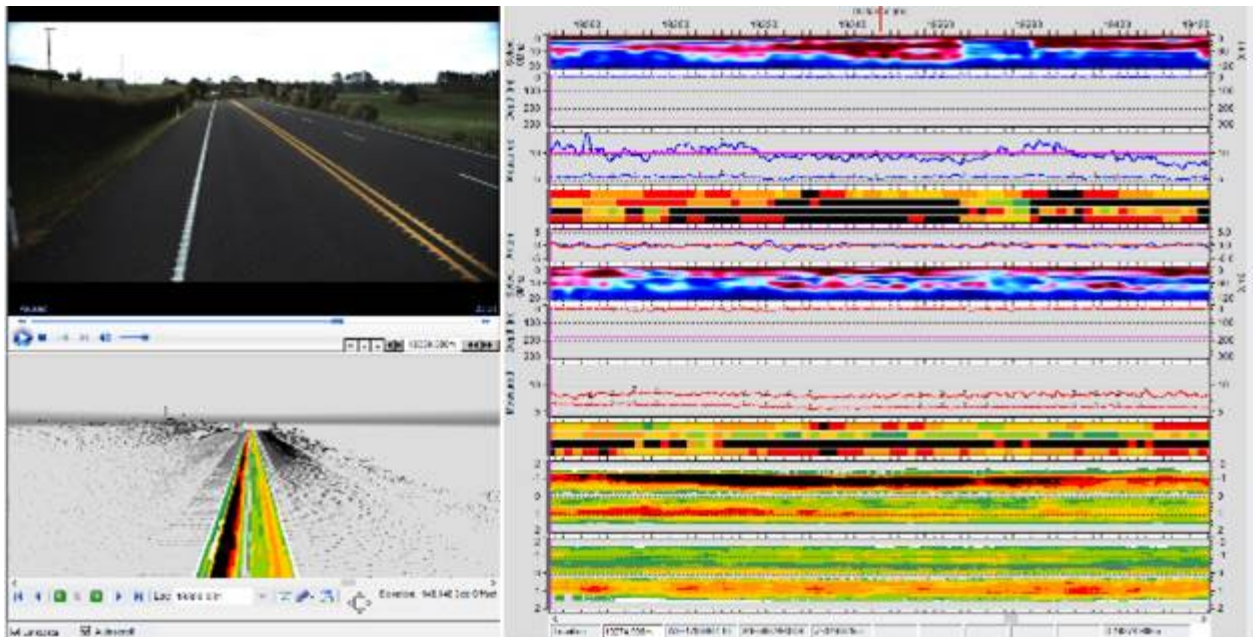
Texture deterioration



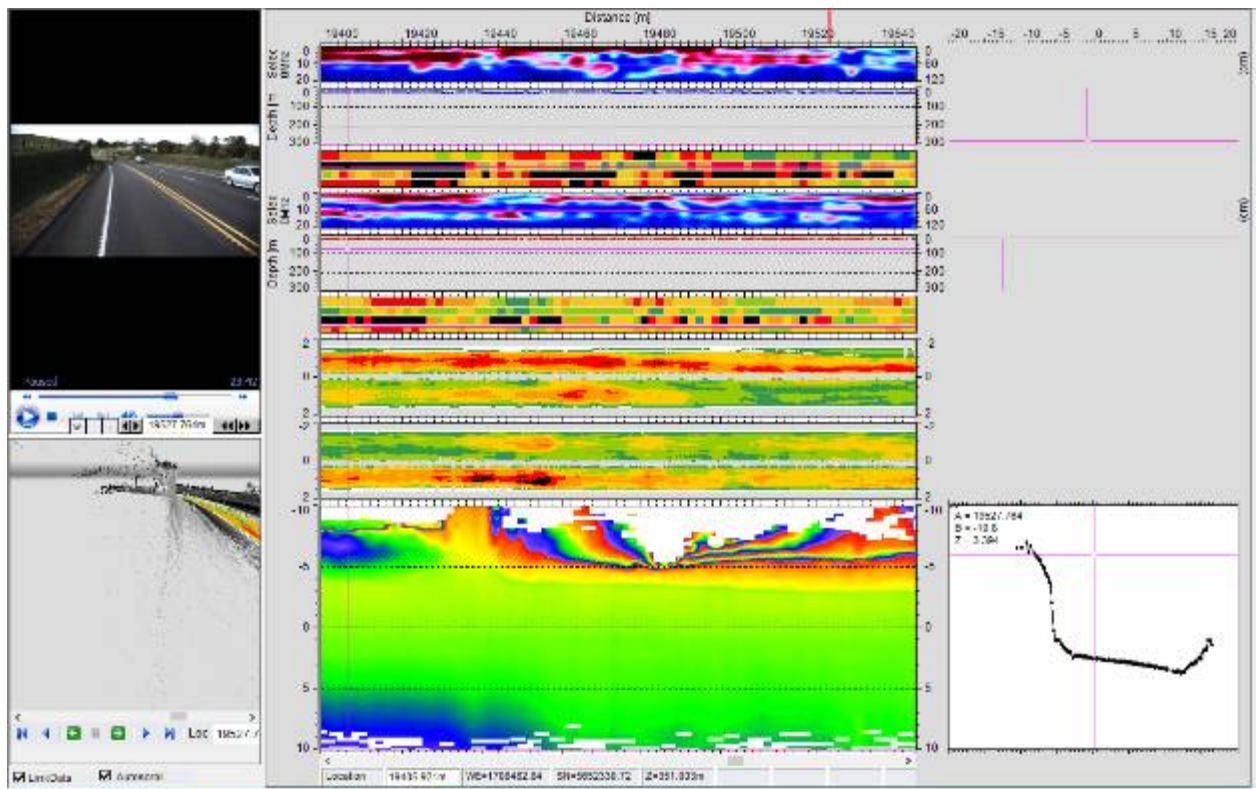
Rutting deterioration

**B7.2.5 SH3 Egmont to Stratford 19,300-19,450m (RP 269/2.59)**

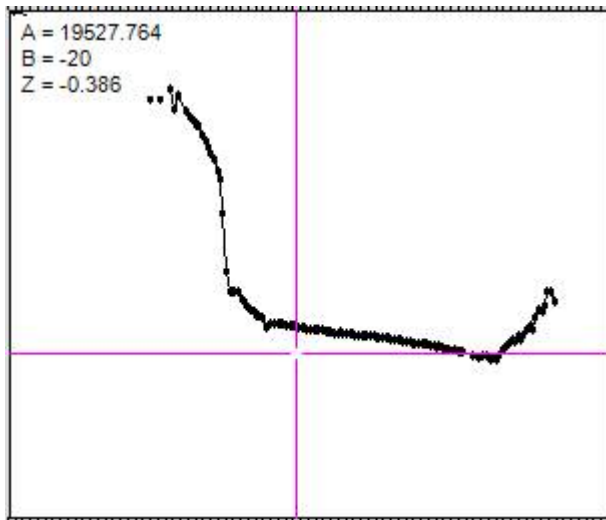
**Figure B.43 Moisture results showing in SH3 Egmont to Stratford 19,300-19,450m (RP 269/2.59)**



**Figure B.44 Moisture results showing in SH3 Egmont to Stratford 19,300-19,450m (RP 269/2.59) with cross section information**



**Figure B.45** Cross section measured by LIDAR laser during moisture survey



This section shows high moisture rutting, which is probably due to the higher ground on the left-hand side. This may be a good location to cut deeper drains and/or install deep subsoil drains to intercept the water travelling under the road.

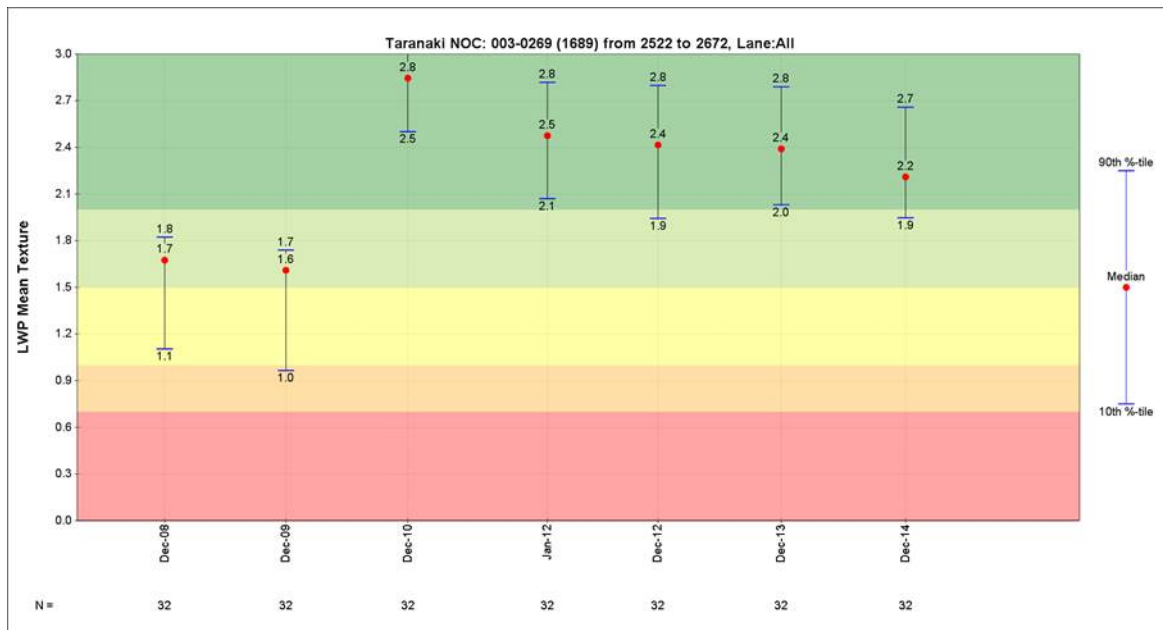
This section of highway is typical of the area with what appear to be good drains either side, bounded by rail and open farmland. A passing lane was constructed here about 2002 with four seal coats over this section and a further two over the entire width.

No significant maintenance activities have been recorded since the pre-reseal repairs in 2001, and no defects are present in the all faults programme. Visually, however, there is evidence of rutting and some flushing albeit isolated and minor in nature.

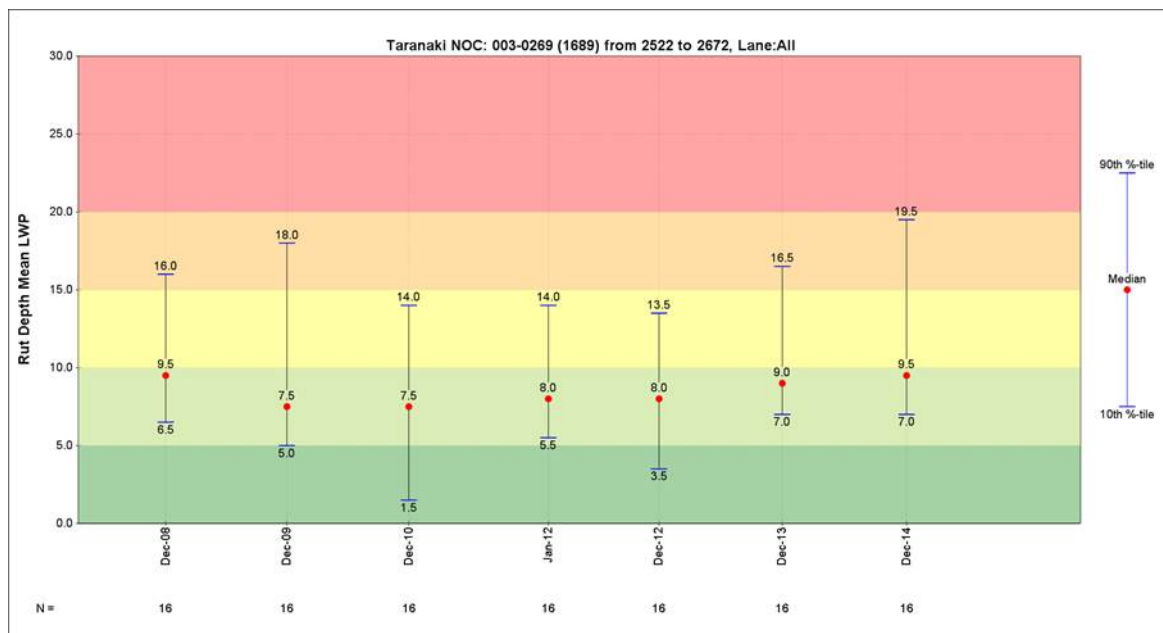
No area rehabilitation or reseal treatment has been identified in the FWP for the next five years.



Figure B.46 SH3 Egmont to Stratford 19,300–19,450m: rutting and texture measurements from 2008 to 2014



Texture deterioration



Rutting deterioration

Figure B.47 Results of moisture survey on SH3 Egmont to Stratford (RP 9150)

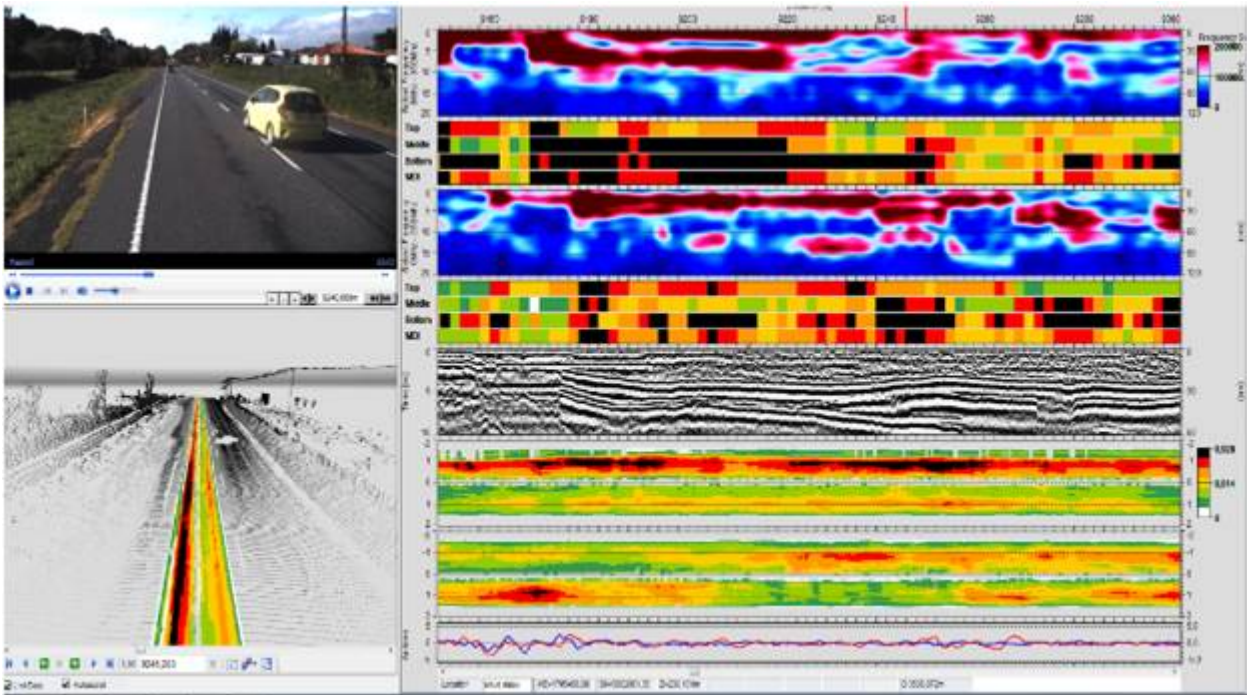


Figure B.47 shows an area with high moisture at depths >250mm and a small area near the top of the pavement. High moisture is supported by the fact that high rutting is recorded in the left-hand wheel path as indicated by the laser survey.